Pedro Miguel Miranda de Sousa Gonçalves Pereira

Severity and Extent of Tissue Damage in Human and Experimental Temporal Lobe Epilepsy



Instituto de Ciências Biomédicas de Abel Salazar

Universidade do Porto

Porto, 2005

The Prinsengracht, in Amsterdam, as painted by the Author´s mother (2003)

Pedro Miguel Miranda de Sousa Gonçalves Pereira

Severity and Extent of Tissue Damage in Human and Experimental Temporal Lobe Epilepsy

Instituto de Ciências Biomédicas de Abel Salazar
Universidade do Porto
Porto, 2005

Pedro Miguel Miranda de Sousa Gonçalves Pereira

Severity and Extent of Tissue Damage in Human and Experimental Temporal Lobe Epilepsy

Dissertação de candidatura ao grau de Doutor em Ciências Médicas submetida ao Instituto de Ciências Biomédicas de Abel Salazar da Universidade do Porto.

Orientador: Professor Doutor Fernando Lopes da Silva

Co-Orientador: Professor Doutor António Martins da Silva

To my Parents

In memory of my Brother

ACKNOWLEDGMENTS

I can date the beginning of this thesis on a late summer night at the "Martinho da Arcada" restaurant, in Lisbon, in 1999. Me, Professor Lopes da Silva and Professor Martins da Silva meet to discuss the possibilities of a research project on epilepsy. The dinner was splendid and ended with a solid possibility to pursue an assignment in experimental neurobiology at the Faculty of Science at the University of Amsterdam.

Throughout the following years, I've learned some of the essential aspects related with committed scientific research and was embebed by the enthusiasm for epilepsy, neurobiology and neuroradiology.

The book you are about to read contains much more than a simple collection of data of neurobiology and neuroradiology experiments. It certainly contains hypothesis and possible explanations for current epilepsy questions; but, mostly, it contains the passionate flavor for science that I had the chance to gather from so many different people.

I owe them much.

They own my friendship.

This study was carried out at the following European institutions, during years 1999-2003:

- the Institute of Neurobiology, Faculty of Science at the University of Amsterdam, in Amsterdam, the Netherlands,
- the Departments of Neurology and Radiology at the Kuopio University Hospital, in Kuopio, Finland,
- the Human Neuroanatomy Laboratory, School of Medicine at the University of Castilla-la Mancha, in Albacete, Spain,
- the Department of Neurology at the "Egas Moniz" Hospital, in Lisboa, Portugal,
- the "Caselas" Magnetic Resonance Center, in Lisboa, Portugal.

I am grateful to the principal supervisor of this study, Professor Fernando Lopes da Silva, M.D., Ph.D. for providing me an unparalleled introduction to the world of epilepsy and research. The attitude and enthusiasm he had for the field of neuroscience has been an example for me to finish this thesis. Further, I am in debt for his thoughtful and supportive observations regarding all aspects of this work.

I owe my full appreciation to co-supervisor, Professor António Martins da Silva, M.D., Ph.D. for his decisive encouragement given during all periods of the research and for the expert

knowledge in clinical neurology. I take as a professional example the persistent developmental work carried out at the Department of Neurophysiology ("Santo António" Hospital), which I've assisted since I was a medical student.

Their proficiency has been vital in designing and executing the study. They have also been my qualified and critical, but also understanding, support during this work.

I owe warmest thanks to Jan Gorter, Ph.D. and Paul Lucassen, Ph.D., and all the colleagues and personnel (including Suarti Maslam) at the Institute of Neurobiology for their valuable contributions on **Study I** of this thesis.

I am greatly indebted to Professors Asla Pitkänen, M.D., Ph.D., Reetta Kälviäinen, M.D., Ph.D. and Ricardo Insausti, M.D., Ph.D. for having accepted the challenge to study the human piriform cortex (**Study III**) and for their professional teaching on the anatomy of the temporal lobe and on the pre-surgical workout of candidates with pharmacologically intractable epilepsy. I further acknowledge the friendly and stimulating working atmosphere they provided at the Departments of Neurology and Radiology at the Kuopio University Hospital (Reetta Kälviäinen) and at the A.I. Virtanen Institute for Molecular Sciences (Asla Pitkänen), and at the Medical School at the University of Castilla-la-Mancha (Ricardo Insausti).

I am also particularly grateful to Tuuli Salmenperä, M.D., Ph.D. for participating on the research conducted for **Study III** and for all the assistance given on data collection and analysis. I am further in debt for her close friendship and support.

My special thanks go to Pedro Rosado, M.D. for his contribution to the **Studies IV** and **V** and for his effort to append the first multimodal quantitative imaging protocol on the pre-surgical evaluation of patients with pharmacoresistant epilepsy, in Portugal. Particular thanks also to Alberto Leal, M.D., BsC.

I express my gratitude to Professor Mário Forjaz Secca, Ph.D. for providing the facilities to carry out a part of the imaging work in Portugal. I am also in debt for the knowledge in imaging physics he has thought.

Thanks also to Romeu Cruz, M.D. who suggested the MRI acquisition protocol used for the volumetric studies.

I would like to thank all the colleagues at the Department of Neurology at the "Egas Moniz" Hospital, in particular Orlando Leitão, M.D. and Luís Guerra M.D.

I also express my gratitude to Professor Pratas Vital, M.D., Ph.D. for his support and teaching on the aspects of temporal lobe surgery.

Warmest thanks go to the colleagues at the "Caselas" Magnetic Resonance Center, in Lisbon, in particular Constança Ribeiro, M.D. and Pedro Evangelista, M.D. for their allowance in developing a comprehensive multimodal imaging protocol at the outpatient clinic and for all their skillful collaboration and helpful criticisms.

I thank Eduardo Oliveira, BsC. for his important and relevant contribution to the statistical analysis on **Studies II, IV** and **V** and for the suggestions added. His expertise was also vital for study design and data selection.

I want to owe special acknowledgments to João Amoedo and the Grünenthal Foundation, who believed in this project since its early days at the Gulbenkian Institute for Science (Gulbenkian PhD Programme in Medicine and Biology). I express my special gratitude to Teresa Carracho and to all the staff at the Department of Design of the Grünenthal Foundation, for the technical assistance provided on the figures of the manuscript and for composing the text for background printing.

Unique and exceptional acknowledgments go to all the old friends that where around since the beginning of this adventure (Pedro Sottomayor, Sofia Lois, Silvia Leal, Ricardo Bettencourt, Frederico Pimentel and Marta Guinot, you are here!) and to all the new friends gathered in-between (and because) of this work (Rita Salema, Thomas Wissen, Lino Ramos and his family, "Mike" Howard, João Amoedo, Lurdes Lopes, Rosália Fonte, Leena Jutila, Gabriela Laranjo, Patricia Magalhães, Sara Gonçalves, Eduardo Oliveira and Célia Leitão). I further add warmhearted thanks to everyone at the *Universiteit van Amsterdam* swim team, including our trainer "Nisco", for their relaxing company.

The greatest thanks for me reaching this goal in my life belong to my loving parents, for their affection and patience, and for their support and encouragement.

This study was financially supported by the Ministry of Science of Portugal, through a scholarship of the Science and Technology Foundation (Fundação para a Ciência e Tecnologia – BD 18498/98).

Further indispensable support was granted by the Grünenthal Foundation.

The Gulbenkian Foundation, the Luso-American Foundation, the Portuguese Medical Association and the International Society for Magnetic Resonance provided specific funding on several occasions.

The Tecnifar, GlaxoSmithKline and Merck Sharp & Dohme industries provided other limited support.

There was indirect support given by the Nationaal Epilepsie Fonds and the Dutch Organization for Scientific Research (NWO), in The Netherlands; the Department of Science and Technology of the Government of Castilla-La Mancha, in Spain; the Academy of Finland, the Sigrid Juselius Foundation, the Kuopio University Hospital Research Fund, the University of Kuopio, and the Vaajasalo Foundation, in Finland, which I acknowledge.

Porto, September 2005



Pedro M. Gonçalves Pereira

Luck ?!
Luck has nothing to do with it ! It's skills !
Skills !!

Asla Pitkänen on 05 of April 2002, getting ready to go for an ice-fishing competition in Kuopio, Finland.

CONTENTS

I – ABSTRACT / RESUMO / RÉSUMÉ

II – INTRODUCTION

III – REVIEW OF THE LITERATURE

1. EPILEPSY
    - 1.1 Definition
    - 1.2 Epidemiology
    - 1.3 Classification
    - 1.4 Etiology
    - 1.5 Epileptogenesis
    - 1.6 Prognosis and Treatment
    - 1.7 Epilepsy Surgery and Outcome
    - 1.8 Status Epilepticus
2. THE LIMBIC SYSTEM AND THE FUNCTIONAL ANATOMY OF THE MESIAL TEMPORAL LOBE
3. THE CONCEPT OF TEMPORAL LOBE EPILEPSY (TLE)
    - 3.1 Definition and Epidemiology
    - 3.2 Semiology and Electroencephalographic Findings
    - 3.3 Etiology and Pathogenesis
4. HISTOPATHOLOGY OF TLE
    - 4.1 The Hippocampus
    - 4.2 The Amygdala
    - 4.3 The Entorhinal Cortex
    - 4.4 The Piriform Cortex
    - 4.5 The Extratemporal Limbic System
5. CAUSES OF MEDIAL TEMPORAL LOBE DAMAGE
    - 5.1 Initial Insult *vs* Recurrent Seizures
        - 5.1.1 Epilepsy patients studies
        - 5.1.2 Experimental studies
            - 5.1.2.1 Experimental animal model of kindling
            - 5.1.2.2 Model of self-sustaining status epilepticus

6. CONSEQUENCES OF MESIAL TEMPORAL LOBE DAMAGE
7. COURSE OF TLE
8. MAGNETIC RESONANCE IMAGING (MRI) STUDIES
8.1 Qualitative MRI of the Hippocampus
8.2 MRI Volumetry of the Hippocampus
8.3 T2-Relaxometry of the Hippocampus
8.4 MR Spectroscopy
8.5 Diffusion Imaging
8.6 MRI of Specific Brain Structures in TLE
8.6.1 Bilateral hippocampal damage
8.6.2 Hippocampal damage in extratemporal epilepsy
8.6.3 MRI of the amygdala and the para-hippocampal cortices
8.6.4 Damage outside mesial temporal lobe structures
8.7 Anatomical Reproducibility and Normative Values
8.7.1 Reference lines and landmarks
8.7.2 Normative values and precision
IV – AIMS OF THE THESIS
V – STUDIES OF THE THESIS
I. NEURONAL CELL DEATH IN A RAT MODEL FOR MESIAL TEMPORAL LOBE EPILEPSY IS INDUCED BY THE INITIAL STATUS EPILEPTICUS AND NOT BY LATER REPEATED SPONTANEOUS SEIZURES
II. ASSESSMENT OF THE PREFERRED SCOUT SAGITTAL ORIENTATION FOR TEMPORAL LOBE IMAGING WITH MAGNETIC RESONANCE
III. MAGNETIC RESONANCE VOLUMETRIC ANALYSIS OF THE PIRIFORM CORTEX AND CORTICAL AMYGDALA IN DRUG-REFRACTORY TEMPORAL LOBE EPILEPSY
IV. ADC-MAPPING OF THE HIPPOCAMPUS AND THE AMYGDALA IN PHARMACORESISTANT TEMPORAL LOBE EPILEPSY
V. RELATIVE LOCALIZING VALUE OF AMYGDALO-HIPPOCAMPAL MR BIOMETRY IN TEMPORAL LOBE EPILEPSY
VI – CONCLUSIONS
VII – DISCUSSION
VIII – FUTURE STUDIES
IX – REFERENCES

I – ABSTRACT

Epilepsy refers to a common group of disorders of brain function that are characterized by recurrent seizures. Temporal lobe epilepsy (TLE) is the most prevalent and least medically responsive form of epilepsy. Up to 30% of patients continue to have seizures despite intensive medication and may be referred for surgical treatment. Mesial temporal sclerosis is the most frequent lesion found in patients with TLE. About 70% of these patients present hippocampal sclerosis, oftenly extending to the amygdala and adjacent cortices. Accordingly amygdalo-hippocampectomies are generally effective in TLE patients. Nevertheless it is not known whether recurrent seizures are a determinant factor underlying the development of hippocampal sclerosis. In any case the non-invasive identification of hippocampal sclerosis in patients with TLE is clinically very useful.

The extent of tissue damage occurring in TLE patients is incompletely known. In recent years there has been a wealth of experimental evidence implicating multiple limbic sites in the generation and propagation of seizures. In addition to the hippocampal formation and the amygdala, the piriform cortex, which is a highly excitable limbic region overlying the fundus of the endorhinal sulcus, may play an important role in TLE, although this area has been less studied.

The investigations reported in this Thesis were carried out with the aim of determining the progression, severity and extent of mesial temporal sclerosis. This should lead to an improvement of the diagnostic and prognostic capabilities of state-of-the-art magnetic resonance imaging (MRI) by selecting appropriate quantitative methods.

In order to avoid the inherent limitations of human studies, an experimental model of TLE, in the rat, was used to analyze the spatio-temporal development of (para) hippocampal lesions and their evolution in the course of TLE. MRI studies were further conducted in human patients using quantitative methods to highlight the pattern of atrophy in the piriform cortex and the diagnostic and prognostic utility of newly emerging techniques, such as diffusion-weighted imaging (ADC-mapping), in the context of pre-surgical evaluations.

In the rat model we tested the hypothesis that a relationship between the occurrence and frequency of epileptic seizures and the progression of (para) hippocampal cell loss might exist. However, this hypothesis was not substantiated by the experimental results. On the contrary, the largest part of (para) hippocampal cell death occurs early at a sub-clinical stage (the latent period), shortly after an initial insult (*status epilepticus*), while recurrent seizures occur only much later.

In human TLE patients we pursued a similar quantitative approach in order to obtain relevant diagnostic and prognostic information that may overcome the limitations of qualitative studies. In this context we quantified structural changes in different brain areas in these patients using multimodal MRI.

An interesting novel observation was that the piriform-cortical amygdala, which includes the piriform cortex, is an area extensively damaged in chronic TLE, as demonstrated by MR volumetry. Nearly 50% of the patients had a mean of 20% volume loss on the side of the site of seizure onset as assessed by electroencephalography, which associated specifically with the severity of hippocampal sclerosis.

We assessed the performance of different quantitative MRI approaches: volumetry, T2 relaxation times, multi-voxel spectroscopy and diffusion-weighted imaging (DWI), particularly with respect to their capacity of predicting the postoperative outcome, in terms of seizure freedom. We found that DWI, which is the most rapid method of imaging the brain, is capable to predict postoperative outcome reliably. We determined that major determinants of a successful postoperative outcome are the concordant lateralization of the hippocampal ADC increase ipsilateral to the side of major electroencephalographic abnormalities and a larger side-to-side difference in hippocampal ADCs. These determinants have a similar predictive value as hippocampal volumetry and T2-relaxometry. Hippocampal spectroscopy and amygdala measures are less precise in predicting post-operative outcome.

The findings of the present series of studies allow us to conclude that damage of the mesial temporal lobe involves multiple limbic sites besides the hippocampus, and its severity can be diagnosed accurately by means of DWI.

RESUMO

A Epilepsia é um conjunto de doenças da função cerebral caracterizadas por crises epilépticas recorrentes. A epilepsia do lobo temporal é a forma mais prevalente e mais resistente ao tratamento farmacológico. Cerca de 30% destes doentes são fármaco-resistentes e podem ter indicação cirúrgica. A esclerose temporal mesial é a lesão que se encontra com maior frequência nos doentes com epilepsia do lobo temporal. Setenta por cento desses doentes têm esclerose do hipocampo, a qual pode incluir o complexo amígdalino e os cortices adjacentes. Dessa forma, a cirurgia com amigdalo-hipocampectomia é um tratamento geralmente eficiente. Actualmente, desconhece-se se a recorrência de crises epilépticas é um factor determinante no desenvolvimento da esclerose temporal mesial. Por outro lado, o diagnóstico não-invasivo da esclerose do hipocampo em doentes com epilepsia do lobo temporal é particularmente importante.

A completa extensão da lesão de esclerose mesial não é conhecida. Recentemente, diversos trabalhos científicos demonstraram que múltiplas regiões do Sistema Límbico podem participar na geração e propagação de crises epilépticas. Além do hipocampo e da amígdala, o cortex piriforme é uma região límbica com grande excitabilidade neuronal, e que tem sido pouco estudada. O cortex piriforme situa-se na profundidade do sulco endorrinal e pode desempenhar um papel importante na fisiopatologia da epilepsia do lobo temporal.

Os trabalhos de investigação realizados para esta Tese, tiveram como objectivos determinar a progressão, severidade e extensão da esclerose temporal mesial. Este conhecimento permitirá uma selecção adequada de métodos neurorradiológicos avançados de Ressonância Magnética (RM) com a finalidade de melhorar as capacidades de diagnóstico e prognóstico.

De forma a obviar as limitações próprias dos estudos com humanos, foi utilizado também um modelo animal experimental da epilepsia do lobo temporal, para analisar a progressão espacio-temporal das lesões do hipocampo e região para-hipocampal e sua evolução no decurso da doença. Subsequentemente, realizaram-se estudos em humanos utilizando métodos de RM quantitativa para determinar o padrão de atrofia do cortex piriforme e a relativa utilidade diagnóstica e prognóstica de novas técnicas, nomeadamente a imagem ponderada em difusão, no contexto das avaliações pré-cirurgicas.

No modelo experimental, testámos uma hipótese que sugere existir uma relação directa entre a ocorrência e frequência de crises epilépticas e a progressão da morte neuronal no (para) hipocampo. Verificámos, pelos resultados experimentais, que essa hipótese não se verifica no modelo experimental estudado. Pelo contrário, a maior parte da morte neuronal no (para)

hipocampo ocorre num estadio sub-clínico (o período de latência), imediatamente após o insulto inicial (*estado de mal epileptico*), sem que ocorram crises epilépticas recorrentes (as quais se iniciam posteriormente).

Em doentes com epilepsia temporal, realizaram-se estudos quantitativos similares para obter informação diagnóstica e prognóstica que permitisse superar as limitações das análises qualitativas. Nesse contexto, quantificámos as alterações estruturais de distintas regiões do lobo temporal utilizando um protocolo de RM multimodal.

Uma das observações mais originais, consistiu na demonstração por volumetria por RM da existência de lesão na região dos cortices piriforme-amigdalino, região esta que ínclui o cortex piriforme. Cinquenta por cento dos doentes estudados, aproximadamente, mostraram uma redução média de 20% do volume do cortex piriforme, no mesmo lado da origem do foco epiléptico tal como fora avaliado electroencefalográficamente. Adicionalmente, a atrofia do cortex piriforme correlaciona-se especificamente com a severidade da esclerose do hipocampo.

Finalmente, analisámos a performance de vários métodos de RM quantitativa: volumetria, relaxometria T2, espectroscopia *multi-voxel* e imagem ponderada em difusão, particularmente quanto à capacidade predictiva do resultado pós-cirúrgico, avaliado em termos de recorrência de crises. Verificámos que a imagem ponderada em difusão, actualmente o método mais rápido para obter imagens cerebrais, consegue prever o resultado pós-cirúrgico com precisão. Concluímos que os principais factores determinantes do sucesso pós-cirúrgico são: (1) existir concordância entre as alterações quantitativas da imagem ponderada em difusão no hipocampo e a lateralização do foco epiléptico demonstrada por electroencefalografia, e (2) existir grande assimetria nos valores de difusão entre os dois hipocampos. Estes factores, têm um valor predictivo comparável aquele obtido pelos métodos de volumetria e relaxomeria T2 do hipocampo. A espectroscopia *multi-voxel* e as análises quantitativas da amigdala são menos robustas na previsão do resultado cirúrgico.

Os resultados da presente série de estudos, permitem concluir que a lesão do lobo temporal envolve múltiplas regiões límbicas além do hipocampo e a sua severidade pode ser diagnosticada com precisão através da imagem ponderada em difusão.

RÉSUMÉ

L´épilepsie est un ensemble de maladies de la fonction cérébrale caractérisé par crises épileptiques récurrentes. L'épilepsie du lobe temporale est la forme le plus dominante et plus résistante au traitement pharmacologique. Environ 30% de ces malades sont résistants à la pharmacothérapie et peuvent avoir indication chirurgicale. La sclérose temporale médiale est le substrat pathologique le plus fréquent dans les malades avec épilepsie du lobe temporale. Soixante-dix pour cent de ces malades ont sclérose de l´hippocampe, que peut s´élargir pour l´amygdale et les cortex adjacents. En conséquence, la chirurgie que consiste dans la amygdalo-hippocampectomie est un traitement généralement efficace. À présent, on méconnaît si la récurrence de crises épileptiques est un facteur déterminant dans le développement de la sclérose temporale médiale. D'autre part, le diagnostique par imagerie par résonance magnétique (IRM) de la sclérose de l´hippocampe est particulièrement important.

La complète extension pathologique de la sclérose temporale médiale n'est pas connue. Récemment, de divers travaux scientifiques ont démontré que multiples régions du Système Limbique peuvent participer dans la génération et la propagation de crises épileptiques. Par rapport au l´hippocampe et l´amygdale, le cortex pyriforme est une région limbique avec de grande excitabilité neuronale, et qui a été peu étudié. Le cortex pyriforme se place dans la profondeur du sillon endorrinal et peut jouer un rôle important dans la physiopathologie de l'épilepsie du lobe temporale.

Les travaux de recherche qui ont réalisé pour cette Thèse ont eu pour objectif déterminer la progression, la sévérité et l'extension de la sclérose temporale médiale. Cette connaissance permettra une sélection appropriée de méthodes d´étude avancées de l´IRM avec la finalité d'améliorer les capacités de diagnostique et de pronostique.

De manière à remédier les limitations propres des études avec des humains, on a utilisé un modèle animal expérimental de l'épilepsie du lobe temporale, pour analyser la progression spatiale et temporale de la pathologie de l'hippocampe et du gyrus du para- hippocampe, plus son évolution au cours de la maladie. Ultérieurement, se sont réalisées des études dans des humains en utilisant méthodes d'IRM quantitative pour déterminer le degré d'atrophie du cortex pyriforme et la relative utilité diagnostique et pronostique de nouvelles techniques, notamment la séquence pondérée en diffusion, dans le contexte des études chirurgicales.

Chez le modèle expérimental, nous avons verifié l´hypothèse que suggère une relation directe entre la présence et fréquence de crises épileptiques et la progression de la perte neuronale du (para) hippocampe. Nous avons vérifié, par les résultats expérimentaux, que cette hypothèse ne

peut pas être soutenue. Par contre, la plupart de la perte neuronale du (para) hippocampe se produit dans la période de latence, immédiatement après l'insulte initiale (*status de mal épileptique*), sans se produirent des crises épileptiques récurrentes (qui s'initient ultérieurement).

Dans des malades avec épilepsie du lobe temporale, se sont réalisées des études IRM quantitatives semblables pour d'obtenir des informations diagnostiques et prognostiques qui permettaient de dépasser les limitations des analyses qualitatives. Dans ce contexte, nous avons quantifié les modifications structurelles de distinctes régions du lobe temporale en utilisant un protocole d´IRM plurimodale.

Une des observations la plus original a consisté de démontrer par volumétrie IRM de l'existence d'une atrophie dans la région du cortex pyriforme-amygdale, région qu'inclut le cortex pyriforme. Cinquante pour cent des malades étudiés, approximativement, avaient une réduction moyenne de 20% du volume de cortex pyriforme, dans le même côté de l'origine du foyer épileptique évaluée pars l´electroencephalographie. Supplémentairement, l'atrophie de cortex piriforme a une relation spécifique avec la sévérité de la sclérose de l´hippocampe.

Finalement, nous avons analysé la performance de plusieurs méthodes de l´IRM quantitative: volumétrie, relaxométrie-t2, spectroscopie *multi-voxel* et image pondérée en diffusion, en évaluant particulièrement la capacité prédictive du résultat chirurgical, dans des termes de récurrence de crises épileptiques. Nous avons vérifié que l'IRM pondérée en diffusion, actuellement la méthode le plus rapide pour d'obtenir des images du cerveau, réussit à prévoir le résultat chirurgical avec précision. Nous concluons que les principaux facteurs déterminants du succès de la chirurgie sont: (1) l'accord entre les valeurs pathologiques quantitatives de l'image pondérée en diffusion dans l´hippocampe et l´electroencephalographie, et (2) l'existance d'une grande asymétrie dans les valeurs de diffusion entre les deux hippocampes. Ces facteurs ont une valeur prédictive comparable à celui obtenu par les méthodes de volumétrie et de relaxométrie-t2 de l´hippocampe. La spectroscopie *multi-voxel* et les analyses quantitatives de l´amygdale sont moins plus robustes dans la prévision du résultat chirurgical.

Les résultats de la présente série d'études permettent de conclure que la pathologie du lobe temporale ce rapport a multiples régions limbiques et sa sévérité peut être diagnostiqué avec précision à travers l'image pondérée en diffusion.

II – INTRODUCTION

Epilepsy is a common chronic brain disorder characterized by recurrent seizures due to excessive discharge of cerebral neurons. More than 10% of the population will experience a seizure at some time and around 1% of the population has epilepsy [1]. Up to about 30% of all epilepsy patients develop medically intractable epilepsy [2, 3]. Despite prolonged drug treatment these patients continue to have seizures or other symptoms restricting their ability to lead a full life [4]. The majority of medically intractable epilepsy patients referred for surgical consideration have complex partial seizures [5].

Most commonly, the origin of recurrent complex partial seizures is in the temporal lobe. Patients with mesial temporal lobe epilepsy (TLE) have typical clinical and electroencephalographic characteristics. Furthermore, a distinctive pattern of structural damage is frequently found in the medial temporal lobe structures of TLE patients. Neuropathological studies indicate that 70% of medically intractable TLE patients have hippocampal damage characterized by neuronal loss and gliosis in the dentate hilus and in Ammon's horn [6]. The structural damage often extends beyond the confines of the hippocampus to the amygdala and the adjacent cortex [6-9]. However, the full extent of brain damage associated with TLE and hippocampal sclerosis is incompletely known.

The etiology and the pathogenesis of this frequently encountered mesial temporal lobe damage is also a matter of debate. Several human studies have reported a correlation between severe childhood illness (encephalitis/meningitis, complex prolonged febrile convulsions, *status epilepticus*) and hippocampal atrophy in TLE [6, 7, 10-12]. However, not all TLE patients with hippocampal damage have a clear history of initial insult. Some experimental and human data suggest that recurrent seizures may cause progressive damage to the hippocampus [13-15].

Experimental animal models of TLE offer a unique means to study the temporal and spatial effects of the pathogenesis of epilepsy over the entire brain, while controlling for illness-related variables such as duration of the disease, frequency of seizures, medication and genetic background, that hamper human studies [16]. Importantly, results obtained with animal models of chronic TLE often provide clues that may lead to new investigations in human subjects.

In human studies, magnetic resonance imaging (MRI) is the most sensitive noninvasive technique to investigate the temporal lobe, and associated structures, of TLE patients during the course of the disease. Quantitative MRI volumetric analysis of the hippocampus proved to be highly sensitive and specific for hippocampal sclerosis in a series of surgically treated TLE patients [17, 18]. Furthermore, the quantification of transverse relaxation time (T2)-weighted

signal intensity, and of metabolite peak frequency by means of chemical-shift imaging, may help to compensate for the inherent bias of visual neuroradiological analysis and allow MRI diagnosis of hippocampal damage in cases with mild structural abnormalities. However, the existing quantitative imaging methods used for the depiction of hippocampal sclerosis are time-consuming if used routinely in a clinical setting, and may yield data difficult to interpret. For these reasons we investigated new emerging MRI methods, such as diffusion-weighted imaging, which are rapid to acquire and precise to quantify.

In line with previous histopathological results, current neuroimaging data indicate that TLE affects the hippocampal formation and involves other brain regions, in particular those that belong to the limbic system. Nevertheless, some areas known for their possible role in seizure generation remain to be studied in human patients.

This series of studies investigated by means of quantitative experimental neuropathology and human MRI the pattern of mesial temporal lobe and limbic damage in TLE patients. The questions addressed were (i) whether recurrent or prolonged seizures contribute to the damage, (ii) whether tissue damage extends beyond the confines of the hippocampus and (iii) which quantitative MRI method would be most suited to unveil the neuropathology associated to TLE on a time-efficient and sensitive manner.

The human studies, however, do not allow a precise analysis of the evolution of the epileptic condition and the underlying cellular changes, since the large majority of patients are analyzed using MRI many years after the initiation of the disease process. The lesions found in the hippocampi and in the remaining of the mesial temporal lobe of pharmacoresistant TLE patients represent an advanced stage of the disease; early stages of epilepsy development are not available for structural analysis in humans. Animal models of TLE appear particularly helpful to study the cellular and structural mechanisms of highly dynamic processes such as the development of hyperexcitability and pharmacoresistance. Therefore we carried out an experimental study with the main objective of investigating whether cell loss in the (para) hippocampal region is related to the severity of chronic seizure activity in a rat model for temporal lobe epilepsy (TLE).

III – REVIEW OF THE LITERATURE

1. EPILEPSY

1.1. Definition

Epilepsy is not a single entity or disease. Rather, epileptic seizures can be defined as manifestations of abnormal and sudden excessive activity of cerebral neuronal networks [19] caused by a large number of processes. The entire brain or parts of it may be involved; the extent of involvement largely determines the type of seizure.

The Commission on Epidemiology and Prognosis of the International League Against Epilepsy defines Epilepsy as "a condition characterized by two or more recurrent epileptic seizures over a period longer than 24 hours, unprovoked by any immediate identified cause" [20].

The clinical features of seizures are manifest as sudden alterations of sensory experiences and/or motor activities. Such clinical symptoms can include stereotyped alterations of consciousness, behavior, emotion, motor function or sensation. Seizures can be caused by a variety of pathologic conditions, including acquired brain injuries and genetic abnormalities. Many disturbances of brain functions can also provoke seizures [19, 21, 22]. A single seizure, occurring after a brain insult such as severe brain trauma, is not sufficient to label a person an epileptic patient. Only when unprovoked seizures occur recurrently the pathological condition may be called epilepsy [20]. Thus, epilepsy might be considered a "dynamical disease" of brain systems [19, 23], in the sense that seizures are manifestations of the property of neuronal networks to display multistable dynamics due to an abnormal organization of cerebral networks, both in time and space [24].

1.2. Epidemiology

In the general population, the lifetime prevalence rate for epilepsy is 4-8 cases per 1000 [25] and the annual incidence rate including patients with recurrent unprovoked seizures is estimated to be between 40-70 cases per 100.000 per year [3, 25, 26].

The point prevalence (that is, the proportion of a defined population carrying the disease at a given point in time) is estimated at about 0.5-0.8% in Europe [3] with similar figures reported for the United States [27].

Epidemiological studies carried out in the two European countries where the present series of clinical studies took place, indicated relatively similar incidence and prevalence rates; in Northern Portugal, Lopes Lima reported an incidence rate of 30.6/100.000 and a prevalence of

4.2/1000 in adult patients with epilepsy [28]; in East-Central Finland, Keränen reported an incidence rate of 24/100000 and a prevalence of 6.3/1000, also in the adult population [29].

Considering the entire population of Europe (about 810 million persons, including Russia), as many as 40 million people will have a history of seizures at some time in their lives, and as many as 6 million currently have active epilepsy [30].

The estimates of lifetime prevalence, which is the measure of people in a population who have ever had epilepsy, vary from 2 to 6% of the population [1, 25, 26, 31]. These statistics suggest that 1 in 20 persons will have suffered epilepsy at some point in their lives and, conservatively, 1 in 200 will currently have epilepsy [21]. In the United States, prevalence rates increased steadily from 2.7/1000 in 1940 to 6.8/1000 in 1980 [32].

1.3. Classification

The classification of epileptic seizures by the Commission on Classification and Terminology of the International League Against Epilepsy (ILAE) [33] is based on the seizure type, and on clinical and electroencephalographic (EEG) characteristics. According to this classification, epileptic seizures are divided into partial and generalized seizures. In general, partial seizures are those in which the first clinical and EEG changes indicate initial activation of a system of neurons limited to part of one cerebral hemisphere. Partial seizures are classified as simple when consciousness is retained and complex when consciousness is impaired. Simple partial seizures can progress to become complex and they are further classified according to symptoms: motor, sensory, autonomic and psychic. Both simple and complex partial seizures can further evolve into secondarily generalized seizures with characteristic tonic and clonic motor manifestations. Generalized seizures are those in which the first clinical changes indicate initial involvement of both hemispheres. The initial ictal EEG patters are bilateral and presumably reflect neuronal discharge, which is widespread in both hemispheres. Generalized seizures are further divided into tonic-clonic, tonic, clonic, absence, myoclonic and atonic seizures.

According to the classification, the disorder of the brain may be apparently localized and known as “localization related” (partial) or generalized. Both localization related and generalized epilepsies and syndromes are divided according to the etiology into idiopathic and symptomatic varieties.

1.4. Etiology

Certain postnatal insults such as brain trauma, central nervous system (CNS) infections, cerebrovascular disease, and brain tumors greatly increase the incidence of epilepsy [34]. In a classical study in Rochester, Minnesota, 1935-1984, the presumed predisposing cause of epilepsy was vascular in 11% of all the incident cases of epilepsy, followed by congenital (8%), traumatic

(5.5%), neoplastic (4.1%), degenerative (3.5%) and infective (2.5%) causes [32]. These data agree with other recent prospective cohort population-based studies that reported a vascular etiology of epilepsy in 15%, cerebral tumor in 6%, alcohol-related in 6% and post-traumatic in 3% of the patients [3]. The etiology of epilepsy varies considerably in different age groups and may be multifactorial. Notably, epidemiological studies have reported that in about 65% of cases the etiology of seizures was idiopathic, that is not associated with brain lesions, neurologic abnormalities other than seizures, or cognitive impairment [3, 25].

It is evident that the more extensive the investigation, the more likely etiological factors are to be identified. Brain magnetic resonance imaging (MRI) identifies a high rate of positive causes in hospital-based surveys [35]. Therefore, it is likely that the true incidence of symptomatic epilepsies is higher than reported in previous studies, and that MRI will have an important impact on the diagnosis of previously undetectable structural abnormalities underlying epilepsy (such as cortical dysplasias [36], or hamartomas [37], for example).

The majority of epilepsies lack an overt genetic determinant. However, genetics may contribute to susceptibility to epilepsy arising after a brain insult [38].

1.5. Epileptogenesis

Epileptogenesis refers to the development of an epileptic disorder (**Figure 1**) and it is considered a progressive process [19]. In general, all epilepsies follow a similar pattern of development. It is clearly documented from experimental studies with animal models [39, 40] as well as from studies with patients [41] that there is a latent period between the induction of an initial precipitating insult such as head trauma or *status epilepticus* and the appearance of a chronic epileptic condition. During the latent period major changes occur at the cellular and molecular level, namely neuronal loss and abnormal synaptic reorganization [42-44]. This reorganization of the neuronal integration progressively establishes an epileptogenic network characterized by abnormal excitability and synchronization, leading eventually to the occurrence of spontaneous seizures [39, 40]. Once developed, epilepsy should be viewed as a dynamic process, which results in both ictal phenomena and interictal functional abnormalities, related to structural abnormalities in the brain [19, 45, 46]. Patients who develop chronic intractable epilepsy demonstrate progression in both the number of seizures and in seizure-related neurological symptoms such as cognitive decline and behavioral disorders [46-49]. A challenge arising from the existing experimental data is how to counteract the progression of epileptic damage. In the future, neuroprotective therapy could be developed either for the time period after a brain insult, or even after the diagnosis of epilepsy was made as a part of a rational antiepileptic therapy if the patient is not seizure-free [50].

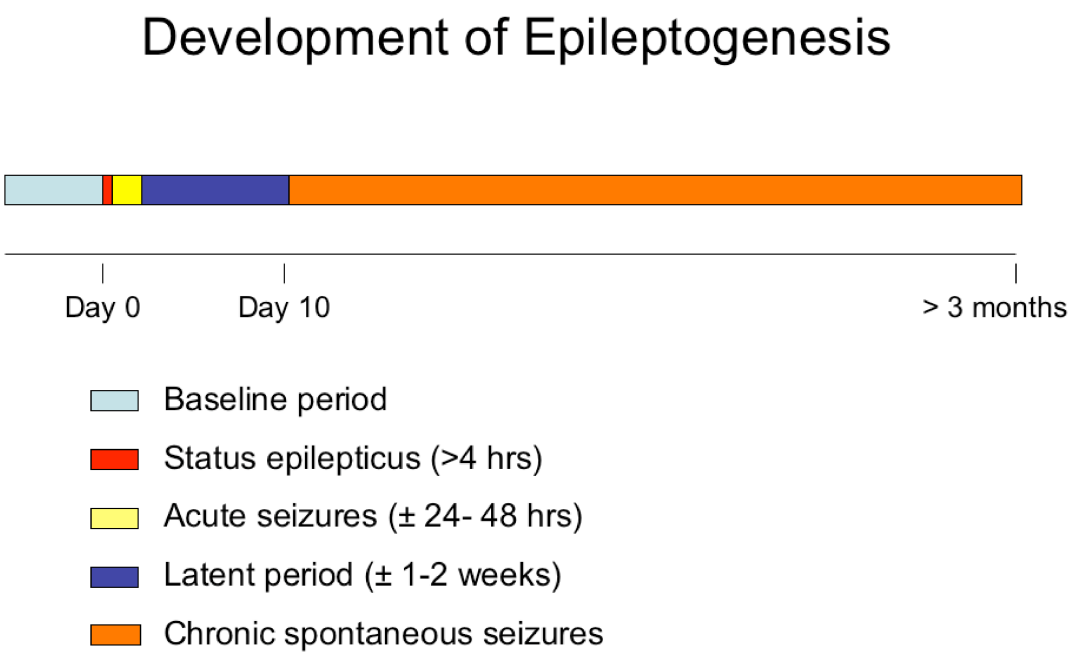


Figure 1. Model of development of epilepsy – epileptogenesis – in the animal model of chronic partial epilepsy used in the experimental studies conducted for Study I of this thesis. The major steps leading to the state of chronic seizures match those of the human condition (only the time-lag varies; weeks are equivalent to years in humans). After initial cerebral insult, the damaged brain reorganizes during the latent period in a manner that ultimately predisposes to the development of chronic spontaneous seizures.

1.6. Prognosis and Treatment

Overall, the prognosis for most epilepsy patients undergoing antiepileptic treatment is good in terms of seizure control. Population-based studies have shown that 70-80% of patients will become seizure-free with the appropriate medication [31, 51, 52]. An interesting observation is that the long-term outcome of epilepsy is often predictable by the early outcome of seizure control [31, 53, 54]. In 50-70% of the patients, seizures can be controlled with an initial antiepileptic drug [52, 55]. Switching to a second antiepileptic drug affords control in about one-third of initially uncontrolled patients [52]. There are no clear differences in efficacy between first line monotherapy drugs such as carbamazepine, phenytoin, valproate, lamotrigine and oxcarbazepine [52, 56], nor have the newer antiepileptic drugs (gabapentin, levetiracetam, tiagabine, topiramate, vigabatrin and zonisamide) shown significant difference in efficacy or tolerability in a meta-analysis of trials in drug-resistant partial epilepsy [57].

Up to 35% of all epilepsy patients become pharmacoresistant and will develop intractable epilepsy [4, 58-60]. Up to 60% of these patients may benefit from surgery [61, 62]. The surgically treatable disorders include mesial temporal sclerosis, benign neoplasms, developmental abnormalities and other focal lesions such as arteriovenous malformations.

The epilepsy is considered intractable when a patient has epileptic seizures, or other symptoms of an epileptic syndrome, despite adequate treatment, while these symptoms restrict the patient's ability to lead a full and safe life [4]. Some known risk factors that predict the development of intractable epilepsy are a large number of seizures before treatment, combined seizure types, early age at onset, and prolonged disease duration [63]. Additionally, other factors associated with intractable epilepsy include syndromes of secondarily generalized epilepsies (e.g., Lennox-Gastaut syndrome, West syndrome), certain seizure types such as atonic and tonic seizures, and etiologies such as sequelae of cerebral infections or severe trauma. Epilepsy patients with associated neurologic deficits and detectable structural brain damage are prone for lower remission rates [21, 59, 64]. Patients with drug-resistant seizures and associated neurological disabilities are further related to poor social outcome and higher mortality rate [65]. Overall, patients with epilepsy have a mortality rate two to three times higher than expected in the general population [66]. The greatest increase in mortality occurs in the early years of diagnosis, in the symptomatic group and in patients with high frequency of tonic-clonic seizures [2, 67].

1.7. Epilepsy Surgery and Outcome

For certain groups of patients with partial seizures resistant to pharmacological treatment, surgery is an effective treatment option.

The modern era of epilepsy surgery started in the nineteen fourties with the pioneering work of Otfried Foerster in Germany and later Herbert Jasper together with the neurosurgeon Wilder Penfield at the Montreal Neurological Institute [61]. Since then, the number of epilepsy surgery centres has increased rapidly.

The comprehensive epilepsy surgery evaluation of patients involves a combination of clinical, electrophysiological, neuroimaging and neuropsychological evaluations [61, 154, 272, 295]. The electrophysiological investigations include routine EEG, and seizure monitoring with continuous video-EEG recording. In some cases, intra-cranial electrodes are used to achieve a more precise location of the seizure focus.

The more favorable outcome after surgery is achieved in patients with a known lesion [62, 120, 154, 274]. Recent advances in neuroimaging have improved the prospects of finding lesions that could be related to the seizure focus. The development of structural imaging using high-resolution MRI has been most important [35]. However, it is known that a structural lesion is not necessarily the origin of the seizure focus. Functional imaging techniques, such as positron emission tomography (PET) [177, 178] and single-photon emission computed tomography (SPECT) [176] often provide additional information in the quest for the seizure focus.

Concordance of results from different investigations, especially EEG and imaging data, is necessary for the decision to perform surgery.

The efficacy of epilepsy surgery has been recently confirmed in a randomized, controlled study [154] of surgery versus pharmacological treatment in poorly controlled TLE patients, confirming many observational studies [62, 120, 266, 274, see also 61 for a review].

Postoperative outcome after epilepsy surgery is usually estimated with regard to seizure freedom. The most frequently used seizure outcome classification was introduced by Engel et al in 1993 [312] and, recently, the ILAE Commision on Classification suggested a revised classification scheme [418] that hopefully will improve the possibilities for comparisons amongst epilepsy surgery centres. Nontheless, other post-surgical outcome measurements such as memory and language functions, quality of life and psychiatric morbidity, have been used [49, 266, 272, 313].

1.8. Status Epilepticus

Status epilepticus is a condition characterized by series of epileptic seizures that are frequently repeated or so prolonged as to create a lasting state [68]. The present operational definition of *status epilepticus* was introduced by Lowenstein and Alldredge [69] and includes either continuous seizures lasting at least 5 minutes, or two or more discrete seizures between which there is incomplete recovery of consciousness. *Status epilepticus* in early life is often seen as the kind of initial insult that predisposes to chronic epilepsy [70]. Since such a convulsive status may induce the development of structural damage and functional incapacity it is commonly agreed that it should be terminated as soon as possible. Time is a crucial variable in the treatment of *status epilepticus*. The therapy for status epilepticus currently consists of agents such as benzodiazepines, phenytoin or barbiturates [71].

Any type of seizure can develop into *status epilepticus*, although the form most often seen in adults is tonic-clonic *status epilepticus* [72]. The incidence of *status epilepticus* reaches 41/100000, and the mortality rate 22% [73]. The majority of *status epilepticus* patients had no history of epilepsy. Furthermore, infants less than one year of age had the highest incidence of *status epilepticus*, but the elderly population represented the largest number of *status epilepticus* cases [71, 73]. Frequent causes of *status epilepticus* include noncompliance with antiepileptic medication, cerebral vascular disease, drug abuse (including ethanol) and anti-epileptic drug withdrawal, CNS infection, metabolic disorder, tumor, and trauma [74]. In some cases, the cause is multifactorial; in others, no cause can be identified.

The morbidity and mortality from status epilepticus are related to three factors: damage to the CNS caused by acute insult precipitating the *status epilepticus*, systemic stress from repeated

generalized tonic-clonic convulsions, and injury from repetitive electrical discharges within the CNS [71, 72]. Neuropathological and imaging studies have shown damage in the hippocampus and in the amygdala, piriform cortex, thalamus, cerebellum and cerebral cortex after convulsive and nonconvulsive status epilepticus episodes in patients [75-79].

The three broad types of sequelae of *status epilepticus* include epileptic brain damage, neurological/cognitive deficits, and spontaneously recurrent seizures [80]. This latter feature is the rationale to create animal models of chronic spontaneous seizures in the limbic system [81].

2. THE LIMBIC SYSTEM AND THE FUNCTIONAL ANATOMY OF THE MESIAL TEMPORAL LOBE

The limbic system forms a border (limbus) around the upper brain stem, diencephalons and corpus callosum. “Le grand lobe limbique” (the limbic lobe) first defined by Broca [82], includes cortical components (subcallosal, cingulated, hippocampal and parahippocampal gyri) and subcortical structures, such as the amygdala, thalamus and hypothalamus (see [83] for a review). Functionally, it was proposed that these structures play a role in memory and emotive mechanisms [84-86], and are highly interconnected so to consider them collectively as a system [85, 87].

The connectivity of the various components of the limbic cortex is broad and complex (**Figure 2**). The limbic cortical areas receive multimodal sensory information, which are processed by a number of interconnected and parallel loops and circuits. These cortices are specialized in forming associations between stimuli of different kinds in relation to the behavioral context in which the stimuli occur. The outputs modulate multiple target structures responsible for somatomotor, autonomic, and/or hormonal functions.

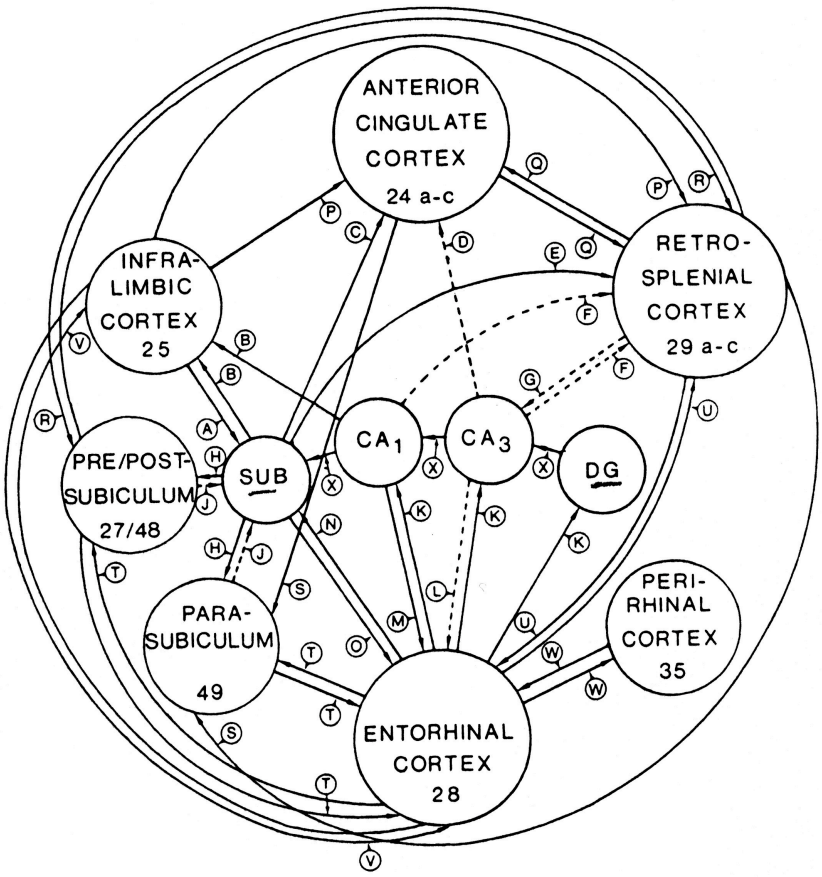


Figure 2. Diagram of connectivity of various components of limbic cortex. Reprinted from [83] with permission.

The temporal lobe is far more often than any other area the seat of an epileptogenic focus. The reasons for this probably relates to the distinct anatomophysiological properties of the limbic portion of the temporal lobe and to a particular vulnerability of its neocortical and limbic components to some forms of pathology.

The temporal lobe contains the brain-functioning elements of speech, memory and hearing.

Morphologically, the temporal lobe has the form of a truncated pyramid, with the (anterior) pole as the top while the base appers to merge with the parietal and occipital lobes. It has four surfaces.

On the lateral aspect of the hemisphere (**Figure 3**), the superior, middle and inferior temporal gyri can be distinguished; they are separated by the superior and inferior temporal sulci. The sylvian fissure borders superiorly the superior temporal gyrus.

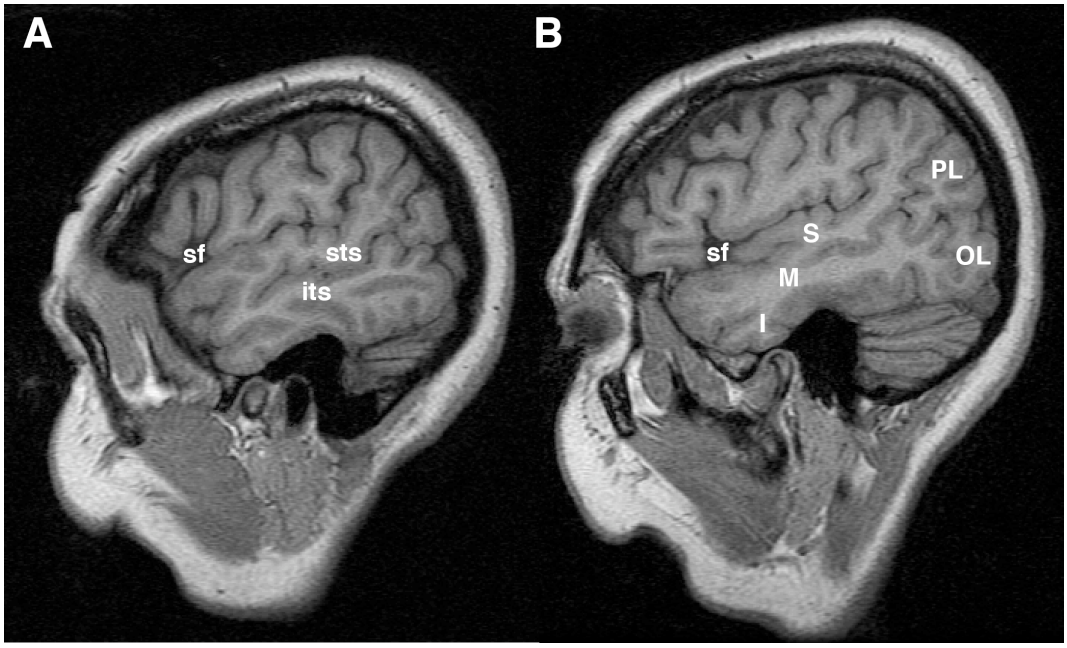


Figure 3. T1-weighted magnetic resonance images of the lateral surface of the human temporal lobe on the sagittal plane of view. ***A*** is more lateral and ***B*** more medial. Subject had 37 years-old and was included as a control for Studies III to V. Abbreviations: S, superior temporal gyrus; M, medial temporal gyrus; I, inferior temporal gyrus; sts, superior temporal sulcus; its, inferior temporal sulcus; sf, sylvian fissure; PL, parietal lobe; OL, occipital lobe.

The inferior (basal) surface includes the inferior temporal, the fusiform and the para-hippocampal gyri. The medial (mesial) surface consists of the para-hippocampal and the hippocampal gyri, and the amygdala (**Figure 4**). The perirhinal and entorhinal cortices are located in the fusiform and para-hippocampal gyri, respectively.

The superior surface (opercular, because it corresponds to the temporal operculum) has three distinct parts (the planum polare, the Heschl´s gyrus and the planum temporale). The temporal horn of the lateral ventricle occupies the deep part of the pyramid.

Deep to the sylvian fissure is the insula, which is bounded by the fronto-temporal opercular regions. The inferior part of the insula near the sylvian fissure is called the *limen* of the insula (*limen insulae*, for short). The *limen insulae* (**Figure 4**) is a critical reference for neuroanatomical co-localization of mesial temporal cortices, such as the entorhinal and piriform cortices.

Histologically, there are four areas with different cortical organization. The three-layered *allocortex* includes the piriform and periamygdalar cortices, the ambiens and semilunar gyri (that constitute the uncus), and the hippocampus. The *mesocortex*, which has six layers, comprise the anterior third of the para-hippocampal gyrus, named the entorhinal area. The *isocortex*, also with six layers, consists of the superior, middle and inferior temporal gyri, the Heschl´s gyrus and the

fusiform gyrus. There is a *transitional area* in the mesial temporal lobe from the primitive allocortex to the meso and isocortices, named amygdalo-hippocampal transitional area.

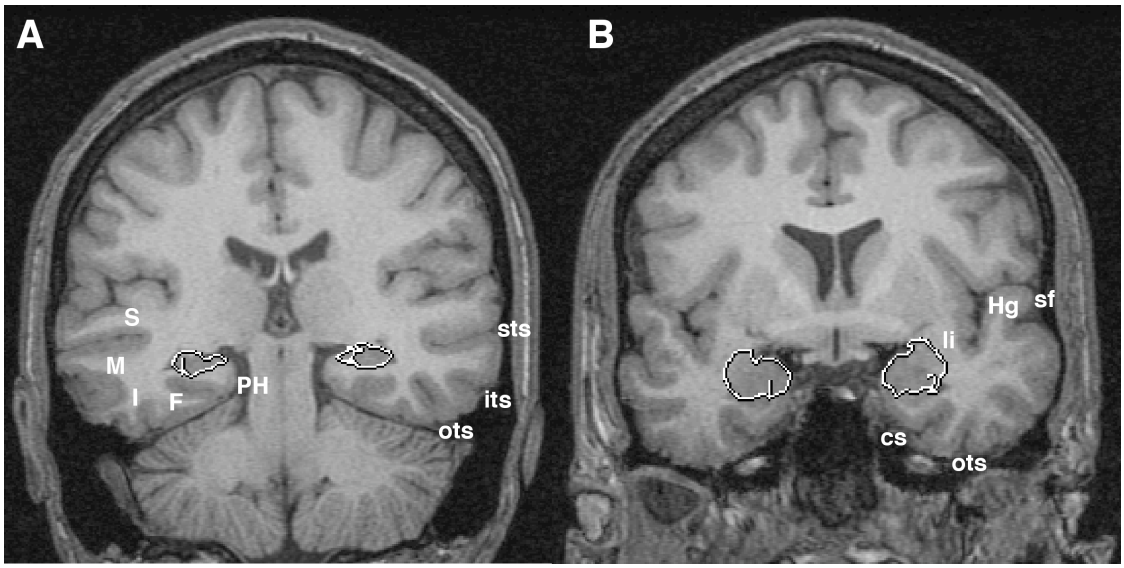


Figure 4. T1-weighted magnetic resonance images of the human temporal lobe on the coronal plane of view. Lateral and infero-medial cortices are seen. ***A*** is more posterior and shows the segmentation of the hippocampus. The hippocampus is an oval-shaped structure, isointense to gray matter, located inferior to the choroid fissure (also known as the endorhinal sulcus) and inferior and medial to the temporal horn. ***B*** is more anterior and shows the segmentation of the amygdala. Subject had 28 years-old and was included as a control for Studies III to V Abbreviations: S, superior temporal gyrus; Hg, Heschl´s gyrus; M, medial temporal gyrus; I, inferior temporal gyrus; F, fusiform gyrus (perirhinal cortex); PH, para-hippocampal gyrus (entorhinal cortex); sts, superior temporal sulcus; its, inferior temporal sulcus; ots, occipito-temporal sulcus; cs, collateral sulcus; sf, sylvian fissure; li, *limen insulae*.

Physiologically, two main divisions may be distinguished in the temporal lobe. The limbic temporal lobe, mainly constituted by the mesial structures, and the neocortical temporal lobe, which includes the cortical ribbons of the superior, lateral and inferior surfaces.

The main components of the limbic system that are located in the medial temporal lobe (**Figures 5 and 6**) consist of (l) the hippocampal formation, (2) the limbic association cortices including the parahippocampal gyrus, and (3) the amygdaloid complex [83]. Both the amygdala and hippocampus are located in the medial part of the temporal lobe, adjacent to the parahippocampal gyrus. This gyrus is a "continuation" of the cingulate gyrus onto the inferior surface of the brain, which is limited inferolaterally by the collateral sulcus (**Figures 4 and 5**). The cortex of the parahippocampal gyrus includes the pre- and parasubiculum, the subiculum, and the entorhinal cortex, both of which are functionally related to the hippocampus.

The presubiculum borders the hippocampus proper (*cornu ammonis*) and dentate gyrus with the fimbria found superomedially and the alveus bordering the *cornu ammonis*.

The hippocampal formation (**Figure 5**) is a prominent, bulging eminence in the floor of the temporal horn of the lateral ventricle. During development, the hippocampal formation (HC) undergoes an enfolding into the temporal lobe. This results in the interdigitation of two c-shaped structures, the *cornu ammonis* (Ammon´s horn) and the dentate gyrus. The *cornu ammonis* is sub-divided into three regions, which are referred to as CA fields. The curling CA includes the CA3 field (Spielmeyer sector) bordering the hilus of the dentate gyrus; the short CA2 field; and the more extensive CA1 filed (Sommer sector), that borders the subiculum [88]. CA1 is also named the "vulnerable sector" because it is exquisitely sensitive area of the brain (with the globus pallidus) to anoxia.

The dentate gyrus includes an area of densely packed granule cells and an area of sparsely distributed cells (the hilus).

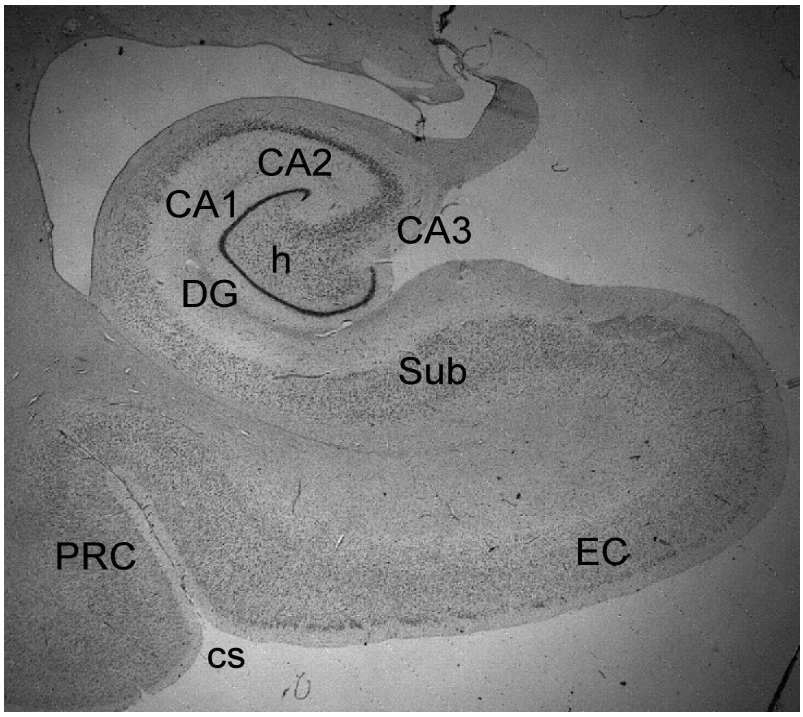


Figure 5. Photomicrograph (Nissl staining) of the hippocampal formation, the subiculum and the entorhinal and perirhinal cortices obtained from the human autopsy studies conducted for Study III of this thesis. Subject had 42 years old and the cause of death was other than a neurological insult. Abbreviations: CA, *cornu ammonis* (with subfields 1, 2 and 3); cs, collateral sulcus; DG, dentate gyrus; EC, entorhinal cortex; PRC, perirhinal cortex (only the medial part is shown); Sub, subiculum.

Within the medial temporal lobe, the hippocampus is critically located so to interact with the principal sources of cortical inputs. It receives major projections from the cingulated cortex, the amygdala, the piriform, per- and post-rhinal and entorhinal cortices [83, 89, 90] (**Figure 6**).

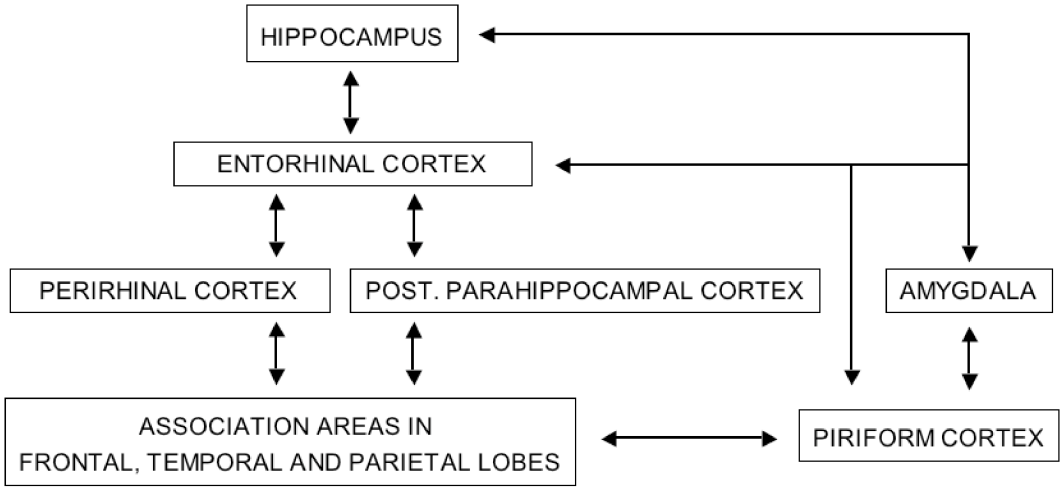


Figure 6. A schematic view of the cortical connections and the inter-connectivity of the medial temporal lobe structures. The entorhinal cortex is the major source of projections to the hippocampus and acts as a relay system for the inputs arriving from the amygdala, perirhinal, posterior parahippocampal and piriform cortices. The amygdala, the perirhinal and the posterior parahippocampal cortices receive projections from unimodal and polymodal areas in the frontal, temporal and parietal lobes. All the projections are reciprocal.

The term entorhinal cortex (EC) was coined by Brodmann [91] as a synonym for his area 28 and it covers the rostral parahippocampal gyrus [92]. The human entorhinal cortex is made up of six layers, of which layer IV does not appear throughout all subfields of the entorhinal cortex [92].

In the most classical hippocampal pathway (the "trisynaptic loop"), cells in layers II and III of the entorhinal cortex give rise to the perforant path that distributes to the hippocampal formation, in particular to the dentate gyrus [93]. From the dentate gyrus, granule cells project to the CA3 field. The CA3 pyramidal cells, in turn, send a major projection to the CA1 field (although some fibers from the CA3 field leave the hippocampus at this point, via the fornix). Much of the input from the CA1 field is sent to the subiculum. From the subiculum, information can be conveyed to the deep layers of the entorhinal cortex and to many other cortical and sub-cortical brain areas [88, 93] (**Figure 6**).

The entorhinal cortex receives prominent cortical innervation [88]. Accordingly to Insausti et al, two-thirds of this cortical input originates in the perirhinal and remaining parahippocampal

cortices [94, 95]. The perirhinal cortex (areas 35 and 36 by Brodmann [91]) is bounded medially by the entorhinal cortex and laterally by temporal association areas. It also extends anteriorly to include the medial portion of the temporal pole [96]. The posterior parahippocampal cortex is caudally adjacent to both the entorhinal cortex and the perirhinal cortex. Direct input to the entorhinal cortex originates in several cortical regions in the frontal and temporal lobes, and in the insular and cingulate cortices, as well as in the adjacent amygdala, perirhinal, parahippocampal and piriform cortices [94]. All these projections (except those between the piriform cortex and the association areas) are reciprocal (**Figure 7A and B**).

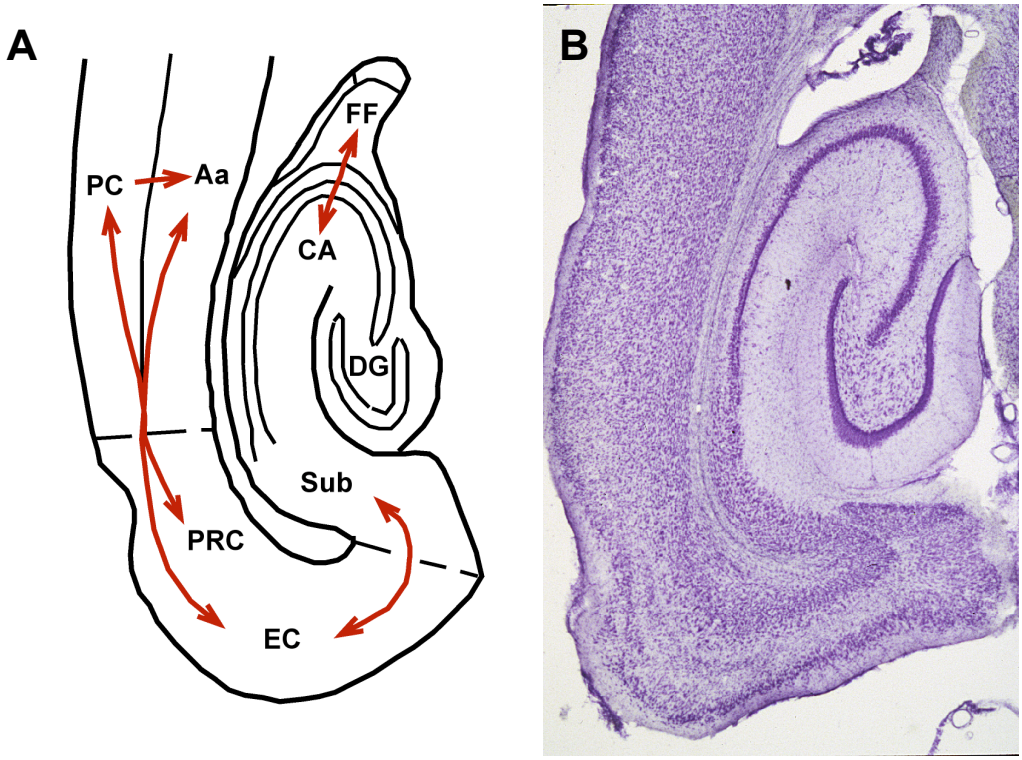


Figure 7. ***A*** – Schematic drawing of the inter-connectivity within the medial temporal lobe structures in the rat brain; all the projections are reciprocal, except for the piriform cortex. ***B*** – Photomicrograph (Nissl staining) at a similar level of panel ***A*** obtained from a control (non-epileptic) rat used in the studies conducted for Study I of this thesis. Abbreviations: Aa, associations areas; CA, *cornu ammonis*; DG, dentate gyrus; EC, entorhinal cortex; FF, fimbria-fornix; PC, piriform cortex (not visible in panel ***B***; the PC is located ventral and anteriorly as depicted in **Figure 8**); PRC, perirhinal cortex; Sub, subiculum.

The piriform cortex (PC) is an olfactory related, small region located rostromedial to the amygdala, overlying the fundus of the endorhinal sulcus (**Figure 8**). It receives primary olfactory projections from the olfactory bulb [97, 98]. The PC has received little attention in human studies [99] although it has a critical role in the generation of epileptogenic and ictiogenic networks in experimental TLE animals [100] (for review, see [101]).

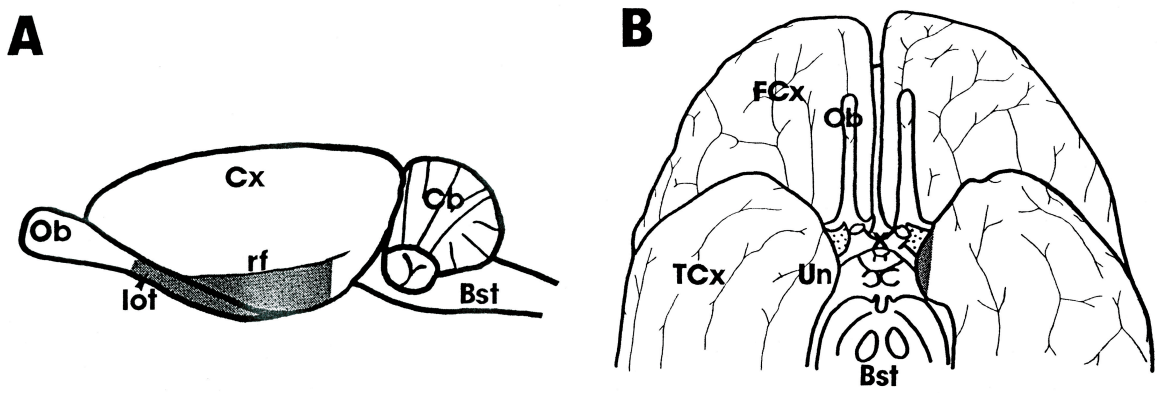


Figure 8. Anatomical location of the piriform cortex in rat and man. The piriform cortex is marked by the shaded area on both panels. ***A*** – Lateral schematic view of the rat brain. ***B*** – Ventral schematic view of the human brain. Abbreviations: Cb, cerebellum; Cx, cortex; FCx, frontal cortex; lot, lateral olfactory tract; Ob, olfactory bulb; rf, rhinal fissure; TCx, temporal cortex; Un, uncus; x, optic chiasm. Reprinted from [101] with permission.

The PC consists of three layers (**Figures 9 and 10**). Layer I is superficial and contains few GABAergic neurons with a dense network of dendritic and axonal fibers arising from the pyramidal cells of the deeper layers II and III [102]. Layer I was further divided according to its connectivity into an external region (Ia) containing afferent fibers from the olfactory bulb and an internal region (Ib) receiving afferent fibers from the neurons of the deep layers of the PC and the adjacent olfactory cortical nuclei, including those that are located in the cortical amygdala [103]. Layer II consists of a great number of glutamatergic semilunar and pyramidal neurons, which are densely packed [104]. Due to its unique characteristic "S" shape, it is easily recognizable on light microscopy (**Figures 9 and 10**). Layer III includes large size multipolar and pyramidal cells, presumably GABAergic [97], and projectional fibers.

The major source of afferent input to the PC are the mitral cells of the olfactory bulb, the axons of which reach the PC via the lateral olfactory tract along the lateral surface of the anterior PC [103]. In the PC, they establish excitatory synapses with the pyramidal cells in layer I. Additional afferents originate in the endopiriform nucleus, the basal forebrain, the thalamus, the hypothalamus and the brainstem, which can be both excitatory or inhibitory.

Output from the PC arises from pyramidal cells axons back to the olfactory bulb and endopiriform nucleus. There are an important number of fibers crossing to the contralateral PC by commissural projections [105]. Connections to areas outside the olfactory system originate mainly in the pyramidal neurons of layers II and III and include pathways to the insula, the cortical and the deep nuclei of the amygdala, the entorhinal cortex and the subiculum, the thalamus and to the hypothalamus and ventral putamen (see [97] and [101] for a review).

Therefore, the PC is connected reciprocally with many nuclei of the ipsilateral olfactory system and additionally has access to the insular areas of the neocortex, to the limbic system, to the hypothalamus, and to the motor systems in the diencephalon.

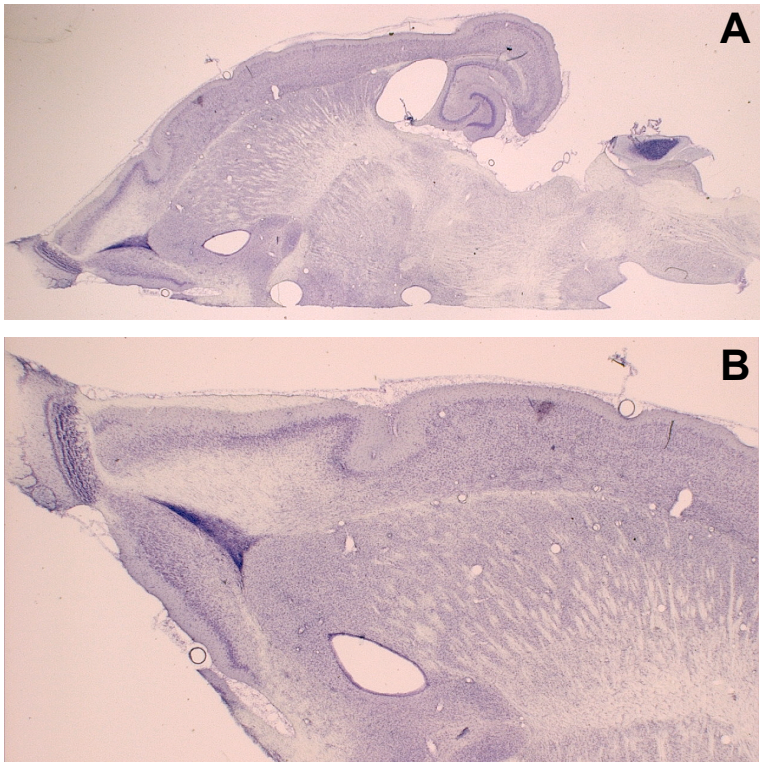


Figure 9. The piriform cortex in the rat. ***A*** – Axial slice of the entire brain. ***B*** – The piriform cortex in detail. Photomicrograph (Nissl staining) obtained from a control (non-epileptic) rat used in the studies conducted for Study I of this thesis. Abbreviations: EC, entorhinal cortex; HC, hippocampus; PC, piriform cortex (I, II, III indicate the cell layers); PRC, perirhinal cortex; lot, lateral olfactory tract; rf, rhinal fissure.

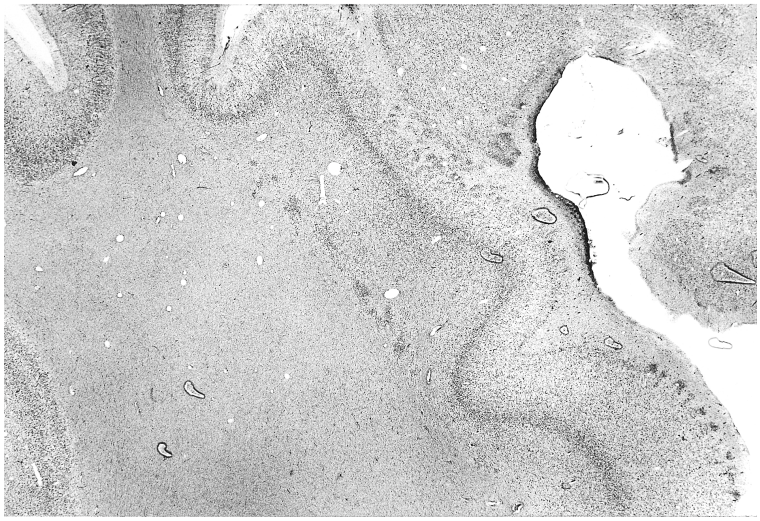


Figure 10. The human piriform cortex. Photomicrograph (Nissl staining) obtained from the human autopsy studies conducted for Study II of this thesis. Subject was 53 years old and the cause of death was other than a neurological insult.

There are extensive reciprocal connections with the hippocampus, the entorhinal cortex and the amygdala [106]. The amygdaloid complex (AMY) is composed of more than ten nuclei and their subdivisions, which have different cytoarchitectonic, chemoarchitectonic, and connectional characteristics [107, 108] (**Figure 11**). The lateral nucleus of the amygdala gives rise to a prominent projection to layer III of the entorhinal cortex [89]. There are also additional

projections from the amygdaloid complex to the hippocampus and to the subiculum [88]. Conversely, the subiculum and the entorhinal cortex originate return projections to the amygdala [89] [107]. In general, the amygdaloid complex projects to a greater number of cortical regions than those from which it receives projections [106, 109]. Essentially, all major divisions of the temporal cortex receive a projection from the amygdala. The piriform cortex, particularly, has prominent interconnections with the cortical amygdala and its deep nuclei [101, 110-112]. Moreover, there is evidence of reciprocal connectivity with the amygdala and portions of the frontal and insular cortices [112]. The general conclusion about the functional connectivity is that the amygdaloid complex is directly and reciprocally linked to a wide variety of cortical regions and can influence and be influenced by sensory information processed to various degrees. In contrast, cortical information is funneled into and out of the hippocampal formation through polysensory border regions and appears to be highly processed before reaching the hippocampus [83, 106, 113].

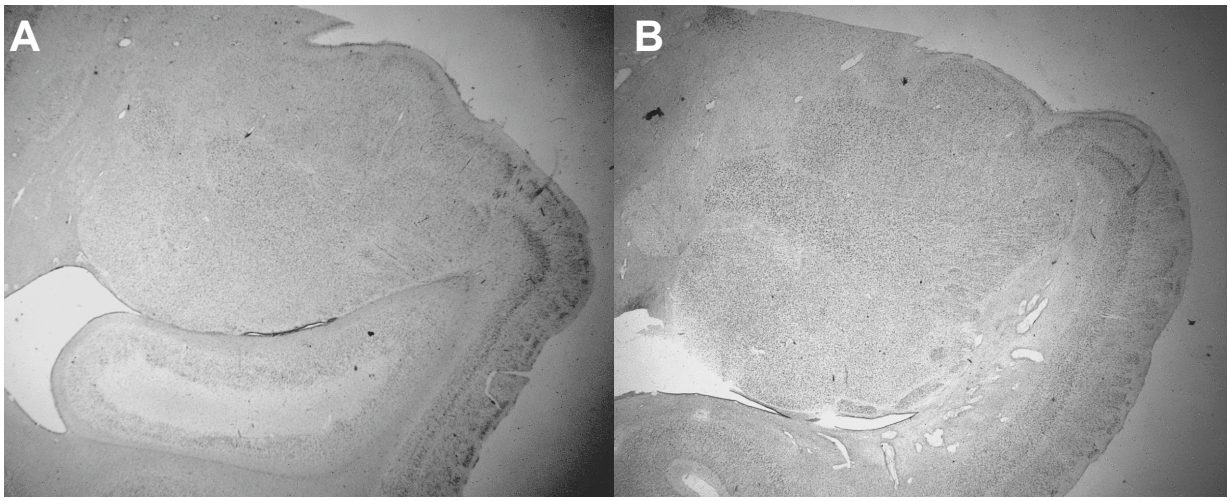


Figure 11. The human amygdala at the level of the subiculum (***A***) and 4mm rostral (***B***). Photomicrographs (Nissl staining) obtained from the human autopsy studies conducted for Study III of this thesis. Subjects were 53 (***A***) and 44 years old (***B***), respectively.

According to the known anatomical connectivity, several hypotheses have been developed concerning the functional anatomy of limbic epilepsy.

The first proposal was hypothesized by Lothman et al [114] and further supported by Pare et al [115]. They suggested that seizures arise in a "trisynaptic loop" that involves the entorhinal cortex, the dentate gyrus and the *cornu ammonis*. As such, seizures would arise at any point in the loop, with further activity reverberating through this loop until it would propagate to other regions of the brain.

A second hypothesis, however, regard the multiple limbic sites as independent seizure generators [116]. Accordingly, every limbic structure located in the mesial temporal lobe can initiate a seizure with further recruitment of the neighboring areas and consecutive spread over the brain.

3. THE CONCEPT OF TEMPORAL LOBE EPILEPSY (TLE)

3.1. Definition and Epidemiology

Mesial Temporal Lobe Epilepsy is a localization related epilepsy with typical clinical and EEG characteristics [33, 118]. Complex partial seizures originating from the temporal lobe are the single most common type of seizure encountered in the adult population [4, 119]. Patients with temporal lobe complex partial seizures constitute the majority of patients referred for surgical consideration [5, 120, 121].

Temporal lobe epilepsy with seizure onset from the mesial temporal lobe structures and with distinctive hippocampal pathology is actually recognized as an individualized syndrome [47, 48, 118]. If seizures begin outside mesial temporal lobe structures in the temporal neocortex, epilepsy is referred to as lateral or neocortical TLE [122]. Seizures may also begin outside the temporal lobe. In large surgical series, seizures originating from the frontal lobe were the second most commonly reported localization related epileptic disorder [5, 123, 124]. When the location of seizure focus is outside the temporal lobe, epilepsy is termed extratemporal partial epilepsy. If the seizure focus is unknown, partial epilepsy remains unclassified.

Temporal lobe epilepsy is one of the most common and frequent medically intractable seizure disorders [125]. Probably, it is *the* most common. However, the true frequency of TLE in the general population is unknown. Population studies show that partial seizures account for up to 50% and 60% of incident and prevalent epilepsy cases, respectively, and that complex partial seizures are the most frequent single seizure class [25]. A worldwide census of 107 epilepsy surgery centers confirmed that TLE is by far the commonest type of localization-related epilepsy. Of 8.234 operations performed between 1985 and 1990, 66% involved the temporal lobe [126]. Of course, these series derive from specialized units. Thus, they are biased toward patients who are surgical candidates, have more severe epilepsy and are more intensely investigated.

3.2. Semiology and Electroencephalographic (EEG) Findings

In general, temporal lobe seizures can be manifested as simple partial seizures, complex partial seizures and secondarily generalized seizures, or a combination of these [117]. Most temporal lobe seizures begin with a simple partial seizure such as abdominal visceral or olfactory

sensations and experiential (e.g., fear or déjà vu) phenomena [47, 127, 128]. Following the initial symptoms, prominent ictal features include an arrest of activity, oral-alimentary automatisms, and motor phenomena; commonly there is amnesia for the seizure [129]. Secondary generalization may occur.

Representative EEG patterns observed in mesial TLE are illustrated in **Figure 12**.

The anterior temporal lobe "spike and wave" discharge is the classical EEG finding in the interseizure interval [130]. The interictal scalp EEG may show unilateral or bilateral, synchronous or asynchronous temporal spikes, sharp waves, and/or slow waves [130], although it may be normal in the majority of partial epilepsy patients at the time of the epilepsy diagnosis. Conversely, the large majority (94%) of intractable TLE patients have paroxysmal abnormalities localized in the anterior temporal region in the preoperative scalp EEG [48, 131]. Bilateral independent paroxysmal activities occur in about 25-40% of the cases but are generally preponderant over the side of seizure origin [48, 131, 132].

Synchronized EEG-video monitoring contributes to a correct identification of the seizure focus lateralization, particularly when acquired during an ictal event. Such method is indispensable for the establishment of the temporal relationships between clinical and electrical phenomena and provides insights into the interpretation of abnormal clinical findings in relation to electrographic activity. If a series of scalp EEGs do not reveal the onset and evolution of the seizure discharges in partial epilepsy patients, intracranial recordings may provide additional information [133, 134].

3.3. Etiology and Pathogenesis

Temporal lobe epilepsy may develop after a variety of insults such as head trauma, birth injury or CNS infection [15, 47]. When seizures result from a specific cerebral pathologic substrate in the temporal lobe, such as a traumatic scar, TLE is classified as remote symptomatic. A common factor predisposing some patients to TLE is the occurrence of complex febrile convulsions. Falconer et al. suggested already in 1964 that prolonged febrile seizure can lead to the development of TLE [11].



Figure 12. An electroencephalographic recording during a complex partial seizure with left fronto-temporal origin in a patient with left hippocampal sclerosis. This patient was included in studies conducted for Study IV of this thesis. The vertical bar (with the word 'crise') signals the beginning of ictal semiology. There is a massive sharp wave activity over the left fronto-temporal regions, maximal in the anterior temporal lead.

Several studies since then have recognized the association between complex febrile convulsions and TLE [47, 135], although its precise role in the development of TLE remains unclear [136].

Idiopathic (or cryptogenic) TLE refers to an epileptic disorder where no etiology of the condition can be determined. A finding frequently encountered in patients with intractable TLE, both idiopathic and symptomatic, is a distinctive pathological change in the hippocampus, i.e. hippocampal sclerosis. However, it is not known whether the damage found in the hippocampus is the cause or the consequence of TLE.

Another concept related with the pathophysiology of TLE states is that the damage is broadly distributed throughout the limbic system. It involves, at least, the hippocampus, the amygdala, the entorhinal cortex, the piriform cortex and the thalamus [6, 7]. Moreover, within each structure, the pathology is not uniform. Cell loss within an affected hippocampus varies among

patients [7] and some cases of TLE have been reported to have a more severe degree of pathology within the amygdala [9, 137]. Such findings suggest, at least, that the TLE syndrome is a general disorder of the limbic system, implicating not just a single structure (such as the hippocampus) but rather extending to extra-hippocampal and even to extra-temporal regions. Additionally, when considering individual patients, there is the possibility that one structure may be more affected and more likely to drive seizures than another.

In most TLE patients, seizures begin in the mesial temporal structures [5], specifically in the hippocampal area [133]. Regional onsets including hippocampus, amygdala, and temporal cortices may account for more than 50% of temporal lobe seizures [138]. The piriform cortex, in particular, is a critical generator of seizure activity within the temporal lobe as spontaneous interictal discharges first appear in the PC in the kindled brain [139] before they spread to other brain areas [140, 141]. Specially the "area tempestas" [142, 143], which is a small region located in the deep piriform cortex, is proposed to have a pivotal role in seizure spread in rodents [144, 145] and in non-human primates [146]. On the other hand, the entorhinal cortex may serve as a gate of seizure propagation and generalization [147-149].

Observations from animal models have shown that most of the sites indicated above are involved in the initial phases of seizure generation [100] and may show a particular pattern of cell damage [150, 151]. Experiments carried out during human depth electrode studies confirm that seizure onset may involve multiple limbic sites [133].

The outcome of epilepsy surgery can also yield useful insights with respect to the pathophysiology of TLE and the functional anatomy of limbic epilepsy. There is a relation between surgical successes and the extension of the mesial temporal tissue that is resected [5, 152] that is, success is linked to the resection of multiple limbic sites including the entorhinal cortex, the amygdala and the hippocampus proper. The current surgical strategy for mesial temporal epilepsy in cases with identified hippocampal sclerosis (on MRI) [153, 151, 118] generally spares the piriform cortex, a region from which it is very easy to initiate seizures in animal models [142, 155]. Thus it is possible that failures of epilepsy surgery to control seizures, at least in some cases, may be attributed to the fact that the epileptogenic network extended beyond the removed brain structures, typically the hippocampus and the amygdala. For example, the epileptogenic network may include the piriform cortex and, if the latter is not surgically removed, seizures would continue uncontrolled.

4. HISTOPATHOLOGY OF TLE

4.1. The Hippocampus

Unilateral atrophy of Ammon´s horn was reported in 1867 by Meynert and in 1880 by Sommer in autopsies of epileptic patients [156]. Since then, a myriad of neuropathological studies have shown that hippocampal damage is by far the most common structural lesion in intractable TLE patients: it is observed in 50 to 85% of surgical and autopsy specimens [6, 7, 10, 11, 157, 158]. Involvement is typically asymmetric, with one side more severely affected. The side of greatest involvement is believed to be the site of seizure origin.

The primary morphological change in the hippocampus consists of neuronal loss. Following neuronal degeneration, glial proliferation and hypertrophy occur, and, as astrocytes and their processes occupy the areas of neuronal loss, the hippocampus generally shrinks in size and appears “sclerotic”.

The classic histological pattern of hippocampal sclerosis in TLE patients is characterized by loss of pyramidal cells in the prosubiculum and CAI field of the hippocampus [158]. The findings also include neuronal loss in the hilus of the dentate gyrus and the adjacent CA3 field of the hippocampus [159, 160]. Another pathologic marker of hippocampal damage in TLE is the reorganization of axons of some groups of cells. Most often, mossy fibers from the dentate granule cells which normally innervate the hilar mossy cells and CA3 pyramidal cells become reorganized and project into the inner third of the molecular layer of the dentate gyrus [42, 161].

The available pathologic data suggest that the hippocampal damage is asymmetrically bilateral in a group of patients with chronic TLE (up to 30%, accordingly to the classical study of Margerison and Corsellis [7]). Bilateral symmetric damage in the hippocampus is less frequent, occurring in ≤ 10% of TLE cases [7, 156, 162].

Hippocampal sclerosis may coexist with an extrahippocampal lesion, for example with a tumor, i.e. there may be dual pathology [156, 163]. Interestingly, Levesque et al. [163] reported that the distribution and severity of hippocampal neuronal damage was could differ according to the pathological type of an extrahippocampal lesion. While the hamartoma and glioma groups had the least cell loss in the hippocampus, the heterotopia group had the most severe damage.

4.2. The Amygdala

Neuronal loss and gliosis extend frequently beyond the confines of the hippocampus to the amygdala and the adjacent cortex in intractable TLE patients [6, 7, 11] (see also [164]). Histopathological studies have reported a concomitant pattern of tissue damage, that is, selective neuronal loss and gliosis extending to the amygdala (10-60% of the cases with a damaged

hippocampus [7, 9, 10]) and the para-hippocampal gyrus (21-68% of the cases [9, 10]). In 9% of postmortem TLE cases, there was a bilateral involvement of both amygdalae [7]. It has also been reported that isolated amygdala damage can be present in up to 10% of the patients referred for surgical treatment [165-167]. Such widespread involvement of more than one mesial temporal lobe structure is usually denoted by the term "mesial temporal sclerosis" (MTS).

Neuronal loss in the amygdala most commonly occurs associated with lesions in the hippocampus [6, 7]. In the study of Margerison and Corsellis [7], there were 27% of cases with amygdala sclerosis, all of which showing concomitant hippocampal damage. In a series of surgically treated TLE patients with hippocampal sclerosis, 76% also had damage in the amygdala and 27% in the adjacent medial temporal cortex [6]. Recently, Zentner et al. [138] reported that up to 85% of patients with surgically treated intractable TLE had a severely altered amygdaloid body.

4.3. The Entorhinal Cortex

In early neuropathological reports, the parahippocampal gyrus, which contains the entorhinal cortex, is often mentioned as one of the affected areas in TLE [10, 11]. Two recent histological studies indicate that specifically the entorhinal cortical layers II and III have remarkable neuronal loss in patients operated on for drug-refractory seizures [8, 168]. Furthermore, as a marker of synaptic reorganization, the polysialylated neural cell adhesion molecule was increased in layer II of the entorhinal cortex [168].

4.4. The Piriform Cortex

To date, there has been no attempt to characterize the histopathology of the piriform cortex in the human TLE condition. Margerison and Corsellis demonstrated in their classic monograph [7] that the cell loss extended outside the boundaries of the hippocampus to include the piriform cortex in a certain number of autopsy specimens that were analyzed.

In addition, data concerning its involvement in TLE obtained by animal studies [100, 140, 151, 169-175] (see also [101] for a review) are consistent and implicate the piriform cortex has a critical generator of seizure activity within the temporal lobe before they spread to other brain areas [139, 142, 143, 145, 146] [140, 141, 144].

To our knowledge, there is only one neuropathological report by Fujikawa et al [99] which analyses the regional distribution of neuronal damage caused by *status epilepticus* in the brains of three deceased patients. According to Fujikawa et al, following an onset of focal motor *status epilepticus*, these patients suffered widespread neuronal loss/reactive gliosis in the hippocampus, amygdala, entorhinal and periamygdaloid (piriform) cortices, dorsomedial thalamic nucleus, and cerebellum.

There is no data specifying the pattern of the piriform cortex damage in chronic TLE.

4.5. The Extratemporal Limbic System

Except for the thalamus and cerebellum [7], additional tissue damage outside the temporal lobe has not been identified hystopathologically. Current data rely on neuroimaging studies.

In vivo positron emission tomography [176-178] and MRI [179] suggest a multifocal pattern of extra-hippocampal pathology concordant with seizure onset [148]. Therefore, less is known about tissue damage in regions other than the medial temporal lobe [180-183], including those involving limbic structures [184].

5. CAUSES OF MEDIAL TEMPORAL LOBE DAMAGE

5.1. Initial Insult *vs* Recurrent Seizures

5.1.1. Epilepsy Patients Studies

The etiology and pathogenesis of structural damage in the mesial temporal lobe of epilepsy patients has been the subject of controversy and debate for years in epilepsy research.

Clinically, TLE often starts as an isolated, prolonged convulsion in early life followed by a period of remission, after which seizures reemerge and may become intractable [5]. Patients with complex febrile seizures (longer than 15 minutes, multiple or focal) are more likely to develop recurrent nonfebrile seizures than those with uncomplicated febrile seizures [185]. Marks et al. (1992) showed that mesial temporal sclerosis was significantly associated with CNS infection before but not after the age of 4 years. Moreover, Cavanagh and Meyer [10] indicated that typical hippocampal sclerosis was found in adult lobectomies more frequently when the habitual seizures started at 5 years of age or earlier.

Other studies, however, have provided evidence that the pathogenesis of sclerosis is not age-dependent and that it is not essential for a TLE patient to have experienced a childhood seizure [70, 186]. For example, Mathern et al. [70] found that patients with an initial precipitating injury such as prolonged seizures, status epilepticus, head trauma or encephalitis before the onset of chronic TLE had severe neuron loss in the hippocampus However, the age at which the initial injury occurred did not influence the amount of hippocampal damage seen at the time of surgery.

Mouritzen Dam [187] was the first to relate neuronal loss and seizure number in epilepsy patients. She found in an autopsy study that generalized seizures occurring more frequently than twice per month and epilepsy with over 30 years of duration was related to more prominent loss of pyramidal neurons in the hippocampus. More recently, Mathern et al. [12, 186] reported in a

cross-sectional study that surgically treated TLE patients with longer duration of disease showed a progressive decrease in the number of hippocampal CA1 neurons. The progression was slow, but after approximately 30 years, all patients showed at least 60% neuronal loss.

As further evidence of ongoing seizure activity resulting in neuronal injury, Beach et al. [188] reported that specimens of temporal lobectomy showed signs of reactive microglia in intractable TLE patients. Since microglial activation is an acute or subacute response to injury, the finding contradicts the hypothesis that hippocampal sclerosis consists of an inactive scar.

Quantitative imaging studies also support the notion that hippocampal sclerosis probably starts with an initial precipitating insult before the onset of chronic epilepsy. Several MRI studies have shown a significant relationship between hippocampal and amygdaloid damage and a history of febrile convulsions in early childhood [189-192]. In a series of drug-resistant epilepsy patients with a history of febrile seizures, hippocampal atrophy was diffuse and located ipsilateral to seizure focus [190, 193, 194]. As diffuse hippocampal volume loss is more strongly associated with febrile convulsions than focal volume loss, some authors have hypothesized that pre-existing hippocampal focal abnormality may facilitate febrile convulsions and contribute to the development of subsequent widespread sclerotic changes in the hippocampus [190, 195]. VanLandingham et al. [196] demonstrated for the first time the development of structural damage in the hippocampus after complex febrile convulsions in a prospective follow-up MRI study. They showed that prolonged, focal febrile convulsions in four infants resulted in acute hippocampal injury and swelling, and this evolved into hippocampal atrophy in two of them.

It is likely that many other etiological factors in addition to febrile convulsions play a part in the development of hippocampal sclerosis. Bigler et al. [197] showed with quantitative MRI that head trauma can produce hippocampal atrophy. Furthermore, 75% of TLE patients with a history of meningitis or encephalitis had bilateral hippocampal volume reductions [198]. Progressive hippocampal damage has also been reported after *status epilepticus* associated with encephalitis both with and without persistent seizures, even when acute increases in T2 signal resolve [76-78, 199]. In the report by Wiehsmann et al. [77], the progression of hippocampal atrophy continued up to 58 months after onset of *status epilepticus* due to herpes encephalitis.

As in previous correlative histopathological studies, quantitative imaging studies investigating the effect of age at seizure onset on hippocampal damage show contradictory results. Trenerry et al. [191] observed that the younger the left temporal lobectomy patients were when spontaneous seizures began, the smaller were the left hippocampal volumes. Hippocampal damage was also related to early onset of habitual epilepsy in a large study of 100 intractable TLE patients [193].

However, in another MRI study of patients with uncontrolled TLE the effect of age at seizure onset was not a significant factor in predicting the severity of hippocampal atrophy [194].

Several imaging studies have failed to find a correlation between MRI-determined hippocampal atrophy and either the estimated severity or the duration of the seizure disorder [189-191, 200-202]. In a retrospective MRI report of 50 patients with intractable TLE, neither hippocampal nor amygdaloid volumes correlated with duration of epilepsy, seizure frequency, or the occurrence of generalized seizures [189]. The study concluded that habitual seizures do not lead to progressive hippocampal damage.

In contrast to other imaging studies, Spencer et al. [203] reported that hippocampal atrophy in quantitative MRI was significantly correlated with longer duration of epilepsy. More recent imaging studies have produced evidence that epilepsy duration has a significant effect on the severity of hippocampal damage in intractable TLE patients [49, 194, 204]. As long duration of drug-resistant TLE is related to a considerable number of focal or secondarily generalized seizures, both hippocampal and hemispheric volume reductions were associated with high seizure frequency in MRI series of TLE patients [202, 205]. VanPaesschen [206, 207] reported that the extent of hippocampal damage correlated with the number of secondarily generalized seizures in both newly diagnosed and chronic TLE patients.

In addition to correlational approaches, one can compare patient groups with different duration and severity of epilepsy, or follow cohorts of patients longitudinally to examine the progression of disease. Quantitative MRI studies have shown that while hippocampal damage is found in 73% of intractable TLE patients [193], only 10% of newly diagnosed patients with partial seizures have volume reduction and T2 time prolongation in the hippocampus [208]. Kälviäinen et al [209] and Salmenperä et al [210] compared hippocampal volumes and T2 relaxation times in newly diagnosed and chronic patients with TLE, and found that those patients with a long history of recurrent seizures had more severe hippocampal damage, and concluded that recurrent seizures may cause damage to the hippocampus throughout the lifetime of the patient.

The cumulative data from neuropathological and imaging studies suggest that TLE begins with an early hippocampal injury occurring asymmetrically, and is followed by a gradual and progressive course of further neuronal damage [211]. The imaging data so far indicate that in some patients the hippocampus is damaged acutely, with enlargement and increased T2 signal, reflecting edema in the acute stages and progression toward MRI features of hippocampal sclerosis such as atrophy with an increased hippocampal T2 signal in the ensuing months, and with onset of TLE months or years later [76, 196, 199]. After the diagnosis of epilepsy, the

epileptic process continues, leading to intractable seizures, functional disability and progressive structural damage. Accordingly, O´Brien et al [212] provided the first prospective MRI evidence that progressive atrophy of the hippocampus may develop in the absence of initial insult such as status epilepticus, due to uncontrolled temporal lobe seizures.

Magnetic resonance proton spectroscopic imaging (^{1}H-MRSI or CSI) is a more sensitive indicator of neuronal dysfunction in vivo than MRI volumetry, since one can detect acute chemical changes with this method [213-215].

Several ^{1}H-MRSI studies of TLE patients have observed reduced signals from the cerebral metabolite N-acepyl-aspartate (NAA) in temporal lobes, reflecting focal neuronal dysfunction and/or cell loss [215, 216]. In patients with partial epilepsy, the decreasing NAA correlated with high seizure frequency, but not with the duration of epilepsy [217]. Tasch et al. [204] found an inverse relationship also between the duration of epilepsy and the ratio of NAA and Creatine/Phosphocreatine (Cr) in the temporal lobes of TLE patients ipsilateral and contralateral to the EEG focus, a finding replicated more recently by Bernasconi et al [218]. Moreover, echoing the previous autopsy results of Mouritzen Dam [187], which showed increased hippocampal cell loss in patients with generalized tonic-clonic seizures, bilateral lower NAA/Cr ratios were associated with generalized seizures [204, 218].

However, the clinical utility of ^{1}H-MRSI and its significance is a matter of debate. Ende at al [219] found that the hippocampal NAA/(Cho+Cre) ratio was concordant with EEG and MRI, but far more sensitive in detecting bilateral changes than MRI. Subsequently, Knowlton et al [220] compared 2-[18F]fluoro-2-deoxy-D-glucose positron emission tomography (FDG-PET) lateralization with hippocampal volumetry, T2-relaxometry, and ^{1}H-MRSI in 13 patients with typical electroclinical characteristics of mesial TLE with hippocampal sclerosis. Their main findings was that ^{1}H-MRSI was better in detecting bilateral disease in combination with hippocampal volumetry and that NAA/(Cho+Cre) was similar to PET for seizure localization. Additionally, they correlated the several imaging modalities with the postoperative outcome and found that only the presence of unilateral hippocampal atrophy is predictive of seizure-free outcome, while bilateral abnormal ^{1}H-MRSI measures do not preclude good surgical outcome (that is, it seems that ^{1}H-MRSI does not reflect any objective structural impairment of hippocampal sclerosis).

In order to determine whether the contralateral reduction of NAA in TLE was a consequence of repeated seizures, Vermathen et al [221] performed hippocampal NAA studies on patients with neocortical epilepsy who had frequent seizures. No reduction in hippocampal NAA were found suggesting that reduction of hippocampal NAA in TLE is a consequence of the disease

process and not a response to repeated seizures. Vermathen et al [222] have also found that following seizure surgery for TLE, there is an increase of contralateral NAA/(Cho+Cre), but the mechanism of this change is speculative.

More recently, Kuzniecky et al [223], reported a detailed prospective study relating a multimodal set of data (hippocampal volumes and ^{1}H-MRSI on one hand, and quantitative neuronal-glial ratio from resected specimens) of 33 patients with intractable mesial TLE who underwent surgery. Significant interdependence was only obtained between the neuronal-glial ratio and hippocampal volumes, implying that metabolic dysfunction measured by ^{1}H-MRSI and structural MRI don't have the same neuropathologic basis.

In conclusion, although ^{1}H-MRSI adds considerable new diagnostic information in the assessment of epilepsy, its additional diagnostic value is unclear.

There is a similar incongruence of data regarding amygdaloid damage as with respect to hippocampal damage, since the severity of amygdaloid damage in some studies does not differ between TLE patients with different durations of epilepsy or seizure frequency [224], while in others there is an inverse correlation between the number of epileptic seizures and the amygdaloid volume [225] or T2 relaxation times [226] on the focal side.

Therefore, due to the cross-sectional design of these studies, most authors do not exclude the possibility that there is an association between the duration of epilepsy and the severity of hippocampal damage, as well as the propensity to develop refractory epilepsy.

Longitudinal prospective quantitative MRI studies have also been conducted to address this issue. Liu et al [227] reported that 16% (4/24) of the patients with chronic active TLE had significant loss in hippocampal volume after 3.5 years. Fuerst et al [228] analyzed the hippocampal volume of 12 patients with refractory TLE at baseline and after a 3.4 years interval; in 9 patients with ongoing seizures, progressive ipsilateral atrophy was found, but not in the 3 patients who remained seizure-free. Although these findings should be considered preliminary, due the small number of cases used and to the fact that histopathologic studies demonstrate that it takes approximately 30 years for neuronal loss to decrease by about 60% [12], they imply that hippocampal changes may be progressive in those patients with uncontrolled focal epilepsy.

With the present set of data relying only on cross-sectional and preliminary longitudinal studies, it's challenging to determine which is the relative contribution of each illness-related factor and whether hippocampal sclerosis is the cause or the consequence of seizure activity. Variables such as the period of seizure onset and duration of TLE are not statistically independent from each other. The contribution of these factors to the underlying neuropathology likely depends on the patient's age, as well as on the age of onset and on the total duration of

TLE. Additionally, other factors may play a role, such as frequency of seizures, medication and genetic background. At present, the role of these factors on the dynamical aspects of pathogenesis of TLE can only be controlled appropriately in animal models of chronic TLE. In naturally occurring human epileptic conditions, all illness-associated variables tend to be strongly related and are difficult to disentangle.

5.1.2. Experimental Studies

Animal models provide a wealth of information regarding the functional anatomy, biochemistry, and neuropathology of epilepsy. They are particularly useful to study the development of epileptogenesis and to characterize the regional pattern of cell damage in the limbic system. They allow to determine the nature of injuries that might contribute to the subsequent development of epilepsy, to observe and intervene in the disease process subsequent to an injury but prior to the onset of spontaneous seizures, and also to study the chronically epileptic brain in exquisite detail, using state of the art physiological, pharmacological, molecular, and anatomical techniques. In this respect, experimental models can be used to address the critical questions of the pathogenesis of TLE without the limitations of human studies. The relevance of such comparisons is enhanced by the observation that the physiological properties of human and animal celss of the limbic cortical areas are basically similar [229, 230]. On the other hand, experimental data provide additional clues on the histopathology of TLE by localizing regions displaying tissue damage that are rarely studied in the human brain since they are not removed by the surgical procedure used to treat patients who are refractory to pharmacotherapy.

Neuropathological abnormalities typically precede the appearance of recurrent seizures in several animal models of human partial epilepsies. *Status epilepticus* induced by systemic injection of pilocarpine causes selective structural brain damage in rats. Cell loss is observed in the hilus and CA3 region of the hippocampus with prominent mossy fiber sprouting, as well as neuron loss in the amygdala, entorhinal cortex, thalamus and cerebral cortex [39]. A similar widespread pattern of neuronal changes in the hippocampus and amygdala as in the pilocarpine model is observed after *status epilepticus* induced by kainate and corticotrophin releasing hormone [231, 232]. In these experimental designs, recurrent spontaneous seizures occur after a latent period, which is reminiscent of the evolution in time of human TLE [233, 234]. Recently, Koh et al. [235] reported that kainate seizure activity induced during the second week of life in rats predisposes to more extensive neuronal injury in the hippocampus than after kainate-induced seizures in adulthood. Such data suggest that seizures occurring at an early time point in life contribute to the later development of epilepsy and selective hippocampal neuronal loss [235].

5.1.2.1 Experimental Animal Model of Kindling

Kindling is an animal model of TLE where increasingly stronger seizures are induced by stimulating the undamaged brain [236, 237]. Its main disadvantage is that for seizures to occur an electrical stimulus must be applied recurrently. In addition, the electrical threshold to produce seizure-like activity increases with time. This model has been used to study the short-term effects of seizure-like activity so, ultimately, it is difficult to disentangle whether the cellular and tissue damage are a consequence of the stimulus or a result of epileptogenesis. General conclusions driven from kindling experiments, associate progressive hippocampal damage with repeated seizures [14, 238]. However, in the kindling model spontaneous seizures are rarely recorded and kindling-induced damage is controversial since cell loss due to repeated seizures is not always confirmed when cell densities calculations are used to analyze the various limbic regions [239, 240].

In this model, neuronal loss has been described in the hilus of the dentate gyrus and CA1 after three generalized tonic-clonic seizures, and with increasing number of seizures the tissue damage may eventually evolve into a pattern that resembles hippocampal sclerosis [13, 14]. Repeated seizures induce progressive cellular alterations not only in the hippocampus, but also in the amygdala, and the entorhinal cortex [14, 237, 241, 242]. Several studies have demonstrated that the neuronal loss is accompanied by aberrant mossy fiber axonal growth of dentate granule cells in the hippocampus [16, 243].

5.1.2.2 Experimental Animal Model of Self-sustaining Status Epilepticus

The self-sustained limbic *status epilepticus* (SSLSE) is an electrogenic model of TLE that uses a single continuous pulse of focal electrical stimulation to induce a period of *status epilepticus* [244, 245]. Additionally, the improvements introduced by Lothman and co-workers [81], allows for both stimulation within the hippocampus and monitoring of the electrographic activity throughout the period of stimulation and beyond. A closed circuit television system can also be incorporated [246] which permits to perform a combined observation of the EEG and the animal's behavior, as in the human video-EEG studies. Furthermore, the behavioral seizures noted in the animals show great similarities with the human TLE condition [81, 246, 247].

In this model, chronic spontaneous seizure ultimately develop after a latent period without further need of chemical or electrical exogenous stimulus. This chronic period can last for several months and even persist for more than a year [246].

In our studies we used an electrogenic model [40] (**Figure 13**), which is similar to previously described ones [81, 242, 246]. Its main difference resides in the stimulation site. Instead of using the hippocampus [81, 246] or the amygdala [242], we implanted the stimulation electrodes in the

left angular bundle of the rat [40, 151]. In order to record hippocampal EEG, a pair of insulated stainless steel electrodes was implanted into the left dentate gyrus of the hippocampus under electrophysiological control.



Figure 13. The set-up used in the experimental model of self-sustaining status epilepticus includes the possibility to record the EEG continuously.

This model displays the characteristic neuropathological aspects of the TLE syndrome, showing hippocampal sclerosis (selective neuronal loss and gliosis), synaptic reorganization (mossy fiber sprouting), and the recurrence of seizures. Also, its time-frame is similar: after the *status epilepticus* is achieved, a latent period follows (where no abnormal behavior is detected although interictal EEG epileptiform activity can be recorded) and, after 1-2 weeks recurrent spontaneous seizures develop (**Figure 14**).

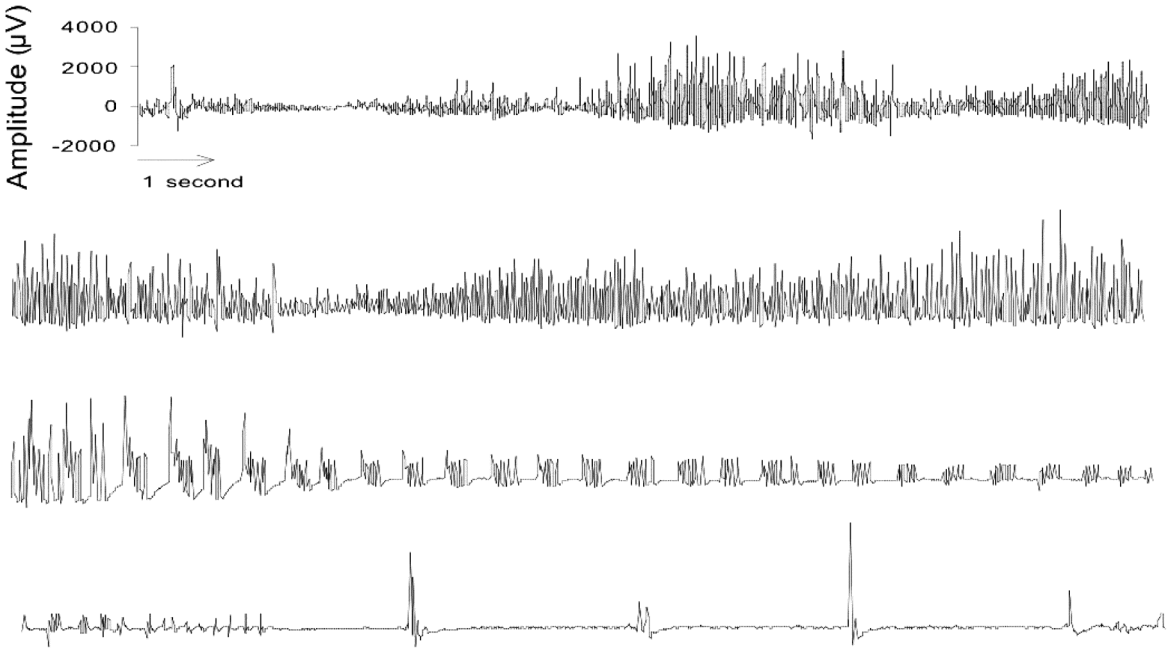


Figure 14. A spontaneous seizure recorded from a successfully stimulated rat in the model of self-sustaining status epilepticus. The massive sharp wave activity is similar to the ictal recordings of human patients (see Figure 12 for comparison).

6. CONSEQUENCES OF MESIAL TEMPORAL LOBE DAMAGE

The neuropsychological observations of patient H.M. [248] demonstrated the importance of the medial temporal lobe in memory, more specifically in what has been termed episodic or declarative memory.

After H.M. experience, a number of studies carried out in patients suffering either unilateral or bilateral damage of limbic structures have enlarged our knowledge of the functions associated with this system.

Kroll et al [249] studied two patients with combined temporopolar and prefrontal damage in the dominant left-hemisphere. They found out that combined temporofrontal damage results in marked retrograde memory deficits while leaving intelligence and new learning relatively unimpaired.

Stone et al [250], reported a patient (R.M.) with extensive bilateral limbic system damage due to trauma, affecting the orbitofrontal cortex, the temporal pole, and the amygdala. In the following months, R.M. suffered severe retrograde amnesia. After two years, R.M. developed a specific impairment of social contract reasoning, making it impossible to detect cheaters and forms of social misconduct.

Behaviorally, a general result of lesions of cortical limbic areas is the impairment of memory functions [83], a characteristic finding of the TLE syndrome with hippocampal sclerosis [118].

The hippocampus and the parahippocampal cortices, form the neural system for declarative memory (memory for facts and events) [251]. The amygdala is not critically involved in memory functions [252], rather its major role is in emotional behavior [253]. The piriform cortex is a highly specialized cortical area for olfactory perception and discrimination [101] albeit it may be also involved in the processing of memory functions [254].

A bilateral lesion limited to field CA1 of the hippocampus leads to permanent loss of ability to consolidate short-term to long-term memory in adults [255]. Although most sensory input to the hippocampus formation enters via the entorhinal cortex [94], complete bilateral lesion of the entorhinal cortex produced only mild and transient memory deficits in monkeys [251]. In humans, damage involving the parahippocampal gyrus produces a syndrome of topographic disorientation [256].

The amygdala is linked by numerous cortical and subcortical routes to brain regions involved in behaviors ranging from sexual behavior, aggression and defense to the highest level of cognitive function [106]. Studies in animal models show that the amygdala is crucial for the normal regulation of emotions [257]. Even partial lesions involving less than two-thirds of the amygdala significantly altered fear and manual exploration of objects. In monkeys, partial or complete damage to the amygdala caused marked alterations in emotional behavior [253]. Specifically, the monkeys were less fearful than normal and unusually willing to touch and otherwise interact with novel stimuli.

There is also experimental evidence supporting distinct functions of the hippocampal formation and the amygdala [253]. In monkeys with amygdaloid damage, memory evaluated by delayed non-matching-to-sample task was intact unless there was also damage to the hippocampal formation or the adjacent cortex. However, the amygdala is critically involved in learning and storage of information about the emotional significance of events [252]. Selective damage in the emotional memory system, such as inability to identify emotional facial expressions, has been observed in some epileptic patients after amygdalectomy.

The piriform cortex, also known as the “primary olfactory cortex" is the largest area of the mammalian olfactory cortex and receives direct projections from the olfactory bulb via the lateral olfactory tract. Beside the obvious involvement in olfactory perception and discrimination, the PC, because of its unique intrinsic associative fiber system and its various connections to and from other limbic nuclei, has been implicated in memory processing and perceptual learning [258]. Neurons in piriform cortex serve as sites of convergence of peripherally extracted odorant

features, and thus encode complex feature ensembles rather than the simple features encoded by mitral cells of the olfactory bulb. Patient H.M., who received bilateral surgical resection of the medial temporal lobe (including the piriform cortex) for chronic epilepsy, has been tested for both odor sensitivity and qualitative discrimination. Eichenbaum et al [259] reported that he showed broadly normal olfactory sensitivity on a range of tests, but performed at chance level when identifying whether two odors of similar intensity but differing quality, were the same or different. These deficits appeared to be limited to olfaction, in that HM could discriminate objects visually and by touch and identify them. Similar findings have been observed in Alzheimer's disease and in other conditions known to affect explicit memory [260].

Patients with epilepsy complain of memory problems more frequently than other cognitive impairments. Studies evaluating memory performance have shown that mild verbal memory dysfunction as shown in delayed recall of word lists is present already at the time of diagnosis in patients with partial epilepsy, and the severity of hippocampal cell loss correlates with the memory scores [261]. Moreover, the presence of verbal memory impairment is a significant predictor of seizure outcome [262]. In chronic intractable TLE, patients with left focus have memory deficits especially on verbal memory tests, and patients with right focus have such deficits on visual and olfactory memory tests [263, 264]. In addition to material-specific memory effects, Hermann et al. [265] reported that the syndrome of mesial temporal lobe epilepsy was associated with considerable generalized cognitive impairment in intelligence, academic achievement, language, and visuospatial functions, reflecting possibly not only the primary neuropatlological substrate *per se* but also the generalized neurobiological consequences of intractable seizures.

One of the possible drawbacks of temporal lobe surgery for mesial sclerosis is that it may introduce additional cognitive deficits due to the removal of regions, not necessarily affected by the pathological changes of TLE. However, as to its effect on general intelligence (usually evaluated by the Wechsler Adult Intelligence Scale) several studies have demonstrated exactly the opposite [266, 267]. At long-term, there is a functional recovery of the parameters used to assess verbal and performance IQ when compared with the initial pre-surgical evaluations [267].

7. COURSE OF TLE

Temporal lobe epilepsy patients have an increased incidence in family history of epilepsy, suggesting a genetic predisposition [268]. Consequently, the familiar and genetic background could be a necessary precursor that permits noxious insults to give rise to epileptogenesis in TLE.

After a presumed initial insult such as complex febrile convulsions, status epilepticus, CNS infection or trauma, a retrospective evaluation of intractable TLE patients reported a mean seizure-free interval of 7.5 years before the development of unprovoked recurrent seizures [47]. Habitual seizures usually begin during the first 10-l5 years of life [5, 47, 119], although in a large survey of patients the range of age of onset varied between 1 year and 77 years [64]. A very young age of onset (less than 2 years) is a predictor of unfavorable outcome [32]. Other factors suggestive to poor prognosis of TLE include intelligence quotient under 90, more than five secondarily generalized seizures, daily partial seizures, and left-sided focus [269].

The drug of choice for the first line monotherapy in TLE is carbamazepine, oxcarbazepine, valproate, or lamotrigine [270, 271]. Some patients reach complete remission after the antiepileptic treatment has been started. Other patients who develop intractable TLE have a seizure-free interval initially. However, seizures may recur during adolescence or later, and often then become intractable [272]. There are also intractable patients who have an evolutionary pattern of TLE, with seizures becoming progressively more elaborate over time [47].

Of all TLE patients treated with antiepileptic medication, 60 to 70% are not satisfactorily controlled [269, 272] If temporal lobe seizures persist, the disorder may lead to neuronal damage followed by impaired neuropsychological performance and behavioral disturbances [272]. Therefore, when the clinical situation of TLE points to a progression of the disorder despite the appropriate antiepileptic medication, the patient should be evaluated for surgical treatment. Previous studies have shown that patients with mesial temporal lobe epilepsy syndrome have an excellent response to surgical treatment, reaching seizure-freedom in 70-80% of cases [62, 65, 152, 273, 274].

8. MAGNETIC RESONANCE IMAGING (MRI) STUDIES

8.1 Qualitative MRI of the Hippocampus

Magnetic resonance imaging is both a sensitive and specific noninvasive technique for detecting pathology in medial temporal lobe structures of epilepsy patients [275].

However, analysis of MR scans from epileptic patients is time consuming since the subtle nature of many epileptogenic abnormalities requires that more time should be spent in the evaluation of MR examinations for seizure patients than for most other patients who undergo brain imaging.

In a qualitative MRI study, temporal lobe abnormalities were observed in 180 (81%) of 222 consecutively referred TLE patients [276]. The most common structural change was hippocampal atrophy (55%), followed by developmental abnormality (7.2%), tumors (6.8%), scars (5%) and cavernous angiomas (4.5%).

The magnetic resonance properties of longitudinal (T1) and transverse relaxation (T2) are processes by which the system of spins reaches thermal equilibrium in the external magnetic field [277]. T1 and T2 represent properties of the tissue [277]. An increased T2-weighted signal and the signal's confinement to a unilaterally small hippocampus were the initially identified MRI features of hippocampal damage [278]. Imaging was performed in coronal and axial planes, specially orientated along and perpendicular to the long axis of the hippocampus. Further findings included (1) decreased T1-signal intensity, (2) disruption of the internal structure of the hippocampus, (3) unilateral atrophy of the columns of the fornix and (4) unilateral atrophy of the white matter bundle in the para-hippocampal gyrus [279, 280]. Dilatation of the temporal horn is an unreliable indicator of hippocampal volume loss because it is a common normal variant.

Hippocampal atrophy and an increased T2-weighted signal can be found in about 80 to 85% of patients with pathologically identified hippocampal sclerosis, using optimized images and visual inspection [281, 282]. Bronen et al [282] achieved sensitivies of 87-98% and specificities of 45-100% when comparing qualitative MRI findings with the histology of the hippocampus. In most patients, signal and volume changes associated with hippocampal sclerosis affect the entire hippocampus. However, Bronen et al [283] reported that 44% of the patients with pathologically proven sclerosis had abnormal qualitative MRI findings regionally. The most frequently affected region found with qualitative MRI segmentation in TLE patients was the body of the hippocampus [283].

Nevertheless, standard MRI may be inadequate for the diagnosis of focal epileptogenic lesions (including mesial temporal sclerosis). Several studies, demonstrated that qualitative assessment might yield a considerable number of so-called "MRI-negative" results in cases where tissue changes are subtle [203, 284-286] and whenever appropriate sequences are missed [285-287]. The main reasons for this underdetection were failure to program sequences accordingly to the orientation of the temporal lobe of each individual, absence of the coronal FLAIR sequence and

thin slice thickness with high-resolution, as well as a three dimensional T1-weighted acquisition for further postprocessing analysis such as reformatting and quantitative evaluation (**Figure 15**).

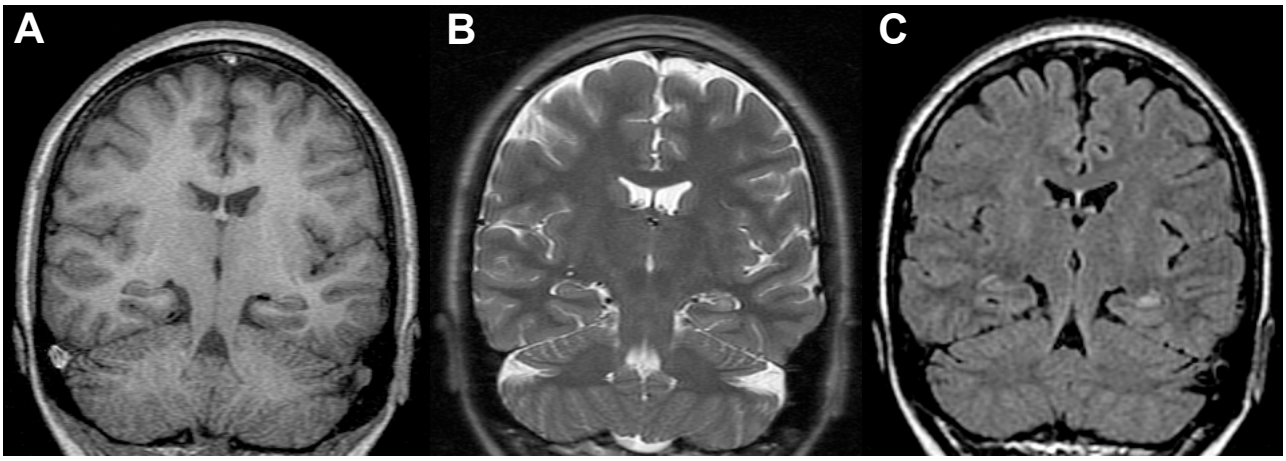


Figure 15. An example of hippocampal sclerosis with subtle imaging features. ***A*** – Oblique coronal T1-weighted with 1.5mm slice thickness and 512x224 matrix. ***B*** – Oblique coronal T2-weighted with 3mm slice thickness and 256x256 matrix. ***C*** – Oblique coronal T2-weighted FLAIR with 3mm slice thickness and 256x256 matrix. Unilateral atrophy and signal changes are equivocal on the T1 and T2-weighted images (***A*** and ***B***). FLAIR imaging clearly depicts a high signal on the left hippocampus. This patient had TLE with a left fronto-temporal EEG focus and a previous "negative" MRI report. Further analysis with quantitative MRI demonstrated significant hippocampal volume asymmetry (left < right) with corresponding increased T2-relaxometry and ADC values. Patient was 24 years old and her clinical data were included in Studies IV and V of this Thesis.

8.2 MRI Volumetry of the Hippocampus

Volumetric analysis can quantify hippocampal atrophy in TLE patients [288-290]. This quantitative measurement improves the diagnostic yield of MRI evaluation, as it may reveal subtle disease-related changes not apparent by routine clinical inspection and not associated with a visible lesion [291, 292]. Although neuropathological examination rather than MRI is the reference standard for the diagnosis of hippocampal sclerosis, measurements of unilateral hippocampal atrophy have proven to be the most accurate method of detecting hippocampal sclerosis.

The current evaluation of hippocampal (but also amygdala and entorhinal cortex) atrophy is based on optimized visualization techniques directed to the mid-portions of these structures (in the case of the hippocampus, that's the body) on T1-weighted coronal MR images with 1.5-3.0 mm thick. However, the shape of the body of the hippocampus is a truncated cone (the amygdala has a middle oval dilatation acutely narrowed on its two extremes, and the entorhinal cortex has a typical cortical comma shape), and this approach introduces errors due to the difficulty in

matching symmetrical positions on each side. Such difficulty is known in clinical practice to lead to incorrect or doubtful conclusions about tissue atrophy. In reality, the current expedient used to estimate tissue atrophy and volume is based on the visual inspection of a number of thick slices and can lead to errors in all but the most severely affected cases.

In a multicentric study, Von Oertzen et al [286] demonstrated that standard MRI failed to detect 57% of focal epileptogenic lesions. They evaluated 123 MRI scans of patients referred for surgery due to intractable epilepsy between 1996 and 1999 and showed that with the use of a dedicated MRI protocol (which included volumetry) 85% of patients with a "negative" standard MRI report had in fact a structural epileptogenic lesion. In particular, hippocampal sclerosis was missed in 86% of cases. Moreover, although the technical quality of standard MRI improved during the study period (upgrading from 1.0 Tesla equipments to 1.5 T), the corresponding diagnostic accuracy did not. Since patients without an identifiable MRI lesion are less likely to be considered candidates for epilepsy surgery, the clinical implications of a negative-MRI are evident. These observations clearly argue in favor of tailored imaging protocols and quantitative MRI in TLE evaluation.

The preferred approach is one that requires no a priori assumptions about shape; this is provided by stereology, which is a mathematical technique to transform 2D information into 3D data. In order to reliably detect atrophy, most comprehensive Epilepsy Centers now use a method that is similar to that described below [62, 215, 286, 289, 290, 293-297].

The Cavalieri principle states that a systematic volume sampling is equal to the product of the sum of a series of area measurements made through a whole structure multiplied by the distance between those measurements [298] (**Figure 16**).

$$V = h \times A$$

$$[V] = h \times \sum A_i$$

Figure 16. The stereology formula used for volumetric analysis of the hippocampus, amygdala and piriform-cortical amygdala region. Abbreviations: V- volume, h- slice thickness (slice spacing), A- cross-sectional area, i- slice position.

One critical advantage of this method is that it does not require precision in the fixing of slice positioning, namely the first and last slices, which would introduce observer bias and errors. The accuracy of the volume calculation depends mainly on slice spacing (sampling frequency) and the complexity of the shape (this is the reason why volume estimations of cortical areas have

larger coefficient of error and observer variability's if performed without proper anatomical protocols). It is possible to calculate a coefficient of error for the volume estimate of a structure of any shape for every number of slices [299]. In the case of the hippocampus, the minimum number of equally spaced slices required to hold error to 5% or less has been determined as 15 [290].

Sampling rate is not the only source of error. Each increase in slice thickness of 2mm introduces a variance of approximately 10%, and greater slice thickness introduces much greater and unpredictable variance [300]. There also are errors associated with the procedure used to identify the boundaries of the hippocampus, what depends on the expertise of the observer. As such, we avoided some of these systematic errors by calculating volumes from the largest number of slices possible (using thin, 1.5-2mm slices), by excluding undefinable amounts of tissue in each measurement and by relying exclusively on described anatomical protocols (including our own [301]) to quantify the tissue volumes (**Figure 17**).

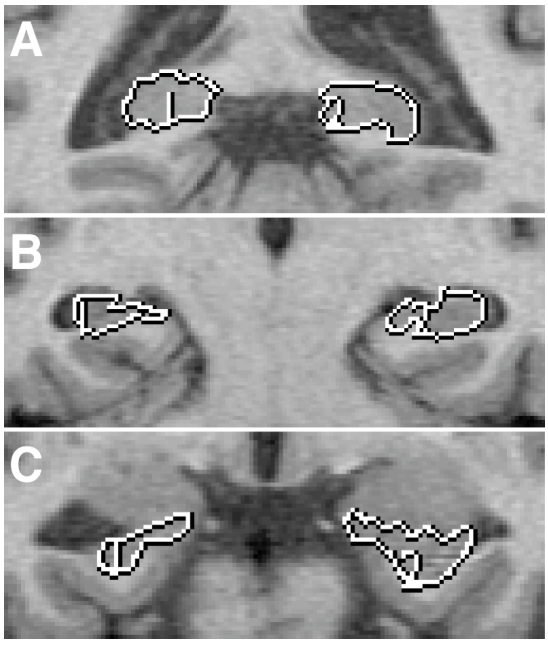


Figure 17. Representative slices of hippocampal volumetry in a TLE patient with a right temporal EEG focus. ***A*** – Hippocampal tail. ***B*** – Hippocampal body. ***C*** – Hippocampal head. There is a clear-cut atrophy on the right side. Patient was 31 years old and his clinical data were included in Studies IV and V of this Thesis.

However, there is a large variance in the normal population, which is related to individual morphometric characteristics (for instance height, as we have determined for the hippocampal volumes [301]). No significant age-group difference in the mesial temporal volumes (that is, the hippocampus, amygdala, entorhinal and perirhinal cortices, and the piriform cortex) has been found in normative groups of healthy volunteers aged from 16 to 65 [96, 301-304]. Thus, in

healthy persons, mesial temporal volumes remain stable from late adolescence through the mid-seventh decade of life.

Absolute volumetric abnormality is difficult to define because of the large variation in the volumes of medial temporal lobe structures of controls. A small female control subject may have smaller absolute volumes than a large male patient with a sclerotic hippocampus. Therefore, measures such as the cerebral volume or the cranial area may be used as correlates to enable normalized absolute volumes to be calculated [305]. The correction procedures reduce the variance in absolute volumes in controls, and provide a method for defining abnormally small volumes. In essence, the normalization procedure allows obtaining comparable volumes of the structures of interest in every subject, taking into account the differences in volume of the total brain. As subjects differ in morphometric parameters, including cranial size, overestimations of volumes (and thus misdiagnosis) will occur if two subjects with a proportionally similar hippocampal size (or of any other structure) are compared without correction, when one of the subjects has a bigger brain volume. Furthermore, the method overcomes the problem of detecting the bilateral volume loss [305].

As such, we have chosen not to use absolute volumes as a measure of tissue atrophy. Instead we express the calculated volumes as estimates of normalized volumes to an individual cranial reference that directly correlates with the total brain volume. We used, as others do [225], the individual brain area obtained at the level of the anterior commissure measured in the coronal plane (**Figure 18**). As subjects differ in morphometric parameters, including cranial size, such a normalization procedure is necessary.

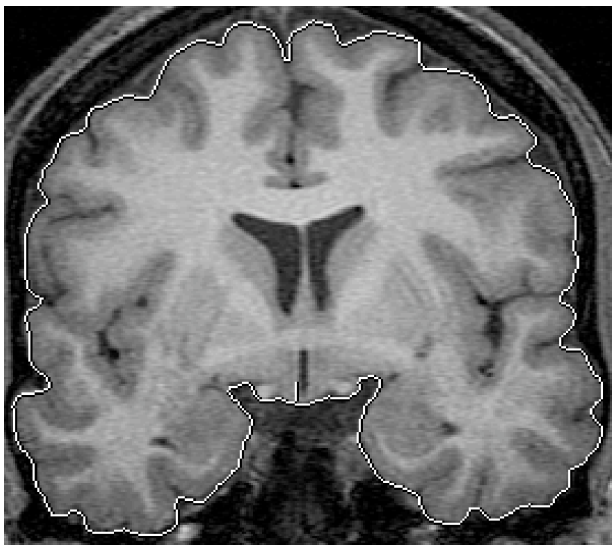


Figure 18. The correction factor used to "normalize" volumes of the regions of interest accordingly to the individual cranial size. In our control population, the correlation between the individual's brain area and volume was highly significant ($n = 10$, $r = 0.91$, $p < 0.01$). The mean, standard deviation (range) brain volume was 1173 , 143 cm^3 (993 – 1443) [301]. T1-weighted image at the level of the anterior commissure of a control subject included in Studies III, IV and V of this Thesis.

One limitation of expressing control values as confidence intervals (usually with 95% confidence, that is 2SD) is that it does not allow for recognition of bilateral lesions and minor (but rather significant) asymmetries. Usually, such methodology implicates additional calculations in order to determine ratios (smaller to larger) or asymmetry indexes. We have overcome these difficulties by using 99% confidence ellipses calculated by means of Hotelling´s statistics [306], which produces a single and clear graphical representation to plot both right and left sides volumes and allow for direct conclusions about meaningful atrophies and asymmetry (**Figure 19**).

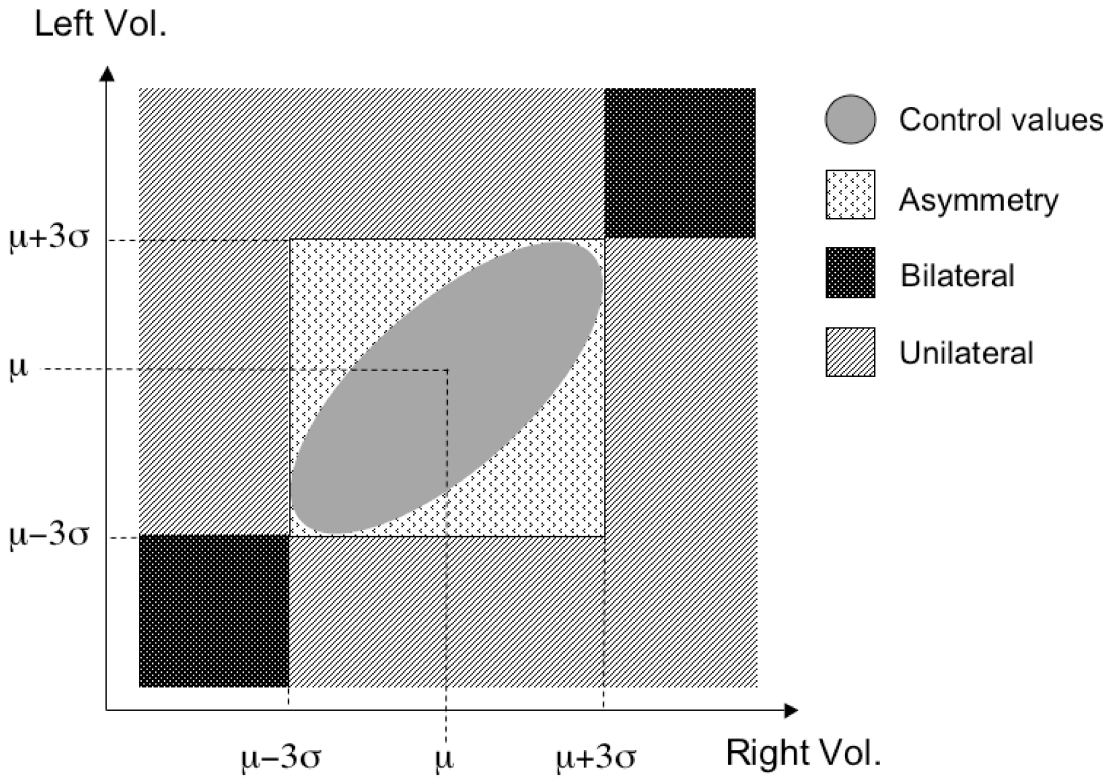


Figure 19. A representation of the general confidence ellipse for quantitative MRI calculated with 99% confidence over normal control values. With a simple graphic illustration, every case localized outside the ellipse is immediately categorized as "Asymmetrical", "Unilateral" or "Bilateral". Such method can be used to plot every data (besides the volumes) obtained from paired structures with a normal distribution within the brain. Abbreviations: μ – mean value, σ – standard deviation, $\mu \pm 3\sigma$ – mean ± 3 standard deviations.

Volumetric MRI studies have reported that 45-88% of the patients with intractable TLE have hippocampal damage [17, 206]. In studies of patients who had temporal lobe surgery for intractable seizures, such quantitative MRI demonstration of hippocampal atrophy was nearly 100% sensitive and specific for mesial temporal sclerosis [17, 307]. The mesasured hippocampal

volume reduction correlates with the severity of neuropatlological evidence of cell loss [165]. In a study by Lencz et al. [291], hippocampal volumetric ratio (ipsilateral/contralateral to the seizure focus) correlated significantly with the neuronal density in all hippocampal subfields except CA2. Many MRI studies have also found a positive correlation between the reduced hippocampal volumes and EEG lateralization of the epileptogenic region in TLE [203, 291, 307, 308]. Cendes et al [308] showed that hippocampal volumes alone agreed with the extracranial and/or intracranial EEG lateralization of the epileptogenic region in 87% of cases, and that combined hippocampal and amygdaloid volumes agreed with EEG lateralization in 93% of cases. The specificity of MRI-detected hippocampal damage is high in clear-cut TLE cases, but relative in those patients with partial and undefined focus. Spencer et al [203] reported that among chronic epilepsy patients who required intracranial EEG localization of seizure onset because of a lack of concordance of noninvasive studies, there was a subgroup of patients with unilateral hippocampal volume reduction who had EEG localization of seizure onset elsewhere in the brain.

The predictive value of MRI-determined hippocampal atrophy and outcome following temporal lobectomy has been established in several studies [296, 309, 310]. Arruda et al [311] reported that patients with unilateral medial temporal atrophy in volumetric MRI had excellent postoperative result (class I outcome according to Engel's classification [312]) in 94% of cases. Moreover, according to Jack et al [309] 97% of intractable TLE patients had a favorable postoperative outcome if hippocampal MRI volumetric data were concordant with the clinical and EEG localization. However, if the hippocampal measurements were nonlateralizing, the percentage of patients with a favorable outcome dropped to 42%.

Preoperative memory function of intractable TLE patients is associated with the severity of hippocampal atrophy in volumetric MRI [291, 313]. Studies correlating postoperative memory outcome with hippocampal volumetric measurements indicate that the group at least risk for a postoperative verbal memory deficit after a dominant left temporal lobectomy comprises those with marked unilateral left hippocampal atrophy [314]. Conversely, the patients at greatest risk for a decline of verbal memory are those with bilateral symmetric severe atrophy of both left and right hippocampi [315].

8.3 T2-Relaxometry of the Hippocampus

Quantitative measurement of hippocampal transverse relaxation time (best known as T2-relaxometry) is an unbiased, objective way of assessing the frequency and severity of signal abnormalities in patients with TLE and has been shown to confer additional sensitivity over qualitative assessment.

T2-relaxometry, along with estimates of metabolite concentrations and diffusion coefficients, are *intensive* quantities, as opposed to volumes that are *extensive* quantities[1]. T2-relaxometry measures the time it takes for the nuclear signal to decay within a magnetized tissue (**Figure 20**); it is a function of the tissue/material that the signal comes from and the local magnetic environment of the nuclei (see [316] for a review).

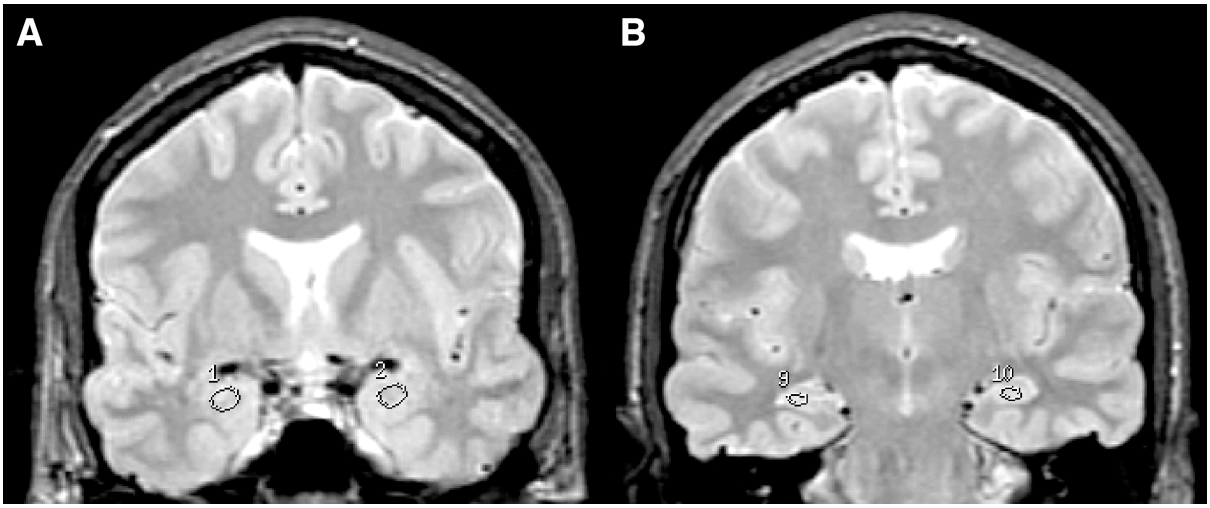


Figure 20. T2-relaxometry performed with a four-echoes protocol on a control subject included in Studies III, IV and V of this Thesis. Regions of interest are superimposed on mesial temporal structures. ***A*** – Amygdala T2-relaxometry map. ***B*** – Hippocampal T2-relaxometry map.

Visually assessed hippocampal T2-weighted signal hyperintensity has been reported in 70% of TLE patients with hippocampal sclerosis [275]. Other studies conducted during the same period demonstrated a considerable range of variability from 8 to 90% [317-321], which may be partly attributed to the subjective nature of visual assessment of subtle signal abnormalities in images of varying quality [320]. In an analogous way to the quantification of hippocampal atrophy by volumetric analysis, T2-weighted signal intensity may be quantified reproducibly by measurement of hippocampal T2-relaxation time [322]. The main advantage of this technique is that since the range of normal hippocampal T2-relaxation times is small, the measured values are absolute and immediately comparable against controls [323]. Furthermore, the T2 values allow detection of mild, bilateral abnormalities, and can be measured within a few minutes (although the acquisition times are still difficult to implement in clinical practice) [324-326].

[1] An *intensive* quantity describes the characteristics of a piece of tissue, which are irrespective of its size, and does not alter as the tissue is subdivided (other examples: density, magnetization, perfusion). An *extensive* quantity is a characteristic that changes whenever fragments are obtained from the original piece (other examples: mass and shape).

Hippocampal and amygdala T2 time reflects the pathology of the tissue. As water content is often higher in tissue with a pathological change than in the surrounding normal tissue, the change results in longer T2 relaxation time. Van Paesschen et al [207] found a positive correlation between hippocampal T2 time and the ratio of glial to neuronal density in the hippocampus of TLE patients. Moreover, hippocampal T2 time prolongation inversely correlated with the severity of hippocampal volume loss in TLE [211, 327] implying that atrophy and elevated T2 do not have the same neuropathological basis. In fact, Briellmann et al [328] provided sound evidence that T2-relaxometry is a reflection of the quantity of glial cells present in tissue sclerosis. Furthermore, about one-third of the glial cells were reactive astrocytes, suggesting an ongoing pathological transformation, as that that may accompany synaptic reorganization. Additionally, elevated hippocampal T2 relaxation has been reported in the presence of normal hippocampal volumes [324].

Jackson et al [320] studied patients suffering from intractable partial epilepsy and found abnormal ipsilateral hippocampal T2 values in 70% of them. Marked elevations (>10 ms) were observed in 65% of TLE patients, correlating strongly with the presence of pathologic evidence of hippocampal sclerosis [320]. Volumetric measurement showed no abnormality in a subgroup of 5 to 10% of intractable TLE patients with hippocampal sclerosis [329]. In these difficult cases, hippocampal T2 signal quantification allows the MRI diagnosis of unilateral hippocampal sclerosis [324, 329].

Despite T2 values being significantly elevated in the vast majority of cases of hippocampal sclerosis, some patients with confirmed sclerosis had a normal T2 value [327]. This may have reflected the methodological constrain of using only a single slice form which T2 values were determined.

In addition to improved sensitivity in the identification of hippocampal abnormalities, analyses of T2-relaxometry are independent predictors of neuropsychological impairment following epilepsy surgery [330-332]. Elevated T2 values in the left hippocampus in left TLE patients were associated with a better verbal memory outcome than high T2 values in the left hippocampus in right TLE patients, suggesting that T2-relaxometry is useful in predicting pre-operatively the risk of post-surgical memory impairment.

T2 relaxation times can be measured accurately, given careful modeling and sufficient image time.

Currently, T2-relaxometry is performed with an interleaved, multislice/multiecho sequence, in which the whole temporal lobe is imaged either in the axial or coronal planes [211, 322, 333]. However, some methodological issues remain to be addressed when performing T2-relaxometry

that may bias the measurements. These include partial volume effects from surrounding cerebrospinal fluid (CSF) or sulcal encystments within the hippocampus [334], and asymmetrical positioning of the head resulting in measurements derived from different hippocampal regions (which may have different T2 values). The use of a multislice, contiguous sequence circumvents this latter limitation [322, 325]. CSF artifacts can also be nulled by adding an inversion-recovery pulse to the multiecho sequence [335]. Still, no significant differences were obtained when measurements were performed in the same patients with the use of both CFS-nulled and non-CSF-nulled sequences [335]. As such, parenchymal changes, rather than CSF contamination is the predominant determinant for prolonged T2 times in tissue sclerosis.

One critical advantage of T2 measurements over volumetry is that T2 values are absolute, so they can be directly compared to control values and in-between patients groups. The range of control values reported in the literature is overall narrow (a maximum of 7 ms [329]). However, one cannot compare T2 values obtained at different MR scanners, since the T2 decay is an intrinsic factor of each machine.

T2 values remain one of the most sensitive indicators of tissue pathology since it is independent of the lesion morphology and volume. It is also a method of choice over standard MRI since significant alterations may be left unnoticed in routine images, either because the difference is too small, or because the change is too diffuse for a boundary to be recognized.

8.4 MR Spectroscopy

Unlike conventional MRI, which provides structural information based on signals from water protons, proton magnetic resonance spectroscopic imaging (^{1}H-MRSI) provides information about the chemical composition of the brain.

Water suppressed H^{1} spectra obtained in patients with TLE have revealed changes in intermediary metabolites in the affected temporal lobe that are moderately consistent. The changes observed are diffuse, and their significance remains largely speculative [223, 336]. Bilateral changes are common findings in patients with clear unilateral hippocampal sclerosis and recover on the unaffected side after temporal lobectomy [337, 338].

Spectroscopy is a highly specific technique for measuring the concentration of brain metabolites. Metabolites of interest to epilepsy studies are *N*-acetyl-aspartate (NAA), Choline (Cho) and Creatine/Phosphocreatine (Cre). Their concentrations are measured from the peak signal intensities at 2.0 p.p.m. (NAA), 3.0 p.p.m. (Cre) and 3.2 p.p.m. (Cho) and they are obtained using long echo-time sequences (**Figure 21**). As such, ^{1}H-MRSI does not provide information regarding the structural status of tissues, although it may be related to the cellular content of the sample.

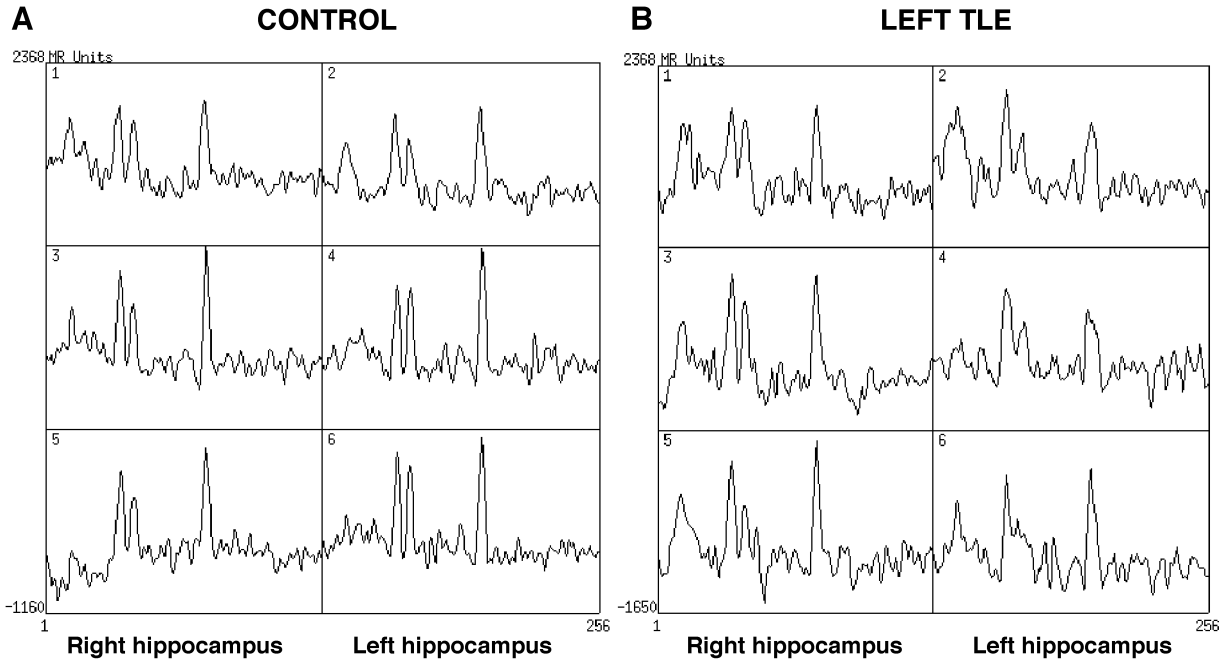


Figure 21. Multivoxel spectroscopy performed for Studies IV and V. Hippocampal peak frequencies from NAA, Cho and Cre obtained from a control subject, aged 22 (***A***), and a left-TLE patient, aged 26, with hippocampal sclerosis (***B***).

Immunohistochemical studies have suggested that NAA is localized exclusively in neurons and their processes throughout the CNS [339-341]. As such, NAA can be used as a neuronal marker [342] and a reduction in NAA levels as assessed by ^{1}H-MRSI has been a useful tool for quantifying brain neuronal and axonal integrity in vivo [336, 343, 344].

^{1}H-MRSI detects hippocampal sclerosis, but the overall added value of the technique in the clinical and pre-surgical context is difficult to define. Nonetheless ^{1}H-MRSI is currently used to obtain complementary information in relation to hippocampal size and T2 measurements available from structural sequences.

There are two different techniques for obtaining a chemical spectrum using MRI: single-voxel spectroscopy and multi-voxel spectroscopy (^{1}H-MRSI or chemical-shift imaging). In general, single-voxel spectroscopy has the advantages of more explicit spatial localization, more homogeneous shimming, better water suppression, and shorter acquisition time; but only one spectrum can be obtained from one data acquisition [345]. On the other hand, ^{1}H-MRSI has the advantage of obtaining multiple spectra simultaneously during one measurement (that is, a higher temporal resolution). This technique is useful for evaluating an area or a lesion with multiple regions of interest and to compare side-to-side differences in paired brain structures such as the

hippocampus (**Figure 22**). However, the post-processing of ^{1}H-MRSI data is more complex [346]. Moreover, although the spatial reproducibility of spectroscopic measurements reaches 100% (measured voxels are fixed volumes within the tissue), the temporal reproducibility of both single- and multi-voxel techniques critically depend on a multitude of technical parameters (such as magnetic homogeneity) and have been showed to vary in standard MR machines operating at 1.5 T [347].

A recent study compared the ability of both techniques to detect mesial temporal sclerosis [348] and found a similar ability for detecting hippocampal abnormalities in patients with complex partial seizures.

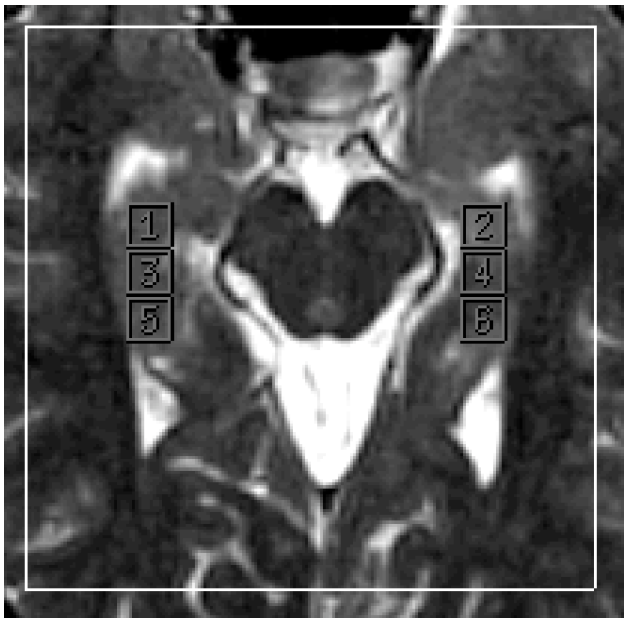


Figure 22. The window of spectroscopy performed for chemical-shift analysis of the hippocampus in Studies IV and V. At least 3 voxels can be quantified on either side.

Both proton single-voxel spectroscopy [349-351] and ^{1}H-MRSI [218, 223, 336, 343, 352, 353] have been used to evaluate metabolic abnormalities in patients with complex partial seizures, especially those with mesial temporal sclerosis. A decrease in hippocampal NAA intensity has been demonstrated in most patients and indicates the neuronal loss underlying mesial temporal sclerosis [215, 349, 350]. Increased intensities of Cho or Cr have also been reported and probably reflect the associated astrocytosis in the affected hippocampus [219, 349, 350]. Although the ability of single-voxel spectroscopy and ^{1}H-MRSI to detect metabolic abnormalities in seizure patients is reportedly satisfactory, diverse quantitative or semiquantitative results due to different measurement techniques, acquisition parameters, and data presentation have been noted [215, 218, 223, 349, 350, 353]. This methodological

inconsistency may hinder the widespread application of MR spectroscopy in clinical practice and prevent comparison of data from different research centers.

8.5 Diffusion Imaging

The diffusion-weighted MR imaging (DWI) sequence is a recent development in clinical practice. Stejskal and Tanner originally introduced its physical principles in 1965 [354], but it was only during the 1990s that *in vivo* water diffusion measurements entered the medical field [355].

The diffusion process is a physical property of water molecules, which refers to their capability of displacement in biological tissues. In a normal tissue, this movement occurs randomly (it is named Brownian movement) and it is induced by the thermal energy of the molecules. Unless there is a restriction, it occurs over all directions.

DWI yields information about the ease of water diffusion within the local tissue environment. The diffusion of water in the brain is characterized by its apparent diffusion coefficient (ADC), which represents the mean displacement of water along all directions. In isotropic tissues, such as the grey matter, ADC-mapping measures the displacement of water within any direction (it is independent of the orientation). In anisotropic tissues, such as the white matter, where the microstructure follows the orientation of the fiber tracts, the diffusion varies accordingly to the direction. Thus, ADC analysis gives potential information about the size, orientation and tortuosity of both intra and extra-cellular spaces. In chronic lesions, such has tissue scars, the largest component detected by DWI is restricted molecular diffusion, and so ADC rises.

Most current scanners can generate the DWI sequence, but only those equipped with large additional field gradients are able to construct DW images with good contrast and spatial resolution. Gradient pulses are applied before and after a radio-frequency pulse of 180º and its effect is to reduce the signal of diffusing protons relative to stationary protons. The orientation of the gradients affects the appearance of the diffusion images of an abnormal tissue, reflecting the fact that molecular motion suffers restriction or facilitation to movement along the axis of the gradients [355]. DWI is sensitive to the signal loss occurring within individual image volume elements (voxels) due to the molecular movement of water within stationary tissue. Signal loss and phase differences due to this mechanism can produce contrast in images.

Recently, DWI emerged as a promising technique to identify pathological changes in human TLE [356-361]. The preliminary studies were limited to observations of the hippocampus. In this way the relative specificity, but not the prognostic utility of interictal DWI to capture the imaging abnormalities of hippocampal sclerosis was evaluated.

The work performed so far, yielded consistent results regarding the diagnostic utility of hippocampal DWI analyses. One common observation is that hippocampal abnormalities are poorly identified on the visual inspection of current diffusion-weighted images. As such, it is unlikely that DWI becomes part of the routine MR sequences to study the mesial temporal lobe in chronic partial epilepsy.

ADC-mapping, however, is a rapid method to produce quantitative and consistent information regarding the status of structural integrity of any brain region.

In the studies published, the lateralizing ability of hippocampal ADC in chronic TLE was reported to be rather similar [356-362]. The initial studies of Hugg et al [356] and Wieshmann et al [357] reported significant larger hippocampal ADC values on the side of the focus and in accordance with MRI findings of hippocampal sclerosis. ADC values obtained in pathological tissue were significantly higher than control values (ranging from a mean difference of 10% [356] to 24% [357] relative to the mean of controls). The results of Yoo et al [359] enlarged the spectrum of hippocampal abnormalities detected by ADC-mapping. These authors reported a significant increase in ADC by about 6%, in the hippocampi contralateral to the focus when compared to the mean of controls, and concluded for the presence of micro-structural changes in the normal-appearing contralateral hippocampus. However, these authors used the axial hippocampal plane for ADC quantification, and partial volume effects may have biased their measurements (**Figure 23**).

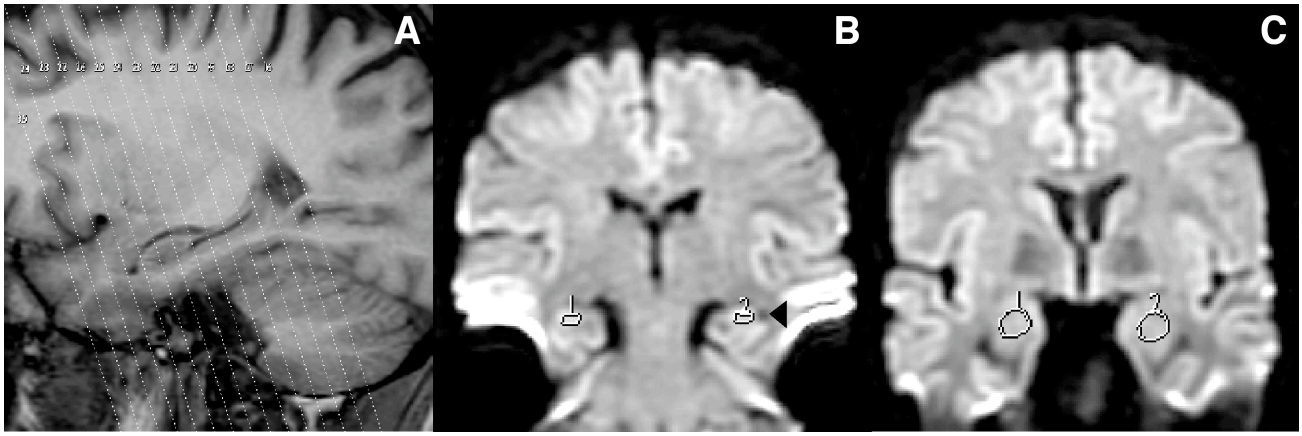


Figure 23. Mesio-temporal ADC-mapping performed perpendicular to the main axis of the temporal lobe (***A***), with regions of interest superimposed on the hippocampus (***B***) and the amygdala (***C***) (control subject included in Studies IV and V of this Thesis). Arrowhead points to the temporal horn.

Londono A. et al [362] provided further insight regarding the utility of hippocampal ADC-mapping in TLE. They compared standard MRI with data provided by ADC in the diagnosis of

hippocampal sclerosis and found that ADCs may be abnormal when MR images are unremarkable and that MR imaging plus ADCs was better than either technique alone in the identification of the pathology.

As such, there is an ongoing interest in this technique and its applications in TLE.

8.6 MRI of specific brain structures in TLE

8.6.1 Bilateral Hippocampal Damage

In line with the previous pathologic data [7, 162], an increasing number of imaging studies suggest a bilateral involvement of hippocampal damage in TLE patients [193, 202, 315, 320, 363-365].

King et al [366] assessed the frequency of bilateral hippocampal damage using absolute hippocampal volumes in 53 medically refractory TLE patients: 5 (9%) patients had hippocampal atrophy bilaterally, and four of them were undetected by volumetric ratios. This finding agrees with the results of Fish and Spencer [367] who observed significant bilateral atrophy in 10% of intractable patients with hippocampal volume decrease. In a series of drug-resistant TLE patients, the mean volume reduction was 30% in the hippocampus ipsilateral to the seizure focus, and 15% in the hippocampus contralaterally [202]. This pattern of bilateral reductions was seen in two-thirds of patient's altogether. Moreover, bilateral hippocampal volume loss is common in patients with a history of encephalitis or meningitis ([198].

8.6.2 Hippocampal Damage in Extratemporal Epilepsy

Several MRI studies have reported normal hippocampal volumes in patients with extratemporal epilepsy [290, 368]. However, experience with large numbers of patients has shown that some extratemporal epileptic patients may demonstrate MRI features of hippocampal damage [367, 369]. Adam et al [370] reported that 29% of patients with intractable complex partial seizures of extratemporal origin had hippocampal atrophy although the degree of atrophy was milder than in TLE patients.

The data agree with those of imaging studies reporting dual pathology in 10 to 15% of cases with lesional epilepsy [369, 371-373]. In a multicenter study involving 167 patients with extratemporal or extrahippocampal temporal lesions, Cendes et al. [371] found only 25 patients (l5%) with dual pathology. However, developmental abnormalities exhibited a higher incidence of coexisting hippocampal sclerosis, in the range of 25 to 30%. Watson et al [368] reported that 25% of their patients with pathologically proved hippocampal sclerosis exhibited dual pathology, and 80% of those patients had neuronal migration disorders. The simultaneous presence of hippocampal damage and developmental changes could create potential multiple epileptogenic zones in these patients.

8.6.3 MRI of the Amygdala and the Para-Hippocampal Cortices

The volume and T2 relaxation time measurements can be used as tools to study not only the hippocampus but also other structures involved in the epileptic process, such as the amygdaloid complex [225, 289, 308, 374-377].

Watson et al [289] and Convit et al [378] showed that measurement of the amygdaloid volume is reliable when special attention is paid to the differentiation of the amygdala from adjacent structures.

Cendes et al [379] and Achten et al [380] demonstrated that amygdala volumetry was reproducible among different observers, although it had a larger coefficient of variation (7.3%) when compared with that of the hippocampus (4.7%).

MRI studies of the amygdala reported a 10 to 20% decrease in volume in patients with drug-refractory TLE when compared to reference values [225, 308, 381]. In these studies up to 30% chronic TLE patients had a significant reduction of the amygdala volumes in the side of the epileptic focus and accordingly with the diagnosis of hippocampal sclerosis. Amygdala T2-relaxometry studies, however, have detected higher number of patients with pathological values, varying between 30-50% of the cases [225, 374, 376].

In some patients, the damage in the amygdala is isolated, although the majority of cases had lesions in both the amygdala and the hippocampus [225, 308, 374, 381]. Most of amygdala pathology is unilateral, but up to 12% of patients may show bilateral abnormalities [225, 376].

Using a qualitative MRI segmentation analysis, Kuzniecky et al. [201] studied the patterns of atrophy in the amygdala and hippocampus of 47 patients with histologically confirmed hippocampal sclerosis. They found amygdaloid atrophy in 23% of cases with hippocampal damage [201]. Furthermore, in a quantitative MRI study by Van Paesschen et al. [374] an abnormal amygdaloid T2 signal was present ipsilaterally in 52% of patients with unilateral hippocampal sclerosis. The volumetric measurements of both the amygdala and hippocampus lateralize the epileptogenic concordantly with the EEG to an accuracy of over 90% in TLE patients [382]. A series of TLE patients also demonstrated that amygdaloid damage was associated with the clinical symptom of ictal fear [383]. Moreover, the study showed a good correlation with the volume of the amygdala and the postoperative pathology.

MR spectroscopy of the amygdala is not technically feasible, due to its close vicinity with air and bone interfaces in the medial temporal lobe. Up to date, there has been no attempt to study water diffusion of the amygdaloid complex in TLE. As such, data is lacking concerning the abnormalities of the epileptogenic amygdalae that may be revealed by DWI.

Until the pioneering works of Insausti et al [96], Bernasconi et al [384] and Salmenpera et al [385], the parahippocampal gyral abnormalities received little attention in imaging studies of epileptic process. Previously Saukkonen et al [386] reported that in patients with intractable left TLE the rostral portion of the ipsilateral parahippocampal gyrus (the area that is mostly composed of the entorhinal cortex) was 12% smaller than in controls. It was only after the establishment of a comprehensive anatomo-radiological protocol for entorhinal and perirhinal (but also temporo-polar) volumetrics by Insausti et al [96], that accurate MRI analyses of the mesial temporal cortices became possible. Several quantitative MRI studies have been conducted since then. These studies evaluated more specifically the volume of the entorhinal, perirhinal and temporo-polar cortices in TLE patients [375, 381, 384, 385, 387-389]. In agreement with previous volumetric studies of the hippocampus and amygdala, the volume of the entorhinal cortex ipsilateral to the epileptic focus was significantly reduced suggesting an involvement of the structure in seizure generation. Moreover, there was a sub-population of chronic TLE patients (64%, that is 14 out of 22) with selective entorhinal atrophy on the side of seizure focus exhibiting normal hippocampal or amygdala volumes (and without further signs of hippocampal or amygdala sclerosis) [387].

There is a myriad of experimental data linking the remaining limbic structures of the mesial temporal lobe to the pathophysiology of TLE. One critical region is the piriform-cortical amygdala ribbon (see sections **2** and **4.4**). Given the lack of human data concerning the involvement of the piriform cortex in TLE, we devised an anatomo-radiological protocol (Study III) for the identification and quantification of tissue damage in this area (**Figure 24**), and applied it to a population of chronic TLE patients.

8.6.4 Damage Outside Medial Temporal Lobe Structures

Magnetic resonance imaging studies of epileptic patients demonstrated volume deficits not only in the medial temporal lobe structures but also in the ipsilateral temporal lobe or hemisphere. Briellmann et al [390] found that TLE patients had smaller hemicranial volume ipsilateral to the seizure focus, irrespective of the presence or absence of hippocampal sclerosis. Other reports suggested a bilateral temporal lobe or cortical volume reduction in patients with TLE [205, 391]. The fornix and mamillary body, which are parts of the limbic system, were smaller ipsilateral to an abnormal hippocampus [181, 283, 392, 393]. Furthermore, the diverse range of structural abnormalities observed in MRI outside the temporal lobe include the ipsilateral thalamus, and caudate, gyrus cingulate, bilateral frontoparietal gray matter, cerebellum, and, in some cases, ventricular enlargement [182-184, 205].

These findings were generally replicated by unbiased voxel-based analyses [394-400].

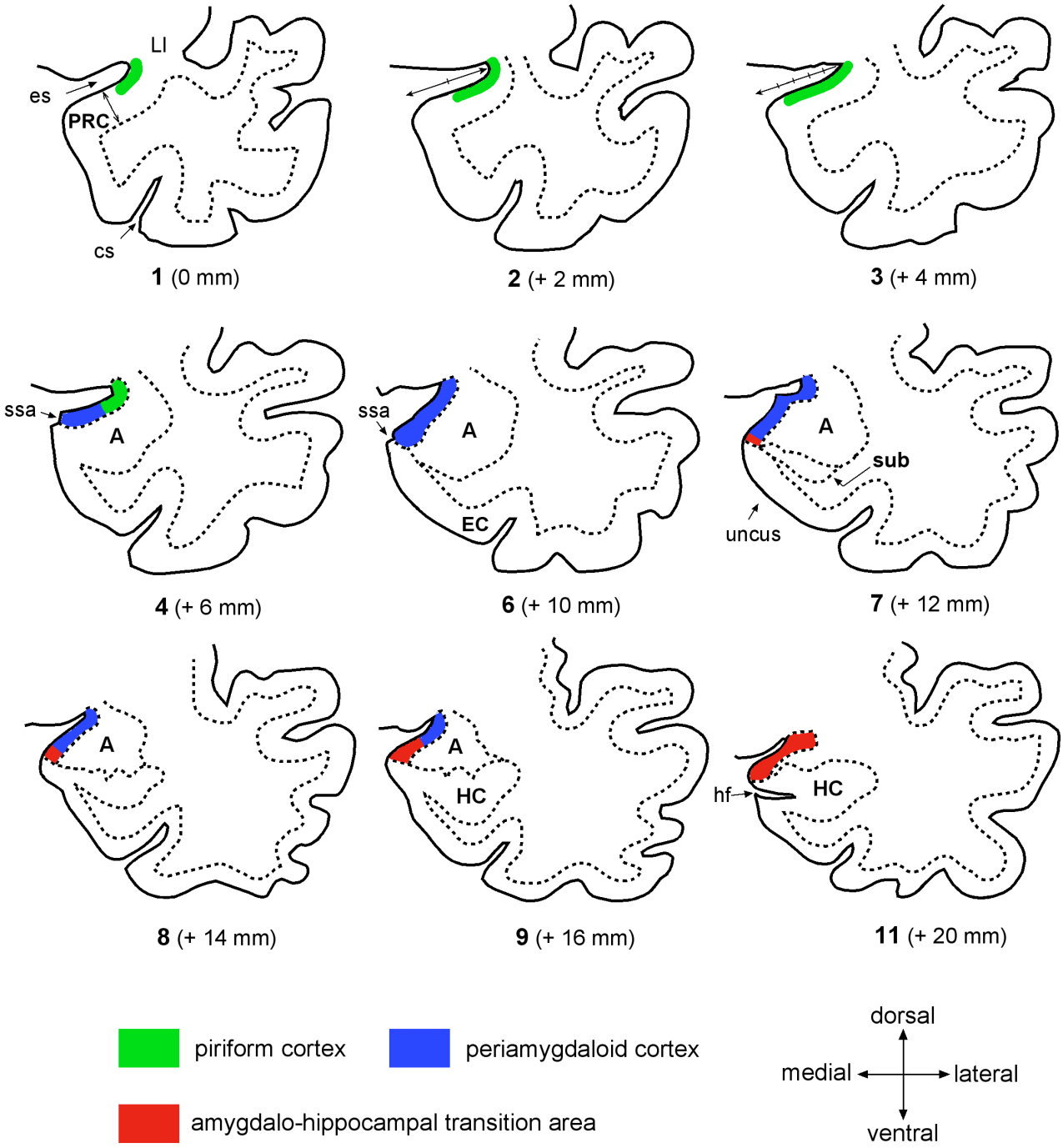


Figure 24. Line-drawings summarize the anatomic landmarks of the piriform-cortical amygdala. Only the images displaying critical landmarks are shown. Section #1 is the more anterior (at the level of the *limen insulae* - LI). The remaining sections are marked accordingly to its posterior-most distance from the LI. Abbreviations: LI - *limen insulae*, es - endorhinal sulcus, PRC - perirhinal cortex, ssa- sulcus semiannularis. EC - entorhinal cortex, cs - collateral sulcus, Sub - subiculum, HC – hippocampus, hf - hippocampal fissure, A - amygdala. Scale bar equals 10 mm (all panels).

8.7 Anatomical Reproducibility and Normative Values

Quantitative measurements of variables characteristic of a given disease tend to become more and more incorporated in medicine in general. Namely in neuroradiology, appropriate quantification can overcome problems due to bias, and enhance reproducibility and make interpretations more reliable. Moreover, quantitative methodologies allow more robust statistical modeling and produce data that can be pooled over multiple centers. The process of measuring parameters in the brain necessarily takes more time and effort than straightforward qualitative studies. For MRI, this also means that more scanner time is needed along with investment in computing resources. As demonstrated previously, quantitative MRI (qMRI) depend on several methodological issues to be accurate. One that is critical, and affects equally every method used, despite its intrinsic technical specificities, is the anatomical orientation that is chosen to obtain the MRI sequence. Another one is the criterion used to pool out the normative values with respect to which pathology is inferred. Finally, partial volume effects, subject positioning and the inherent properties of the NMR – nuclear magnetic resonance – technique (examples: field homogeneity, field gradients, slice profile variations, image noise) may also have a role.

8.7.1 Reference lines and landmarks

The orientation of the acquired images, along with the criteria used for MR analysis and the knowledge of normal and abnormal mesial temporal lobe anatomy are key factors for the interpretation of MR images. Moreover, in qMRI one should assure reproducibility of the measurements by taking a constant tilted orientation to the temporal lobe in successive exams, minimizing in this way, partial volume effects.

Different MR sequences, including several anatomical planes have been used to evaluate the mesial temporal lobe structures [401]. One preferential anatomical orientation is the tilted coronal plane obtained at right angles to the main hippocampal axis [289, 401, 402]. For volumetric and relaxometric studies of the hippocampus and amygdala this is the plane mostly used, while multi-voxel spectroscopy benefits most if performed on a tilted axial orientation perpendicular to this angled coronal view [289, 320, 403].

In the clinical setting it is likely that different radiologists and radiographers are responsible for the examinations of different patients. Thus, the importance of using a stable sagittal reference line as a scout for angulated planes to the temporal lobes cannot be overestimated. A simple, reproducible and well-defined anatomical landmark can contribute to the accurate comparisons of the MRI exams and increase the consistency of qMRI measurements.

The lines that are currently used in radiological practice as anatomical landmarks for the tilted orientation of the temporal lobe include one that is “perpendicular to the main (or long) hippocampal axis” [286, 289, 401, 404, 405] and, for axial imaging, the line “parallel to the longitudinal axis of the hippocampus” (obtained at right angles from the previous) [403, 406]. However, recently [407], the posterior commissure-obex line has been proposed as an accurate reference to obtain angulated coronal and axial images to the main axes of the temporal lobes. This line offers some advantages over the remaining: it joins two well recognizable structures, it is independent of the structures of interest and it can be applied to scout both coronal and axial MRI studies of either temporal lobe. However, to date, there has been no attempt to compare the several anatomical options available.

As such, we devised a test to verify the usefulness of the posterior commissure-obex line in clinical practice (**Figure 25**). We have further compared the intra and inter-observer reproducibility of the posterior commissure-obex line with the remaining landmarks available for temporal lobe imaging (Study II). We were particularly interested to define which may be considered the less variable line so that differences among observers’ peformances of MRI evaluations may be minimized.

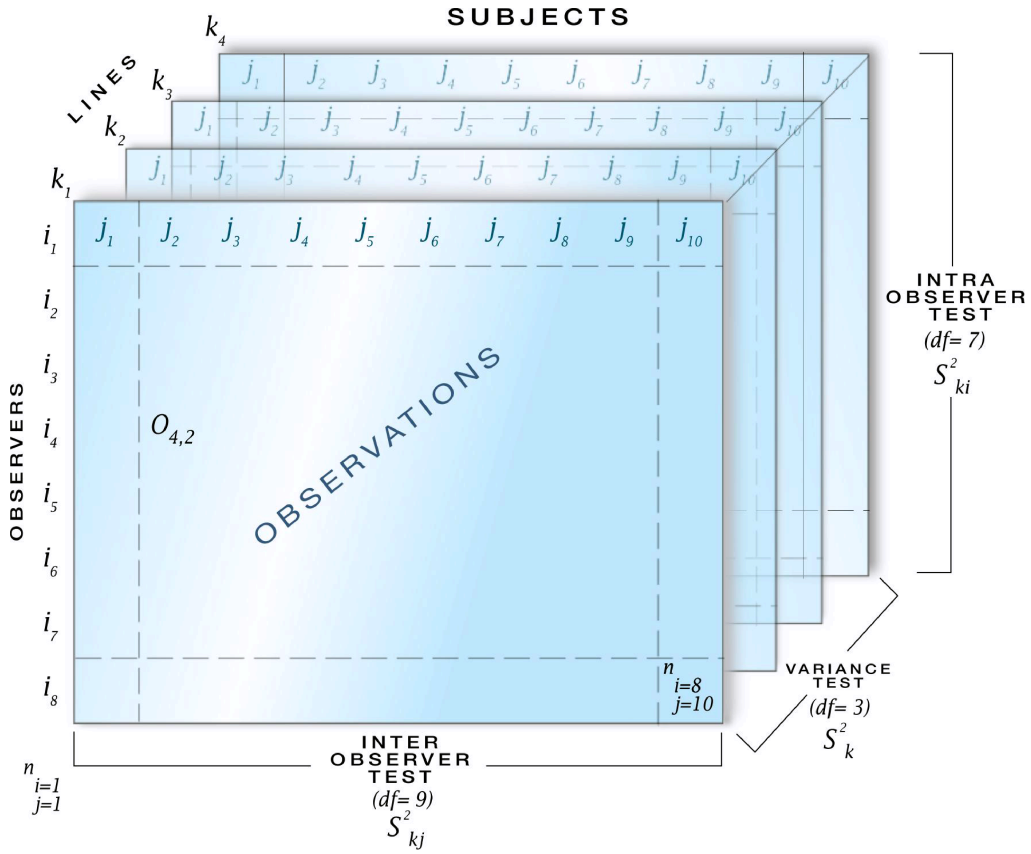


Figure 25. A diagram of the statistical design used to compare the reproducibility of four anatomical lines. Refer to Study II for abbreviations.

8.7.2 Normative values and precision of the measurements

The use of the term *normal* is intended to refer to structural characteristics of mesial temporal regions that are acceptable in a *normal*, healthy population used for control purposes. This does not exclude the possibility that some of these characteristics may be encountered in TLE patients.

It is well known that certain processes influence the normal brain development over time but are not manifestations of disease. One such process is aging. Thus, control groups must be build taking into consideration the distribution of the age-range of patients and of gender[2]. An adequate number of control individuals must be included to account for the intersubject variability of reference values. A minimum of 20 subjects recruited from an environment that is similar to that of the patients group, is generally sufficient to guaranty statistical power and validity of the data.

Additional screenings are necessary to ensure that the volunteers had no prior history of health insults that may have secondary effects within the brain (e.g. head trauma or hypertension can produce selective mesial temporal atrophy [408-410]). Thus, a meticulous inquiry of the past and present health status must be performed, including a complete neurological evaluation and a Mini-Mental State Examination [411] adjusted for the local settings.

Precision is concerned with whether a measurement agrees with a second measurement of the same quantity. Two types of tests (inter-observer and intra-observer) are performed to evaluate the quality of the principal observer of the study. As a rule, quality must be established early at the beginning of the study, in the period where the control group is usually built. Thus, tests of reproducibility are made on normal subjects serving both for assessing the observer's performance and to affine the scanning protocol.

There is, however, other reasons for using this methodology. First, reproducibility may be worse in patients than in normal controls, since patients are less predisposed to support long examination times while keeping still in the MRI apparatus. Second, statistical tests used to assess repeatability depend on the mean value of the parameter [412], which may be significantly different in patients (for example if there is gross atrophy). With respect to the volumetry, it has been showed that the intra-observer variance increases by a quadratic factor accordingly to the mean lesion volume (that is, $Variance = k \times MLV^2$, where k is a constant) [412, 413].

[2] Age and gender have distinct effects in the adult brain. Age primarily influences grey matter characteristics, while gender has differential consequences in white matter.

IV – AIMS OF THE STUDY

How TLE progresses is not precisely known. Whether mesial temporal sclerosis concurs with the beginning of the symptomatology or develops along a course of recurrent seizures is a matter of debate.

The pathophysiology of TLE is not solely dependent on hippocampal, para-hippocampal and amygdala damage. Patients with chronic intractable TLE may have pathological changes in other limbic structures. There is no data concerning the involvement of potentially highly epileptogenic regions such as the Piriform Cortex in human TLE.

Images of hippocampal and amygdala sclerosis are readily detected with tailored MRI sequences, specifically build to highlight the morphological and signal changes of these regions. However, the ability to detect mesial temporal damage depends largely on subjective factors and on the expertise of the reader. Recent quantitative MRI methods can contribute to overcome the inherent subjectivity of visual analyses and provide more robust diagnosis. However, in order to estimate the sensitivity/specificity of different methods, quantitative MRI methods must be compared in large series of patients, taking into account post-surgical outcome such that their diagnostic and prognostic relative value may be established.

The purpose of the present series of studies (I-V) was to investigate experimentally and with MRI the appearance of medial temporal lobe damage during the course of partial epilepsy, and, particularly, to determine the spectrum of tissue damage across limbic mesial temporal structures. More generally we aimed at getting more insight into the basic question whether mesial temporal sclerosis is a progressive disease. In addition we wished to formulate a practical proposal for an efficient quantitative MRI protocol to be used in the diagnosis of TLE.

The specific aim of the present series of experimental (I) and human studies (II-V) was to answer the following questions:

1. Do recurrent seizures cause hippocampal, para-hippocampal and piriform cortex damage in Temporal Lobe Epilepsy? (**Study I**)

a) Is the damage in the hippocampus, para-hippocampus and piriform cortex present already at the time of the first spontaneous seizures?

b) What is the spatio-temporal progression of cell death across the hippocampus, para-hippocampal gyrus and piriform cortex?

c) What is the relation between the extent of neuronal cell death observed in chronic TLE with either the frequency of seizures and the duration of the initial insult (the *status epilepticus*)?

2. Does the mid-sagittal posterior commissure-obex line provide additional stability and reproducibility to general MRI studies of the temporal lobes, and, in particular, to quantitative MRI? (**Study II**)

3. Do human patients with chronic TLE have damage in the piriform cortex? (**Study III**)

a) Is it possible to detect and quantify tissue damage in the piriform cortex in human subjects?

b) Does this damage associate specifically with that of the hippocampus, amygdala, and entorhinal cortex?

d) Does this damage correlate with the duration of TLE or seizure frequency?

e) Should we broaden the concept of mesial temporal sclerosis so to include the piriform cortex?

4. What is the sensitivity of diffusion-weighed imaging (DWI) in detecting hippocampal and amygdala sclerosis? (**Study IV**)

a) Does interictal ADC-mapping localizes amygdalo-hippocampal abnormalities corresponding to electroencephalographic and clinical manifestations?

b) What is the predictive value of the ADC data of the hippocampus and amygdala in the surgical context? Does it relate to and predict outcome?

c) Does interictal ADC-mapping associate with the corresponding measures of volumes, T2-relaxation times and hippocampal NAA/(Cho+Cre) ratios?

d) What is the effect of the subject's age and gender, the age of onset and the duration of epilepsy in amygdalo-hippocampal ADCs?

5. What is the relative value of volumetry, T2-relaxometry and spectroscopy as such and in combination, in the evaluation of the mesial temporal integrity (hippocampus and amygdala) given the context of pre-surgical screening? (**Study V**)

a) Do these techniques provide complementary or redundant information about the status of the mesio temporal structures?

b) Can we use an optimized algorithm in order to obtain accurate quantitative information in a time-efficient manner?

c) Do differences exist in the predictive value of volumetry, T2-relaxometry and spectroscopy regarding post-operative outcome?

d) Are these techniques useful both as diagnostic and prognostic tools?

V – STUDIES INCLUDED IN THE THESIS

I.

Neuronal cell death in a rat model for mesial temporal lobe epilepsy is induced by the initial status epilepticus and not by later repeated spontaneous seizures

Gorter J.A. and Gonçalves Pereira P.M (*), van Vliet E.A, Aronica E, Lopes da Silva F.H, Lucassen P.J.

Epilepsia vol 44, (5) 647-58 **2003**.

(*) co-first authors for citation purposes

II.

Assessment of the preferred scout sagittal orientation for temporal lobe imaging with magnetic resonance

Gonçalves Pereira P.M, Oliveira E, Forjaz Secca M.

MAGMA Magnetic Resonance Materials in Physics, Biology and Medicine vol 18, (1) 19-25 **2005**.

III.

Magnetic resonance volumetric analysis of the piriform cortex and cortical amygdala in drug-refractory temporal lobe epilepsy

Gonçalves Pereira P.M, Insausti R, Artacho-Pérula E, Salmenperä T, Kälviäinen R, Pitkänen A.

AJNR American Journal of Neuroradiology vol 26, (2) 319-32 **2005**.

IV.

ADC-mapping of the hippocampus and the amygdala in pharmacoresistant temporal lobe epilepsy

Gonçalves Pereira P.M, Oliveira E, Rosado P.

AJNR American Journal of Neuroradiology (accepted for publication; to appear in February/March **2006**).

V.

Relative localizing value of amygdalo-hippocampal MR biometry in temporal lobe epilepsy

Gonçalves Pereira P.M, Oliveira E, Rosado P.

Epilepsy Research (submitted).

STUDY I.

Neuronal cell death in a rat model for mesial temporal lobe epilepsy is induced by the initial status epilepticus and not by later repeated spontaneous seizures

Gorter J.A. and Gonçalves Pereira P.M (*), van Vliet E.A, Aronica E, Lopes da Silva F.H, Lucassen P.J.

Epilepsia vol 44, (5) 647-58 **2003**.

(*) co-first authors for citation purposes

Epilepsia, **44**(5):647–658, 2003
Blackwell Publishing, Inc.
© 2003 International League Against Epilepsy

Neuronal Cell Death in a Rat Model for Mesial Temporal Lobe Epilepsy Is Induced by the Initial Status Epilepticus and Not by Later Repeated Spontaneous Seizures

*†[1]Jan A. Gorter, *[1]Pedro M. Gonçalves Pereira, *Erwin A. van Vliet, †‡Eleonora Aronica, *†Fernando H. Lopes da Silva, and *Paul J. Lucassen

**Swammerdam Institute for Life Sciences, Section Neurobiology, University of Amsterdam, Amsterdam; †Stichting Epilepsie Instellingen Nederland, Heemstede; and ‡Department of (Neuro)Pathology, Academic Medical Center, University of Amsterdam, Amsterdam, The Netherlands*

Summary: *Purpose:* To determine whether repeated seizures contribute to hippocampal sclerosis, we investigated whether cell loss in the (para) hippocampal region was related to the severity of chronic seizure activity in a rat model for temporal lobe epilepsy (TLE).

Methods: Chronic epilepsy developed after status epilepticus (SE) that was electrically induced 3–5 months before. The presence of neuronal damage was assessed by using Fluoro-Jade and dUTP nick end-labeling (TUNEL) of brain sections counterstained with Nissl.

Results: We found a negative correlation between the numbers of surviving hilar cells and the duration of the SE ($r = -0.66$; $p < 0.01$). In the chronic phase, we could discriminate between rats with occasional seizures (0.15 ± 0.05 seizures per day) without progression and rats with progressive seizure activity (8.9 ± 2.8 seizures/day). In both groups, the number of TUNEL-positive cells in parahippocampal regions was similar and higher than in controls. In the hippocampal formation, this was not significantly different from controls. Fluoro-Jade staining showed essentially the same pattern at 1 week and no positive neurons in chronic epileptic rats.

Conclusions: Cell death in this rat model is related to the initial SE rather than to the frequency of spontaneous seizures. These results emphasize that it is of crucial importance to stop the SE as soon as possible to prevent extended cell loss and further progression of the disease. They also suggest that neuroprotectants can be useful during the first week after SE, but will not be very useful in the chronic epileptic phase. **Key Words:** Necrosis—Apoptosis—Parahippocampal region—TUNEL—Fluoro-Jade—Sclerosis—Epileptogenesis—Progression.

Since the discovery that a specific neuropathologic syndrome of temporal lobe epilepsy (TLE) is associated with hippocampal mesial sclerosis, there has been a controversy whether the sclerosis is the cause or consequence of repeated complex partial seizures [reviewed in (1,2)]. Various reports on experimental TLE models, in particular the kindling model, suggest that repeated seizures cause progressive hippocampal damage (3,4). However, the kindling model is a model for repeated seizures in which seizures are triggered by electrical stimulation, whereas spontaneous seizures are rarely recorded. Moreover, kindling-induced damage is relatively mild, and the claim of cell loss due to repeated seizures is not always confirmed when cell densities are taken into account (5,6). Previous research in animal models in which chronic seizures developed after a pharmacologically or electrically induced status epilepticus (SE) have shown that extensive cell death occurs almost immediately after the SE in various brain regions (7–9). However, studies that investigated the effects of chronic seizures on cell death have relied mainly on morphologic/stereologic measurements (10,11), so that subtle seizure-induced cell loss might have remained undetected.

In this study we used the post-SE model in which an SE was induced by electrical stimulation of the angular bundle (12). By using continuous hippocampal EEG monitoring, we reported previously that the SE can produce two types of epileptic evolutions in the rats: (a) epileptic rats that display an increasing number of seizures after a latent period, called "progressive post-SE rats" (p-SE); and (b) epileptic rats that display only occasional spontaneous seizures without an increase in seizure frequency for ≥5 months after the SE, called

Accepted December 14, 2002.
Address correspondence and reprint requests to Dr. J. A. Gorter at Kruislaan 320, 1098 SM, Amsterdam, The Netherlands. E-mail: gorter@science.uva.nl
[1]Co-first authors for citation purposes.

"nonprogressive post-SE rats" (np-SE) (12). These two different groups offer the possibility to test the hypothesis that the number and frequency of spontaneous recurring seizures contribute to cell loss.

To investigate whether repeated spontaneous seizures contribute to the specific neuropathology, we used two different markers to detect neuronal loss/damage in combination with cell density counts (Nissl stain): terminal deoxynucleotidyl transferase–mediated biotinylated UTP nick end-labeling (TUNEL), which identifies apoptotic and necrotic neurons in situ, and Fluoro-Jade (FJ) staining that shows degenerating neuronal cells (13). With these methods, we determined the spatiotemporal relation between the extent of cell death during the chronic epileptic phase and the frequency of seizures on the one hand, and the duration of the initial SE, on the other.

MATERIALS AND METHODS

Experimental animals

Male Sprague–Dawley rats (Harlan CPB laboratories, The Netherlands) weighing 350–450 g were used in this study. The rats were housed in individual cages under a controlled environment (21 ± 1°C; humidity, 60%; lights on, 08.00–20.00 h). Food and water were available ad libitum. To record hippocampal EEG and to stimulate the angular bundle, a pair of insulated stainless steel electrodes was implanted under electrophysiologic control by using the following coordinates: 3.9 mm anterior–posterior (AP), –3.5 mm dorsoventral 1.7 mm mediolateral, nosebar –3.9 mm, for recording. For stimulation of the angular bundle, a pair of stainless steel electrodes was implanted (7.2 mm AP, 4.5 mm mediolateral). After the electrode implantation, the rats were individually housed for ≥2 weeks to recover from the operation. The rats were then transferred to the EEG recording cage, and a week after habituation to the new condition, the rats underwent a series of tetanic stimulations (50 Hz) of the hippocampus in the form of a succession of trains of pulses, each of 13 s. Each train had a duration of 10 s and consisted of biphasic pulses (pulse duration, 0.5 ms; maximal intensity, 500 μA), similar to the protocol of Lothman et al. (14). During the electrical stimulation, the behavior of the rat was observed, and stimulation was stopped when the rats displayed sustained forelimb clonus and strong salivation for minutes. This behavioral condition was usually reached within 1 h; if not, stimulation was continued, but it never lasted >90 min.

Differential hippocampal EEG signals were amplified (10×) via an FET transistor that connected the headset to an amplifier (50×; CyberAmp; Axon Instruments, Burlingame, CA, U.S.A.), filtered (1–60 Hz) and digitized by a Pentium computer. A seizure-detection program (Harmonie; Stellate Systems, Montreal, Quebec, Canada) sampled the incoming signal at a frequency of 200 Hz per channel, but because seizures were sometimes missed by automatic detection software, we recorded the EEG continuously. Every 24 h, recordings were interrupted briefly to transfer previous day's recordings to a central review computer. EEG recordings were reviewed afterward to quantify seizure frequency and seizure duration and stored on compact disks; this procedure was repeated daily until the rats were killed for histologic and immunocytochemical processing. The length of the electrographic seizures was measured by using the duration cursor in "Reviewer" software (Stellate Systems). Additional information concerning behavioral seizure activity was obtained by using video-monitoring. Days before killing, a video recording was made of each rat during 6 h, and the behavior during an electrographic seizure was scored according to the scale of Racine (15). Behavioral scoring also was performed when seizures were observed during the daily transfer of EEG recordings.

Usually, immediately after the termination of the stimulation, periodic epileptiform discharges (PEDs) at a frequency of 1–2 Hz were evident in the hippocampal EEG. If these rats displayed PEDs for ≥4 h without interruption after the electrical stimulation, we considered that the rats belonged to the SE group. Note that we did not include in this definition a criterion regarding the occurrence of behavioral seizures, because the latter could have a variety of forms of appearance whereas the EEG criterion was more reliable. Rats were intraperitoneally injected with pentobarbital (Nembutal; Sanofi Santé B.V, France; 60 mg/kg) 4 h after termination of the tetanic stimuli to avoid a severe and prolonged SE possibly leading to death. After recovery from the anesthesia (1–2 h), PEDs could still continue for many hours, but at this time, rats only showed several behavioral seizures. Rats in which the electrical stimulation did not induce SE were defined as belonging to the non-SE group. These rats experienced several stage IV–V seizures during stimulation but not immediately thereafter; after a latent period of about a month, a seizure is registered occasionally (12). Sham-operated electrode-implanted control rats (n = 11) were handled in the same way but not stimulated. The experimental protocols followed the European Communities Council directive 86/609/EEC and the Dutch Experiments on Animal Act (1997) and were approved by the University welfare committee.

Tissue preparation

At 4 h (n = 1 SE; 1 non-SE), 24 h (n = 6 SE; n = 4 non-SE), 48 h (n = 6 SE; n = 4 non-SE), 1 week (n = 7 SE; n = 4 non-SE), 4 weeks (n = 1 SE), 6 weeks (n = 3 SE), and 3–5 months (n = 25 SE; n = 5 non-SE) after electrical stimulation, rats were anaesthetized with pentobarbital (Nembutal, Sanofi Santé B.V., France; 60 mg/kg) and perfusion-fixed through the ascending aorta

with 0.37% Na_2S solution followed by perfusion of 4% paraformaldehyde in 0.1 *M* phosphate buffer (PB) and 0.2% glutaraldehyde (pH 7.4). After in situ postfixation overnight (at 4°C), the brains were dissected and transferred to 30% sucrose in PB. After one night at +4°C, the brains were dissected into two halves by a cut along the interhemispheric fissure and frozen at −20°C to −30°C in 2-methylbutane. Ipsilateral and contralateral midbrains were stored separately at −80°C. Age-matched sham-operated controls (n = 11) underwent the same procedures. Ipsilateral brain sections were cut on a cryostat at 20 μm and pasted directly onto glass slides (SuperFrost Plus; Menzel-Glaser, Merck, Amsterdam, Holland) and stored at −80°C until use. Contralateral sections were cut at 40 μm on a sliding microtome and stored in glycerol/DMSO at −25°C. Both sides were used for TUNEL and immunostaining. Counts at the contralateral site were corrected for section thickness by using a correction factor based on the control counts (i.e., the number of cells counted in the hilar region on Nissl stain at ipsilateral site divided by the contralateral site count).

TUNEL staining

To identify dying cells, TUNEL staining was applied on tissue sections from dorsal (−4.10 mm to –4.60 mm relative to bregma) and ventral (−6.82 mm to −7.34 mm) horizontal levels of the hippocampus, as described previously with minor modifications (16,17). Prostate sections of a castrated Wistar rat were included as positive control (18). In brief, after a short wash in 0.1 *M* PB, pH 7.4, mounted sections were placed in plastic jars, filled with 0.05 *M* citrate buffer, pH 6.0, and pretreated in a microwave oven for 5 min at 800 W, after which the jars were allowed to cool for 20 min (19). Slides were then washed twice with 0.01 *M* PB saline (PBS), pH 7.2, and preincubated in proteinase K (PK) buffer (10 m*M* Tris/HCl; 2.6 m*M* $CaCl_2$; pH 7.0), followed by 20 μg/ml PK (Sigma Aldrich, Zwijndrecht, Holland) in PK buffer for 15 min at room temperature (RT), washed and incubated with terminal deoxynucleotidyl transferase (TdT) buffer (1 *M* sodium cacodylate, 0.125 *M* Tris/HCl in 1.25 mg/ml bovine serum albumin (BSA); pH 6.6) for 15 min at RT before incubation for 60 min at 37°C in TdT buffer, containing per 100 μl, 0.2 μl TdT (Boehringer Mannheim, Germany), 0.5 μl biotin-16-dUTP (Boehringer Mannheim, Germany), and cobalt chloride (25 mmol; 5% of the final volume). After rinsing in PBS (pH 7.4), endogenous peroxidase was blocked with 3% hydrogen peroxide (H_2O_2) in PBS, and sections were preincubated with PBS/1% BSA before peroxidase-conjugated avidin (ABC-Elite kit; Vector Laboratories, Inc., Burlingame, CA, U.S.A.) 1:1,000 in PBS/1% BSA for 1.5 h at RT. Labeled DNA was visualized with 10 mg/ml diaminobenzidine (DAB; Sigma Aldrich, Zwijndrecht, Holland) in 0.05 *M* Tris/HCl (pH 7.5) with 0.02% H_2O_2, during which DAB development was monitored continuously. Sections were then washed and counterstained with cresyl violet.

Fluoro-Jade staining

Horizontal sections of control (n = 4), 1 week (n = 5), 6 weeks (n = 3), and 3–5 months post-SE rats (n = 8) and non-SE rats (n = 4) were stained with FJ by using the method described by Schmued et al. (13). Sections were mounted onto Superfrost Plus slides and dried overnight (37°C). They were immersed in absolute alcohol for 3 min followed by 70% ethanol for 1 min and distilled water for 1 min. The slides were transferred to 0.06% potassium permanganate for 15 min. After rinsing with distilled water (1 min), the slides were transferred to a 0.001% FJ solution (Histo-Chem, Inc., Jefferson, AR, U.S.A.) made in 0.1% acetic acid. Slides were rinsed in water, dried at 37°C, immersed in xylene, and coverslipped with entallan. Sections were analyzed with a laser scanning confocal microscope (Bio-Rad, MRC1024, Hercules, CA, U.S.A.).

Double immunofluorescence

To reveal the cellular identity, a subset of free-floating sections was double labeled by using fluorescent TUNEL that followed incubation with primary antibodies (Abs) against glial fibrillary acidic protein (GFAP; monoclonal mouse, Boehringer Mannheim, Germany; 1:500) as astrocyte marker, anti-rat CD11b/c (monoclonal mouse, OX42; Pharmingen, CA, U.S.A.; 1:100) as microglia marker, and NeuN (Mouse clone MAB377; Chemicon, Temecula, CA, U.S.A.; 1:1,000 all in PBS-BSA + 0.1% Triton) as neuronal marker.

Fluorescent TUNEL was identical as described earlier, except for the biotin-16-dUTP that was replaced with fluorescein-12-deoxy-UTP (Boehringer) and the TdT and PK concentrations were reduced to 50%. Primary antibodies were incubated overnight, and after washing, sections were incubated with CY3 goat anti-mouse immunoglobulin G (IgG) antisera (Zymed, San Francisco, CA, U.S.A.; 1:200), washed and mounted on Superfrost Plus slides for subsequent TUNEL staining. Sections were embedded in Vectashield and analyzed with a laser scanning confocal microscope (Bio-Rad, MRC1024, Hercules, CA, U.S.A.) equipped with argon-ion laser. In a subset of sections, we used NeuN (as neuronal marker) or OX42 (as microglial marker) immunostaining (with CY3 goat anti-mouse IgG antisera (Zymed, San Francisco, CA, U.S.A.; 1:200) followed by incubation with FJ.

Quantification of neuronal loss (Nissl stain)

The extent of structural cell loss in Nissl-stained sections in various brain regions of the ipsilateral and contralateral hemispheres was assessed at ×400 magnification by using grid morphometric techniques. Two sections per rat and per level (dorsal, ventral) were quantified. To avoid confusion with glial cells, neurons were

defined as profiles >10 μm (hilus) or 7 μm (cortex) having an identifiable nucleolus. An ocular grid consisting of 5 × 5 box segments (240 × 240 μm), was placed over the region of interest. For the entorhinal cortex (EC) layer, the medial part was analysed (mEC). Boundaries of each region were taken from the recent description of the hippocampal formation (20). The anterior piriform cortex was evaluated at the ventral level (–7.1 mm to –7.4 mm relative to bregma; see also diagram in Fig. 3E). Layer II, III, dorsal endopiriform nucleus, and claustrum were separately analyzed. For the different cortical layers, a linear 1 × 5 box was used. Typically nearly all of any specific layer would be included in the field. For hilar cell counts, a slightly different technique was used. To express the results as cell densities, we measured the hilar area by using Scion Image software (Scion Corporation, Maryland, U.S.A.) over digital images (camera HCS MXR Vision Technology, The Netherlands). The hilus was defined as the inner border of the granule cell layer (GCL) together with the area formed by two imaginary straight lines connecting the two tips of the GCL with the proximal end of the CA3c area. The number of hilar neurons was counted at ×200 magnification. Final neuron counts were calculated as the number of neurons per square millimeter. It should be emphasized that our neuron-counting methods are relative estimates and not absolute calculations of the number of hippocampal (parahippocampal, etc.) neurons. The neuron counts as used in this study can be considered reliable relative estimates at the specific dorsal and ventral level. Statistical differences in neuron counts between groups of animals can be accurately determined.

Quantification of TUNEL-positive cells

TUNEL-positive cells were quantified in the different hippocampal subfields as well as in the parahippocampal region and anterior piriform cortex (layer II, layer III, and dorsal endopiriform nucleus) of both hemispheres. Quantification was performed at ×400 magnification with a microscope rectangular grid. Two sections per level and per rat were analyzed. To account for tissue changes (swelling and/or shrinking), we measured the areas of the different regions (hippocampus, hilus, and the parahippocampal region) by using Scion Image software. TUNEL-positive cell numbers were then expressed as densities per region. Because the number of TUNEL-positive cells was very low in control and chronic epileptic rats, the number of cells also was expressed per region in a dorsal/ventral section. The parahippocampal area included the presubiculum, parasubiculum, the six-layered medial and lateral entorhinal cortex (mEC and lEC). Within the hippocampus, TUNEL cell counts were performed in the DG, CA1-3, and subiculum. To obtain the local distribution of TUNEL-positive cells in hippocampal and parahippocampal region and anterior piriform cortex, the labeled cells were plotted from sections with the aid of camera lucida and drawn in diagrams obtained from *The Rat Brain* atlas (21). In several rats, TUNEL distributions were compared with a FJ stain distribution in a consecutive brain section.

Statistics

Mean values and SEMs were calculated. Differences in mean values were determined by use of one-way analysis of variance (ANOVA) followed by a post hoc test (Bonferroni, $p < 0.05$) or Kruskal–Wallis test followed by a Mann–Whitney test ($p < 0.05$). Statistics were determined from the raw data. Data on cell densities were normalized to the control densities (100%); a correlation between two ordinal variables was calculated by using a Spearman rank correlation test ($p < 0.01$) with statistics software (SPSS, Inc., for Windows, release 10).

RESULTS

Relation between duration of the SE and neurons in the hilar region

The SE was stopped after 4 h, but PEDs reappeared again after some time and could continue for several hours afterward. SE duration was quantified based on the duration of the period during which PEDs occurred in 17 rats that had developed a progressive form of epilepsy (p-SE rats; six of which were submitted to TUNEL evaluation) and in nine rats that had developed a non-progressive form of epilepsy (np-SE rats; seven of which were evaluated with TUNEL) starting after the stimulation was stopped. The SE duration and number of daily seizures (during the last 2 weeks of EEG recording before killing) for individual p-SE and np-SE rats are indicated in Fig. 1A; the corresponding mean SE duration for each group is indicated in the inset. The average SE duration appeared to last 1.7 times longer in p-SE rats (7.0 ± 1.1 hs in np-SE and 11.8 ± 0.9 h in p-SE rats; Student's t, $p < 0.001$). The average duration of an individual seizure also was measured. During the last 2 weeks before killing, seizures lasted at average ~1 min, (72 ± 4 in np-SE rats and 58 ± 5 s in p-SE rats; $p < 0.01$). In chronic epileptic rats, at 3–5 months after SE, Nissl cell counts indicated that there was a significant negative correlation between the number of hilar cells and the duration of the SE (Fig. 1B; Spearman rank correlation, $r = -0.66$; $p < 0.01$).

Nissl densities in hippocampal and extrahippocampal regions

First we evaluated cell loss quantitatively by analyzing Nissl cell densities in selective hippocampal and extrahippocampal regions at different times after the SE. More specifically, we analyzed the hilus at dorsal and ventral levels, mEC layers II, III, and V/VI at the ventral level, and anterior piriform cortex including dorsal endopiriform nucleus and claustrum at the ventral level.

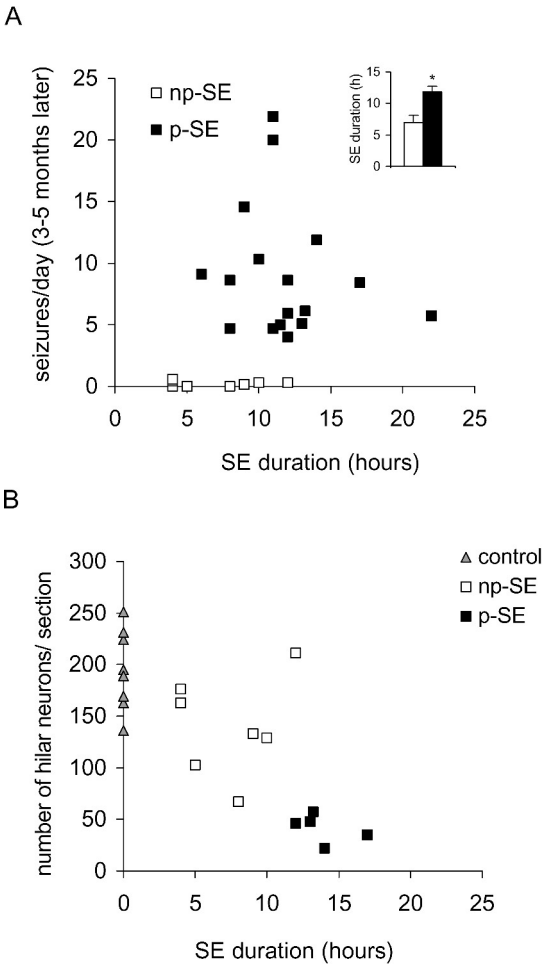


FIG. 1. **A:** Relation between the duration of the status epilepticus (SE) and the later individual seizure activity in progressive epileptic rats (solid squares) and nonprogressive epileptic rats (open squares) during the last 2 weeks before perfusion. The average group data (inset 1A) indicate that rats with a progressive form of epilepsy had a significant longer SE than did rats with a nonprogressive form of epilepsy. **B:** Relation between the duration of the SE and the number of hilar Nissl cells at dorsal hippocampus after SE. There is a significant negative correlation ($r = -0.66$; $p < 0.01$) between the duration of the SE and the hilar cell number of the three groups.

Figure 2 shows changes in Nissl cell counts after SE on the ipsilateral site. There was a dramatic reduction in Nissl cell density within 1–2 days after SE at the ipsilateral hilus (A), mEC layer II/III (C), and layer II of the piriform cortex including the dorsal endopiriform nucleus/claustrum (E). Layers V/VI of the mEC and the deep layer of the piriform cortex were not significantly affected at this ventral level (7.1–7.4 mm below bregma). At more ventral levels, all piriform cortical layers (anterior and posterior) were very severely affected and almost completely filled with vimentin-positive astrocytes (not shown). These Nissl density measurements suggested that cell loss did not increase further beyond 1 week after SE. In other areas including the midline thalamic nuclei, perirhinal cortex, septal areas, and amygdaloid nuclei, cell loss was also observed during the earlier time points, but these areas were not further analyzed in detail. On the contralateral side, cell-density changes were essentially the same or slightly less than observed ipsilaterally, except in the hilus and piriform cortex, in which the reduction of cell density was far less dramatic in rats that had developed a nonprogressive form of epilepsy versus rats with a progressive form of epilepsy [see also (12)]. In sections of non-SE rats, no significant change in cell density was observed in the entorhinal cortex (not shown) and piriform cortex (Fig. 2F).

Evolution of TUNEL/Fluoro-Jade staining in hippocampal and extrahippocampal regions after SE

TUNEL analysis in hippocampal and parahippocampal regions of controls revealed only a few positive cells. In stimulated rats, TUNEL cell numbers varied considerably over time, as did their morphology. During the first week, cells that were TUNEL positive showed mainly a shrunken morphology, whereas at later times (>3 months), the few cells that were TUNEL positive revealed sometimes apoptotic bodies. All TUNEL cells were quantified irrespective of their morphologic appearance. As indicated in Fig. 3A and B, TUNEL cell numbers were already robustly increased at 1 day after stimulation. The numbers reached a peak within 1 week after SE in all subregions of the hippocampus. After that, TUNEL cell numbers dramatically decreased. No significant difference was seen between the amount of stained cells at the dorsal and the ventral levels of the hippocampus or between ipsi- and contralateral sides (data not shown). Examples of the TUNEL labeling are shown in Fig. 4A (gcl, control) and 4B and C (CA3, CA1, 1 week after SE). In chronic epileptic rats (3–5 months after SE), the number of TUNEL cells in the hippocampus was low and not statistically different from that in control rats. In rats that had not experienced SE (non-SE rats), there was a small but nonsignificant increase of TUNEL cells during the first week after SE (Fig. 3C).

TUNEL positivity in the parahippocampal region also showed a large increase during the first week after SE (Fig. 3B), but the evolution was somewhat different compared with hippocampus. Most TUNEL positivity appeared during the first days after SE. Extensive TUNEL labeling in entorhinal cortex 1 week after SE was found mainly in layer III and parasubiculum where cell loss is prominent. In the anterior piriform cortex, cell death also was extensive during the first week and more extensive in layer II than in layer III (Fig. 3E; 6B and C). In the dorsal endopiriform nucleus, TUNEL labeling was extensive during the first week (Fig. 3E).

In epileptic non-SE rats that had not experienced SE after electrical stimulation, an increase of TUNEL cells was observed in the ventral parahippocampal region dur-

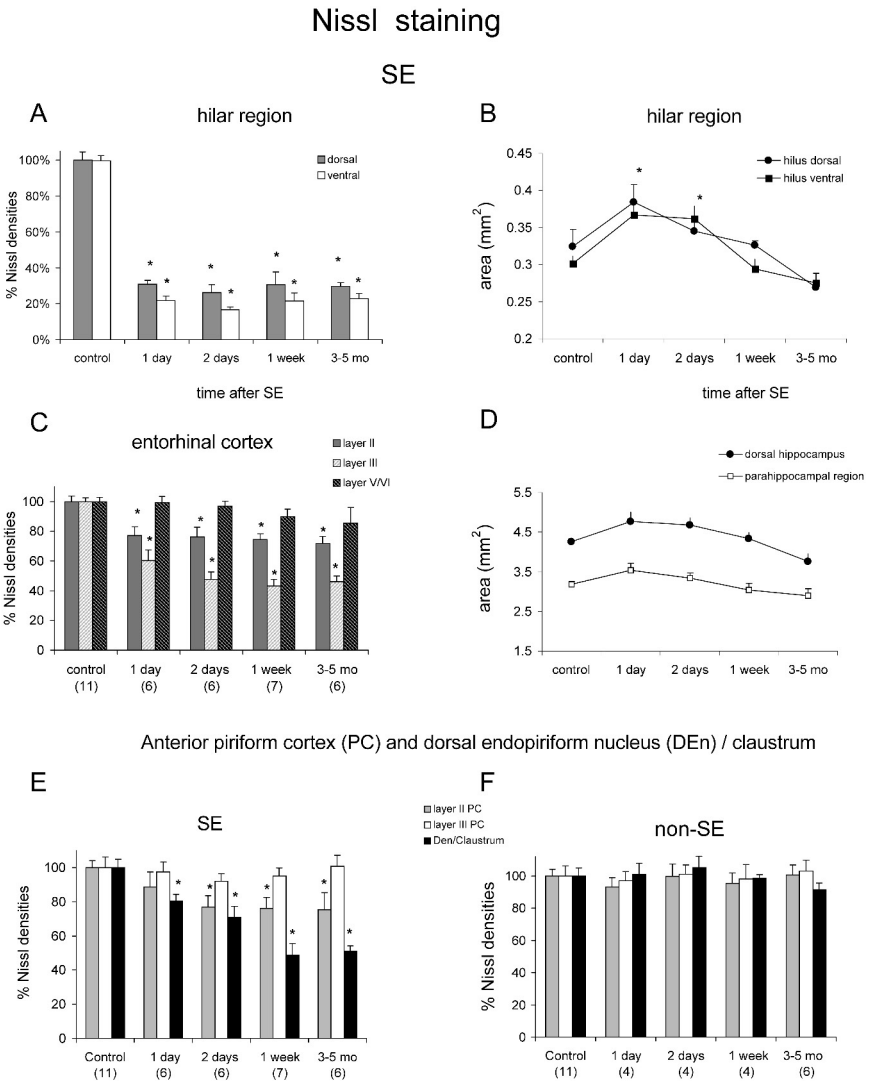


FIG. 2. Evolution of Nissl cell densities after status epilepticus (SE). **A:** Ipsilateral hilar cell densities in dorsal and ventral hippocampus. **B:** Changes in dorsal and ventral hilar surface areas after SE. **C:** Evolution of Nissl cell densities in each layer of the medial entorhinal cortex. **D:** Changes of total surface area of the hippocampus and parahippocampal region after SE. **E, F:** Changes of Nissl cell densities in layers of the anterior piriform cortex and dorsal endopiriform nucleus and claustrum in post-SE **(E)** and non-SE rats. Control densities are normalized to 100%. *Significantly different from control value; Bonferroni $p < 0.05$).

ing the first week after SE, which was significant at 1 week after stimulation (Fig. 3D). Non-SE rats did not show increased numbers of TUNEL cells at later times (3–5 months).

The fact that a large number of TUNEL cells was present during the first week after SE led us to investigate whether these cells were astrocytes or microglial cells, because particularly these cell types proliferate extensively during the first week after SE (22,23). After double immunolabeling of TUNEL with NeuN, GFAP, and OX42 (identifying neurons, astrocytes, and microglia, respectively), no double labeling could be detected for any of these markers. Reactive microglia enwrapping TUNEL-labeled cells was frequently observed (Fig. 4C).

FJ staining of brain sections of post-SE rats showed essentially the same pattern as observed with the TUNEL labeling (Compare Fig. 4B–E and 4C–F). The advantage of the FJ stain lies in the fact that the neuronal morphology still can be visualized, including dendritic processes (see, for instance, Fig. 4F and H). Despite the clear neuronal morphology, double labeling of post-SE sections with NeuN showed that FJ-positive cells were not still recognized by the antibody (e.g., Fig. 4 H and I). In the same sections, the granule neurons were NeuN positive.

Chronic seizure activity and cell death

SE can lead to distinct evolution of spontaneous seizure activity with either a progressive increase of seizure activity in 67% or a nonprogressive form in 33% of the rats (12). We investigated tissue of p-SE rats ($n = 6$) and np-SE rats ($n = 7$) and compared this with tissue of non-SE rats ($n = 2$; these also experience a nonprogressive form of epilepsy after a longer latent period) and control tissue ($n = 11$, age matched). Figure 5 shows the relation between individual seizure activity, expressed as the number of daily seizures during the last 2 weeks before perfusion, and the number of TUNEL cells encountered in hippocampal (A) and parahippocampal sec-

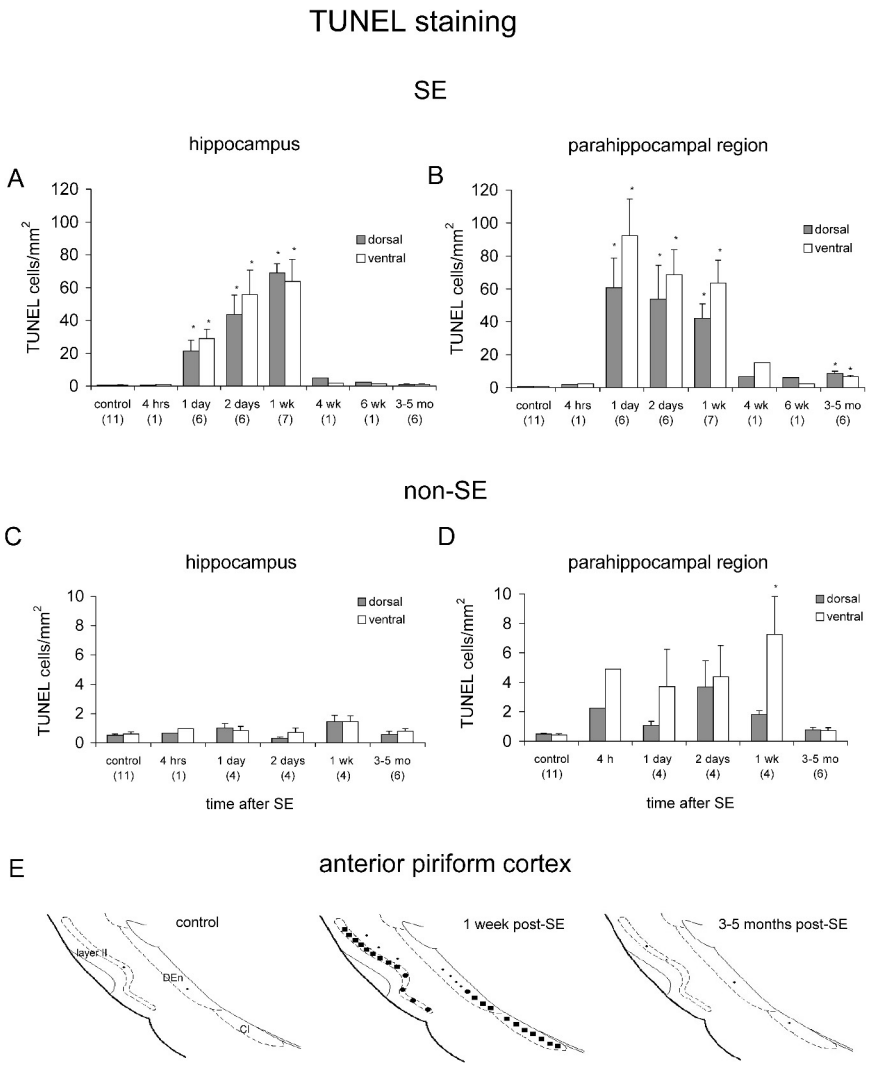


FIG. 3. Quantification of TUNEL-positive cells (TUNEL cells) in the hippocampal and parahippocampal region. **A:** Development of the pattern of TUNEL cells (expressed as density: number per mm^2) in the dorsal and ventral hippocampus (ipsilateral) at different times after status epilepticus (SE). **B:** Cell loss in the parahippocampal region occurs also during the first week but with a somewhat different pattern from that in the hippocampus. **C:** Evolution of TUNEL positivity in the hippocampal region of non-SE rats. **D:** Evolution of TUNEL positivity in the parahippocampal region of non-SE rats. During the first week after stimulation, no change is seen in the hippocampus, but an increase in TUNEL cells occurs in the parahippocampal region (note different scale compared with A, B). **E:** Schematic diagrams showing an overview of the distribution of TUNEL-positive cells in the different layers of the anterior piriform cortex and the dorsal endopiriform nucleus (Den)/claustrum (Cl). *Significantly different from control; Bonferroni $p < 0.05$).

tions (B) of the three groups (indicated with different symbols), including the control group. In the chronic phase, TUNEL cell numbers were very low, but they could be encountered in all regions including the relatively seizure-resistant GCL and presubiculum. The averages of the hippocampal and parahippocampal TUNEL-positive cell counts (here expressed as TUNEL cells per region) and several seizure-activity parameters of each group are shown in Table 1. TUNEL cells were not increased in p-SE rats with more frequent and more recent seizures compared with rats of the np-SE group. In the hippocampus, the number of TUNEL cells was quite comparable between the two epileptic post-SE groups and tended to be slightly (not significantly) higher than that in controls. In the parahippocampal region, the number of TUNEL cells was comparable for both post-SE groups but considerably higher than in controls ($p < 0.05$; Table 1). In non-SE rats that also experienced chronic seizures without progression, TUNEL cell numbers were comparable to those of controls.

FJ stain corresponded largely to the TUNEL stain, as shown by others (24,25), especially during the first weeks after SE (compare Fig. 4B and 4E). FJ stain in 6-week post-SE rats still revealed some positive cells in the CA1-3 region (Fig. 4J) and the piriform cortex (Fig. 6D). They were positioned in the pyramidal cell layer and did not colocalize with microglia (Fig. 4J). In sections of rats of >3 months, no individual neurons were labeled anywhere in the hippocampus (Fig. 4L) and parahippocampal region in dorsal and ventral brain sections. In some ventral sections, there was still increased fluorescence in piriform cortex, but individual cells with neuronal morphology were not observed. In several regions (hilus, parasubiculum), though, FJ-positive cells with astrocyte-like morphology were observed (Fig. 4K).

DISCUSSION

The new and most important finding of this study is that (para)-hippocampal cell loss is related not to the

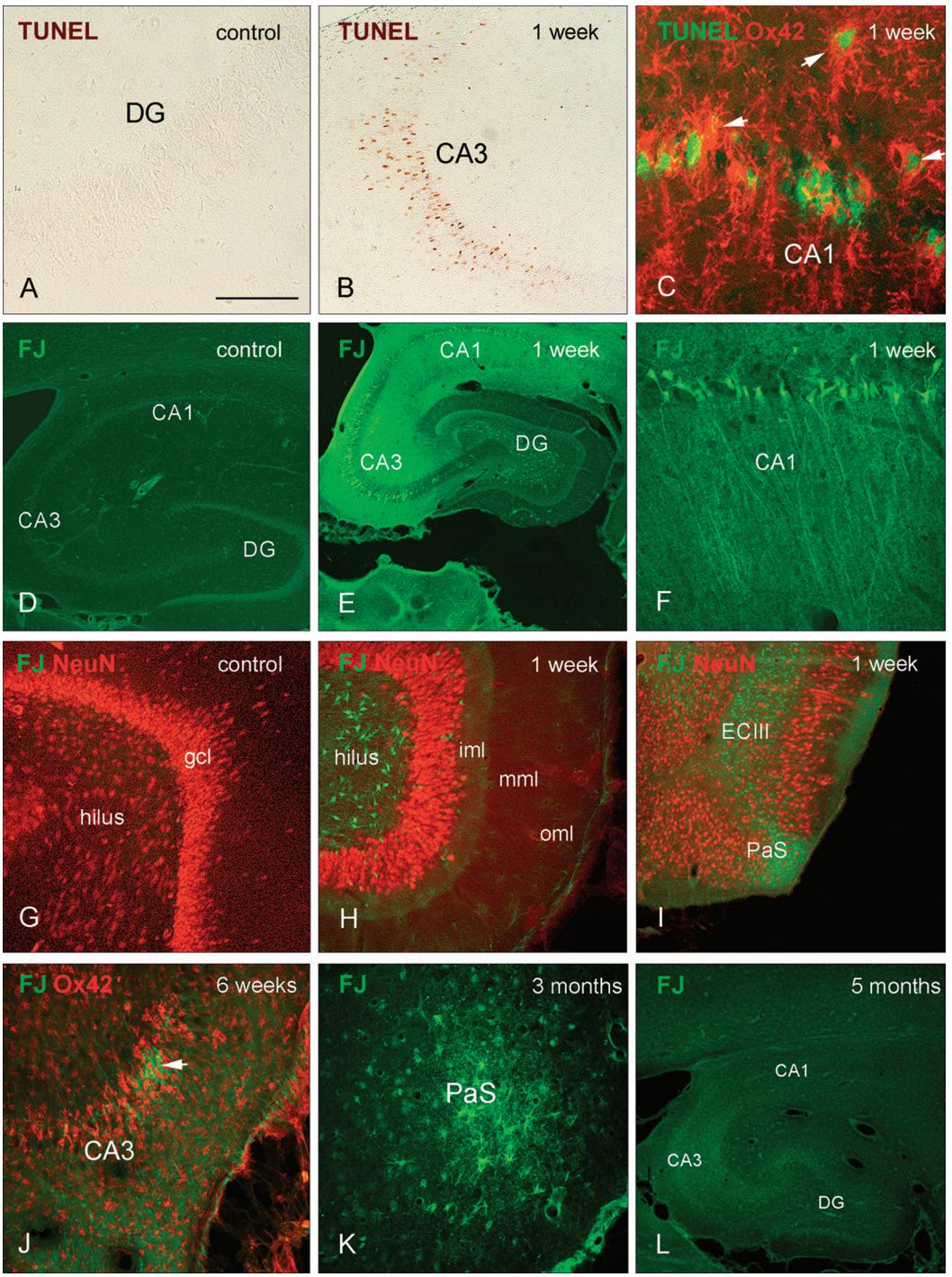


FIG. 4. Examples of TUNEL and of Fluoro-Jade (FJ) staining in (para)hippocampal sections of control rat **(A, D, G)** and rats at different times after status epilepticus (SE). **A–C:** TUNEL staining: **(A)** no labeling in control DG; **(B)** a large number of CA3 neurons are also TUNEL positive, corresponding to the FJ stain of the same 1-week post-SE rat, as shown in E. **C:** TUNEL staining in CA1 at 1 week after SE shows a fluorescent stain of OX42 (marker for microglia, in red) and TUNEL (green); white arrows indicate reactive microglia enwrapping TUNEL-labeled cells. **D–F:** Examples of an FJ stain; in a control rat **(D),** there is only a background stain. **E:** FJ stain of a hippocampal area at 1 week after SE with increased fluorescence in CA1–CA3 and hilar neurons. **F:** CA1 neurons show somatic and dendritic staining with Fluoro-Jade. **G–I:** Double labeling of FJ (green) and NeuN (red). **G:** Detail of dentate gyrus (DG) with hilar cells and granule cell layer (gcl). **H:** Details of the DG including the GCL of a 1-week post-SE rat. Note that most hilar neurons are FJ positive but do not stain for NeuN. **I:** Detail of parahippocampal region of the same 1-week post-SE rat, showing multiple FJ-positive cells in layer III of the entorhinal cortex and parasubiculum but no double labeling with NeuN. **J:** FJ-positive CA3 neurons surrounded by activated microglia at 6 weeks after SE. **K:** FJ staining in parasubiculum at 3 months post-SE with FJ-positive staining of astrocytes. **L:** FJ stain in hippocampal section of rat that displayed 12 seizures per day shows no neuronal labeling anywhere in the hippocampus. Bar in **A**, 100 μm for **A** and **K**; 200 μm for **B, F, G**, and **H, J**; 75 μm for **C**; 400 μm for **D-E, I** and **L**.

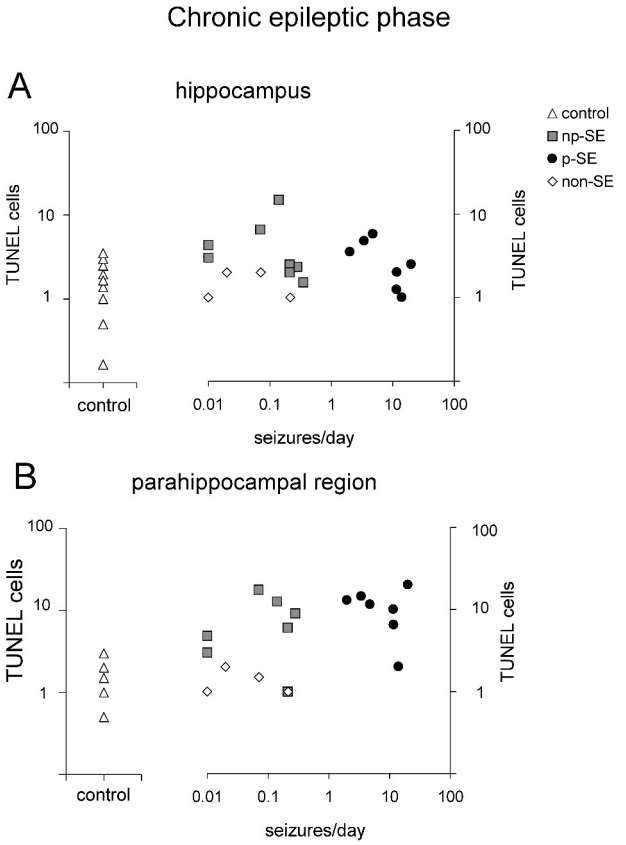


FIG. 5. Relation between individual seizure activity (expressed as seizures per day during the last 2 weeks of EEG recording) and the individual number of TUNEL cells in the dorsal hippocampus **(A)** and parahippocampal region **(B),** respectively (expressed as TUNEL cells per section). Numbers of hippocampal TUNEL cells in np-SE, p-SE, and non-SE rats overlap with controls and are not significantly different from each other. In the parahippocampal region, significantly more TUNEL cells are encountered in the np-SE and p-SE rats than in control rats (Mann–Whitney, $p < 0.05$). The two non-SE rats are in the range of controls.

frequency of spontaneously occurring seizures, but rather to the duration of the initial SE. Furthermore, we show that the majority of cells that die as a consequence of the initial SE, degenerate in the course of the first week after SE, which is in agreement with previous reports (9,26–29). Finally, the extent of hilar cell death is related to SE duration and to the later progression of the disease. These findings extend previous reports because we investigated a longer time period, including both the latent period (first week after SE) and the chronic epileptic phase (3–5 months after SE). These findings can have important implications for the management of TLE, in particular, with respect to the timing of the treatment with neuroprotectants.

Duration of status epilepticus and cell death

In our model, most TUNEL- and FJ-positive cells were encountered during the first week after SE. Cell death was more obvious in specific regions (hilus, EC layer III) but occurred in all regions investigated. A significant negative correlation was seen between the number of surviving hilar neurons and SE duration. Interestingly, rats that experienced a shorter SE appeared to have a better prognosis to develop a nonprogressive form of epilepsy (Fig. 1A). Although the exact pathway remains controversial, both apoptotic and necrotic cell death occur after SE (29–32), and cells with both apoptotic and necrotic morphology were found in our current model as well. This issue might be relevant for therapeutic intervention because neuronal degeneration could be attenuated by inhibition of caspase-3–like enzyme activity (33). The Nissl density counts indicated that the decrease in density was obtained within the first day after SE with no significant change thereafter, suggesting that cell loss beyond 1–2 days after SE is minimal. However, because the hilar area is larger at these times, indicating swelling of tissue, a considerable additional number of cells die during the first week. Even at 6 weeks after SE, a significant number of TUNEL/FJ-positive neurons were still observed. This illustrates that stereologic measurements alone are not sufficient to assess whether cell loss occurs. Our finding that the majority of degenerating cells die during the first week suggests that the time window for a possible intervention to influence the epileptogenic process could last for at least several days in this rat model.

The fact that the pattern of TUNEL-labeled cells largely corresponded with the pattern of FJ-stained cells with clear neuronal morphology emphasizes that it is likely that the majority of TUNEL-labeled cells also were neurons. We were not able to double-label these cells with glia markers in similar tissue. However, in our hands, double labeling of FJ-positive cells with NeuN also was not possible, although the cells had a clear neuronal morphology including dendritic processes (13). This may relate to the fact that TUNEL- or FJ-positive cells in this stage of their death have lost their protein markers and therefore cannot be identified by double-label immunocytochemistry. Apparently during the first week after SE, increasing and additional numbers of neurons show DNA fragmentation and are not removed immediately. In view of the high number of TUNEL-positive cells during the first week after SE, it is at least likely that these labeled cells have a more extended expression than generally thought.

Brief spontaneous seizures do not cause cell death

At first glance, the increased number of TUNEL cells encountered in p-SE rats might suggest that the occurrence of seizures indeed contributes to progression of cell death. However, this is not the case, taking into consideration the following findings: (a) rats with frequent progressive seizure activity (more than eight seizures per day) had their last seizure within several hours

TABLE 1. *Overview of important EEG parameters and the number of TUNEL-positive cells in the dorsal and ventral hippocampal and parahippocampal region sections*

	n	Days after SE	Lifetime seizures	Seizures/day last 2 wk	Time since last seizure (d)	TUNEL cells dorsal hippocampal section	TUNEL cells ventral hippocampal section	TUNEL cells dorsal parahippocampal section	TUNEL cells ventral parahippocampal section
Control	8	—	0	0	—	1.9 (0.5–3.5)	1.2 (0–2)	1.4 (0.5–3)	0.9 (0–1.5)
Non-SE	2	157.5 ± 7.5	16.0 ± 2.0	0.14 ± 0.07	6.32 ± 3.21	1.5 (1–2)	2.25 (2–2.5)	1.25 (1–1.5)	1.75 (1–2.5)
np-SE	7	111.4 ± 9.7	22.1 ± 6.7	0.15 ± 0.05	20.4 ± 15.8	5.0 (2.5–15)	3.3 (0.5–6)	8.8 (3–17.5)[b]	5.7 (3–10)[b]
p-SE	6	104.7 ± 7.8	557 ± 178[a]	8.9 ± 2.8[a]	0.14 ± 0.07[a]	3.3 (1.5–6)	4.1 (1.5–12)	11.1 (6.5–20)[b]	10.2 (4.5–16)[b]

Ipsi- and contralateral site are pooled and expressed as cells per region. Ranges of cell counts are indicated between brackets. Statistical comparisons of seizure parameters are made between np-SE and p-SE groups (Student's t, [a]$p < 0.01$). Statistical comparisons of TUNEL data are made between np-SE or p-SE group and the control group (Mann–Whitney, [b]$p < 0.05$).

before perfusion. Nevertheless they did not have more TUNEL-positive cells in the hippocampal or parahippocampal region than did rats that had their last seizure several days before perfusion (Table 1), with on average only one to two seizures per week; (b) rats that had not had SE (non-SE) showed significantly fewer TUNEL cells in these areas than did either of the post-SE groups, although they had had a comparable number of seizures during their lifetime to those of the np-SE rats; (c) with FJ, we did not observe any positively labeled neurons in rats at >3 months, suggesting that the TUNEL-positive cell counts may include some nonneuronal elements as well. These data indicate that the increased TUNEL labeling is a consequence of the aftermath of the SE and not of the individual seizure activity. The FJ staining strengthens this conclusion even more, because no individually damaged neurons were found in 3–5 months post-SE rats. Because the window for which the cells would be TUNEL/FJ-positive may be only a few hours, one could argue that we have missed ongoing cell death because of the limited sampling of TUNEL- and/or FJ-positive neurons in the chronic epileptic phase. However, the fact that rats with progressive seizure activity had an average 8.9 seizures per day (Table 1) means that the mean interval between seizures was 2.7 h. Nevertheless, the rats did not show increased positivity in comparison

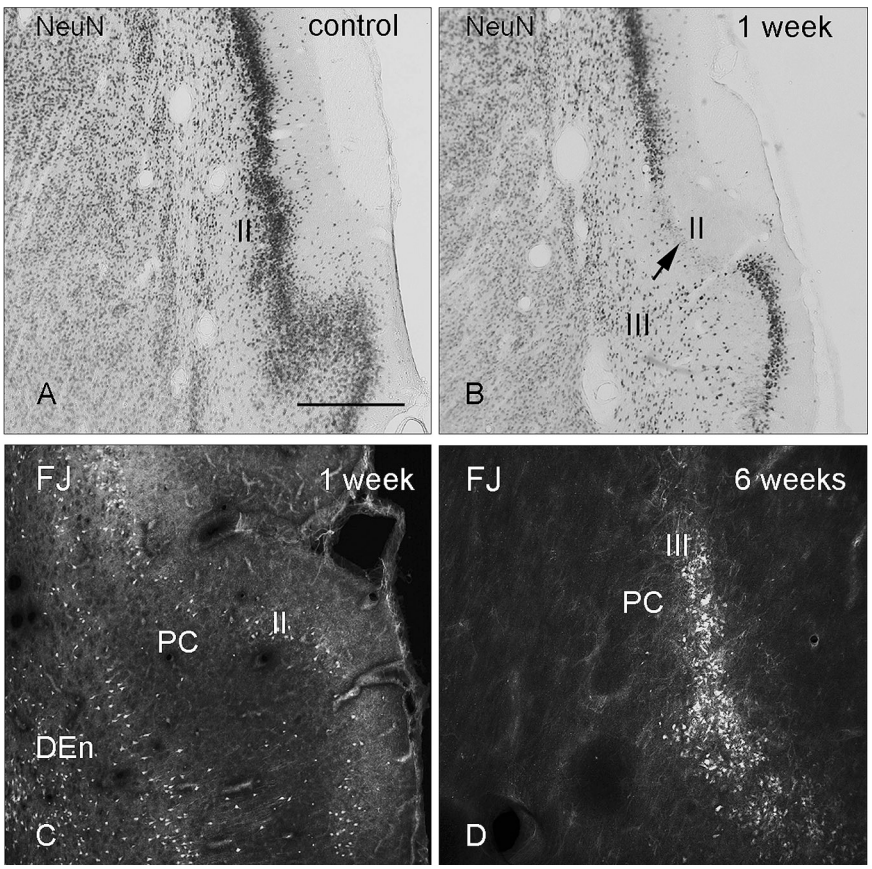


FIG. 6. Immunostaining for neuronal marker NeuN in anterior piriform cortex in control **(A)** and 1-week post-status epilepticus (SE) rat **(B).** Arrow, extensive cell loss. **C:** Fluoro-Jade (FJ) staining of anterior piriform cortex showing labeling of layer II and dorsal endopiriform nucleus at 1 week after SE. **D:** FJ labeling of layer II/III of the piriform cortex 6 weeks after SE. Calibration bar in **A:** 500 μm in **A, B**, and 100 μm in **C** and **D**.

to rats that had their last seizure several days before death ("nonprogressive"). Therefore we think that it is not very likely that TUNEL/FJ positivity could have been missed because of a too-long time interval after the last seizure. Moreover, the fact that we did not find a further decrease in neuronal densities argues also against this point. Our data contrast to what has been reported in pilocarpine-treated rats, in which rats with multiple seizures had more damaged neurons than did animals with single seizures (34). This discrepancy might be related to the different staining technique or to other factors (shorter time window after the initial SE used in the latter study). However, our findings are in agreement with a recent study that appeared during revision of our article, in which similar staining techniques were used in tissue of chronic epileptic rats (35). Cell damage 2 months after kainate-induced SE also was observed in CA1, thalamus, and piriform cortex, using the FJ B staining method (36). At this time, we still found increased fluorescence in piriform cortex, but individual cells with neuronal morphology could not be discriminated. Astrocytes in severely affected regions such as hilus and parasubiculum also showed increased fluorescence. This might reflect astrocytic activation (36).

Our findings show that the extent of cell death in the chronic epileptic phase in our rat model is not related to the frequency of spontaneous seizures. Previous studies had indicated that electrically evoked seizures actually cause progressive cell loss, suggesting that hippocampal sclerosis in human epilepsy may be acquired as a consequence of repeated seizures (2,3,37,38). Apparently neurons are more sensitive to seizures evoked by electrical stimulation than to spontaneously occurring seizures. However, the previously published kindling studies associated neuronal loss with stage 5 or greater seizures. These are very robust significant seizures with secondary generalization and perhaps secondary hypoxic ischemia during the events. In humans, an association with hippocampal neuronal loss and the presence of secondarily generalized seizures was found (39). In all rats that we included in this study, we observed generalized tonic–clonic seizures [stage 4–5 on the scale of (15)] during the chronic epileptic phase, although partial seizures also were observed. Therefore, we cannot exclude that the difference between these studies may relate to the severity of the evoked or spontaneous seizure. Our present findings indicate that seizures do not lead to cell death when they occur spontaneously and are generalized with restricted duration (on average, 1–2 min). This suggests that the sclerosis is likely related to events other than the frequency of spontaneous seizures. Accordingly, it is possible that in human patients, hippocampal sclerosis is induced by a previous brain insult or by some kind of predisposition. This latter possibility is supported by the observation of a preexisting hippocampal lesion, as encountered by using magnetic resonance imaging (MRI) studies in humans (40,41).

Notwithstanding these observations, several longitudinal MRI studies suggested that a progressive decrease of hippocampal volume may result from the cumulative effect of brief recurrent seizures in humans (42–45) and in pilocarpine-treated rats (46). Nevertheless, a decrease in hippocampal volume was found in only four of 33 epilepsy patients in a 3.5-year follow-up study (47). Moreover, it must be realized that a reduction in volume does not necessarily indicate neuronal loss. Shrinkage of neurons and surrounding cells could also contribute to the observed volume reductions. In addition, it is not clear from patient studies whether the TLE syndrome is the only underlying etiology and/or whether medication can have an effect on hippocampal volumes. We should note that the duration of the epilepsy in the rat model is quite different from that in the human. Although the time scales are very different, we may assume that a 3- to 5-month post-SE rat is comparable with a patient that has TLE for a couple of years.

CONCLUSIONS

In conclusion, our data indicate that cell death is not related to seizure frequency when seizures occur spontaneously and are of restricted duration. Therefore it is unlikely that drugs that interfere with cell-death pathways or reorganization will be of any use at the chronic epileptic phase, if seizures are relatively short (<2 min). These data emphasize the importance of an early intervention directed to minimize the effects of SE to prevent progression of epilepsy.

Acknowledgment: We thank S. Maslam for histologic assistance. Grant sponsors: Nationaal Epilepsie Fonds "Power of the Small"; grant 20-03 and 03-03 (J.A.G. and E.A.V.) and Fundação para a Ciência e a Tecnologia BD 18498/98 of Portugal (P.M.G.P.), Dutch Organization for Scientific Research (NWO) (P.J.L.).

REFERENCES

1. Mathern GW, Babb TL, Leite JP, et al. The pathogenic and progressive features of chronic human hippocampal epilepsy. *Epilepsy Res* 1996;26:151–61.
2. Sutula TP, Pitkanen A. More evidence for seizure-induced neuron loss: is hippocampal sclerosis both cause and effect of epilepsy? *Neurology* 2001;57:169–70.
3. Bengzon J, Kokaia Z, Elmer E, et al. Apoptosis and proliferation of dentate gyrus neurons after single and intermittent limbic seizures. *Proc Natl Acad Sci U S A* 1997;94:10432–7.
4. Cavazos JE, Das I, Sutula TP. Neuronal loss induced in limbic pathways by kindling: evidence for induction of hippocampal sclerosis by repeated brief seizures. *J Neurosci* 1994;14:3106–21.
5. Bertram EH, Lothman EW. Morphometric effects of intermittent kindled seizures and limbic status epilepticus in the dentate gyrus of the rat. *Brain Res* 1993;603:25–31.
6. Adams B, Sazgar M, Osehobo P, et al. Nerve growth factor accelerates seizure development, enhances mossy fiber sprouting, and

attenuates seizure-induced decreases in neuronal density in the kindling model of epilepsy. *J Neurosci* 1997;17:5288–96.
7. Schwob JE, Fuller T, Price JL, et al. Widespread patterns of neuronal damage following systemic or intracerebral injections of kainic acid: a histological study. *Neuroscience* 1980;5:991–1014.
8. Nevander G, Ingvar M, Auer R, et al. Status epilepticus in well-oxygenated rats causes neuronal necrosis. *Ann Neurol* 1985;18: 281–90.
9. Du F, Eid T, Lothman EW, et al. Preferential neuronal loss in layer III of the medial entorhinal cortex in rat models of temporal lobe epilepsy. *J Neurosci* 1995;15:6301–13.
10. Bertram EH, Lothman EW, Lenn NJ. The hippocampus in experimental chronic epilepsy: a morphometric analysis. *Ann Neurol* 1990;27:43–8.
11. Liu Z, Nagao T, Desjardins GC, et al. Quantitative evaluation of neuronal loss in the dorsal hippocampus in rats with long-term pilocarpine seizures. *Epilepsy Res* 1994;17:237–47.
12. Gorter JA, Van Vliet EA, Aronica E, et al. Progression of spontaneous seizures after status epilepticus is associated with mossy fibre sprouting and extensive bilateral loss of hilar parvalbumin and somatostatin-immunoreactive neurons. *Eur J Neurosci* 2001; 13:657–69.
13. Schmued LC, Albertson C, Slikker W Jr. Fluoro-Jade: a novel fluorochrome for the sensitive and reliable histochemical localization of neuronal degeneration. *Brain Res* 1997;751:37–46.
14. Lothman EW, Bertram EH, Bekenstein JW, et al. Self-sustaining limbic status epilepticus induced by "continuous" hippocampal stimulation: electrographic and behavioral characteristics. *Epilepsy Res* 1989;3:107–19.
15. Racine RJ. Modification of seizure activity by electrical stimulation, II: motor seizure. *Electroencephalogr Clin Neurophysiol* 1972;32:281–94.
16. Gavrieli Y, Sherman Y, Ben-Sasson SA. Identification of programmed cell death in situ via specific labeling of nuclear DNA fragmentation. *J Cell Biol* 1992;119:493–501.
17. Lucassen PJ, Chung WC, Vermeulen JP, et al. Microwave-enhanced in situ end-labeling of fragmented DNA: parametric studies in relation to postmortem delay and fixation of rat and human brain. *J Histochem Cytochem* 1995;43:1163–71.
18. English HF, Kyprianou N, Isaacs JT. Relationship between DNA fragmentation and apoptosis in the programmed cell death in the rat prostate following castration. *Prostate* 1989;15:233–50.
19. Lucassen PJ, Negoescu A, Labat-Moleur F, et al. Microwave enhanced in situ end labelling of apoptotic cells in tissue sections; pitfalls and possibilities. In: Shi SR, Gu J, Taylor CR, eds. *Antigen retrieval techniques.* Natick, Mass.: Eaton Publishing, 2000:71–91.
20. Amaral DG, Witter MP. Hippocampal formation. In: Paxinos G, ed. *The rat nervous system.* 2nd ed. London: Academic Press, 1995:443–93.
21. Paxinos G, Watson C. *The rat brain in stereotaxic coordinates*. San Diego: Academic Press, 1998.
22. Aronica E, Yankaya B, Troost D, et al. Induction of neonatal sodium channel II and III alpha isoform mRNAs in neurons and microglia after status epilepticus in the rat hippocampus. *Eur J Neurosci* 2001;13:1261–6.
23. Eriksson C, Van Dam AM, Lucassen PJ, et al. Immunohistochemical localization of interleukin-1beta, interleukin-1 receptor antagonist and interleukin-1beta converting enzyme/caspase-1 in the rat brain after peripheral administration of kainic acid. *Neuroscience* 1999;93:915–30.
24. Kubova H, Druga R, Lukasiuk K, et al. Status epilepticus causes necrotic damage in the mediodorsal nucleus of the thalamus in immature rats. *J Neurosci* 2001;21:3593–9.
25. Sato M, Chang E, Igarashi T, et al. Neuronal injury and loss after traumatic brain injury: time course and regional variability. *Brain Res* 2001;917:45–54.
26. Ingvar M, Morgan PF, Auer RN. The nature and timing of excitotoxic neuronal necrosis in the cerebral cortex, hippocampus and thalamus due to flurothyl-induced status epilepticus. *Acta Neuropathol* 1988;75:362–9.
27. Covolan L, Mello LE. Temporal profile of neuronal injury following pilocarpine or kainic acid-induced status epilepticus. *Epilepsy Res* 2000;39:133–52.
28. Poirier JL, Capek R, De Koninck Y. Differential progression of dark neuron and Fluoro-Jade labelling in the rat hippocampus following pilocarpine-induced status epilepticus. *Neuroscience* 2000; 97:59–68.
29. Tuunanen J, Lukasiuk K, Halonen T, et al. Status epilepticus-induced neuronal damage in the rat amygdaloid complex: distribution, time-course and mechanisms. *Neuroscience* 1999;94: 473–95.
30. Sloviter RS, Dean E, Sollas AL, et al. Apoptosis and necrosis induced in different hippocampal neuron populations by repetitive perforant path stimulation in the rat. *J Comp Neurol* 1996;366: 516–33.
31. Fujikawa DG, Shinmei SS, Cai B. Lithium-pilocarpine-induced status epilepticus produces necrotic neurons with internucleosomal DNA fragmentation in adult rats. *Eur J Neurosci* 1999;11:1605–14.
32. Roy M, Sapolsky R. Neuronal apoptosis in acute necrotic insults: why is this subject such a mess? *Trends Neurosci* 1999;22:419–22.
33. Kondratyev A, Gale K. Intracerebral injection of caspase-3 inhibitor prevents neuronal apoptosis after kainic acid-evoked status epilepticus. *Brain Res Mol Brain Res* 2000;75:216–24.
34. Mello LE, Covolan L. Spontaneous seizures preferentially injure interneurons in the pilocarpine model of chronic spontaneous seizures. *Epilepsy Res* 1996;26:123–9.
35. Pitkanen A, Nissinen J, Nairismagi J, et al. Progression of neuronal damage after status epilepticus and during spontaneous seizures in a rat model of temporal lobe epilepsy. *Prog Brain Res* 2002;135: 67–83.
36. Hopkins KJ, Wang G, Schmued LC. Temporal progression of kainic acid induced neuronal and myelin degeneration in the rat forebrain. *Brain Res* 2000;864:69–80.
37. Cavazos JE, Sutula TP. Progressive neuronal loss induced by kindling: a possible mechanism for mossy fiber synaptic reorganization and hippocampal sclerosis [published erratum appears in *Brain Res* 1991 Feb 8;541:179]. *Brain Res* 1990;527:1–6.
38. Zhang LX, Smith MA, Li XL, et al. Apoptosis of hippocampal neurons after amygdala kindled seizures. *Brain Res Mol Brain Res* 1998;55:198–208.
39. Mouritzen-Dam AM. Epilepsy and neuron loss in the hippocampus. *Epilepsia* 1980;21:617–29.
40. Fisher PD, Sperber EF, Moshe SL. Hippocampal sclerosis revisited. *Brain Dev* 1998;20:563–73.
41. Fernandez G, Effenberger O, Vinz B, et al. Hippocampal malformation as a cause of familial febrile convulsions and subsequent hippocampal sclerosis. *Neurology* 1998;50:909–17.
42. Jackson GD, Chambers BR, Berkovic SF. Hippocampal sclerosis: development in adult life. *Dev Neurosci* 1999;21:207–14.
43. Kalviainen R, Salmenpera T, Partanen K, et al. Recurrent seizures may cause hippocampal damage in temporal lobe epilepsy. *Neurology* 1998;50:1377–82.
44. O'Brien TJ, So EL, Meyer FB, et al. Progressive hippocampal atrophy in chronic intractable temporal lobe epilepsy. *Ann Neurol* 1999;45:526–9.
45. Tasch E, Cendes F, Li LM, et al. Neuroimaging evidence of progressive neuronal loss and dysfunction in temporal lobe epilepsy. *Ann Neurol* 1999;45:568–76.
46. Roch C, Leroy C, Nehlig A, et al. Magnetic resonance imaging in the study of the lithium-pilocarpine model of temporal lobe epilepsy in adult rats. *Epilepsia* 2002;43:325–35.
47. Liu RS, Lemieux L, Bell GS, et al. A longitudinal quantitative MRI study of community-based patients with chronic epilepsy and newly diagnosed seizures: methodology and preliminary findings. *Neuroimage* 2001;14:231–43.

STUDY II.

Assessment of the preferred scout sagittal orientation for temporal lobe imaging with magnetic resonance

Gonçalves Pereira P.M, Oliveira E, Forjaz Secca M.

MAGMA Magnetic Resonance Materials in Physics, Biology and Medicine vol 18, (1) 19-25 **2005**.

MAGMA (2005) 18: 19–25
DOI 10.1007/s10334-004-0074-4

RESEARCH ARTICLE

P. M. Gonçalves Pereira
E. Oliveira
M. F. Secca

Assessment of the preferred scout sagittal orientation for temporal lobe imaging with magnetic resonance

Received: 17 May 2004
Revised: 12 July 2004
Accepted: 7 September 2004
Published online: 3 December 2004
© ESMRMB 2004

P. M. Gonçalves Pereira (✉)
Department of Neuroradiology,
'Egas Moniz' Hospital,
Rua da Junqueira 126
1349-019 Lisboa Portugal
E-mail: pmgp@fct.unl.pt
Tel.: +351-21-3031140,
Fax: +351-21-3018140,

P. M. Gonçalves Pereira
Department of Medical Science,
Medical School,
University of Beira Interior,
Polo I, Rua Marquês d'Ávila e Bolama
6201-001 Covilhã
Portugal

P. M. Gonçalves Pereira · M. F. Secca
Department of Physics, CEFITEC,
School of Science and Technology,
New University of Lisboa,
Quinta da Torre 2825-114
Monte de Caparica
Portugal

E. Oliveira
Departement of Statistics,
'Egas Moniz' CRL,
Health Science Institute (ISCS),
Campus Universitário,
Quinta da Granja 2829-511
Monte de Caparica
Portugal

M. F. Secca
'Caselas' Magnetic Resonance Center,
Rua Carolina Ângelo,
1400-045 Lisboa
Portugal

Abstract Oblique magnetic resonance imaging of the temporal lobe (tilted orientation) requires a stable reference line with minimum variability. In the clinical setting, where several observers carry out examination of the patients, there is a need to assure minimum inter-observer variability, in order to obtain comparable tilted anatomical planes. This is particularly relevant when performing quantitative imaging (qMRI) of the hippocampus, amygdala and para-hippocampal cortices. In this study, eight experienced observers tested the stability of four sagittal reference lines by manually tracing the posterior commissure-obex (PC-OB) line, the line tangential to the anterior surface of the pons at its most convex point and the lines orthogonal to the main axis of both hippocampi, in ten exams of healthy subjects. The stability of the tracing was assessed by comparing the inter-observer variability expressed by the variances of the measurements. The observers' performance was assessed by comparing the precision of the tracing for each line. We tested the results statistically using Bartlett's test (analysis of the variances of the four lines) followed by Fischer–Snedecor (in order to compare the two lines that had the smallest variance). The PC-OB line and the line tangential to the anterior surface of the pons had smaller inter-observer variances than the orthogonal lines ($p < 0.01$). In addition, the variance of the PC-OB line was smaller than that of the line tangential to the pons ($p < 0.01$). There were no significant intra-observer differences in the precision of tracing of any of the lines. We show quantitatively that the PC-OB line is the scout reference that yields the smallest inter-observer variance. Thus, this line should be preferred to improve the reproducibility of temporal lobe imaging while performing tilted coronal and axial sequences, to make quantitative assessments of the hippocampus, amygdala and para-hippocampal cortices.

Introduction

The temporal lobe is the main target structure of temporal lobe epilepsy (TLE) [1], Alzheimer-type dementia [2], memory disturbances [3], including mild cognitive deficits [4], schizophrenia [5] and brain trauma [6]. In neurodegenerative disorders and epilepsy, the core limbic structures of the temporal lobe, that is, the hippocampus, the amygdala and the para-hippocampal cortex (see [7] for a review) are particularly affected.

Magnetic resonance imaging (MRI) is an essential tool to evaluate the abnormalities of even the smallest brain structures, due to its non-invasive multi-planar capabilities. Currently, qualitative and quantitative MRI is often used to study mesial temporal areas. Qualitative assessments are based on morphological and signal intensity appearances and depend heavily on the expertise of the radiologist. Quantitative imaging (qMRI) yields numerical information (for example: volumes, relaxation times, water diffusibility, metabolite concentration, blood perfusion measurements) that can be compared with normative values, but it depends on the identification of exact anatomical landmarks in order to be reproducible (see [8] for a review). Therefore, to be able to compare different MRIs and to perform serial or longitudinal studies, using either visual inspection or qMRI, it is essential that the landmarks of cross-sectional images are unambiguously defined.

Selective hippocampal atrophy can be found in patients with intractable partial seizures [9], Alzheimer-type dementia [10], amnesic syndromes [11] or schizophrenia [12]. In the pathophysiology of TLE, it is assumed that the degree of hippocampal, amygdala and para-hippocampal atrophy associates with the magnitude of neuronal loss [9], as the amount of reactive hippocampal astrocytes correlates with the measured T2-relaxometry times [13]. Hippocampal damage can also be detected by spectroscopy [14]. Morphological criteria, including indirect signs are also important to detect hippocampal or amygdala sclerosis. Subtle loss of the digitations of the hippocampal head [15], disruption of the internal architecture [16] and fornix and mamillary bodies' atrophy [17] are reliable indicators of hippocampal damage. Signal changes are also common in the hippocampus and amygdala of TLE patients [16, 18]. Thus, early and accurate diagnosis depends on the ability to identify small variations in the structures' volume, morphology and signal intensity.

The orientation of the acquired images, along with the criteria used for MR analysis and the knowledge of normal and abnormal mesial temporal lobe anatomy are key factors for the interpretation of MR images. Moreover, in qMRI one should assure reproducibility of the measurements by taking a constant tilted orientation to the temporal lobe in successive exams, minimizing in this way, partial volume effects.

Different MR sequences, including several anatomical planes have been used to evaluate the mesial temporal lobe [19]. One preferential anatomical orientation is the tilted coronal plane obtained at right angles to the main hippocampal axis [19–21]. For volumetric and relaxometric studies of the hippocampus and amygdala this is the plane mostly used, while multi-voxel spectroscopy benefits most if performed on a tilted axial orientation perpendicular to this angled coronal view [14, 20, 22].

In order to define a suitable and stable anatomical guideline for temporal lobe MRI studies, and to find out which reference line corresponds to the smallest inter-observer variation, we examined how eight different observers performed with respect to four different sagittal reference lines in ten MR exams of healthy persons. Two of the lines tested are commonly used as scouts of MR studies of the temporal lobe, that is, the lines perpendicular to the main axes of both hippocampi [19, 20] (either the right or left hippocampal body). The other two, the posterior commissure-obex (PC-OB) line and the line tangential to the anterior surface of the pons at its most convex point, have been also proposed as appropriate references in some studies [23, 24].

Materials and methods

Test subjects

The test group included ten subjects (five women) with a mean age [± 1 standard deviation (SD)] of 31.6 ± 3.2 (range: 27–36) years. All the volunteers were interviewed to exclude those with neurologic diseases and were submitted to detailed neurological examination and a "mini-mental state" test [25] [obtained mean score ± 1 SD and range was: 28.4 ± 1.3 (27–30)].

Test observers

Eight different observers with a mean number of years of experience of MRI work of 10.6 ± 6.5 (range: 2–17), volunteered to trace manually the chosen reference lines on a set of sagittal images, since this is the scout plane which is mostly used to define the coronal and axial sequences.

MR image acquisition and processing

All imaging studies were obtained on the same 1.5-T scanner (GE CV/i–NV/i. General Electric, Milwaukee, WI).

A standard sagittal spin-echo T1-weighted sequence, covering the whole brain was obtained with TR = 600 ms, TE = 15 ms, NEX = 2, FOV = 24 cm, section thickness = 5 mm, gap = 1 mm and acquisition matrix = 512×192 pixels.

Standard whole-brain coronal T1 and T2 images and axial T2 were acquired to exclude any structural abnormality.

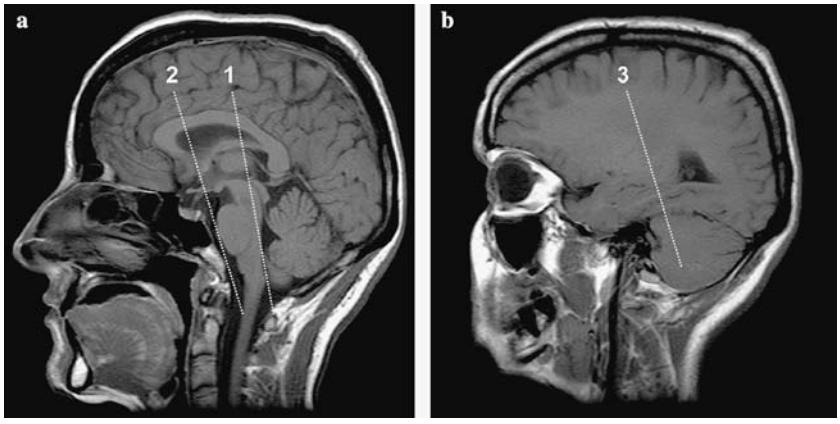


Fig. 1 Sagittal MR images demonstrate the location of three of the four lines tested. (a) mid-sagittal level showing the posterior commissure-obex line [1] and the line tangential to the anterior surface of the pons [2] (b) para-sagittal image showing the line orthogonal to the long axis of the right hippocampus [3]. The fourth line was orthogonally placed on the opposite hippocampus

Imaging processing was performed with the manufacturer's software GE Advantage Windows 3.1 (Viewer module), running on a workstation (SPARC 4.1, Sun Microsystems, Mountain View, Calif.). The software uses a graphical interface that allows to perform measurements (areas, lengths and angles). The measurements are displayed directly in absolute values (mm^2, mm or degrees), benefiting from the automatic calibration performed at the MR scanner during the acquisition of the images. For every graphic element introduced on top of an image, the software calculates automatically the measured values, which are shown on the workstation with the correspondent spatial coordinates.

Reference lines and coordinate system

Four anatomical lines (Fig. 1) were chosen to test the inter-observer variability. These lines represent standard references and anatomical axes used in daily practice [23].

Line 1 (k_1), connects the posterior commissure to the obex of the IV ventricle (PC-OB), joining two well-recognizable anatomical structures.

Line 2 (k_2), was marked tangentially to the anterior surface of the pons, at the point where the surface has maximal convexity.

Lines 3 (k_3) and 4 (k_4) were marked at right angles to the main axis of the hippocampal bodies, respectively in the right and the left hippocampus, as indicated by Watson et al. [20].

After tracing each anatomical line, the value of the angle (α- in degrees) between k and the vertical axis (set at zero degrees – see Fig. 2) was displayed directly on the workstation. The angles are calculated in relation to the vertical axis on the workstation screen and the value that is obtained measures the tilt of the line draw relatively to zero degrees (0°). The origin of the coordinate system (the center, where the three main axes cross zero) and the directions of these axes are defined with respect to the magnet's geometry. The center is defined as the geometric center of the magnetic field. The axes are defined as superior-inferior, anterior-posterior and left-right. The superior-inferior axis is defined as the line passing through the center and parallel to the main axis of the magnetic field, which is parallel to the basis of the magnet (and longitudinal to the scanner). The anterior-posterior axis is perpendicular to the superior-inferior axis, passing through the center, and perpendicular to the basis of the magnet. The left-right axis is perpendicular to the superior-inferior axis, passing through the center, and parallel to the basis of the magnet. The directions of the axes are characterized by the position of the subject in the scanner. In our case, the subjects were introduced head first and supine (and centered with the aid of the scanner's laser-cross beam). Therefore, superior-inferior is directed anatomically from head to feet, anterior-posterior from the back of the head to the nose and left-right is directed to the left-right of the subject.

The mean and the standard deviation of the angles for each anatomical line obtained in each test-subject MRI were further calculated.

Since each test subject underwent only one examination and the observers used the same sagittal image sets from each volunteer to mark the lines $k_1 - k_4$, the tilt of the head of the test subjects does not influence the results. We were specifically interested in studying the relative variances of these anatomical lines, not their absolute αvalues.

Statistical analysis

For the four lines, the mean and standard deviation of the angles as defined above (Fig. 2) were computed for each test subject and by each observer as indicated by Eq. 1 and 2:

$$S_{kj}^2 = \sum_{i=1}^{n_i} \left(\frac{\alpha_{kij} - \bar{\alpha}_{kj}}{n_i - 1} \right)^2 \quad (1)$$

$$S_k^2 = \sum_{j=1}^{n_j} \frac{S_{kj}^2}{n_j} \quad (2)$$

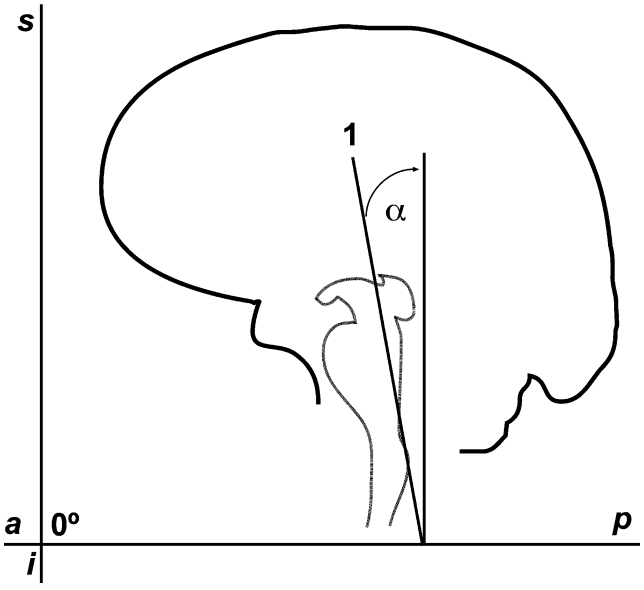


Fig. 2 Schematic drawing illustrates the angle α obtained from line 1 – posterior commissure-obex – in a sample case. Two of the axes of the coordinate system are depicted on the left side of the figure; *a –p*, on the horizontal line, represent the anterior–posterior axis and *s-i*, on the vertical line, corresponds to the superior-inferior axis. The value of α is calculated in regard to the anterior-posterior axis (zero degrees)

where

S_{kj}^2 - inter-observer variance of the angle for line k for a given test-subject j
n_i - number of observers
α_{kij} - value of the angle (relative to the vertical axis) measured by observer i for the test-subject j with respect to the line k
$\bar{\alpha}_{kj}$ - mean of the values of the angle with respect to line k for all observers for a given test-subject j
S_k^2 - mean of the variances for all test subjects with respect to line k (inter-subject variance for line k)
n_j - number of test subjects

The line with the smallest inter-observer variance S_k^2 of the angle α was considered the most stable. Differences in stability of the four lines were tested using Bartlett's test comparing S_k^2 with the mean total variance S^2 for all lines obtained by equation (3):

$$S^2 = \sum_{k=1}^{n_k} \frac{S_k^2}{n_k} \tag{3}$$

where

n_k - number of lines

The two lines with the smallest variance were further compared with each other using the Fischer–Snedecor test.

An intra-observer test for the precision of the measurements was performed in order to verify if the observers were equally consistent. In this step, we were interested in analysing whether there was any variability on each observer's execution regarding the measurements performed on all the test subjects for each line. First, we calculated the variance of each observer i obtained for all the test subjects, for every line k (S_{ki}^2); then, the variances S_{ki}^2 of the angles corresponding to line k were compared using the Bartlett test Eq. 4:

$$B = \frac{2.30259}{C}\left\{(n-n_i)\,.\,\ln\left(S^2\right) - \sum_{j=1}^{n_i}\left(n_j-1\right)\,.\,\ln\left(S_{ki}^2\right)\right\}$$
$$\overset{\bullet}{\cap}\ \chi^2_{(n_i-1)} \tag{4}$$

where

$$C = 1 + \frac{1}{3(i+1)}\left\{\sum_{j=1}^{i}\left(\frac{1}{n_j-1} - \frac{1}{n-1}\right)\right\}$$

n - total number of observations for each k (our case: 80)
S_{ki}^2 - intra-observer variance of the angle for line k for a given observer i
$\chi^2_{(n_i-1)}$ - theoretical value of χ^2 statistics with $(n_i-1)df$.

Results

The results regarding the variance of the four lines for each test subject ($\bar{\alpha}_{kj}$; mean ± 1 SD) as performed by the observers are presented on Table 1.

The mean variances S_k^2 corresponding to each line are shown in Table 2.

Table 3 shows the mean values corresponding to the angles measured in all subjects by every observer ($\bar{\alpha}_{ki}$; mean ± 1 SD).

Of the four lines, the line k_1 (PC-OB - Fig. 3) yield the least inter-observer variance. According to Bartlett' test, significant differences between the mean variances of the four reference lines were obtained (χ^2: χ^2 (3) = 82.54,

Table 1 Inter-observer study for the stability of the lines. $\bar{\alpha}_{kj} \pm 1$SD for α_{kij} in each reference line in every test subject j obtained by the eight observers

Test subject n°	Line k_1	Line k_2	Line k_3	Line k_4
j_1	8.4 ± 0.9	18.6 ± 2.9	18.4 ± 5.0	21.3 ± 7.6
j_2	3.4 ± 1.2	12.0 ± 2.1	24.0 ± 1.2	17.3 ± 2.3
j_3	3.8 ± 0.7	14.8 ± 2.5	18.6 ± 4.6	18.4 ± 2.9
j_4	6.9 ± 1.0	14.4 ± 2.4	14.6 ± 3.6	17.6 ± 3.5
j_5	16.1 ± 1.2	17.1 ± 3.8	27.1 ± 3.6	25.6 ± 4.3
j_6	7.5 ± 0.5	11.6 ± 1.2	18.1 ± 1.9	15.4 ± 2.8
j_7	6.9 ± 0.6	11.8 ± 1.7	17.6 ± 3.7	13.6 ± 2.5
j_8	20.1 ± 0.8	26.8 ± 1.7	27.8 ± 4.8	25.6 ± 3.4
j_9	12.3 ± 1.0	18.4 ± 1.7	24.8 ± 3.6	24.6 ± 5.0
j_{10}	9.3 ± 0.5	24.3 ± 5.6	32.8 ± 3.4	14.1 ± 7.8

$\bar{\alpha}_{kj}$ in degrees, measured with respect to the x-axis (set to zero)

Table 2 Variability for each line assessed. Mean of the variances S_k^2 in the eight observers

Line n°	S_k^2
k_1	0.8
k_2	8.1*
k_3	13.9
k_4	21.3

*significantly different from line 1 with the Fischer–Snedecor test ($p < 0.01$); Bartlett's test has shown that the variances of the groups were not equal

Table 3 Intra-observer study for the technical precision of the observers. $\bar{\alpha}_{ki} \pm 1SD$ for α_{kij} in each reference line for all test subjects obtained by the eight observers i

Observer n°	Line k_1	Line k_2	Line k_3	Line k_4
i_1	9.1 ± 5.4	16.8 ± 5.7	23.2 ± 5.4	21.8 ± 6.2
i_2	9.4 ± 5.2	18.2 ± 4.9	24.6 ± 5.2	22.9 ± 5.6
I_3	9.4 ± 5.5	16.2 ± 5.6	27.0 ± 6.2	23.9 ± 6.3
I_4	9.4 ± 5.8	16.9 ± 5.7	21.0 ± 7.5	16.8 ± 4.8
i_5	9.3 ± 5.8	16.6 ± 6.5	20.2 ± 8.1	17.3 ± 6.1
i_6	9.4 ± 5.0	17.4 ± 5.6	21.0 ± 6.1	16.5 ± 5.3
i_7	9.8 ± 4.9	16.5 ± 5.9	20.3 ± 7.3	17.9 ± 4.8
i_8	9.8 ± 5.3	17.1 ± 5.9	21.7 ± 4.6	17.7 ± 6.8

$\bar{\alpha}_{ki}$ in degrees, measured with respect to the x-axis (set to zero)

$p < 0.0001$). To further verify which line had the smallest variability, we tested the lines with the smallest variance (k_1 and k_2) using the Fischer–Snedecor test. There were significant differences between k_1 and k_2 [$F(9,9) = 103.2$, $p < 0.01$), indicating that k_1, the posterior commissure-obex line (PC-OB), has the smallest variance.

There were no significant intra-observer differences (Table 3) in the precision of the tracing for each line (Bartlett's test: $p > 0.05$ for lines $k_1 - k_4$: χ^2 for k_1: $\chi^2(7) = 0.47$, $p = 0.99$; χ^2 for k_2: $\chi^2(7) = 1.28$, $p = 0.98$; χ^2 for k_3: $\chi^2(7) = 5.49$, $p = 0.60$; χ^2 for k_4: $\chi^2(7) = 2.49$, $p = 0.93$).

Discussion

Topographic imaging provides information about individual brain structures. MRI, due to its multi-planar capabilities and high contrast resolution is a preferred method to analyse the morphometry of the core limbic structures of the temporal lobe.

In qMRI, the validity of hippocampal and amygdala quantification using volumetry, relaxometry or spectroscopy (and of para-hippocampal cortices volumetrics), depends on the quality of the images from which measurements are made.

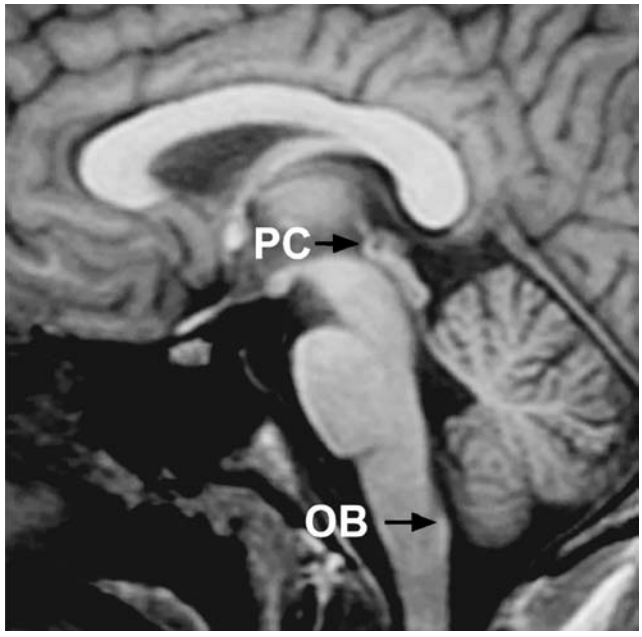


Fig. 3 Highlight of a mid-sagittal MR image showing the PC-OB anatomical details

In this study we sought to determine the stability of four sagittal reference lines, by assessing the variability of the manual tracing performed by a group of eight experienced observers in the evaluation of MR images using ten healthy controls.

Among all observers in this study, the PC-OB line showed the smallest variation while the orthogonal lines to both the right and left hippocampal axis had the largest standard deviations. These results are not surprising. In principle it is simpler to trace a line that joins two well-recognized anatomical structures, such as the posterior commissure and the obex of the IV ventricle, than an arbitrary line perpendicular to the main axis of the hippocampus, whose normal structure encompasses several cortical infoldings [26]. Further, on para-sagittal images the axis of the hippocampal head is frequently disparate to that of the body (see figures 96E and 97C in [26]). This angulation can be a source of error with respect to the choice of the appropriate orthogonal plane.

The lines tested are currently used in radiological practice as anatomical landmarks for the tilted orientation of the temporal lobe. In particular the line referred by several authors as "perpendicular to the main (or long) hippocampal axis" [10, 19, 20, 27, 28] is widely used. Also, for axial imaging the line "parallel to the longitudinal axis of the hippocampus" (obtained at right angles from the previous) is considered [14, 29]. Recently [23], the posterior commissure-obex line has been proposed as an accurate

reference to obtain angulated coronal and axial images to the main axes of the temporal lobes.

In the clinical setting it is likely that different radiologists and radiographers are responsible for the examinations of different patients. Thus, the importance of using a stable sagittal reference line as a scout for angulated planes to the temporal lobes cannot be overestimated. A simple, reproducible and well-defined anatomical landmark can contribute to the accurate comparisons of the MRI exams and increase the consistency of qMRI measurements.

Hippocampal and amygdala lesions include structural changes that disrupt their normal morphology and appearance. Moreover, the highly variable sulcal pattern of the basal and para-hippocampal temporal lobe can be an additional adverse source of variation to the imaging analysis of the subdivisions of the mesio-temporal region [30, 31]. Thus, when planning the appropriate imaging axis for the temporal lobes of a patient, it is advisable to rely on references other than the structure of interest, which may be damaged. The PC-OB line provides a stable choice since it is simple to identify and to trace. Moreover, to date, the involvement of both the posterior commissure and the obex of the IV ventricle has never been reported in the pathology of neurodegenerative disorders and TLE, which may alter their morphometry.

Conclusion

The stability and reproducibility of temporal lobe MRI can be improved by using the posterior commissure-obex line as an anatomical scout for the tilted coronal and axial sequences. Quantitative assessment of the hippocampus and amygdala, but also of the para-hippocampal cortices can benefit most from this improved stability since it predicts higher inter-observer reproducibility.

Acknowledgements This research was funded by a grant from The Science and Technology Foundation (BD 18498/98) awarded to P.M.G.P. Other support was provided by The Grünenthal Foundation. We thank the observers of the study, the Neuroradiologists Constança Jordão, Pedro Evangelista and Jorge Cannas, the Residents in Neuroradiology (at the date of the study) Teresa Palma and Carla Conceição and the Radiographers Cristina Menezes and Alfredo Raio. Alberto Leal is acknowledged for stimulating discussions regarding this project. We wish to thank Professor Fernando Lopes da Silva for his insightful comments on the manuscript.

References

1. Falconer MA, Serafetinides EA, Corsellis JAN (1964) Etiology and pathogenesis of temporal lobe epilepsy. Arch Neurol 10:233–248
2. Mouton PR, Martin LJ, Calhoun ME, Dal Forno G, Price DL (1998) Cognitive decline strongly correlates with cortical atrophy in Alzheimer's dementia. Neurobiol Aging 19:371–377
3. Amaral DG (1987) Memory: anatomical organization of candidate brain regions. In: Plum F, Mountcastle V (eds) Higher functions of the brain, handbook of physiology, Part I. Am Physiol Soc, Washington, pp211–294
4. Petersen RC, Doody R, Kurz A, et al. (2001) Current concepts in mild cognitive impairment. Arch Neurol 58:1985–1992
5. Gur RE, Turetsky BI, Cowell PE, et al. (2000) Temporolimbic volume reductions in schizophrenia. Arch Gen Psychiatry 57:769–775
6. Bigler ED, Blatter DD, Anderson CV, et al. (1997) Hippocampal volume in normal aging and traumatic brain injury. AJNR Am J Neuroradiol 18:11–23
7. Gloor P (1997) The temporal lobe and the limbic system. Oxford University Press, New York
8. Tofts PS (2003) Quantitative MRI of the brain: measuring changes caused by disease. Wiley, Chichester
9. Bronen RA, Cheung G, Charles JT, et al. (1991) Imaging findings in hippocampal sclerosis: correlation with pathology. Am J Neuroradiol 12:933–940
10. Jack CR, Petersen RC, O'Brien PC, Tangalos EG (1992) MR-based hippocampal volumetry in the diagnosis of Alzheimer's disease. Neurology 42:183–188
11. Soininen HS, Partanen K, Pitkänen A, et al. (1994) Volumetric MRI analysis of the amygdala and the hippocampus in subjects with age-associated memory impairment: correlation to visual and verbal memory. Neurology 44:1660–1668
12. Velakoulis D, Pantelis C, McGorry PD, et al. (1999) Hippocampal volume in first-episode psychoses and chronic schizophrenia: a high-resolution magnetic resonance imaging study. Arch Gen Psychiatry 56:133–141
13. Briellmann RS, Kalnins RM, Berkovic SF, Jackson GD (2002) Hippocampal pathology in refractory temporal lobe epilepsy: T2-weighted signal change reflects dentate gliosis. Neurology 58:265–271
14. Ng TC, Comair YG, Xue M, et al. (1994) Temporal lobe epilepsy: presurgical localization with proton chemical shift imaging. Radiology 193:465–472
15. Oppenheim C, Dormont D, Biondi A, et al. (1998) Loss of digitations of the hippocampal head on high-resolution fast spin-echo MR: a sign of mesial temporal sclerosis. AJNR Am J Neuroradiol 19:457–463
16. Jackson GD (1995) The diagnosis of hippocampal sclerosis: other techniques. Magn Reson Imaging 13:1081–1093
17. Kim JH, Tien RD, Felsberg GJ, Osumi AK, Lee N (1995) Clinical significance of asymmetry of the fornix and mamillary body on MR in hippocampal sclerosis. AJNR Am J Neuroradiol 16:509–515
18. Jack CR Jr, Rydberg CH, Krecke KN, et al. (1996) Mesial temporal sclerosis: diagnosis with fluid-attenuated inversion-recovery versus spin-echo MR imaging. Radiology 199:367–373
19. Achten E, Boon P, De Poorter J, et al. (1995) An MR protocol for presurgical evaluation of patients with complex partial seizures of temporal lobe origin. AJNR Am J Neuroradiol 16:1201–1213
20. Watson C, Andermann F, Gloor P, et al. (1992) Anatomic basis of amygdaloid and hippocampal volume measurement by magnetic resonance imaging. Neurology 42:1743–1750

21. Meiners LC, Valk J, van Gils PG, et al. (1997) Assessment of the preferred plane and sequence in the depiction of mesial temporal sclerosis using magnetic resonance imaging. Invest Radiol 32:268–276
22. Jackson GD, Connelly A, Duncan JS, Grunewald RA, Gadian DG (1993) Detection of hippocampal pathology in intractable partial epilepsy: increased sensitivity with quantitative magnetic resonance T2 relaxometry. Neurology 43:1793–1799
23. Tamraz JC, Comair YG (2000) Cephalic reference lines suitable for neuroimaging. In: Tamraz JC, Comair YG (eds) Atlas of regional anatomy of the brain using MRI – with functional correlations. Springer, Berlin Heidelberg New York, pp.11–50
24. Bartlett PA, Richardson MP, Duncan JS (2002) Measurement of amygdala T2 relaxation time in temporal lobe epilepsy. J Neurol Neurosurg Psychiatry 73:753–755
25. Folstein MF, Folstein SE, McHugh PR (1975) "Mini-mental state". A practical method for grading the cognitive state of patients for the clinician. J Psychiatr Res 12:189–198
26. Duvernoy HM (1998) The human hippocampus. Functional anatomy, vascularization and serial sections with MRI. Springer, Berlin Heidelberg New York
27. Du AT, Schuff N, Amend D, et al. (2001) Magnetic resonance imaging of the entorhinal cortex and hippocampus in mild cognitive impairment and Alzheimer's disease. J Neurol Neurosurg Psychiatry 71:441–447
28. Von Oertzen J, Urbach H, Jungbluth S, et al. (2002) Standard magnetic resonance imaging is inadequate for patients with refractory focal epilepsy. J Neurol Neurosurg Psychiatry 73:643–647
29. Capizzano AA, Vermathen P, Laxer KD, et al. (2001) Temporal lobe epilepsy: qualitative reading of 1H MR spectroscopic images for presurgical evaluation. Radiology 218:144–151
30. Novak K, Czech T, Prayer D, et al. (2002) Individual variations in the sulcal anatomy of the basal temporal lobe and its relevance for epilepsy surgery: an anatomical study performed using magnetic resonance imaging. J Neurosurg 96:464–473
31. Insausti R, Juottonen K, Soininen H, et al. (1998) MR volumetric analysis of the human entorhinal, perirhinal, and temporopolar cortices. AJNR Am J Neuroradiol 19:659–671

STUDY III.

Magnetic resonance volumetric analysis of the piriform cortex and cortical amygdala in drug-refractory temporal lobe epilepsy

Gonçalves Pereira P.M, Insausti R, Artacho-Pérula E, Salmenperä T, Kälviäinen R, Pitkänen A. **AJNR American Journal of Neuroradiology** vol 26, (2) 319-32 **2005**.

AJNR Am J Neuroradiol 26:319–332, February 2005

MR Volumetric Analysis of The Piriform Cortex and Cortical Amygdala in Drug-Refractory Temporal Lobe Epilepsy

Pedro M. Gonçalves Pereira, Ricardo Insausti, Emilio Artacho-Pérula, Tuuli Salmenperä, Reetta Kälviäinen, and Asla Pitkänen

BACKGROUND AND PURPOSE: **The assessment of patients with temporal lobe epilepsy (TLE) traditionally focuses on the hippocampal formation. These patients, however, may present structural abnormalities in other brain areas. Our purpose was to develop a method to measure the combined volume of the human piriform cortex and cortical amygdala (PCA) by using MR imaging and to investigate PCA atrophy.**

METHODS: **The definition of anatomic landmarks on MR images was based on histologic analysis of 23 autopsy control subjects. Thirty-nine adults with chronic TLE and 23 age-matched control subjects were studied. All underwent high-spatial-resolution MR imaging at 1.5T, including a tilted T1-weighted 3D dataset. The PCA volumes were compared with the control values and further correlated with hippocampal, amygdale, and entorhinal cortex volumes.**

RESULTS: **The normal volume was 530 ± 59 mm^3 (422–644) [mean ± 1 SD (range)] on the right and 512 ± 60 mm^3 (406–610) on the left PCA (no asymmetry, and no age or sex effect). The intraobserver and interobserver variability were 6% and 8%, respectively. In right TLE patients, the mean right PCA volume was 18% smaller than in control subjects ($P < .001$) and 15% smaller than in left TLE ($P < .001$). In left TLE, the mean left PCA volume was 16% smaller than in control subjects ($P < .001$) and 19% smaller than in right TLE ($P < .001$). Overall, 46% (18/39) of the patients had a greater than 20% volume reduction in the ipsilateral PCA. There was bilateral atrophy in 18% (7/39). Patients with hippocampal volumes of at least 2 SDs below the control mean had an 18% reduction in the mean PCA volume compared with patients without hippocampal atrophy ($P < .001$). Ipsilaterally, hippocampal ($r = 0.756$, $P < .01$), amygdaloid ($r = 0.548$, $P < .01$), and entorhinal ($r = 0.500$, $P < .01$) volumes correlated with the PCA volumes.**

CONCLUSION: **The quantification of PCA volume with MR imaging showed that the PCA is extensively damaged in chronic TLE patients, particularly in those with hippocampal atrophy.**

Temporal lobe epilepsy (TLE) is a localization-related epilepsy with typical clinical and electroencephalographic characteristics (1, 2). Complex partial seizures originating from the temporal lobe are the single most common type of focal-onset seizure encountered in the adult population (3, 4).

One of the histopathologic landmarks of TLE (5) is hippocampal sclerosis (HS), present in up to 90% of surgically treated drug-refractory patients (6). Tissue damage to temporal lobe structures other than the hippocampus, including the amygdaloid complex and the adjacent entorhinal, perirhinal, and parahippocampal cortices, contributes to a lowered seizure

Received February 26, 2004; accepted after revision July 6.

From the Department of Neuroradiology (P.M.G.P.), Pedro Hispano Hospital, Matosinhos, Portugal; the Department of Medical Science (P.M.G.P.), Medical School, University of Beira Interior, Covilhã, Portugal; the Institute of Electronics Engineering and Telematics of Aveiro (P.M.G.P.), University of Aveiro, Aveiro, Portugal; the Department of Health Sciences and Regional Center for Medical Investigations (R.I., E.A.-P.), Human Neuroanatomy Laboratory, School of Medicine, University of Castilla-la Mancha, Albacete, Spain; the Department of Neurology (T.S., R.K.), Kuopio University Hospital, Kuopio, Finland; and the Epilepsy Research Laboratory (A.P.), A. I. Virtanen Institute for Molecular Sciences, University of Kuopio, Kuopio, Finland.

Sponsored by Grant BD 18498/98 for P.M.G.P. (The Science and Technology Foundation), the Grünenthal Foundation and the Gulbenkian Foundation, Portugal, Grant FIS 00/468 (Ministry of Health), and Grants PAI 02–022 and GC 02–022 (Department of Science and Technology, Government of Castilla-La Mancha), Spain, and the Academy of Finland, The Sigrid Juselius Foundation, the Kuopio University Hospital Research Fund, the University of Kuopio, and the Vaajasalo Foundation, Finland.

Address reprint requests to Asla Pitkänen, MD, PhD, Epilepsy Research Laboratory, A.I. Virtanen Institute for Molecular Sciences, University of Kuopio, P. O. Box 1627, FIN-70 211 Kuopio, Finland, E-mail: asla.pitkanen@uku.fi.

© American Society of Neuroradiology

threshold, seizure spread, and cognitive decline in TLE (7–14).

An additional mesio-temporal region that may be involved in the physiopathologic findings of TLE comprises the piriform and periamygdaloid cortices. These structures share with the hippocampus an allocortical organization (15) and are core elements of the limbic system.

The piriform cortex (PC) is an olfactory-related, small region located rostromedial to the amygdala, overlying the fundus of the endorhinal sulcus. It receives primary olfactory projections from the olfactory bulb, as well as from other olfactory structures such as the anterior olfactory nucleus, sends projections to different limbic structures such as the entorhinal cortex (16–18), and is a major recipient of sensory afferents, but additional targets also comprise the periamygdaloid and the entorhinal areas. The efferent circuitry from the PC terminates mainly in the neighboring periamygdaloid cortex (PAC) and in the anterior and posterior cortical amygdala nuclei (19). Additionally, the PC, PAC and cortical amygdala nuclei share a similar functional processing of sensory-evoked activity (20) and therefore can be grouped as a PC-cortical amygdala area.

The PC has received little attention in human epilepsy studies (21), although it has a critical role in the generation of epileptogenic and ictogenic networks in experimental TLE (22, 23).

A number of studies carried out in animal models of TLE demonstrated that the PC is activated early during focal seizure activity. For example, studies by using c-Fos immunohistochemistry (24, 25) or deoxyglucose autoradiography (26) indicate that the PC becomes activated and damaged during the first hour after the initiation of prolonged seizure activity (24, 27). If status epilepticus is not stopped, neuronal loss becomes more severe and extensive (28–30). Consistent with histologic observations, MR imaging studies of rat tissue *ex vivo* after SE demonstrate that the PC is one of the most sensitive areas to damage caused by prolonged focal seizure activity (31, 32). Moreover, PC damage is associated with the development of spontaneous focal-onset seizures after SE (33).

The PC is also prone to activity-dependent plasticity. In studies of the kindling model of TLE, the PC is easier to kindle than the amygdala, hippocampus, or adjacent cortex (34–36). Further, the PC is a critical generator of seizure activity within the temporal lobe as spontaneous interictal discharges first appear in the PC in the kindled brain (37) before they spread to other brain areas (35, 38). In particular, the area tempestas (39), which is a small region located in the piriform cortex, is proposed to have a pivotal role in seizure spread in rodents (40, 41) and in nonhuman primates (42). Finally, the PC and PAC plus the adjacent cortical amygdaloid nuclei are key areas for processing olfactory information (18, 43).

Based on previous studies, olfactory sensations are not uncommon as an early sign of seizure onset in patients with TLE, particularly if the primary focus is in the amygdala (44), which is probably related to the heavy interconnections between the cortical amygdaloid nuclei and the PC (rodents: [45, 46]; primates: [47]). Together, these data suggest a role for the PC in ictogenesis as well as in the symptomatology of TLE. To date, however, there have been no attempts to investigate the contribution of piriform and cortical amygdala (PCA) atrophy to the human TLE syndrome.

We hypothesized that the piriform and cortical amygdala is damaged in a subpopulation of patients and, further, it is most damaged in patients with lesions in other temporal lobe structures (e.g., amygdala, hippocampus, entorhinal cortex). Therefore, we first defined the anatomic landmarks of the PCA in histologic sections of control brains as a guide for identification of the PCA in coronal MR images. We then investigated the occurrence of PCA damage by quantifying the degree of atrophy as well as its association with the volumes of hippocampus, amygdala, and entorhinal cortex in patients with chronic TLE. Part of this work was published in abstract form (48).

Methods

Subjects and Tissue Preparation for Histologic Examination

Twenty-three temporal lobes from 21 cases (two cases had both hemispheres studied) from a series of 44 autopsies were analyzed (12 men, nine women; mean age, 41 ± 14 years; range, 16–65 years). All the subjects were reported as clinically neurologically normal at the time of death. All cases had coronal sections cut perpendicular to the line between the anterior and posterior commissures and covered the entire PCA area. The right hemisphere was available for study in 14 cases and the left in nine cases. No differences were observed in the lamination, subfields, or topographic relation between the piriform and adjacent perirhinal and periamygdaloid cortices and amygdalo-hippocampal transitional area between the left and right hemispheres. All cases were determined neuropathologically normal, thus excluding abnormalities of the central nervous system that could impair the identification of the cytoarchitectonic boundaries.

Protocols for fixation, cryoprotection, cutting, and storage of human brain were performed as described previously (49) and the cytoarchitectonic analysis followed the methodology of Insausti et al (50). Sections were spaced 250 μm, and every eighth section was analyzed, that is, with an interval of one-half mm.

The piriform and periamygdaloid cortices areas were grouped together (PCA) first because they are closely related both anatomically and functionally (15, 18–20, 43). The periamygdaloid cortex (PAC) is located underneath the PC in the rostral medial temporal lobe and is made up of five subfields (PAC_0, PAC_1, PAC_2, PAC_3, PAC_S). The PC originates a great number of associational projections to other olfactory and cortical structures. Furthermore, the PC and PAC grouped together offered a more sizeable amount of tissue to be determined volumetrically.

A volume was estimated by using the Cavalieri method, an unbiased stereological procedure that allows an efficient and precise estimation of the volume of a structure of arbitrary size and shape through a series of parallel planes of the structure spaced at a constant distance (51, 52). Applying a test point graticule on the PCA regions and counting those test points hitting the PCA region, we obtained the unbiased estimate of volume of the PCA [estV(PCA)] according to the following equation,

$$estV_{(PCA)} = t \cdot (a/p) \cdot (P_1 + P_2 + \ldots + P_n)$$

TABLE 1: Normalized volumes and asymmetry ratios of the right and left hippocampus, amygdala complex and entorhinal cortex

Group	Hippocampus	Δ HC	Amygdala	Δ AMY	Entorhinal Cortex	Δ EC
Controls (n = 23)						
Right	3623 ± 468 (2825–4579)		2333 ± 263 (1983–2882)		1400 ± 279 (965–2088)	
Left	3412 ± 347 (2898–4186)	8.1 ± 6.2	2484 ± 400 (2041–3372)	9.0 ± 7.4	1399 ± 210 (1038–1809)	9.3 ± 7.3
Right TLE (n = 18)						
Right	3131 ± 1082 (1288–4404)		2336 ± 404 (1501–3303)		1272 ± 240 (999–1904)	
Left	3434 ± 539 (2507–4474)	25.4 ± 21.4	2459 ± 244 (2149–3027)	11.2 ± 11.0	1230 ± 176 (942–1580)	13.3 ± 9.8
Left TLE (n = 21)						
Right	3488 ± 591 (2360–4189)		2351 ± 352 (1774–3286)		1370 ± 272 (839–1929)	
Left	2851 ± 912 (1237–3840)	26.2 ± 24.5	2355 ± 395 (1657–2909)	10.1 ± 10.7	1248 ± 220 (934–1782)	12.8 ± 10.3

All volumes are presented as mean ± one standard deviation of the mean (range) and given in mm^3. Asymmetry ratios (Δ) are presented as mean ± one standard deviation of the mean and given in percentages. HC indicates hippocampus; AMY, amygdala; EC, entorhinal cortex; TLE, temporal lobe epilepsy.

where $P_1, P_2, \ldots, P_n$ denote the number of test points hitting PCA on each consecutive section, t is the sectioning interval for the n consecutive sections, and a/p is the area associated with each test point (in our study, $t = 0.5$ mm. and $a/p = .49$ mm^2). We estimated that about 6% of the PCA sections were lost (damage, interval between blocks, etc.), and the quantification could not be made by interpolation of previous and following sections.

The precision of the volume estimates when using the Cavalieri method and the point counting method was assessed by the equation (53),

$$CE(estV) = \left(\sum_{i=1}^{n} P_i\right)^{-1} \cdot \left(\frac{1}{12}\left(3\sum_{i=1}^{n} P_i^2 + \sum_{i=1}^{n-2} P_iP_{i+2} - 4\sum_{i=1}^{n-1} P_iP_{i+1}\right) + 0.0543\left(\frac{\bar{B}}{\sqrt{\bar{A}}}\right)\left(n\sum_{i=1}^{n} P_i\right)^{1/2}\right)^{1/2}$$

where $\bar{A}$ and $\bar{B}$ denote the mean transect area and boundary length respectively. The estimation of the $\bar{B}/\sqrt{\bar{A}}$ is a shape coefficient that measures the shape of the PCA profiles through the sections. Shape coefficient was measured in all cases despite the great stability of it. The range of values between different samples was 4.8–5.4 with a mean of 5.1.

The contribution of the point counting to overall estimation of the CE (estV) is, in general, negligible compared with the contribution of differences between sections. The study includes the estimation of the contribution of the point counting to the precision of the Cavalieri estimate of volume of the PCA according to the following equation,

$$estCE\left(\sum_{i=1}^{n} P_i\right) = \left[0.0724 \cdot \frac{\bar{B}}{\sqrt{\bar{A}}} \cdot \frac{\sqrt{n}}{\left(\sum_{i=1}^{n} P_i\right)^{3/2}}\right]^{1/2}$$

Thus, the contribution to the overall CE due to the variation between section areas of the PCA can be predicted from the equation,

$$CE^2(estV)_s = CE^2(estV)_t - CE^2\left(\sum P\right)$$

where subscript s and t means section and total respectively.

MR Imaging

Subjects for MR Imaging. The control group included 23 healthy individuals (11 men, 12 women), with a mean age of 32 ± 10 years (mean ± 1 SD; range: 21 –52 years) who were interviewed to exclude any neurologic or psychiatric diseases.

The patient group included 39 adults (17 men, 22 women) with chronic TLE, evaluated at the Department of Neurology at the Kuopio University Hospital in Finland. Only patients that did not have any identified etiology underlying their epileptic disorder were chosen to minimize the contribution of various etiologic factors to the cortical atrophy. Diagnosis of TLE was established on the basis of medical history, neurologic examination, electroencephalography (EEG), and qualitative MR imaging, including high-resolution T1- and T2-weighted, proton attenuation, inversion-recovery, and fluid-attenuation inversion recovery scans. Seizure symptomatology and noninvasive EEG data were used to determine the laterality of TLE. On the basis of EEG recordings, 18 patients had TLE with a unilateral seizure focus on the right and 21 patients had a seizure focus on the left. At the time of the MR image, the mean age of the patient group was 34 ± 9 years (range: 16–53 years). Total lifetime seizure number was calculated as described previously (54).

MR Image Acquisition. Patients and control individuals underwent imaging on a 1.5T Magnetom (Siemens, Erlangen, Germany) by using a standard head coil and a tilted coronal 3D magnetization-prepared rapid acquisition gradient-echo sequence with the following parameters: (TR/TE/NEX), 10/4/1; inversion time, 250 ms; flip angle, 12°; FOV, 250 mm; matrix, 256 × 192. This resulted in 124–128 contiguous T1-weighted images with a 1.5- to 2.0-mm section thickness oriented perpendicular to the long hippocampal axis, which were further reconstructed to 2.0-mm-thick contiguous sections oriented perpendicular to the line drawn between the anterior and posterior commissures at the individual midsagittal level (similar to the histologic plane of section). Consequently, the reconstructed MR images and the histologic sections had an identical in-plane orientation and spacing, which facilitated the identification of the anatomic boundaries. Using a different in-plane orientation on MR imaging would make the histologic boundaries difficult to reproduce and another MR imaging section thickness would impair the definition and contrast of the images (if less than 2.0-mm-thick) or enhance the partial volume effects (if larger than 2.0-mm-thick). According to the histologically defined landmarks, the boundaries of the PCA were drawn manually by using a trackball-driven cursor.

To minimize the effect of a possible bias, the cases were analyzed in random order without knowledge of the side of the epileptic focus.

The volumetric analysis of the hippocampus (55), amygdala (7) and entorhinal cortex (54), from these cases was previously reported (see Table 1 for a brief description of the results).

Definition of the PC and Cortical Amygdala Borders in Histologic Sections

The histologic appearance and location of the PC (area 51 of Brodmann [56]), the cortical amygdaloid nuclei including the

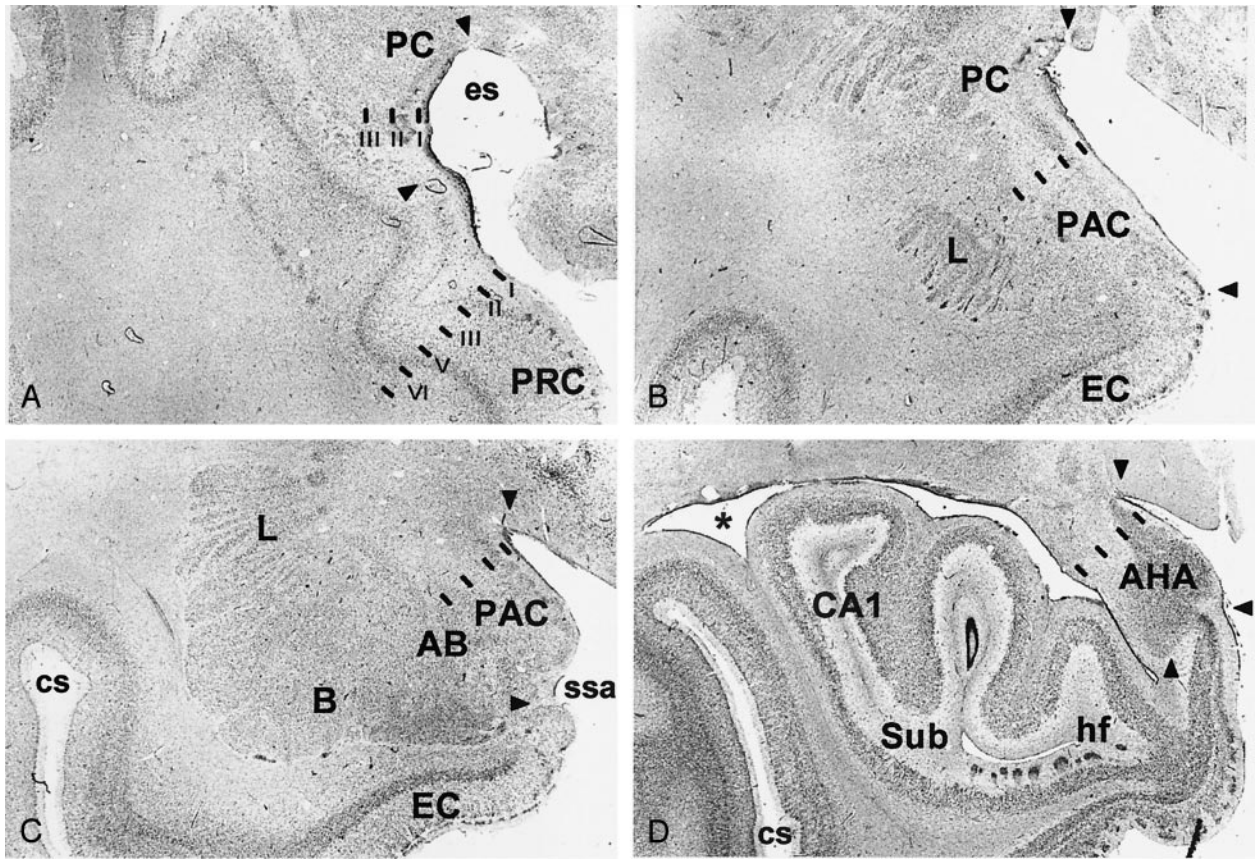


FIG 1. Brightfield photomicrographs of thionin-stained sections on the coronal plane show cytoarchitectonic borders (*arrowheads*) of the different components of the piriform cortex-cortical amygdala (PCA) region as defined in the present study. *A* is the most rostal (at the level of the *limen insulae*) and *D* is the most caudal (hippocampal head). PC indicates piriform cortex; PRC, perirhinal cortex; es, *endorhinal sulcus*; PAC, periamygdaloid cortex; L, amygdala lateral nucleus; EC, entorhinal cortex; AB, amygdala accessory basal nucleus; B, amygdala basal nucleus; ssa, *sulcus semiannularis*; cs, *colateral sulcus*; AHA, amygdalo-hippocampal area; CA1, hippocampal field 1; Sub, subiculum; hf, hippocampal fissure; asterisk, lateral ventricle. Scale bar equals 2 mm.

anterior cortical nucleus, medial nucleus, and periamygdaloid cortex, as well as the amygdalo-hippocampal area are shown in Figure 1 (for nomenclature of the human amygdala, see [57]). Together they form a ribbon located around the *limen insulae* and share a common trilaminated structure (58–61) that defines the paleocortex. Next, we describe the major anatomic landmarks used to identify each of these cortical regions in a rostral to caudal direction (Fig 2).

Piriform Cortex. The most rostral aspect of the PC is located in the caudolateral portion of the orbitofrontal cortex where it is situated lateral and ventral to the lateral olfactory tract. From there, it extends to the dorsal medial temporal lobe where its major portion is located, and terminates in the periamygdaloid region where it fuses with the cortical amygdala. In Nissl preparations, the PC has a characteristic prominent S-shape, due to a cell-sparse layer I and densely packed layer II that is composed of large pyramidal cells. Deep to layer II lies a thicker and less-densely packed layer III of slightly larger pyramidal cells (Fig 1A).

Although the boundaries of the PC can be easily identified from the adjacent cortices in Nissl-stained histologic sections, there are no clues to outline its borders on correspondent MR images, particularly in the frontal lobe. Therefore, to obtain a more reliable estimate of the PC volume, we focused on the temporal extension of the PC. Based on histologic assessment, the frontal aspect of the PC forms a fairly minor portion of the PC (10–15% of the total PC volume)(47). There are also no landmarks for placing the border between the PC and the cortical amygdaloid nuclei (the anterior cortical nucleus). Therefore, the neighboring cortical amygdala and the amygdalo-hippocampal area were included in the analysis. The region of volume measurement was the PCA and includes the PC located in the temporal lobe, anterior cortical nucleus of the amygdala, medial nucleus of the amygdala, nucleus of the lateral olfactory tract, periamygdaloid cortex (PAC_0, PAC_1, PAC_2, PAC_3 and PAC_S subfields), posterior cortical nucleus of the amygdala, and the amygdalo-hippocampal area (Fig 1).

Histologic analysis of 23 hemispheres demonstrated that the PC in the temporal lobe begins at the level of the *limen insulae* (LI, or frontotemporal junction, formed at the junction between the frontal and temporal lobes) in 21 of 23 cases (Figs 3and 4A). In two cases, the rostral border of the PC was approximately 1 mm rostral to the LI. Therefore, the coronal MR imaging section containing the LI was demarcated as the section containing the most rostral portion of the PC (Fig 5). At this level, the dorsal border of the PC was drawn at the fundus of the *endorhinal sulcus* (Figs 1A and 5). In histologic sections, the mediolateral extent of the PC occupies approximately 30% of the distance from the convexity of the rostralmost portion of the *gyrus semilunaris* (the most medial prominence of the medial temporal lobe) (Fig 5) to the fundus of the *endorhinal sulcus* (Fig 5). From this level caudally, and as far as the rostral limit of the amygdala, the PC occupied progressively a larger proportion of the gray matter on the medial aspect of the medial temporal lobe, up to 80% on the section immediately anterior to the begining of the amygdala (Fig 5). The most caudal section where the PC is present is located approximately 6 mm caudal to the LI (Fig 5). At this level, its mediolateral extent is highly variable and no larger than 20% of the total distance between the fundus and the *gyrus semilunaris*. Here,

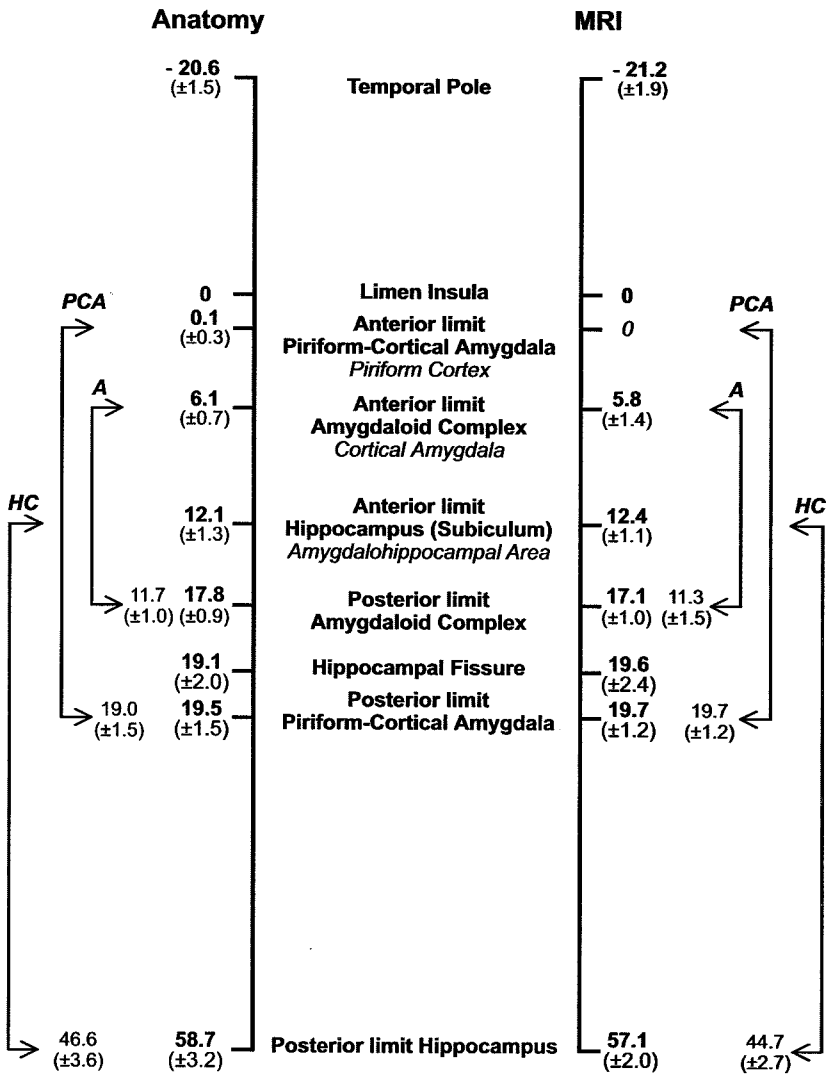


FIG 2. Schematic representation of the rostrocaudal location and extent of the major landmarks relative to the *limen insula* (set at 0) used to define the PCA. Numbers on the left (mean distance in millimeters ± SD) were calculated from control histologic cases (23 temporal lobes) and on the right from the MR imaging control group (46 temporal lobes). The values between arrows depict the mean (± 1 SD) distances between the rostro-caudal limits of the PCA, the amygdaloid complex (A), and the hippocampus (HC).

the cortical amygdala occupies most of the dorsal surface of the medial temporal lobe. In histologic sections, the thickness of the PC reaches 1 mm throughout its full rostro-caudal extent. Because the thickness of the adjacent perirhinal cortex is 4 mm, the thickness of the PC can be estimated to be one-fourth (25%) that of the perirhinal cortex in coronal MR images.

Cortical Amygdala. The cortical amygdala is the most caudal segment of the olfactory allocortex, located on the medial surface of the human temporal lobe (62). It is composed of several superficial amygdaloid nuclei with defined cytoarchitectonic, chemoarchitectonic, and connectional characteristics (for nomenclature, see [57]). The present volumetric analysis included the cortical nuclei of the amygdala (cortical amygdala, for short, composed of the anterior cortical nucleus, the medial nucleus, the nucleus of the lateral olfactory tract, olfactory amygdala [63]), the periamygdaloid cortex (PAC_0, PAC_1, PAC_2, PAC_3, and PAC_S subfields), and the posterior cortical nucleus (Fig 1). Rostrally, the cortical amygdala is located caudal and ventral to the PC (Fig 1B) and caudal to the perirhinal cortex (PRC) (Fig 1A). It extends down to the ventral bank of the *sulcus semiannularis* (ssa) where it borders the entorhinal cortex (Fig 1B-C). At caudal levels it becomes continuous with the amygdalo-hippocampal transitional area (Fig 1D).

Rostrally, the cortical amygdala (including the PACo) appears at the level of the beginning of the amygdala approximately 6 mm caudal to the LI (64) (Figs 1B and 5). At this level, the cortical amygdala occupies approximately 80% of the mediolateral extent of the cortex in the dorsal aspect of the medial temporal lobe (see above). One section caudally, where the amygdaloid complex is larger (Fig 5) and often the temporal horn of the lateral ventricle is present, the cortical amygdala (including the anterior cortical nucleus, nucleus of the lateral olfactory tract, PAC3, and PACs) extends as far as the border with the rostromedial portion of the entorhinal cortex at the fundus of the *sulcus semiannularis* (49). In cases, where the *sulcus semiannularis* is not apparent, the border defined by the line extending medially from the white matter to the surface of the brain was used as the ventral border of the cortical amygdala (Fig 5) (50). At the beginning of the subiculum at the head of the hippocampus (64), the cortical amygdala (medial nucleus, posterior cortical nucleus, PACs) becomes continuous with the amygdalo-hippocampal transitional area (AHA) (Fig 1D).

Amygdalo-hippocampal Transitional Area. This transitional area between the hippocampus and the amygdala (65) continues caudally the *gyrus semilunaris*, approximately at the level of the *diverticulum unci* (66). The caudal end of the cortical amygdala comes into close contact with the amygdalo-hippocampal transitional area (AHA), which establishes the link between the rostral extremity of the uncal hippocampal allocortex and the caudal end of the olfactory amygdala. Due to the lack of any apparent landmarks to separate the AHA from the cortical amygdala, it was included in the volumetric measurement.

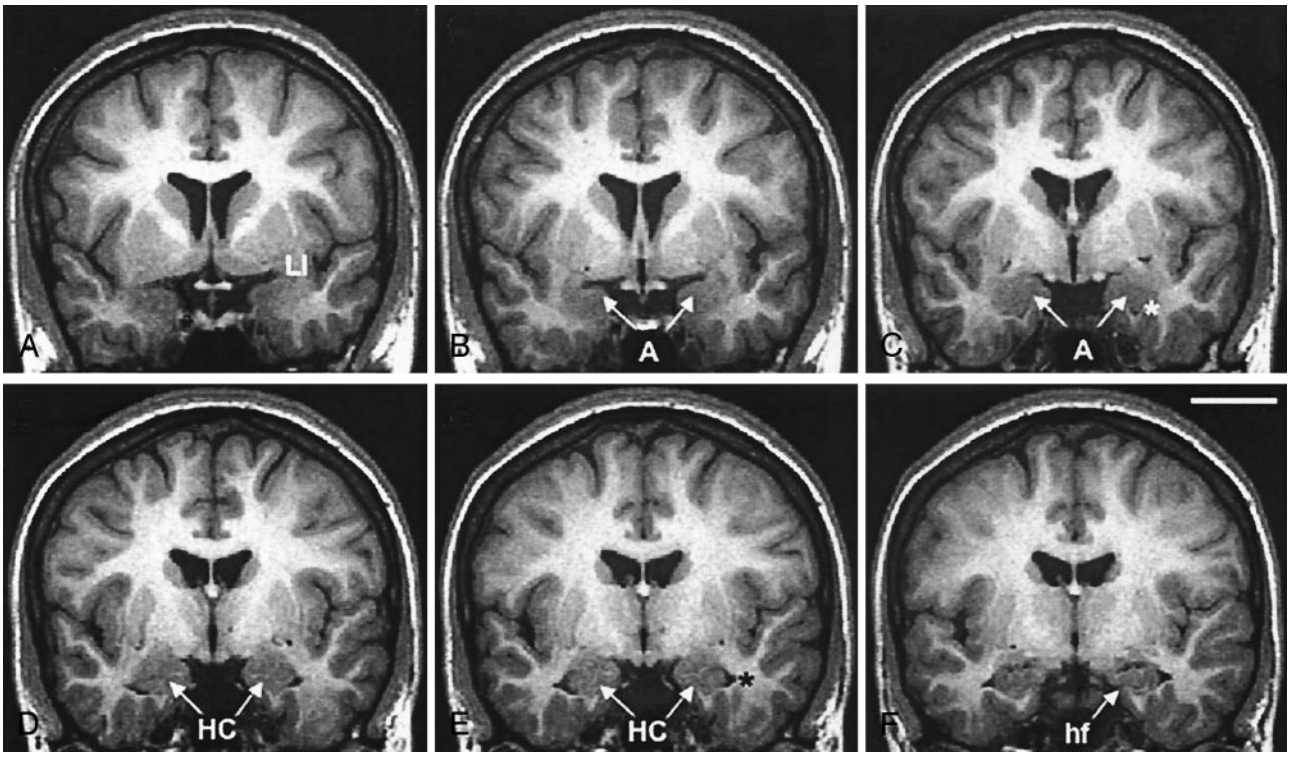


FIG 3. Successive 2-mm coronal MR images demonstrate the location of the PCA. *A* is the most rostral and *F* is the most caudal. A, Shows the limen insulae (LI); B, first section where the characteristic ovoid shape of the amygdala (A) can be recognized; C, full extent of the amygdala (A) with lateral ventricle appearing underneath (asterisk); D, appearance of the rostral hippocampus (HC); E, rostral hippocampus at the level of the hippocampal head and lateral ventricle (asterisk); and F, hippocampal fissure (hf; arrow). Scale bar equals 20 mm (applies to all panels).

The amygdalo-hippocampal area becomes apparent at the caudal part of the *gyrus uncinatus*, rostral to the hippocampal fissure (Fig 1D). The caudal limit of the AHA was coincident with the beginning of the hippocampal fissure in most of the cases.

Definition of the PCA Borders on Coronal MR Images

The PCA was outlined from the rostral to caudal direction, according to the MR imaging step-by-step protocol defined below. Before PCA measurements in TLE patients, ten randomly assigned control subjects were selected for intra- and interobserver tests to assure the reproducibility of the protocol. Measurements of TLE subjects were performed by a single investigator (P.M.G.P.) who was blind to the patient's clinical and electroencephalographic characteristics. In cases where the cortical boundaries were not clear, a second opinion (T.S.) was obtained.

The localization of the PCA region in the medial temporal lobe is presented in coronal MR images in Figures 3 and 4 and schematically in corresponding line-drawings in Figure 5.

Step 1

The coronal MR image containing the LI was selected (Figs 3A, 4A and 5). At this level, the PCA is composed of the PC, which was not identifiable in terms of different contrast. Therefore, based on histologic analysis, the PCA outline was drawn to include 30% (approximately one-third) of the distance from the *endorhinal sulcus* to the most convex point of the medial temporal lobe. Its thickness was determined to be one-fourth (25%) of the thickness of the adjacent perirhinal cortex (PRC), as indicated on Figure 4A.

Step 2

In the next section (Figs 4B and 5), the PCA occupies one-half (50%) of the distance from the *endorhinal sulcus* to the *gyrus semilunaris* (most medial bump of the medial temporal cortex). Caudal to this level, the PCA included three-fourths (75%) of that distance (Figs 4C and 5) up to the appearance of the amygdala. Its thickness was drawn as 25% of that of the PRC, as in step 1, and as indicated on Figure 4B.

Step 3

Next, the characteristic ovoid shape of the amygdala became visible on MR images (Figs 3B, 4D and 5). At this level, the entire cortex from the fundus of the *endorhinal sulcus* to the most medial point of the *gyrus semilunaris* on the medial temporal cortex was included into the PCA. If the *sulcus semiannularis* was already present, the fundus of the sulcus was considered to be the ventral limit of the PCA. The entire thickness of the cortex was included in the PCA.

Step 4

On the next 2.0-mm MR image (Figs 4E-F and 5), the cortex extending from the *endorhinal sulcus* to the fundus of the *sulcus semiannularis* was included in the PCA. The entire thickness of the cortex was included in the PCA.

Step 5

Starting approximately 12 mm from the LI, the amygdala is at its largest and the temporal horn of the lateral ventricle appears ventrolateral to the amygdala (Figs 3C, 4G and 5). At this level, the *sulcus semiannularis* is near its end, and it may be either absent or show a shallow appearance on MR images. If

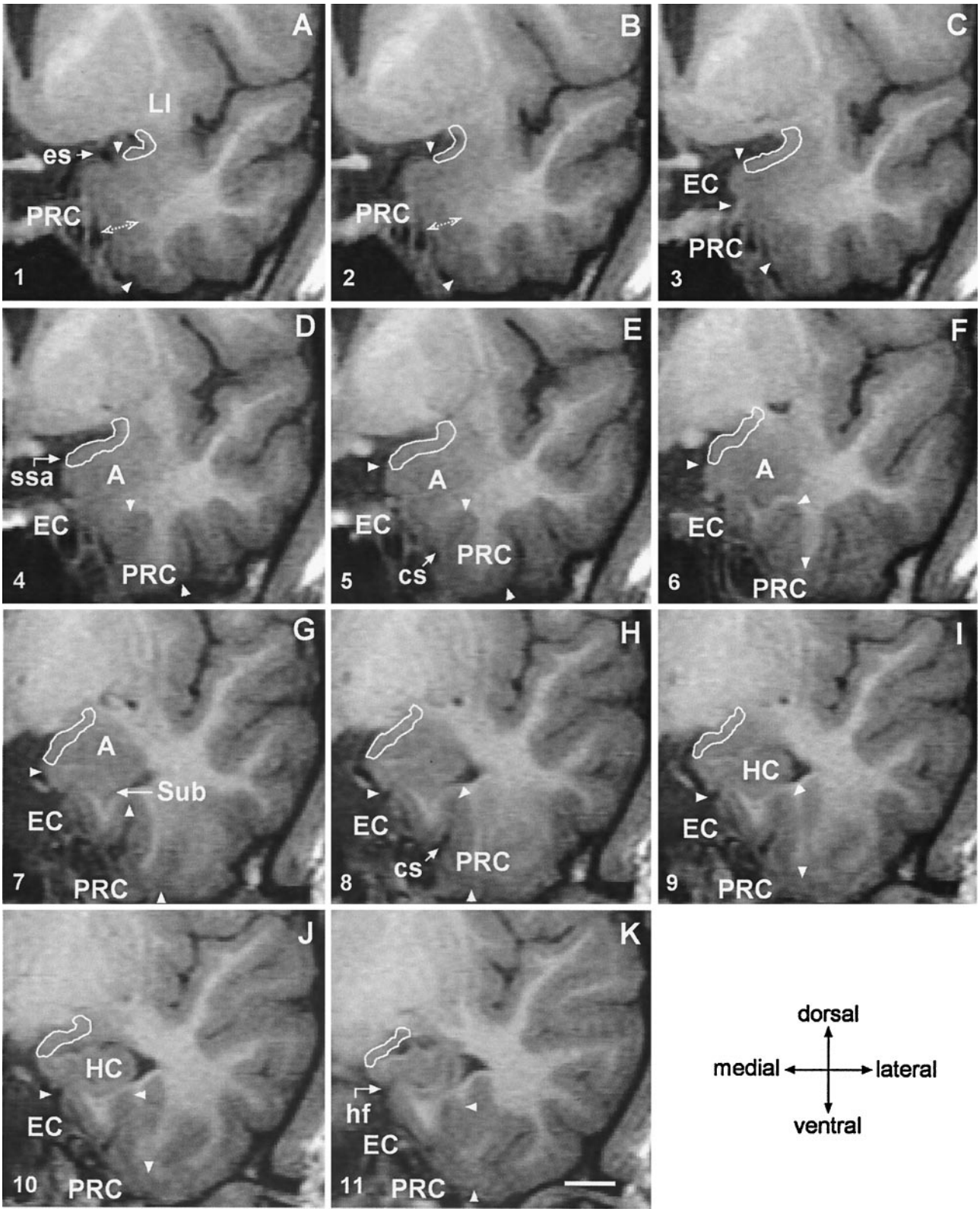


FIG 4. Coronal 2-mm-thick MR images from a control subject demonstrate the outline of the PCA at different rostrocaudal levels. Line drawings of the same MR imaging sections demonstrating more anatomic details are shown in Figure 5 (numbers in the lower left corner correspond to the levels of the line-drawings). *A* is the most rostral and *K* is the most caudal. In panels A and B, the thickness of the perirhinal cortex, which serves as reference for the thickness of the PCA is indicated. Panel *C* marks the anterior-most limit of the entorhinal cortex. In panels *D*, *E* and *F*, the characteristic ovoid shape of the amygdala can be recognized. Panel *G* shows the appearance of the subiculum. Panels *H–K* show the hippocampal head. EC indicates entorhinal cortex; cs, *colateral sulcus* (arrow); A, amygdala; es, *endorhinal sulcus* (arrow); HC, hippocampus; hf, hippocampal fissure (arrow); LI, *limen insulae*; PRC, perirhinal cortex; ssa, s*ulcus semiannularis* (arrow); Sub, subiculum; and arrowheads, boundaries of the entorhinal and perirhinal cortices. Scale bar equals 10 mm (applies to all panels).

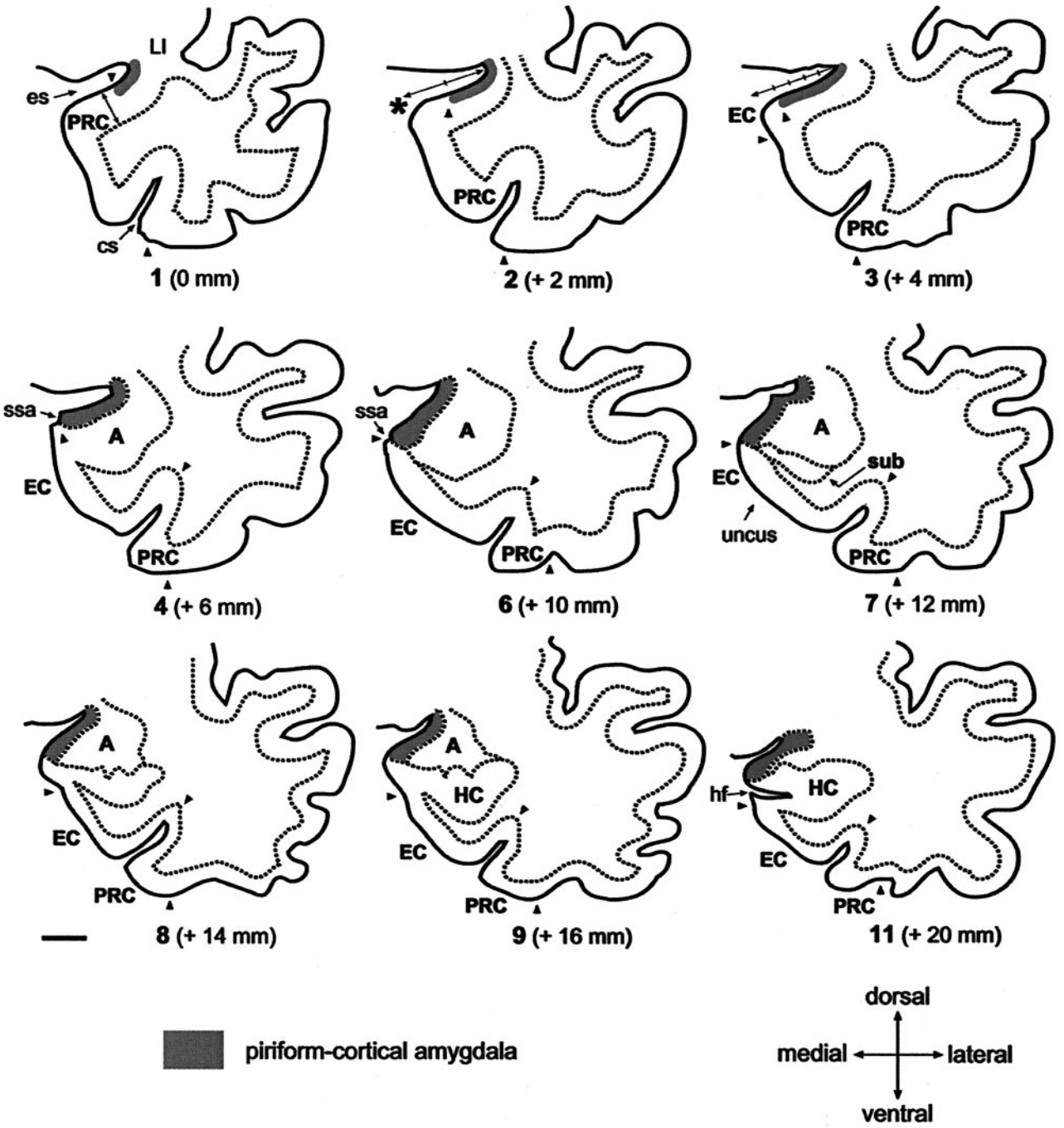


FIG 5. Line-drawings corresponding to MR images in Figure 4 summarize the anatomic landmarks used to draw the outlines of the PCA. Only the images displaying critical landmarks are shown. In section #1 (Fig 4A), the appearance of the *limen insulae* (LI) marks the reference level for outlining the PCA. At this level, the PCA extends 30% of the distance between the *endorhinal sulcus* (es) to the most convex point of the medial temporal cortex (asterisk). Its thickness is reaches 25% that of the adjacent perirhinal cortex (PRC). In section #2 (Fig 4B), the PCA occupies 50% of the distance of the *endorhinal sulcus*-medial temporal lobe convexity (arrow). Its thickness is 25% of that of the adjacent PRC. In section #2 (Fig 4C), the PCA extends down as far as the continuation of the limit of the white matter at its crossing with the pial surface (alternatively, if it were absent, the limit is given by the visualization of the sulcus semiannularis). This distance represents up to 80% of the distance of the es-medial temporal lobe convexity. The PCA borders ventrally the most medial aspect of the entorhinal cortex (EO subfield) (49). Its thickness is 25% that of the adjacent PRC. Section #4 (Fig 4D) is at the level of the rostralmost portion of the amygdala. At this level, the PCA extends from the *endorhinal sulcus* down to the *sulcus semiannularis* (ssa), or in its absence, as in the previous level. Its thickness encompasses the entire cortical gray matter. In section #6 (Fig 4F), the amygdala is larger. The PCA occupies the entire medial temporal cortex down from the *endorhinal sulcus* to the *sulcus semiannularis*. Its thickness encompasses the entire cortical gray matter. In sections 7–9 (Fig 4G–I), the rostral hippocampus appears. The PCA is defined as in level #6. In section #11, the opening of the hippocampal fissure (hf) marks the last image to be quantified. HC indicates hippocampus; cs, *colateral sulcus*; Sub, subiculum. Scale bar equals 10 mm (all panels).

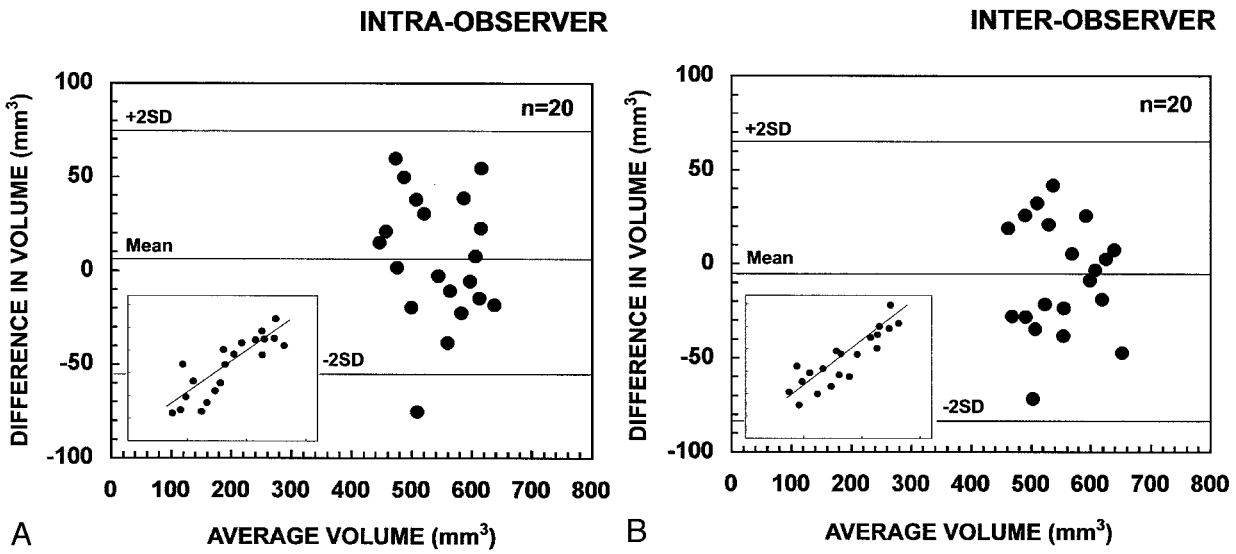


FIG 6. Scatter plots show the intra- and inter-observer variability of repeated measurements in the assessment of the right and left volume of the PCA of 10 control subjects. A, shows intra-observer measurement (P.M.G.P.); and B, inter-observer measurement (P.M.G.P. versus T.S.). The limits of agreement between the first and second measurements are expressed as the mean difference in volume: [volume in the first measurement minus volume in the second measurement (mm^3)] ± 2 SD. Inserts in the lower left corner show the association between the first (x-axis) and second (y-axis). Mean indicates mean difference in volume; +2 SD, mean difference in volume plus two SD; −2 SD, mean difference in volume minus two SD.

the *sulcus semiannularis* is visible, the PCA extends from the fundus of the *endorhinal sulcus* to the fundus of the *sulcus semiannularis*. In the cases were the *sulcus semiannularis* cannot be identified, the approximate ventral limit of PCA was determined by the intersection of the line extending from the white matter under the amygdala (medial extension of the external capsule) to the surface of the brain, as defined previously (50) for the entorhinal cortex. The entire thickness of the cortex was included into the PCA. In more caudal sections where the rostral end of the hippocampus (uncus) appears (Figs 3D, 4H-I, and 5), the PCA is defined accordingly.

Step 6

At the caudal end of the amygdala (Figs 3E, 4J-K and 5), the *gyrus ambiens*, including the medial intermediate subfield of the entorhinal cortex, is replaced by the amygdalo-hippocampal area and the uncus, which is composed of the subiculum and the CA1 subfield (64, 65). At this level, the *endorhinal sulcus* becomes very narrow and locates in close proximity to the optic tract. The last section, in which the PCA was present, was usually coincident with the opening of the hippocampal fissure (Figs 3F, 4K and 5). The outlines of the PCA were drawn as in Step 5.

Once the PCA cortices were outlined on each of the coronal images, the final volume was calculated by using a program developed in-house for a standard work console.

Statistical Analysis

The mean, SD and coefficient of variation of the PCA volume, and the MR imaging data were computed by using SPSS/PC+ Statistical Software Package 11.0 (SPSS, Inc., Chicago, IL), and the normal distribution was analyzed by the Kolmogorov-Smirnov test.

As it is generally accepted that interindividual variability in head size affects the volumes of brain regions, we corrected the PCA volume to the individual brain area obtained at the level of the anterior commissure, according to Cendes et al (67) with modifications (68). Briefly, we used the formula: (overall mean control intracranial area/intracranial area for each subject) x measured cortical raw PCA volume of the subject.

Ten randomly assigned control subjects were selected for intra- and interobserver tests, by using the method introduced by Bland and Altman (69). Repeated measurements were performed for 10 control subjects. The limits of agreement between the first and second measurement were defined as the mean difference in volume (first minus second measurement) ± 2 SD of the mean difference (Fig 6). The clinical significance of the intra- and interobserver variability was assessed by comparing the limits of agreement with (a) the total volume of the PCA, (b) the mean volume reductions, and (c) the volume considered to be a marker of volume reduction in individual analyses (> 2 SD from the mean of control subjects). The mean difference in volume was near zero and thus, not considered significant.

For statistical analysis, the patients were divided into two groups according to localization of the seizure focus: TLE patients with focus on the right and TLE patients with focus on the left. Because the initial statistical survey indicated that the parameters studied were not normally distributed and the number of subjects in each study group was small, nonparametric analyses were used. First, the mean PCA volumes between control subjects and patients with left or right TLE were compared by using the Kruskal-Wallis test. Differences between the study groups were determined by using the Mann-Whitney test with the Bonferroni adjustment (x 3) for multiple comparisons. To assess the degree of volume asymmetry, the PCA asymmetry ratio was calculated according to Bernasconi et al (70): [Asymmetry (%) = (100 x (R-L)/((R+L)/2) where R refers to the volume on the right and L to that on the left. In control subjects, right–left asymmetry in the volumes was analyzed by using Wilcoxon's test with two related samples, and the effect of sex was analyzed by using a Mann-Whitney test. Subsequently, patients were divided accordingly to their measured hippocampal volumes (HCvol) in HS patients, if the volume was less than two SD from the control mean and without HS if HCvol was at least two SD from the control mean. A P value of less than .05 was considered statistically significant.

Results

Stereological Determination of PCA Volume in Control Subjects

The mean ± 1 SD volume of PCA was 280 ± 27 mm^3 (ranged between 254 to 331 mm^3). Figure 7 is the plot of the volume estimation for the PCA areas

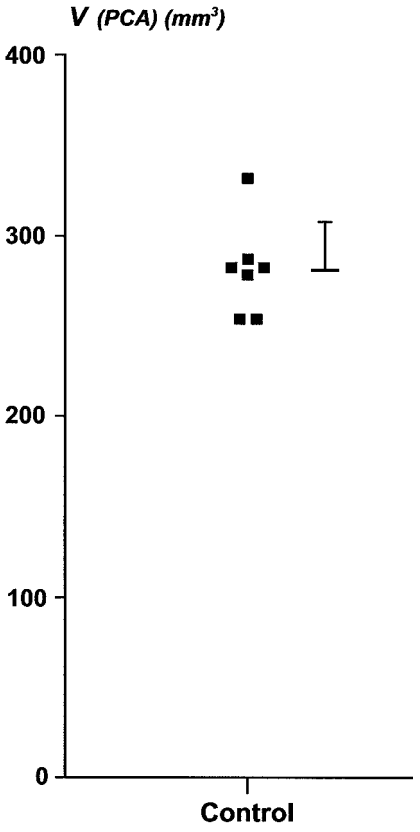


FIG 7. Plot of the individual volume estimation of the PCA, obtained by the stereological assessment of seven brain hemispheres (see Materials and Methods section for details). Each square represents a case. Group mean ± 1 SD is indicated on the right side.

in the seven hemispheres quantified. The variability was not due to the method of volume estimation since the coefficient of error was, in average, less than 2%. In addition, the contribution of the point counting to the overall coefficient of error was approximately half of the contribution of the variability between sections. Values obtained were smaller compared with MR imaging determinations. This difference can be accounted for by the retraction of tissue (up to 48%, [Mouritzen Dam, 1979 #1795]) due to fixation in 4% paraformaldehyde and staining process.

Control Subjects

The mean normalized volumes and the asymmetry ratios of the PCA volumes in control subjects are shown in Table 2. There was no significant right–left asymmetry in the mean volumes. There was no sex difference in the PCA volumes. Also, there was no correlation between PCA volume and age.

Patients with TLE

The sex distribution and mean age did not differ between control subjects and patients with TLE. When control subjects and patients with right or left TLE were compared, there were differences in the mean PCA volumes between groups.

Patients with right TLE

The mean ipsilateral PCA volume was 18% smaller than in control subjects ($P < .001$). The mean contralateral PCA volume did not differ from that in control subjects (Table 2). Also, the mean asymmetry ratio was higher than that in control subjects ($P < .001$). There was a greater than 10% decrease in the right PCA volume in three patients and a greater than 20% volume decrease in 10 patients. Additionally, the mean right PCA volume was 15% smaller than that in left TLE patients ($P < .01$).

Patients with left TLE

The mean left PCA was 16% smaller than in control subjects ($P < .01$) and 19% smaller than in the right TLE group ($P < .001$). The mean right PCA did not differ from that in control subjects. The mean asymmetry ratio was higher than in control subjects ($P < .05$), indicating that PCA volumes were smaller ipsilateral to the focus. In this group, there was a greater than 10% decrease in the left PCA volume in five patients and a greater than 20% decrease in eight.

PCA atrophy was bilateral in 18% (7/39) of the patients (five patients with bilateral PCA volumes reduction were over 20% and two patients presented bilateral reductions over 10%).

PCA Volume in Patients With Hippocampal Atrophy

We assessed whether the volume reduction within the PCA is associated with hippocampal, amygdaloid, or entorhinal atrophy (Table 1). In control subjects, both right and left PCA volumes correlated with the volume of the right ($r = 0.447$, $P < .05$) or the left ($r = 0.524$, $P < .01$) hippocampus, respectively. There was no correlation with amygdala volumes, but the volume of the right PCA correlated with that of the right entorhinal cortex ($r = 0.467$, $P < .05$).

In all patients with TLE (Fig 8), the volume of the PCA ipsilateral to the seizure focus correlated with the ipsilateral hippocampal volume ($r = 0.756$, $P < .01$), ipsilateral amygdala volume ($r = 0.548$, $P < .01$), and ipsilateral entorhinal cortical volume ($r = 0.500$, $P < .01$). The contralateral PCA volume correlated with the contralateral hippocampal volume ($r = 0.363$, $P < .05$), contralateral amygdala volume ($r = 0.397$, $P < .05$), but not with the contralateral entorhinal volume ($r = 0.158$, $P > .05$).

To assess whether TLE patients with a hippocampal volume reduction of at least two SD on the side of the seizure focus have more substantial PCA atrophy than patients with milder hippocampal atrophy, the PCA volume in the TLE subgroups was evaluated (Table 2). Eight patients with right TLE and 11 patients with left TLE had a volume reduction of at least two SDs from the mean of control subjects (at least 19% volume reduction) in the ipsilateral hippocampus, and the mean hippocampal volume was reduced by 45% on average compared with the control group. In patients with right hippocampal atrophy, the mean right PCA volume was reduced by 28% ($P < .001$)

TABLE 2: Normalized volumes and asymmetry ratio of the right and left piriform-cortical amygdala in control subjects and patients groups and subgroups

Group		Right PCA	Left PCA	Δ PCA
Controls	(n = 23)	530 ± 59 (422–644)	512 ± 60 (406–610)	7.2 ± 4.1
Right TLE	All Patients (n = 18)	436 ± 71 (367–585)*** ^ ^	526 ± 59 (408–612)	19.3 ± 12.6***
	HS Patients (n = 8)	384 ± 28 (367–430)***°°	508 ± 59 (408–607)	27.1 ± 14.4***
	Without HS (n = 10)	476 ± 69 (377–585)	541 ± 58 (461–612)	13.0 ± 6.3*
Left TLE	All Patients (n = 21)	512 ± 70 (364–605)	427 ± 68 (307–506)**€€€	19.2 ± 16.0*
	HS Patients (n = 11)	492 ± 83 (364–603)	388 ± 61 (307–488)***¥¥	24.0 ± 18.0*
	Without HS (n = 10)	535 ± 45 (458–605)	470 ± 47 (375–509)	13.9 ± 12.4

All volumes are presented as mean ± one standard deviation of the mean (range) and given in mm^3. Asymmetry ratios (Δ) are presented as mean ± one standard deviation of the mean (range) and given in percentages. Nonparametric analyses with the Bonferroni correction were used to compare means over the study groups and to determine differences between the groups. * $P < .05$, ** $P < .01$, *** $P < .001$ compared to controls. ^ ^ $P < .01$ compared to left TLE patients, €€€ $P < .001$ compared to right TLE patients, °° $P < .01$ compared to right TLE patients without HS, ¥¥ $P < .01$ compared to left TLE patients without HS. HS indicates hippocampal sclerosis; PCA, piriform-cortical amygdala; TLE, temporal lobe epilepsy.

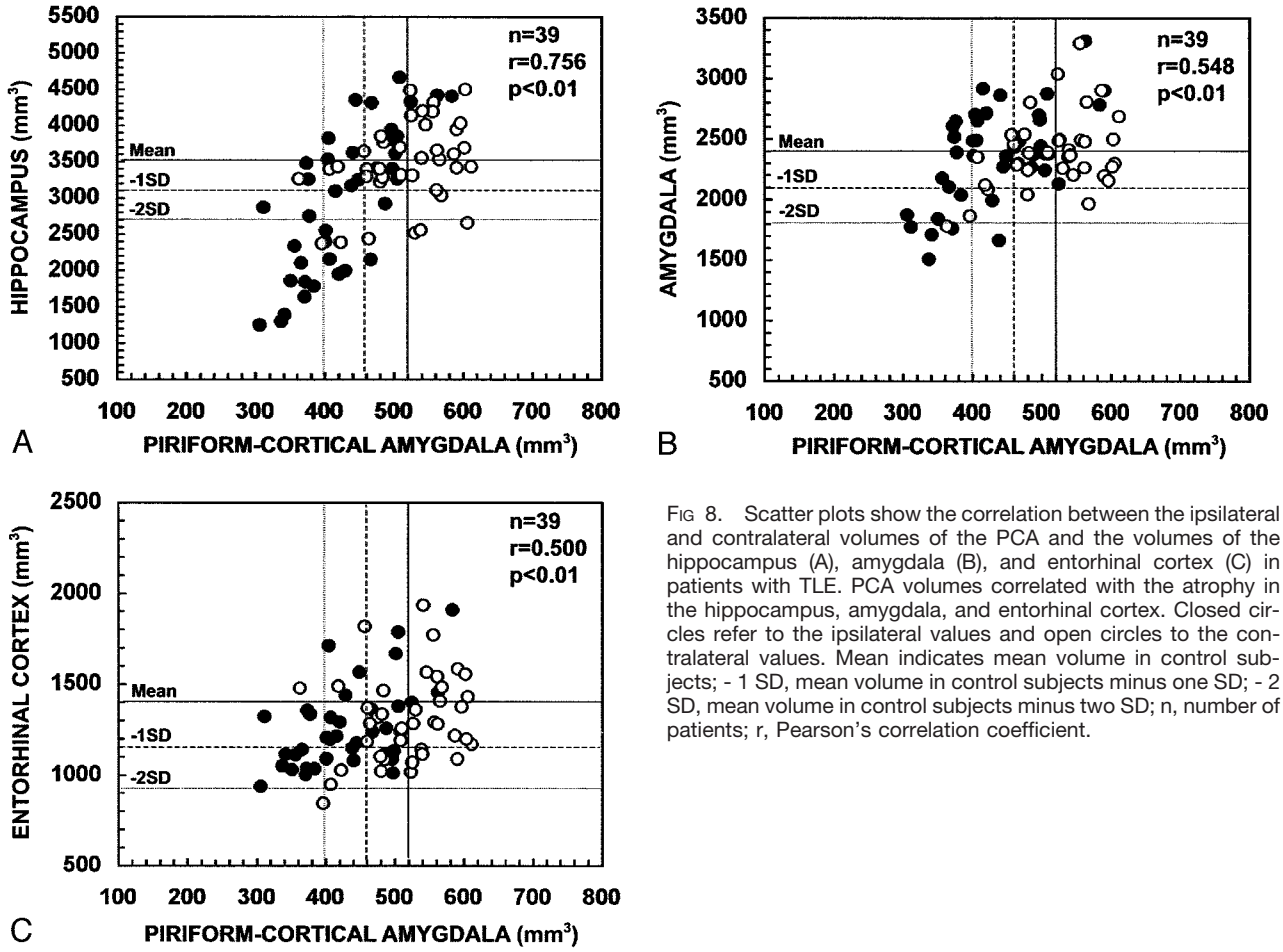


FIG 8. Scatter plots show the correlation between the ipsilateral and contralateral volumes of the PCA and the volumes of the hippocampus (A), amygdala (B), and entorhinal cortex (C) in patients with TLE. PCA volumes correlated with the atrophy in the hippocampus, amygdala, and entorhinal cortex. Closed circles refer to the ipsilateral values and open circles to the contralateral values. Mean indicates mean volume in control subjects; - 1 SD, mean volume in control subjects minus one SD; - 2 SD, mean volume in control subjects minus two SD; n, number of patients; r, Pearson's correlation coefficient.

compared with control subjects. In patients with left hippocampal atrophy, the mean left PCA volume was 24% smaller than in control subjects ($P < .001$). Additionally, the mean PCA volumes were 18% smaller in patients with hippocampal atrophy compared with patients without hippocampal volume reduction ($P < .01$, on both subgroups). Three patients without HS had a reduction of at least two SD in the ipsilateral PCA volume and six patients with HS had normal PCA volumes.

PCA Volume in Patients with Amygdaloid Atrophy

Two patients with right TLE and one with left TLE had a volume reduction of the ipsilateral amygdala of

at least two SDs of the control mean. Both right TLE patients with amygdala atrophy had a PCA volume of at least two SDs below the control mean.

There were no patients with an entorhinal cortex volume reduction of less than two SDs from the mean of the control subjects (54).

Association of the PCA Volumes with Lifetime Seizure Number

The volume of the ipsilateral or contralateral PCA did not correlate with the lifetime seizure number.

Discussion

In the present study, we developed a method to measure the volume of the PCA in coronal MR images of the human brain. This method allowed us to assess the occurrence and severity of PCA atrophy in patients with TLE and its co-occurrence with volume reduction in the hippocampus, amygdala, or entorhinal cortex. Only patients with an unknown etiology for TLE were included in the study. After establishing the adequate methodological considerations, the study revealed four major findings. First, there was no hemispheric asymmetry of the PCA in control subjects. Also, the volume did not vary depending on the sex or age of the subjects. Second, in approximately 40% of patients with TLE there was at least a 20% volume reduction in the ipsilateral PCA. Third, PCA atrophy strongly correlates with HS and the side of the seizure focus. Fourth, there was no association between the PCA volumes and lifetime seizure number.

1. Methodological Considerations

The purpose of this study was to investigate the occurrence of damage in the PC and the cortical amygdala in patients with TLE by means of quantitative MR imaging. Based on histologic analysis, we have elaborated a protocol that can be used to measure the volume of the human PCA in 2.0-mm-thick coronal MR images, which provides additional information on the structural integrity of the medial temporal lobe. Our MR protocol was designed based on anatomic landmarks derived from the analysis of histologic sections from postmortem brains of healthy subjects. Thus, we were able to locate the different segments of the PCA and extrapolate the findings to determine the boundaries on MR images. The major difficulty was in determining the thickness of the piriform cortex. This cortical area appears embedded in the *endorhinal sulcus* on the first three MR images, starting at the LI, and there are no clear reference points to delineate this region on MR images. Therefore, we used the thickness of the neighboring perirhinal cortex as a reference. Consequently, it is possible that atrophy of the perirhinal cortex can bias the estimation of the volume of the PCA. It is, however, important to realize that this would compromise the thickness measurement in only three of 11 coronal sections, and the volume of this portion of the PCA is no more than 18% of the total PCA volume. Also, volume reduction of the perirhinal cortex is relatively uncommon, even in patients with intractable epilepsy (8, 10, 71). Therefore, we concluded that the use of the perirhinal cortex to define the thickness of the piriform component of the PCA does not significantly affect the data evaluation. Contrary to the PC, the cortical amygdala and the amygdalohippocampal transition area (the remaining 82% of total PCA volume) are readily identified on T1-weighted MR images by their different contrast, allowing their separation from the adjacent amygdala and hippocampus.

The thickness and orientation of the MR images was set according to identical thickness and orientation of the histologic sections, facilitating in this way the identification of the boundaries and minimizing partial volume effects. Even so, partial voluming is an inherent property of the discretized image and would still persist if the contrast between tissues were maximal or if the thickness was sub-milimetric. Moreover, at 1.5T, the volumetrics of parahippocampal cortices should rely as much as possible in the correct recognition of the same anatomic boundaries as seen on histologic examination (50, 54, 72–74), which are crucial for accurate delineation of the region of interest (75, 76). Therefore, it is advisable to employ identical section thickness to use the minimum number of MR partitions to estimate the volumes (77).

Except for the hippocampus and amygdala, focal atrophies of the para-hippocampal cortices are virtually indiscernible with current cross-sectional high-resolution imaging. Similarly, PCA atrophies can only be detected quantitatively. It is possible, however, that MR imaging performed at higher fields than 1.5T with tailored sequences for the mesio-temporal cortices, could demonstrate such abnormalities qualitatively.

One novel result of this study was to identify PCA damage in drug-refractory TLE patients. Still, we were unable to confirm our data histologically. Indeed, to date there exists no gold standard consisting of MR imaging and histologic analysis of the same TLE cases. Future post-surgical or autopsy-based studies are needed to substantiate our data and to definitively establish the role that the human PC and cortical amygdala have as critical areas in epileptogenesis.

2. PCA Volume as a Marker for Seizure Lateralization

The results indicate a high concordance between PCA atrophies on one hand, and the EEG findings and the hippocampal atrophies, on the other.

In the present study, 44% patients had a PCA volume reduction of at least 2 SD below the control values. Of these patients, 76% had an asymmetry index higher than 2 SD of control subjects. The remaining 56% of patients had a normal PCA volume (within mean $\pm$ 2 SD limits), but also had an asymmetry index with a trend toward abnormality on the side of the focus (32% of these patients had a volume

asymmetry higher than 2 SD of control subjects). These data suggest that a reduced PCA volume or abnormal asymmetry index can be a useful addition to the tools currently used to determine the side of the seizure focus.

3. PCA Atrophy is One Component of Overall Damage in the Temporal Lobe

Volumetric MR imaging measurements of the amygdala (7, 67), entorhinal (54, 70), perirhinal (10) and parahippocampal (71) cortices, thalamus, lenticular and caudate nuclei (78), fornix, and mammillary bodies (79, 80) support the concept that tissue damage in TLE is not limited to the hippocampus, but involves other associated limbic structures. Our data demonstrate that even though a most of patients with HS also have ipsilateral PCA atrophy, the PCA volume is normal in 31% of HS patients. Further, 15% of patients with normal hippocampal volumes had a volume reduction in the PCA. These data are consistent with previous data suggesting that structural atrophy secondary to cell loss often extends outside the hippocampus. Furthermore, in the absence of clearly identifiable HS in TLE, extrahippocampal damage, including that in the PCA, can be part of the epileptogenic zone responsible for the symptomatic findings. Whether the damage in these various brain areas occurs at the same time or develops in parallel or sequentially later during the epileptogenic process (6) remains to be studied, along with the relative sensitivity, specificity and predictive value of the various quantitative MR imaging protocols that we have at our disposal to characterize the overall brain damage induced by TLE.

Conclusion

The volumetric measurement of the PCA is feasible in human MR images despite its small size. Atrophy of the PCA occurs in a subgroup of patients with TLE and the severity of the volume reduction correlates with hippocampal atrophy. These data demonstrate that the PCA is one component of the damaged temporal lobe network in humans. Furthermore, volumetric assessment of the PCA provides additional information to determine the lateralization of seizure focus.

Acknowledgments

We thank Professor Fernando Lopes da Silva for his constructive comments on the final version of this article. We thank Mrs. Teresa Carracho (the Grünenthal Foundation /Department of Design) for assistance in drawing Figure 5.

References

1. Commission on Classification and Terminology of the International League Against Epilepsy. **Proposal for revised clinical and electroencephalographic classification of epileptic seizures**. *Epilepsia* 1981;22:489–501
2. Commission on Classification and Terminology of the International League Against Epilepsy. **Proposal for revised classification of epilepsies and epileptic syndromes**. *Epilepsia* 1989;30:389–399
3. Hauser WA, Kurland LT. **The epidemiology of epilepsy in Rochester, Minnesota, 1935 through 1967.** *Epilepsia* 1975;16:1–66
4. Williamson PD, Wieser HG, Delgado-Escueta AV. **Clinical characteristics of partial seizures**. In: Engel JJ, ed. *Surgical Treatment of the Epilepsies.* New York: Raven Press, 1987; 101–120
5. Falconer MA. **Mesial temporal (Ammon's horn) sclerosis as a common cause of epilepsy. Aetiology, treatment, and prevention**. *Lancet* 1974;2:767–770
6. Mathern GW, Adelson PD, Cahan LD, Leite JP. **Hippocampal neuron damage in human epilepsy: Meyer's hypothesis revisited**. *Prog Brain Res* 2002;135:237–251
7. Kälviäinen R, Salmenperä T, Partanen K, Vainio P, Riekkinen P, Sr., Pitkänen A. **MRI volumetry and T2 relaxometry of the amygdala in newly diagnosed and chronic temporal lobe epilepsy**. *Epilepsy Res* 1997;28:39–50
8. Bernasconi N, Bernasconi A, Caramanos Z, Andermann F, Dubeau F, Arnold DL. **Morphometric MRI analysis of the parahippocampal region in temporal lobe epilepsy**. *Ann N Y Acad Sci* 2000;911:495–500
9. Salmenperä T, Kälviäinen R, Partanen K, Mervaala E, Pitkänen A. **MRI volumetry of the hippocampus, amygdala, entorhinal cortex, and perirhinal cortex after status epilepticus**. *Epilepsy Res* 2000;40:155–170
10. Jutila L, Ylinen A, Partanen K, et al. **MR Volumetry of the Entorhinal, Perirhinal, and Temporopolar Cortices in Drug-Refractory Temporal Lobe Epilepsy**. *AJNR Am J Neuroradiol* 2001;22:1490–1501
11. Margerison JH, Corsellis JAN. **Epilepsy and the temporal lobes. A clinical, electroencephalographic and neuropathological study of the brain in epilepsy, with particular reference to the temporal lobes**. *Brain* 1966;89:499–530
12. Pitkänen A, Tuunanen J, Kälviäinen R, Partanen K, Salmenperä T. **Amygdala damage in experimental and human temporal lobe epilepsy**. *Epilepsy Res* 1998;32:233–253
13. Lopes da Silva FH, Wadman WJ. **Pathophysiology of epilepsy**. In: Meinardi H, ed. *The Epilepsies, Part I*: Elsevier Science B. V., 1999
14. Lüders HO. **Mesial Temporal Sclerosis. Overview**. In: Kotagal P, Lüders HO, eds. *The Epilepsies. Etiologies and Prevention*: Academic Press, 1999; 121–124
15. Vogt C, Vogt O. **General results of our brain research, second part: The nature of the architectural differences the cerebral cortex [in German]**. *J Psychol Neurol (Leipzig)* 1919:292–360
16. Insausti R, Amaral DG, Cowan WM. **The entorhinal cortex of the monkey: III. Subcortical afferents**. *J Comp Neurol* 1987;264:396–408
17. Price JL. **Olfactory System**. In: Paxinos G, ed. *The Human Nervous System.* 2nd ed. San Diego: Academic Press, Inc., 1990; 979–998
18. Zatorre RJ, Jones-Gotman M, Evans AC, Meyer E. **Functional localization and lateralization of human olfactory cortex**. *Nature* 1992;360:339–340
19. Carmichael ST, Clugnet MC, Price JL. **Central olfactory connections in the macaque monkey**. *J Comp Neurol* 1994;346:403–434
20. Gottfried JA, Deichmann R, Winston JS, Dolan RJ. **Functional heterogeneity in human olfactory cortex: an event-related functional magnetic resonance imaging study**. *J Neurosci* 2002;22:10819–10828
21. Fujikawa DG, Itabashi HH, Wu A, Shinmei SS. **Status epilepticus-induced neuronal loss in humans without systemic complications or epilepsy**. *Epilepsia* 2000;41:981–991
22. Bertram EH. **Functional anatomy of spontaneous seizures in a rat model of limbic epilepsy**. *Epilepsia* 1997;38:95–105
23. Löscher W, Ebert U. **The role of the piriform cortex in kindling**. *Prog Neurobiol* 1996;50:427–481
24. Clark M, Post RM, Weiss SR, Cain CJ, Nakajima T. **Regional expression of c-fos mRNA in rat brain during the evolution of amygdala kindled seizures**. *Mol Brain Res* 1991;11:55–64
25. Maggio R, Lanaud P, Grayson DR, Gale K. **Expression of c-fos mRNA following seizures evoked from an epileptogenic site in the deep prepiriform cortex: regional distribution in brain as shown by in situ hybridization**. *Exp Neurol* 1993;1:11–19
26. Sato M, Racine RJ, McIntyre DC. **Kindling: basic mechanisms and clinical validity**. *Electroencephalogr Clin Neurophysiol* 1990;76:459–472
27. Ebert U, Löscher W. **Strong induction of c-fos in the piriform cortex during focal seizures evoked from different limbic brain sites**. *Brain Res* 1995;671:338–344
28. Fujikawa DG. **The temporal evolution of neuronal damage from pilocarpine-induced status epilepticus**. *Brain Res* 1996;725:11–22
29. Gorter JA, van Vliet EA, Aronica E, Lopes da Silva FH. **Progression of spontaneous seizures after status epilepticus is associated**

with mossy fibre sprouting and extensive bilateral loss of hilar parvalbumin and somatostatin-immunoreactive neurons. *Eur J Neurosci* 2001;13:657–669
30. Gorter JA, Gonçalves Pereira PM, van Vliet EA, et al. **Neuronal cell death in a rat model for mesial temporal lobe epilepsy is induced by the initial status epilepticus and not by later repeated spontaneous seizures.** *Epilepsia* 2003;44:647–658
31. Pirttila TR, Pitkänen A, Tuunanen J, Kauppinen RA. **Ex vivo MR microimaging of neuronal damage after kainate-induced status epilepticus in rat: correlation with quantitative histology**. *Magn Reson Med* 2001;46:946–954
32. Roch C, Leroy C, Nehlig A, Namer IJ. **Magnetic resonance imaging in the study of the lithium-pilocarpine model of temporal lobe epilepsy in adult rats**. *Epilepsia* 2002;43:325–335
33. Roch C, Leroy C, Nehlig A, Namer IJ. **Predictive value of cortical injury for the development of temporal lobe epilepsy in 21-day-old rats: an MRI approach using the lithium- pilocarpine model**. *Epilepsia* 2002;43:1129–1136
34. Honack D, Wahnschaffe U, Löscher W. **Kindling from stimulation of a highly sensitive locus in the posterior part of the piriform cortex. Comparison with amygdala kindling and effects of antiepileptic drugs**. *Brain Res* 1991;538:196–202
35. Löscher W, Ebert U, Wahnschaffe U, Rundfeldt C. **Susceptibility of different cell layers of the anterior and posterior part of the piriform cortex to electrical stimulation and kindling: comparison with the basolateral amygdala and "area tempestas"**. *Neuroscience* 1995;66:265–276
36. McIntyre DC, Kelly ME. **The parahippocampal cortices and kindling**. *Ann N Y Acad Sci* 2000;911:343–354
37. Racine RJ, Moscher M, Kairiss EW. **The role of the piriform cortex in the generation of interictal spikes in the kindled preparation**. *Brain Res* 1988;454:262–274
38. Kelly ME, Staines WA, McIntyre DC. **Secondary generalization of hippocampal kindled seizures in rats: examining the role of the piriform cortex**. *Brain Res* 2002;957:152–161
39. Gale K. **Progression and generalization of seizure discharge: anatomical and neurochemical substrates**. *Epilepsia* 1988;29:S15–34
40. Halonen T, Tortorella A, Zrebeet H, Gale K. **Posterior piriform and perirhinal cortex relay seizures evoked from the area tempestas: role of excitatory and inhibitory amino acid receptors**. *Brain Res* 1994;652:145–148
41. Gale K, Zhong P, Miller LP, Murray TF. **Amino acid neurotransmitter interactions in 'area tempestas': an epileptogenic trigger zone in the deep prepiriform cortex**. *Epilepsy Res Suppl* 1992;8:229–234
42. Gale K, Dubach M. **Localization of area tempestas in piriform cortex of the monkey**. *Soc Neurosci Abstr* 1993;19:21
43. Jones-Gotman M, Zatorre RJ, Cendes F, et al. **Contribution of medial versus lateral temporal-lobe structures to human odour identification**. *Brain* 1997;120:1845–1856
44. Van Paesschen W, King MD, Duncan JS, Connelly A. **The amygdala and temporal lobe simple partial seizures: a prospective and quantitative MRI study**. *Epilepsia* 2001;42:857–862
45. Kevetter GA, Winans SS. **Connections of the corticomedial amygdala in the golden hamster. II. Eferents of the 'olfactory amygdala'**. *J Comp Neurol* 1981;197:99–111
46. Luskin MB, Price JL. **The topographic organization of the assotional fibers of the olfactory system in the rat, including centrifugal fibers to the olfactory bulb**. *J Comp Neurol* 1983;216:264–291
47. Gloor P. *The temporal lobe and the limbic system.* New York: Oxford University Press, Inc., 1997
48. Gonçalves Pereira PM, Insausti R, Salmenperä T, Kälviäinen R, Pitkänen A. **Magnetic resonance volumetric analysis of the piriform cortex and cortical amygdala in chronic temporal lobe epilepsy [Suppl].** *Epilepsia* 2002;43:300–301
49. Insausti R, Tunon T, Sobreviela T, Insausti AM, Gonzalo LM. **The human entorhinal cortex: a cytoarchitectonic analysis**. *J Comp Neurol* 1995;355:171–198
50. Insausti R, Juottonen K, Soininen H, et al. **MR volumetric analysis of the human entorhinal, perirhinal, and temporopolar cortices**. *AJNR Am J Neuroradiol* 1998;19:659–671
51. Gundersen HJ, Jensen EB. **The efficiency of systematic sampling in stereology and its prediction**. *J Microsc* 1987;147:229–263
52. Howard CV, Reed MG. **Estimation of reference volume using the Cavalieri method**. In: Howard CV, Reed MG, eds. *Unbiased Stereology. Three-dimensional measurement in microscopy*: BIOS Scientific Publishers, 1998; 39–54
53. Cruz-Orive LM. **Systematic sampling in stereology**. In: Inst BIS, ed. *Proceedings 49th session.* Florence, 1993; 451–468
54. Salmenperä T, Kälviäinen R, Partanen K, Pitkänen A. **Quantitative MRI volumetry of the entorhinal cortex in temporal lobe epilepsy**. *Seizure* 2000;9:208–215
55. Salmenperä T, Kälviäinen R, Partanen K, Pitkänen A. **Hippocampal damage caused by seizures in temporal lobe epilepsy**. *Lancet* 1998;351:35
56. Brodmann K. *Comparative localization study of the brain according to the principles of cellular structures* [in German]. Leipzig: Barth, 1909
57. Sorvari H, Soininen H, Paljarvi L, Karkola K, Pitkänen A. **Distribution of parvalbumin-immunoreactive cells and fibers in the human amygdaloid complex**. *J Comp Neurol* 1995;360:185–212
58. Rose M. **The allocortex in animal and human; first part [in German]**. *J Psychol Neurol (Leipzig)* 1926:1–260
59. Price JL. **An autoradiographic study of complementary laminar patterns of termination of afferent fibers to the olfactory cortex**. *J Comp Neurol* 1973;1:87–108
60. Haberly LB, Feig SL. **Structure of the piriform cortex of the opossum. II.** *Fine structure of cell bodies and neuropil. J Comp Neurol* 1983;1:69–88
61. Martinez MC, Blanco J, Bullon MM, Agudo FJ. **Structure of the piriform cortex of the adult rat. A Golgi study**. *J Hirnforsch* 1987;28:341–348
62. Price JL, Russchen FT, Amaral DG. **The Limbic Region. II. The amygdaloid complex**. In: Björklund A, Hokfelt T, Swanson LW, eds. *Handbook of Chemical Neuroanatomy.* Amsterdam: Elsevier, 1987; 279–388
63. Turner BH, Gupta KC, Mishkin M. **The locus and cytoarchitecture of the projection areas of the olfactory bulb in Macaca mulatta**. *J Comp Neurol* 1978;3:381–396
64. Amaral DG, Insausti R. **Hippocampal formation**. In: Paxinos G, ed. *The Human Nervous System.* 2nd edition ed. San Diego: Academic Press, Inc., 1990; 711–755
65. Rosene DL, Van Hoesen GW. **The hippocampal formation of the primate brain. A review of some comparative aspects of cytoarchitecture and connections**. In: Jones EG, Peters A, eds. *Cerebral Cortex.* New York City: Plenum Press, 1987; 345–456
66. Klingler J. **The macroscopic anatomy of Ammons' formation [in German]**. *Denkschr Schweiz Naturforsch Ges* 1948;78:1–80
67. Cendes F, Andermann F, Gloor P, et al. **MRI volumetric measurement of amygdala and hippocampus in temporal lobe epilepsy**. *Neurology* 1993;43:719–725
68. Kälviäinen R, Salmenperä T, Partanen K, Vainio P, Riekkinen P, Pitkänen A. **Recurrent seizures may cause hippocampal damage in temporal lobe epilepsy.** *Neurology* 1998;50:1377–1382
69. Bland JM, Altman DG. **Statistical methods for assessing agreement between two methods of clinical measurement**. *Lancet* 1986;1:307–310
70. Bernasconi N, Bernasconi A, Andermann F, Dubeau F, Feindel W, Reutens DC. **Entorhinal cortex in temporal lobe epilepsy. A quantitative MRI study**. *Neurology* 1999;52:1870–1876
71. Bernasconi N, Bernasconi A, Caramanos Z, Antel SB, Andermann F, Arnold DL. **Mesial temporal damage in temporal lobe epilepsy: a volumetric MRI study of the hippocampus, amygdala and parahippocampal region**. *Brain* 2003;126:462–469
72. Naidich TP, Daniels DL, Haughton VM, Williams A, Pojunas K, Palacios E. **Hippocampal formation and related structures of the limbic lobe: anatomic-MR correlation. Part I. Surface features and coronal sections.** *Radiology* 1987;162:747–754
73. Watson C, Andermann F, Gloor P, et al. **Anatomic basis of amygdaloid and hippocampal volume measurement by magnetic resonance imaging**. *Neurology* 1992;42:1743–1750
74. Juottonen K, Laakso MP, Insausti R, et al. **Volumes of the entorhinal and perirhinal cortices in Alzheimer's disease**. *Neurobiol Aging* 1998;19:15–22
75. Convit A, McHugh P, Wolf OT, et al. **MRI volume of the amygdala: a reliable method allowing separation from the hippocampal formation**. *Psychiatry Res* 1999;90:113–123
76. Brierley B, Shaw P, David AS. **The human amygdala: a systematic review and meta-analysis of volumetric magnetic resonance imaging**. *Brain Res Brain Res Rev* 2002;39:84–105
77. McNulty V, Cruz-Orive LM, Roberts N, Holmes CJ, Gual-Arnau X. **Estimation of brain compartment volume from MR Cavalieri slices**. *J Comput Assist Tomogr* 2000;24:466–477
78. DeCarli C, Hatta J, Fazilat S, Gaillard WD, Theodore WH. **Extratemporal atrophy in patients with complex partial seizures of left temporal origin**. *Ann Neurol* 1998;43:41–45
79. Kuzniecky R, Bilir E, Gilliam F, Faught E, Martin R, Hugg J. **Quantitative MRI in temporal lobe epilepsy: evidence for fornix atrophy**. *Neurology* 1999;53:496–501
80. Ng SE, Lau TN, Hui FK, et al. **MRI of the fornix and mamillary body in temporal lobe epilepsy**. *Neuroradiology* 1997;39:551–555

STUDY IV.

ADC-mapping of the hippocampus and the amygdala in pharmacoresistant temporal lobe epilepsy

Gonçalves Pereira P.M, Oliveira E, Rosado P.

AJNR American Journal of Neuroradiology (accepted for publication; to appear in February/March **2006**).

ADC MAPPING OF THE HIPPOCAMPUS AND THE AMYGDALA IN PHARMACO-RESISTANT TEMPORAL LOBE EPILEPSY

Pedro M. Gonçalves Pereira [1,2]*; Eduardo Oliveira* [3] *; Pedro Rosado* [2,4]

[1] Department of Neuroradiology, 'Pedro Hispano' Hospital, Rua dr. Eduardo Torres, 4454-509 Matosinhos – Portugal
Phone: *-351-22-939 10 00, Fax: *-351-22-939 10 05, E-mail: pmgp@estsp.pt

[2] Department of Medical Science, Medical School, University of Beira Interior, Polo I, Rua Marquês d'Ávila e Bolama. 6201-001 Covilhã – Portugal

[3] Departement of Statistics, 'Egas Moniz' CRL, Health Science Institute (ISCS), Campus Universitário, Quinta da Granja, 2829-511 Monte de Caparica – Portugal

[4] Department of Neurology, Centro Hospitalar da Cova da Beira, Quinta do Alvito, 126, 6200-251 Covilhã – Portugal

Keywords: Temporal Lobe Epilepsy, Hippocampus, Amygdala, Apparent Diffusion Coefficient, Magnetic Resonance Imaging, Epilepsy Surgery.

Support:

This study was supported by a grant from the Fundação para a Ciência e Tecnologia (BD 18498/98, awarded to P.M.G.P.) and by the Grünenthal Foundation (Portugal).

Acknowledgements:

We wish to thank neuroradiologists Constança Jordão and Pedro Evangelista for including the DWI sequence on the comprehensive magnetic resonance imaging protocol for temporal lobe epilepsy used at the "Caselas" Magnetic Resonance Center, in Lisbon where all imaging studies were performed. Thanks also to Professor Mário Forjaz Secca and radiographer Cristina Menezes who provided us expert technical assistance. The authors further acknowledge Professor Fernando Lopes da Silva for his insightful comments on the manuscript. All of our clinical epilepsy research occurs in collaboration with neurologists and neurosurgeons from Lisbon and Coimbra. Therefore we are very much indebted to our clinical collaborators, who include Alberto Leal (Hospital Júlio de Matos), Orlando Leitão, José Pratas Vital, Luís Guerra and Dina Pinto (Hospital Egas Moniz), Paula Breia (Hospital Garcia de Orta), António Martins (Hospital Fernando da Fonseca), Francisco Pinto and António Gonçalves Ferreira (Hospital de Santa Maria) and Francisco Sales (Hospitais Universitários de Coimbra).

Corresponding author:
Pedro M. Gonçalves Pereira
Department of Neuroradiology
'Pedro Hispano' Hospital
Rua dr. Eduardo Torres
4454-509 Matosinhos – Portugal
Tel: *-351-22-939 10 00
Fax: *-351-22-939 10 05
E-mail: pmgp@estsp.pt

ABSTRACT

BACKGROUND AND PURPOSE: To determine whether interictal apparent diffusion coefficients (ADC) provide a robust means for detecting amygdalo-hippocampal abnormalities in adult patients with localization-related chronic temporal lobe epilepsy (TLE) undergoing pre-surgical evaluation.

METHODS: Fifty-five patients and 20 age-matched controls were studied with hippocampal and amygdala ADC-maps (HADC and AMYADC), volumes (HCVOL, AMYVOL), T2-relaxometry (HCT2, AMYT2), and hippocampal *N*-acetyl-aspartate to Choline and Creatine/Phosphocreatine ratios (HCSI). Mean values and 99% confidence ellipses were computed for the groups. Individual ADC-mapping was compared with electroencephalography (EEG) data, and further correlated with the quantitative MR measures and with the age at onset and duration of TLE. Moreover, we evaluated the association and the predictive value of HADC and AMYADC with respect to the surgical outcome in a sub-group of patients (n=21) operated on the side of maximal EEG lateralization and with MRI criteria for hippocampal sclerosis, 71% of which became seizure-free.

RESULTS: In controls, there was no relation between ADC values and age, gender or right-left asymmetries. Group comparisons showed, in TLE groups with right (n=29) or left epileptogenic foci (n=26), that ADC-mapping detected changes ipsilateral to the focus in the hippocampus (p<0.01) and the amygdala (p<0.05), accordingly with the volumes, T2-maps and HCSI. Significant Pearson's correlations (two-tailed) were obtained between ADC-maps and the volume of the hippocampus (r=-0.64) and of the amygdala (r=-0.55, both p<0.01), T2 (r=0.70; r=0.29, both p<0.01) but not with HCSI. Individual ADC analysis showed ipsilateral pathology in 82% of cases (hippocampus) and 35% (amygdala) and included a moderate association between ipsilateral HADC and AMYADC (r=0.54, p<0.01). Bilateral abnormalities were found in 7% (hippocampus) and 5% (amygdala). Except for HCSI and the amygdala data, there were significant correlations between the asymmetry indices and the duration of epilepsy (HADC: r=0.42, HCT2: r=0.50, HCVOL: r=0.35, all p<0.01). Age at onset was only associated with ipsilateral HADC (r=0.35, p<0.01), HCVOL and HCT2 (both, p<0.05). The association with post-surgical successes was characteristic of HADC (Fisher´s exact test, two-tailed; p = 0.031; Spearman correlation: r_s=-0.75 ; p=0.0002), not AMYADC. The predictive value regarding a favourable outcome was 0.87 (OR 26; 95% CI 2.33-38.86). As determined by regression models, both larger ipsilateral HADC´s and asymmetry indices predicted surgical success.

CONCLUSION: Interictal ADC-mapping lateralizes efficiently the lesion side in accordance with the EEG data, and might be used to study the differential regional aspects of mesio-temporal sclerosis. Hippocampal (not amygdala) ADC-maps discriminates favourably post-operative outcome and can be added to the multidisciplinary evaluation workout of pharmaco-resistant TLE patients.

INTRODUCTION

Mesial temporal lobe epilepsy (TLE) (1, 2) is one of the most common adult forms of pharmacologically intractable epilepsy (3). In spite of medical therapy, seizures can persist in up to 35 percent of patients with partial epilepsy (4). Patients with refractory TLE can benefit from a resective surgical intervention to treat or relief symptomatology that cannot be controlled satisfactorily with antiepileptic drugs (1, 5). Successful anterior temporal lobectomy or amygdalohippocampectomy requires accurate identification of the site and extent of the epileptogenic zone responsible for habitual seizures, as it may involve several distinct structures within the temporal lobe.

TLE is generally accompanied by a damaged hippocampus and, less frequently by amygdala damage and para-hippocampal cell loss (6-8). Hippocampal sclerosis (HS), which refers to a selective neuronal loss and gliosis in hippocampal subfields CA1, CA3 and dentate hilus (3, 7), is thought to play a decisive role in the origin of limbic seizures (6, 9). Depending on the surgical series, HS has been reported in up to 63% - 100% of the patients (8, 10, 11).

In addition to the hippocampus, epileptogenic lesions can also include the amygdala. Most often, amygdala damage occurs associated with HS, affecting 7% - 76% of these patients (6-8, 10-13) but it may also occur in the absence of HS in a minority (1% - 10%) of cases (11-13). The latter patients are thought to have a different clinical profile than those with HS (13-15). The assessment as to the presence of amygdala sclerosis is therefore of interest.

Quantitative estimation of hippocampal and/or amygdala structural abnormalities belongs now to standard procedures on routine pre-surgical evaluations (16). With this objective several MRI features, mostly volumetry (17), T2-relaxometry (18) and spectroscopy (19) are employed. The relative prognostic value of these techniques regarding surgical outcome has already been demonstrated (volume: (20, 21); T2-relaxometry: (22); spectroscopy: (23, 24)).

More recently, diffusion-weighted MR imaging (DWI) (see (25) for a review) emerged as a promising technique to identify pathological changes in human TLE (26-31). The preliminary studies were limited to observations of the hippocampus. In this way the relative specificity, but not the prognostic utility of interictal DWI to capture the imaging abnormalities of HS was evaluated.

DWI yields information about the ease of water diffusion within the local tissue environment. The diffusion of water in the brain is characterized by its apparent diffusion coefficient (ADC), which represents the mean diffusivity of water along all directions. Thus,

ADC analysis gives potential information about the size, orientation and tortuosity of both intra and extra-cellular spaces.

The main purposes of this study were (i) to extend the DWI analyses to the amygdala whilst assessing the co-occurrence of amygdalo-hippocampal diffusion abnormalities, (ii) to evaluate the lateralizing ability of the interictal ADC data of the hippocampus and amygdala (HADC and AMYADC) in a group of patients with unilateral electroclinical manifestations of TLE and pharmaco-resistance, and (iii) to assess the association of HADC and AMYADC with surgical outcome in the sub-group of patients who underwent selective amygdalohippocampectomy. Moreover we took into account that HADC and AMYADC are associated with the corresponding measures of volumes, T2-relaxation times and hippocampal NAA/(Cho+Cre) ratios and investigated how the subject's age and gender, and the age of onset and the duration of epilepsy correlate with the different measures of hippocampal and amygdala pathology.

This study not only allowed a direct comparison of the individual HADC and AMYADC values against the electroencephalographic (EEG) data and surgical outcome within a patient population, but also enabled us to ascertain the correlations between different MRI measures of pathology in individual patients.

We hypothesized that DWI analyses performed interictally in TLE, reflects the characteristic structural abnormalities found in mesio-temporal sclerosis and therefore could be used as a valid non-invasive mean of diagnosis in the pre-surgical assessment of TLE patients.

PATIENTS AND METHODS

Control subjects

The control group included twenty subjects (10 women) with a mean age (1SD) of 34.1, 10.7 (range: 19 - 52) years. All the volunteers were interviewed to exclude those with neurologic diseases and were submitted to detailed neurological examination and a "mini-mental state" test (32) [obtained average score and range was: 28.9 , 1.2 (26 - 30)].

Patients

A consecutive group of fifty-five patients (29 women) with medically refractory TLE and a mean age of 33.1, 10.2 (18 - 57) years, were enrolled in the study. Classification of the patients syndromes was based on the guidelines proposed by the International League Against Epilepsy (33). All the patients underwent comprehensive presurgical epilepsy evaluations, which included a detailed clinical history, interictal EEG, prolonged video-telemetry monitoring, MRI studies, neuropsychological assessment and intracarotid sodium amobarbital tests (in selected cases at risk for memory problems). Only patients with clinical and EEG evidence of TLE and without any neoplastic, vascular, developmental or non-hippocampal volme loss lesion demonstrated at MR imaging were included.

In addition, an extensive and careful review of hospital records was undertaken in order to obtain for each patient the demographic and illness-related variables used in this study, with the subject's permission. All the patients enrolled had visited a neurologist at the epilepsy units of the Departments of Neurology from main central hospitals in Lisbon and Coimbra at least once a year, depending on seizure frequency, since the time of their diagnosis.

The duration of the illness (years of epilepsy) was determined for every patient from the age of onset of seizures up to the age at which the MRI study was performed. The patients had a mean duration of 15.4, 7.6 (3 - 39) years of medically intractable epilepsy with recurrent complex partial seizures (n = 55), simple partial seizures (n = 17) and secondarily generalized seizures (n = 26).

MR Image acquisition

All MR studies were obtained on the same 1.5T scanner [CV/i-NV/I equipped with high-capacity gradient - amplitude: 40 mT/m, slew rate: 200 (T/m)/s - General Electric (GE) Medical Systems, Milwaukee, Wisconsin, USA], using the manufacturer's standard headcoil, from July 2001-December 2003. Every subject underwent a single MRI session. During the

scanning period (approximately 70-min.; 56 seconds for diffusion-weighted imaging) all participants were comfortably placed and their heads were fixated within the headcoil with customized cushions. Special attention was paid to the symmetric positioning of the subjects head.

Previous to the MR examination, every subject filled a general questionnaire regarding the usual safety precautions of MR examinations and the patients were specifically interviewed to determine the time past since the last seizure up to the MRI study (the minimum time lag was 5,5 days).

All sequences were obtained using an orientation tilted to the temporal lobes and orthogonal to the axis of the hippocampal body (34). Presurgical imaging consisted of standard conventional sequences (multiplanar high-resolution T1- and T2-weighted, proton density, inversion-recovery and fluid-attenuation inversion recovery scans).

For this study, patients and controls were further evaluated with a specific MR protocol in order to obtain quantitative data. Imaging for diffusion (**Figure 1**), volumetry and relaxometry was acquired on the coronal plane, parallel to the posterior comissure-obex line (PC-OB) (34, 35). Hippocampal chemical-shift was acquired on the axial plane perpendicular to PC-OB.

Imaging processing was performed using the manufacturer's software, GE Advantage Windows 3.1 (including research modules), running on Sun workstations (SPARC 4.1, Sun Mycrosystems, Mountain View, California, USA).

A sagittal spin-echo T1-weighted with TR = 600 ms, TE = 15 ms, NEX = 2, FOV = 24 cm, slice thickness = 5 mm, intersection gap = 1 mm, acquisition matrix = 512 x 192 pixels was acquired as a reference series for the conventional and quantitative MRI sequences.

Diffusion - Echo-planar diffusion-weighted imaging was acquired with TR = 10000 ms, TE = Min.full, NEX = 1, FOV = 32 cm, slice thickness = 5 mm, gap = 0 mm, matrix = 128 x 128 pixels. The b coefficient was set at 1000 mm^2/s, as we had previously identified the highest sensitivity of this value when compared to b=1500 mm^2/s and b=3000 mm^2/s in a subset of the patients and controls of this study (36, 37).

HADC and AMYADC were obtained from isotropic maps, by means of the diffusion coefficient calculated on a pixel-by-pixel basis using the manufacturer's diffusion software, which eliminates the T2 "shine-through". An exponential fit of the signals from two different acquisitions, one with the diffusion gradients off (b=0) and another with the diffusion gradients on (b=1000) was applied. Diffusion was measured in three orthogonal directions (x, y and z). HADC represents the average value of the apparent diffusion coefficient (ADC) obtained from ROIs of $20mm^2$ placed over the hippocampi on four successive coronal central slices, paying

particular attention to the anatomical boundaries in order to exclude measurements at the level of the hippocampal head and tail. AMYADC was calculated by averaging the ADC values from ROI's of 40mm^2 in two anterior contiguous slices, where the ovoid shape of the complex could be fully identified (**Figure 1**). Generally we had no difficulties to identify the amygdalo-hippocampal boundaries (even on major atrophies). Nonetheless, current diffusion images lack the morphological definition observed on other MR sequences due to their intrinsic contrast properties independent of T1 and T2. Thus, whenever doubts arose in the identification of the structure's borders we referred to the gapless T1 3D spoiled gradient recalled acquisition in the steady state (SPGR) images (see next) displaying the corresponding in-plane slice of the diffusion image.

Volumetry - For volumetric studies, we used a T1 3D SPGR protocol with TR = 20-30 ms, TE = Min.Full, NEX = 2, FOV = 24 cm, slice thickness = 1.5 mm, gap = 0 mm, acquisition matrix = 512 x 224 pixels, producing a series of 118-126 slices of the entire brain. Right and left hippocampus and amygdala volumes (HCVOL and AMYVOL) were measured following the general guidelines of Watson et al (38) on images magnified four-fold, with some modifications.

We relied on the multi-planar intrinsic signal of the structures of interest to account for the individual's anatomy. Instead of using external anatomical references, we took advantage of the gapless images with high-resolution to measure consecutively the hippocampus and amygdala areas on the coronal plane. For each subject, the posterior and anterior limits of each hippocampus were identified on the right and left para-sagittal sections, where the corresponding in-plane coronal images (with the reference image number) could be displayed. The posterior limit of the amygdala was identified using the same methodology. However, with current MRI, the anterior limit of the amygdala is difficult to identify by means of its contrast differences and, thus we had to refer to external anatomical references. This is a common feature in every volumetric study of the amygdaloid complex (for a review see (39)). We followed the borders described by Cendes et al (40) with modifications. For the anterior limit, we chose the level where the lateral sulcus closes to form the endorhinal sulcus and, simultaneously, the optic chiasm appears continuous.

HCVOL includes the volumes of the dentate gyrus, hilus, cornu ammonis, subiculum, alveus and fimbria (17). Whenever present, hippocampal sulcus remmants (41) were included in the measurements and considered a normal anatomic variation (42).

AMYVOL consists of the volumes of the deep nuclei (lateral, basal, accessory basal, and paralaminar nuclei), the superficial nuclei (anterior cortical and medial nuclei, nucleus of the

lateral olfactory tract, periamygdaloid cortex, posterior cortical nucleus) and the remaining nuclei of the amygdala (anterior amygdaloid area, central nucleus, amygdalohippocampal area and intercalated nucleus) (43).

Volumes were calculated by measuring the hippocampal and amygdala areas within each slice using the manufacturer's interactive mouse-driven software and multiplying them by the thickness of the slice; the resulting volumes were summed to obtain the total volume (Cavalieri slices method: (44, 45)).

Finally, to correct the absolute volumes for the individual variance in head size a ratio was used to obtain 'normalized volumes'. We adopted the procedure of Cendes et al (15), with the modifications of Kälviäinen et al (46), according to the equation:

$$Norm.Vol. = \frac{A_M}{A_I} \times Abs.Vol.$$

where $Norm.Vol.$ indicates the normalized volume; A_M, the mean brain area obtained at the level of the anterior commissure (coronal plane) for the control group, A_I, the individual brain area obtained at the level of the anterior commissure (coronal plane) and $Abs.Vol.$ the measured absolute volume. This method allows obtaining comparable volumes of the structures of interest in every subject, taking into account the differences in volume of the total brain. As subjects differ in morphometric parameters, including cranial size, such a normalization procedure is necessary.

T2-relaxometry - The method used for T2-relaxometry was similar to that described by Jackson et al (18), with some modifications due to time constraints (47). We used a 4-echoes protocol (instead of 16) with TR = 3000 ms, TE = 45 – 90 – 135 – 180 ms, NEX = 2, FOV = 24 cm, slice thickness = 4 mm, gap = 1 mm, acquisition matrix = 256 x 192 pixels, producing a series of 15 oblique slices over the whole temporal lobe. To assure reproducibility, the first slice was placed at the posterior end of the *corpus callosum*, in the mid-sagittal scout plane.

T2 maps were obtained by fitting the data from successive echoes, pixel by pixel, to a mono-exponential decay curve. Regions of interest (ROI) of arbitrary shape (but constant voxel number) were drawn over the hippocampi (20 mm^2) and amygdala (40 mm^2), avoiding borders where partial volume effects could alter the mean T2 value for the ROI. For each subject, the hippocampal relaxometry (HCT2) results were obtained by averaging ROI's values from 3 central slices taken at the level of the body of the hippocampus. Amygdala relaxation times (AMYT2) were calculated by averaging ROI's values from 2 anterior slices, which included the amygdala.

Hippocampal chemical-shift - For HCSI, a T2 fast spin-echo (TR = 4800 ms, TE = 136 ms, NEX = 2, FOV = 24 x 18 cm, section thicknes = 3 mm, gap = 1 mm, matrix = 256 x 224 pixels) localizer was acquired at an oblique transverse orientation, parallel to the long axis of the hippocampus (perpendicular to PC-OB) to reduce partial volume effects due to surrounding cerebrospinal fluid. A 2D proton magnetic resonance spectroscopy imaging sequence with point-resolved spectroscopic (PRESS) multi-volume selection (TR = 1000 ms, TE = 144 ms, NEX = 1, FOV = 24 x 24 cm, 18 x 18 encoding steps, PROBE-SI) was then acquired on the T2 image where the hippocampi were fully visible (48, 49). Shimming (GE Grad-Shim) and water suppression were performed automatically. To exclude the large lipid resonances from the extracranial fat, the length and width of the acquired volume were adjusted for each individual case, depending on head size, whereas section thickness was set to 10 mm in all cases. The volume of interest was placed behind the clivus and oriented in a similar position for all examinations to cover the entire extent of both hippocampi. Each voxel had the following nominal size: 7.5 x 7.5 x 9.9 mm^3 (volume: 557 mm^3).

The acquired chemical-shift imaging raw data were transferred to the manufacturer's workstation for Fourier transformation, curve fitting, plotting and display processing using the standard spectroscopy software (GE FuncTool). To obtain HCSI, two to tree voxels were placed along the longitudinal axis of each hippocampal structure, avoiding areas of low signal to noise ratio. In every subject, technically good-quality spectra were obtained using this standard voxel placement. Mean metabolic concentration was obtained on each hippocampus for *N*-acetyl-aspartate (NAA), Choline (Cho) and Creatine/Phosphocreatine (Cre) from signal intensities at 2.0 p.p.m. (NAA), 3.0 p.p.m. (Cre) and 3.2 p.p.m. (Cho). The NAA/(Cho + Cre) ratio was then calculated for each hippocampus, since this is a reliable measure for optimal lateralization (50). All spectra were inspected thoroughly, and those who were artifactually broadened [i.e., with a full width at half maximum of > 12 Hz (water resonance)] or if Cho and Cre peaks were not resolved, were discarded. In a small number of subjects (n = 7), we had to repeat the PROBE-SI acquisition due to head motion.

For all the MRI variables, an asymmetry index (A.I.) was used to ascertain the degree of asymmetry (in percentage) between the values obtained in the right (R) and left (L) structures (51) as follows:

$$A.I.(\%) = 100 \times \left| \frac{R - L}{(R + L)/2} \right|$$

EEG data

All patients were submitted to prolonged in-patient Video-EEG monitoring, while anti-epileptic medication was reduced. Scalp electrodes were placed according to the International 10-20 System (52) with 3 pairs of additional electrodes over the inferior temporal areas. The EEG signals were digitalized and analyzed by experts with reformatting facilities and synchronized video.

Lateralization was decided based on semiology (video) and on the electrophysiological ictal activity. In the very few patients ($n = 6$) without seizures during video-EEG, the presence of interictal activity preferentially localized to one hemisphere in the fronto-temporal areas was accepted as indicating lateralization (> 80%, that is a ratio greater than 4:1 of interictal spikes) (53). Patients whose EEG didn't fit these criteria were not enrolled in the study.

Because no histological data were available for these patients to confirm their diagnosis, special care was taken that none of the patients had divergent findings in electrophysiology, ictal semiology, conventional MRI and neuropsychological assessments. Neuropsychological evaluation was performed using the protocol of Helmstaedter et al (54). The temporal lobe in which the seizure focus was detected will be referred to as the "ipsilateral" and the other as the "contralateral" temporal lobe throughout this article.

Post-surgical outcome

To date, 21 patients (12 women), with a mean age of 30.7, 9.4 (18 - 57) years underwent selective amygdalohippocampectomy accordingly to the procedure of Yasargil et al (55) and had duration of the follow-up period longer than one year. The mean postoperative follow-up was 23 months (range: 13 - 35). In this group of patients, no reoperations were performed. Patients were assessed by epileptologists on a regular basis (months 3, 6, 12) and yearly afterwards.

The surgical outcome with respect to seizure control was assessed by means of Engel's classification (56). Patients were classified as having a good outcome (Engel's class IA) or a less satisfactory outcome (classes IB to III). Such data was related to the lateralizing ability of amygdalo-hippocampal ADC measures, it´s degree of asymmetry and the co-occurrence of hippocampal and amygdala ADC abnormalities. Post-surgical quality of life, memory and disability were not assessed in this study.

Statistical analysis

Group differences for age were assessed using one-way ANOVA (analysis of variance).

To verify the repeatability of the imaging measurements, the same observer (P.M.G.P.) performed twice quantifications for all the variables in 10 controls independently with a 6-week

interval. To check the inter-observer variability, a second observer quantified also the hippocampal volumes. Intra (and inter) observer variability was tested by analysing the limits of agreement between the first and second measurements and the correlations between measurements, according to Bland and Altman (57), at $p < 0.05$. The intra-observer variability, expressed as the means of the coefficients of variation of each control value, was 2.8% (HADC), 3.3% (AMYADC), 3.6% (HCVOL), 4.8% (AMYVOL), 3.1% (HCT2), 2.4% (AMYT2), and 0.2% (HCSI). The inter-observer variability expressed on the same way for HCVOL was 4.3%. For all the variables, the mean difference between the two measurements was near zero and the limits of agreement were below 2 standard deviations of the mean of controls (**Figure 2**).

In order to compare the means of the variables between groups (control *vs* right TLE; control *vs* left TLE), we tested the equality of variances (Levene's test) and used student's t-test. The significance of the differences between the right and left hippocampus and amygdala values was assessed with paired *t*-test. We further evaluated whether there was any mean difference at the group level in hippocampal and amygdala volumes, T2-relaxometry and ADC values, and hippocampal NAA/(Cho+Cre) between the patients who experienced complex partial plus secondarily generalized seizures ($n = 26$) and complex partial plus simple partial seizures ($n = 17$), and those who had only complex partial seizures ($n = 12$).

To verify the normal distribution of the values obtained by quantitative MRI, we used the Kolmogorov-Smirnov (58) and Lilliefors (59) analysis. As the normal distribution was not rejected, we determined confidence ellipses for the ADC control values, with 99% of confidence.

Confidence ellipses describing selected values for both hippocampus and amygdala were determined for controls using the Hotelling's method (60),

Using STATISTICA software for Windows (Tulsa, OK: StatSoft, Inc.), we computed confidence ellipses according to Hotelling's statistics with the assumption that a pair of variables has a multivariate binormal distribution, as shown in **Figure 5**.

In order to assess the level of interdependence between the MR variables, we used Pearson's correlation (two-tailed) between every hippocampal and amygdala ADC value and corresponding volume and T2-relaxometry measurement. HADCs were further correlated with HCSIs. We also verified whether the magnitudes of the amygdala and hippocampal quantitative values differed in a correlated manner across patients and whether amygdala ADC values could be predicted by the severity of hippocampal ADC.

Additional two-tailed Pearson's correlations were calculated to assess whether decreases in volumes (and hippocampal NAA/(Cr + Cho) ratios), and increases in T2 and ADC values associates with age (in years), age at which TLE had the clinically onset (in years) or

time after the onset of epilepsy (duration in years).

Fisher´s exact test was used to evaluate the probability of association between the ADC measures and surgical outcome. Whether such association was demonstrated, the positive predictive values, odds ratios and Spearman´s correlation´s coefficients were calculated. Additionally, a logistic regression model was used relating outcome (dependent variable) to the side of surgery and ADC values on the operated side.

Finally, receiver operating characteristic (ROC) curves were used to define the optimal cutt-off regarding a satisfactory surgical result.

RESULTS

Patients groups

Based on neurophysiological evaluation, patients were separated in two groups according to the main seizure electrographic lateralization: right TLE (n = 29) or left TLE (n = 26).

The patients with right TLE, left TLE, and normal controls did not differ significantly in age [ANOVA; F (2,72) = 0.92, p = 0.41] or sex distribution [χ^2; $\chi^2(1) = 1.8$, $p = 0.18$ for right TLE, and χ^2; $\chi^2(1) = 0.1$, $p = 0.68$ for left TLE]. The ethnic background of all patients and controls was white. Every subject was right-handed.

Group comparisons

Comparisons were made between right and left hippocampi and amygdalae values in patients groups and controls. In patients groups, values ipsilateral and contralateral to the focus were tested and the asymmetry indices compared to control values.

In **Table I** we present the hippocampal numerical data and the statistics regarding the comparisons between the patients' groups (both left and right TLE) and the controls, as well as between left and right sides.

Regarding the control group, the only significant difference was observed with respect to the hippocampal volumes (right > left; $p < 0.01$). There were no gender differences in the hippocampal and amygdala volumes, T2, and ADC values, and hippocampal NAA/(Cho+Cre) data. Also, there was no correlation between the values and age.

It can be seen that there are a number of comparisons that reach a significant level, since the groups are relatively large, although the differences may be rather small with a considerable overlap of the values for patients and controls.

The most relevant data with respect to the possibility of being used in the diagnosis of patients in clinical practice are the asymmetry indices (A.I's). For the ***Hippocampus***, control data showed that the mean A.I.'s values varied between 1.3 for ADC and 3.8 for volume, but in the two patients' groups the mean A.I.'s were much larger, varying from 9.2 for T2 and 36.1 for Volume. For the ***Amygdala*** the same tendency was seen, but the differences between A.I.s of controls and patients were much smaller, although significant, as indicated in **Table II**.

There was no significant differences in the mean volumes, T2-relaxometry, NAA/(Cho+Cre) and ADC values between the groups of patients with other seizures besides the

complex partial type. However, there was a tendency for patients that experienced complex partial plus generalized seizures to have smaller ipsilateral mean amygdala volumes than patients that had only episodes of complex partial seizures ($p = 0.06$).

Since the main objective of this study was to determine whether ADC values may contribute to localize hippocampal and amygdala abnormalities (**Figures 3 and 4**) we present these data, for patients and controls, in two-dimensional plots (confidence ellipses) where the asymmetries can be put more clearly in evidence for the individual patients.

Confidence ellipses for ADC values (Figure 5)

The ellipse represents the 99% confidence interval for the control group. In the right and left TLE groups ($n = 55$), the HADC values of 82% (45 / 55) of the patients were outside the 99% confidence interval. Seventy-six percent (42 / 55) had a larger ipsilateral HADC, while 3 patients (7%) had a bilateral increased diffusion coefficient, although asymmetric (two right TLE and one left TLE). Interestingly, two of these patients had the highest ipsilateral ADC values of the respective group. The remaining 18% had normal and symmetrical HADC values.

When contrasted with similar analyses performed for HCVOL, there were 89% (49 / 55) of the cases in which HCVOL and HADC provided identical information [74% (41 / 55) had both atrophy and larger ADC values in the ipsilateral hippocampus, while 15% (8 / 55) had normal volumes and ADC values]. In the remaining (11%, 6 subjects), there were 3 patients with normal volumes and ipsilateral larger HADC, 2 patients with bilateral atrophy and ipsilateral larger HADC, and another one subject with ipsilateral atrophy and normal HADC. As for the comparison of HCT2 and HADC, there were 85% (47 / 55) of the patients with concurrent values [being 37 patients (67%) with concomitant ipsilateral pathology and 10 (18%) with normal values on both analyses]. In the remaining 15%, there were 6 patients (11%) with either bilateral or normal HCT2 in which HADC provided ipsilateral localization, and 2 patients (4%) with a normal HADC and a larger HCT2 in the ipsilateral hippocampus. Regarding the correspondence between HCSI and HADC values, 55% (30 / 55) of the patients had concordant values [25 patients (46%) with coexistent ipsilateral pathology and 5 (9%) in which both analyses displayed normal values]. Of the remaining 45% (25 subjects), 33% (18 / 55) had either normal or bilaterally small NAA/(Cho+Cre) ratios and an ipsilateral larger HADC, 9% (5 / 55) had a normal HADC and either a bilaterally small HCSI ($n = 2$) or a bilaterally asymmetric (ipsilateral<contralateral, $n = 3$) HCSI, and 4% (2 / 55) had an ipsilateral high HADC and a contralateral small HCSI.

The combined use of the four modalities provided a slight increase in sensitivity when compared with the single use of HADC, since it allowed to localize ipsilateral pathology in the hippocampus in 87% (48 / 55) of the patients.

AMYADC data showed that only 35% (19 / 55) of the patients (right/left TLE) had a larger ADC value in the amygdala ipsilateral to the EEG focus. Except for 2 cases, all had a concomitant abnormal HADC. Sixty-five percent (36 / 55), however, had values that fell within the 99% confidence ellipse of controls. One right TLE patient (5% - 1/19), had a larger ADC value on both amygdalae, with an A.I. in the range of controls (and an asymmetrical bilaterally high HADC).

When individual AMYADC values were assessed jointly with the data provided by AMYVOL by means of 99% confidence ellipses, there were 64% (35 / 55) of the patients with concordant information in both analysis [of which 10 patients (18%) had coexistent ipsilateral atrophy and large ADC values and 25 patients (46%) where both analyses were normal]. The remaining 16% (9 / 55) had symmetrical volumes and ipsilateral large ADC values, and 18% (10 / 55) had asymmetrical volumes (ipsilateral<contralateral in all, except two cases in which the volume of the contralateral amygdala was smaller) and normal ADC values (except one case with bilaterally large ADC values). As for the comparison of AMYT2 and AMYADC, there were 62% (34 / 55) of the patients with concurrent values [being 13 patients (24%) with concomitant ipsilateral pathology and 21 (38%) with normal values on both analyses]. Fifteen percent (8 / 55) of the patients had an ipsilateral larger AMYADC and a symmetrical AMYT2, while 20% (11 / 55) had ipsilateral larger AMYT2 and symmetrical AMYADC.

The combined use of the 3 modalities enabled to localize 12 other patients (22%) with ipsilateral abnormalities compared with the single use of AMYADC. In 8 of these patients, the additional localizing data was provided by T2-relaxometry.

Relationship between MRI measures

To determine whether the individual MRI measures of pathology provide related information, as suggested by the large number of pathological cases that were commonly identified, we analysed the correlations between ADC-mapping on the one hand, and volumetry, T2-relaxometry and spectroscopy, on the other, for the hippocampus and amygdala.

There were relatively large correlation coefficients between the hippocampal ADC and the corresponding HCVOL (r = - 0.64, $p < 0.01$) and HCT2 (r = 0.70, $p < 0.01$), ipsilateral to the EEG focus. A weak and insignificant correlation was found between HADC and HCSI (r = - 0.18). The correlations between the contralateral values were non-significant.

In the amygdala, both ipsilateral AMYVOL (r = - 0.55, $p < 0.01$) and AMYT2 (r = 0.29, $p < 0.01$) correlated with the correspondent AMYADC values. There were no correlations for the contralateral values.

The correlation between the HADC and AMYADC values assessed the co-occurrence of hippocampal and amygdala damage (**Figure 6**). We found positive correlations with both ipsilateral and contralateral HADC and AMYADC values (ipsilateral: r = 0.54, $p < 0.01$; contralateral: r = 0.61, $p < 0.01$). When we tested the association of the asymmetry indices for HADC/AMYADC, a positive correlation was also obtained (r = 0.40, $p < 0.01$). We performed further *post-hoc* analyses to assess the possibility that the relationship between HADC and AMYADC is a reflection of the severity of hippocampal damage. In fact, we obtained a weak linear regression for both ipsilateral (r^2 = 0.30) and contralateral (r^2 = 0.37) ADC values which, however, were highly significant (both analyses, $p < 0.001$). These data indicate that only up to 37% of the variance of AMYADC is likely shared by the variance of HADC values.

Regarding the relationship between hippocampal and amygdala volumes and T2-relaxometry, we found only significant correlations between the ipsilateral HCVOL and AMYVOL (r = 0.31, $p < 0.05$). As expected, HCSI values did not correlate with any amygdala MR variable.

In the control group, the only significant correlations were verified for hippocampal ADC and their correspondent T2 values (r = 0.40, $p < 0.05$) and in-between the amygdalo-hippocampal ADCs (r = 0.43, $p < 0.01$).

Relationship of MRI measures to age, age at onset and duration of epilepsy

There was no relationship between each hippocampal and amygdala MRI measure and age, both in the controls and in patients groups.

Regarding the relationship between the years of symptomatic epilepsy and hippocampal MRI measures, we found significant correlations between the ipsilateral ADC, volumes and T2 values and the duration of epilepsy. Ipsilateral HADC values (**Figure 7**) increased significantly with the time past after onset of seizures (r = 0.45, $p < 0.001$), along with HCT2 (r = 0.35, p = 0.008) and as HCVOL decreased (r = - 0.37, p = 0.006). There was no association between the individual ipsilateral NAA/(Cho+Cre) ratios and the years of epilepsy. Except for a marginally significant relationship between the contralateral HCT2 values and duration of epilepsy (r = 0.25, p = 0.06), no correlations were encountered with the remaining contralateral MRI measures. The observation that the coexistent increase in HADC/HCT2 plus atrophy was selective to the ipsilateral hippocampus was also captured in the significant correlations between the asymmetry indices of these measures and the duration of epilepsy (HADC: r = 0.42, HCT2: r

= 0.50, HCVOL: $r = 0.35$, all $p < 0.01$). Accordingly, there was no correlation between the A.I. of HCSI and the years of epilepsy.

In the amygdala, there were no significant correlations at α level 0.01 between the ipsilateral or contralateral ADC, volumes and T2 values, and duration of epilepsy. However, a marginally weak significant relationship remained for ipsilateral AMYADC ($r = 0.26$, $p = 0.04$) and years of epilepsy (also verified by the corresponding level of correlation between the AMYADC asymmetry index: $r = 0.25$, $p = 0.06$).

Further correlative analyses were performed to verify whether the hippocampal and amygdala ADC, volumes, T2 values and the hippocampal NAA/(Cho+Cre) ratios were also affected by the age of onset of the disease. In fact, age of onset was moderately correlated with the ipsilateral HADC ($r = - 0.54$, $p < 0.01$) (**Figure 7**), and weakly associated with both the ipsilateral HCVOL ($r = 0.31$, $p < 0.05$) and HCT2 ($r = - 0.33$, $p < 0.05$). There were no significant correlations found between age of onset of epilepsy and the remaining MR values, including those obtained from the amygdalae (all r values < 0.11, with corresponding p values > 0.2).

Post-surgical outcome

During the follow-up period, 15 (71%) patients were in class IA (seizure-free), and 6 (29%) in class IB-III (2 patients in class IB, 3 in class II and 1 patient in class III). All 21 patients underwent surgery on the side of maximal EEG lateralization and had imaging features characteristic of hippocampal sclerosis.

The probability of association between the ADC measures and a good surgical outcome was only demonstrated with respect to the hippocampus, by the concordant lateralization of the HADC increase ipsilateral to the side of major EEG abnormalities and surgery (Fisher´s exact test, two tailed; $p < 0.05$). Thirteen (87%) of 15 patients with ipsilateral HADC pathological values and 2 (34%) of the 6 patients with normal ipsilateral HADC were in class IA [of those in classes IB to III, 67% (4/6) had a normal HADC in both hippocampi and 33% (2/6) had an ipsilateral pathological HADC]. The odds ratio was 26 (95% CI 2.33 – 38.86). A strongly negative ρ correlation was also found between the ipsilateral HADC´s and individual Engel class ($r_s = - 0.75$; $p < 0.001$). The relative impact of ipsilateral HADC has a predictor variable on outcome was significant ($p = 0.049$; Hosmer and Lemeshow test: $p = 0.82$). A lower HADC on the side of surgery was associated with a worse outcome. The regression model allowed estimating that for each 0.1 mm^2/s x 10^5 increase in ipsilateral HADC, the probability of a favorable outcome was multiplied by a factor of 88% ($\beta_0 = 43.52$; $\beta_1 = - 46.44$), and the ROC

analysis determined 0.940 mm^2/s x 10^5 has the corresponding optimal cut-off value (area under the curve = 0.98, LR = 2.6).

Additionally, a derived variable – the asymmetry index – that allows for a straightforward side-to-side comparison between both hippocampi was evaluated (**Figure 8**). A larger A.I. was associated with a better outcome ($p < 0.05$; Hosmer and Lemeshow test: $p = 0.30$). In terms of relative risk, the regression model estimated that a 1-unit increase in the A.I. predicted the probability of a better outcome multiplied by a factor of 84% ($\beta_0 = 1.85$; $\beta_1 = -0.22$). As such, a cut-off value of 5.1 (area under the curve = 0.94, sensitivity = 100% ; specificity = 50%, LR = 2) might be used for clinical evaluation purposes.

The association between the amygdala ADC measures and surgical outcome was not demonstrated in this study (Fisher´s exact test, two tailed; $p = 0.132$). However, this observation may be hampered by the limited amount of cases with ipsilateral pathological AMYADC values: only 6 patients out of 21 (29%). Interestingly, still, all those cases are to date seizure-free.

DISCUSSION

This study is, to the best of our knowledge, the first one to analyse the interictal water diffusion changes (ADC) of the amygdala in human epilepsy, along with the hippocampus simultaneously, in a large population of TLE patients, a part of which (38%) underwent amygdalohippocampectomy. Furthermore the variations in ADC values were put in perspective relative to the surgical outcome and the other quantitative MR values, namely volumetry, T2-relaxometry and the spectroscopic NAA/(Cho+Cre) ratio, and with the age of onset and duration of the disease. Giving the narrow variability of ADC across multiple brain regions and it´s known stability with age and gender (61), we also sought to determine useful cut-off values for the predictor variables.

There were 5 major findings in the study.

First, in the hippocampus there was agreement between the EEG data and the ipsilateral increase in HADC in 82% of the patients. In the amygdala, such agreement was obtained in only 35% of the cases. The remaining had normal ADC values and no incorrect lateralizations were encountered.

Second, in 100% of the patients with pathological HADC, the ipsilateral hippocampus had significantly larger ADC values than the contralateral, so that the asymmetry index (A.I.) differed very significantly with respect to that of controls. In the amygdala, this figure occurred in 95% of the cases (one case with bilateral larger ADC, without asymmetry).

Third, there was a moderate but significant correlation ($r \geq 0.45$) between hippocampal and amygdala ADC values, and their respective volumes, while the corresponding T2 relaxation times were strongly associated ($r = 0.70$) with HADC, but only weakly ($r = 0.29$) with AMYADC. No significant correlation between HADC and HCSI was found. Accordingly, the total number of cases that displayed concomitant hippocampal structural abnormalities was best assessed by the common data provided by HCVOL, HCT2 and HADC with limited increase in sensitivity (+5%, that is 3 additional cases) when all the four modalities (plus HCSI) were jointly assessed. As for the amygdala, additional pathology was uncovered in 22% of the patients by the combined use of ADC-mapping, volumetry, and T2-relaxometry; the latter modality contributed with the majority of the supplementary detections relatively to the AMYADC data.

Fourth, there was a selective relationship between the number of years of symptomatic epilepsy and the hippocampal measures of structural abnormalities on the side of the seizure focus, reflected by the coexistent triad of increased HADC/HCT2 values plus atrophy which, in

addition was unrelated with the age of the patients. Furthermore, ipsilateral increased HADC/HCT2 values plus hippocampal atrophy was associated with the age of onset of the TLE syndrome. Regarding the amygdala, there was a marginal relationship between AMYADC and the time past after onset of seizures, while there were no correlations between all the amygdala MR modalities and the age at which recurrent seizures started or with the patient's age.

Fifth, pos-surgical outcome was only related with hippocampal ADC data. In those patients in whom the EEG lateralization and difference in HADC were concordant, almost all (13 / 15) were classified in Engel´s class IA. If the ADC data was nonlateralizing, only 2 of 6 patients had a satisfactory outcome. Both an ipsilateral HADC and an asymmetry index larger than 0.940 mm^2/s x 10^5 and 5.1 respectively, strongly predicted favourable amygdalohippocampectomy results.

Regarding the control group, we found that in healthy individuals (decades: third to fifth) there was no relation between ADC values and age, gender or right-left asymmetries. The only significant associations captured in this group were between hippocampal ADC values and their correspondent T2 values and between amygdalo-hippocampal ADCs.

1. Lateralizing ability of ADC-mapping and methodological considerations

The lateralizing ability of HADC obtained in our population, is similar to that of published reports (26-31), namely those of Hugg et al (26) and Wieshmann et al (27), who reported only significant ipsilateral larger hippocampal ADC (ranging from a mean difference of 10% (26) to 24% (27) relative to the mean of controls). Yoo et al (29), using the axial hippocampal plane for ADC quantification, reported a significant increase in the contralateral hippocampi by about 6%, when compared to the mean of controls, and concluded for the presence of micro-structural changes in the normal-appearing contralateral structure. In our study, the comparison of the mean values of the contralateral hippocampi either with the controls and the ipsilateral values disclosed insignificant differences in both groups of patients (right and left TLE). In addition, we did not find incorrect lateralizations when compared to the EEG data. These findings suggest that hippocampal ADC mapping has an optimal specificity for damaged hippocampi and can be used as a surrogate marker for focus lateralization.

Our protocol quantifies both the HADC and AMYADC on a coronal plane, perpendicular to the main hippocampal axis, in consecutive 5 mm thick slices. The use of successive isotropic sections oriented perpendicularly to the main anatomical orientation, enabled us to identify the hippocampal and amygdala boundaries and to recognize the presence of CSF space and cortical sulci which could contaminate the measurements due to partial volume artefacts. Despite using ROIs of constant size, we tailored the shape of the ROI to the anatomical boundaries and kept

them placed at a reasonable distance from the interface with the white matter or the CSF spaces. Thus, we believe that this method has improved morphological accuracy and reproducibility when compared with the quantification of ADC-mapping in other anatomical axes (29).

2. ADC-mapping as a marker of hippocampal and amygdala sclerosis

The increases in HADC and AMYADC to values larger than controls reflect the facilitation of water diffusivity in a damaged hippocampus and amygdala. At a cellular level, hippocampal and amygdala sclerosis is mainly characterized by selective neuronal loss and reactive astrogliosis (3, 7) with consequent tissue shrinkage. Thus, this lesional pattern results in an increase in the amount of glial cells, which have a larger cytoplasm-nuclei ratio and, consequently, a larger proportion of intra-cellular freely moving water. Moreover, there is atrophy of the whole structure (which can loose up to 65% in volume, as shown by our results) and a decrease in the neuronal density that is likely reflected in a decrease of interictal metabolic activity. Altogether, these findings can explain the ADC increase, either by the relative increase of unbound water or by the reduction of myelin that accompanies the neuronal cell loss (62).

In addition, the architectural disorganization of the damaged tissue might lessen the proportion of active biological barriers, which in normal conditions reduce the ability of water to diffuse, allowing increased water mobility (25).

These tissue changes have well-established MR correlations. Neuronal loss corresponds to MR volumetric atrophy (22, 63, 64), while the proportion of glial cells correlates with the magnitude of T2-relaxation (65). Eventually, these changes result in a functionally impaired network that can be detected by spectroscopy (66).

Our results with respect to the amygdala showed correlations between ADC values and volumes, and T2-relaxation that mimic what was observed in the hippocampus, supporting the view that ADC is a valid measure of architectural injury. This reinforces the importance of amygdala studies in TLE, since patients with this pathological condition are less likely to become seizure-free (13). Moreover, AMYADC and HADC were strongly correlated but the severity of hippocampal ADC roughly accounted for 1/3 of the variance of AMYADC. Such data, although indicating that there is a pathological association that might be reflected by the disruption of amygdala-hippocampal connections secondary to neuronal loss, suggests, also, that amygdala damage evolves in an independent manner from that of HS.

3. ADC-mapping is the MR measure that shows large correlations with illness-related variables.

Our data demonstrate that both age at onset and duration of TLE are related to the water diffusivity, the volume and T2 values in the ipsilateral hippocampus. However, only the

hippocampal ADC values had a strong level of association and significance with those illness-related variables. Hippocampal NAA/(Cho+Cre) ratios, and amygdala volumes and T2 values did not show such a relationship.

These findings are in line with previous studies of hippocampal sclerosis (67-69).

With the present set of imaging data, however, we cannot determine which is the relative contribution of each illness-related factor we tested. Variables such as the period of seizure onset and duration of TLE are not statistically independent from one another. The contribution of these factors to the underlying neuropathology likely depend on the patient's age, as well on the age of onset and total duration of TLE. Additionally, other factors may play a role, such as frequency of seizures, medication and genetic background. At present, the role of these factors on the dynamical aspects of pathogenesis of TLE can only be controlled appropriately in animal models of chronic TLE (70). In naturally occurring human epileptic conditions, all illness-associated variables tend to be strongly related and are difficult to disentangle.

4. Implications for pre-surgical screening

The surgical prognosis of patients with TLE and a temporal lobe EEG focus varies accordingly to the presence, extent and severity of hippocampal structural damage identified by quantitative MRI (20-23, 71, 72). In general, patients with larger asymmetries yield better outcomes, while temporal lobe damage beyond hippocampal margins is associated with post-surgical failures.

In terms of ADC-mapping, several features can be used to predict outcome. Hippocampal ADC values larger than 2.5 SD related to control mean predicted better results in the patients whose ADC was concordant with the lateralization provided by EEG. In addition, a side-to-side difference larger than 3 SD relative to control mean was a robust predictor of favourable surgical outcomes. Overall, the positive predictive value of HADC was 87%. Such predictive findings were not obtained for the amygdala results. This observation may argue against the relative importance of amygdala studies in the surgical context. While we were completing the present study, Hakyemez et al (73) reported that amygdala ADC measurements were less sensitive to pathological tissue changes associated with TLE, reinforcing the validity of our data. Recently, Urbach H. et al (74) showed that amygdala volumes did not influenced the surgical outcome in 45 patients and that hippocampal atrophy was the single useful predictor of surgery. Such observation conflicts with voxel-based morphometry studies (72), where the amygdala complex, among other temporal lobe regions, appeared with reduced volume in patients with surgical failures relative both to controls and patients with surgical successes. However, as for ADC, only 6 out of 21 patients operated in this study had pathological AMYADC values, a limitation that

may hamper definitive conclusions about the sensitivity of ADC measurements of the amygdala complex.

Marginally interesting, though, was the discrepancy found between HADC and the MR qualitative diagnosis of HS. While all the operated patients had clear criteria for HS, four of those had normal HADC values, and were classified as post-surgical failures.

Many centers for epilepsy surgery include both conventional and quantitative MRI evaluations of mesial temporal lobe structures in the pre-surgical assessment of the seizure focus. None of these methods, however, produce uniformly reliable results, and the need remains for an imaging modality that is both quantitative and widely available that can be used to localize abnormal epileptogenic brain tissue at a regional level. Some quantitative modalities, like hippocampal and amygdala volumetry and relaxometry are quite accurate in the identification of structural lesions but require extensive acquisition and processing times and depend on a trained observer to be reproducible. Others, like 2D multi-voxel spectroscopy depend less on the observer skills and are less time-consuming, but depict frequently bilateral changes and are usually limited to hippocampal analysis.

Current ADC-mapping, despite its crude morphological resolution, in our experience proved sensitive and specific enough for the detection of mesio-temporal sclerosis. Furthermore this is a rapid MR method of diagnosis, since in our hands, the acquisition and processing of temporal lobe ADC-mapping ranged between 10-12 minutes.

CONCLUSION

In conclusion, hippocampal and amygdala ADC maps can be used as an accurate technique, moreover rapid to carry out, to depict hippocampal and amygdala sclerosis in the pre-surgical evaluation of chronic TLE patients. Hippocampal ADC-mapping may be used has an additional, robust method for the predictive counselling of surgical candidates.

REFERENCES

1. Wieser HG, Engel J, Williamson PD, Babb TL, Gloor P. **Surgically remediable temporal lobe syndromes**. In: Engel J, ed. *Surgical Treatment of the Epilepsies*. New York: Raven Press, 1993; 49-63.
2. Najm IM, Babb TL, Mohamed A, et al. **Mesial temporal lobe sclerosis**. In: Lüders HO, Comair YG, eds. *Epilepsy Surgery*. 2nd ed. Philadelphia: Lippincott Williams & wilkins, 2001; 95-103.
3. Babb TL, Brown WJ. **Pathological findings in epilepsy**. In: J. Engel J, ed. *Surgical Treatment of the Epilepsies*. New York: Raven Press, 1987; 511-540.
4. Cascino GD. **Intractable partial epilepsy: evaluation and treatment**. *Mayo Clin Proc* 1990; 65:1578-1586.
5. Wiebe S, Blume WT, Girvin JP, Eliasziw M. **A randomized, controlled trial of surgery for temporal-lobe epilepsy**. *N Engl J Med* 2001; 345:311-318.
6. Falconer MA, Serafetinides EA, Corsellis JAN. **Etiology and pathogenesis of temporal lobe epilepsy**. *Arch Neurol* 1964; 10:233-248.
7. Margerison JH, Corsellis JAN. **Epilepsy and the temporal lobes. A clinical, electroencephalographic and neuropathological study of the brain in epilepsy, with particular reference to the temporal lobes**. *Brain* 1966; 89:499-530.
8. Bruton CJ. **The neuropathology of temporal lobe epilepsy**. Oxford: Oxford University Press, 1988.
9. ILAE Commision on Neurosurgery of Epilepsy (Compiled by Wieser HG). **Mesial Temporal Lobe Epilepsy with Hippocampal Sclerosis**. *Epilepsia* 2004; 45:695-714.
10. Yilmazer-Hanke DM, Wolf HK, Schramm J, Elger CE, Wiestler OD, Blumcke I. **Subregional pathology of the amygdala complex and entorhinal region in surgical specimens from patients with pharmacoresistant temporal lobe epilepsy**. *J Neuropathol Exp Neurol* 2000; 59:907-920.
11. Swartz BE, Tomiyasu U, Delgado-Escueta AV, Mandelkern M, Khonsari A. **Neuroimaging in temporal lobe epilepsy: test sensitivity and relationships to pathology and postoperative outcome**. *Epilepsia* 1992; 33:624-634.
12. Lee DH, Gao FQ, Rogers JM, et al. **MR in temporal lobe epilepsy: analysis with pathologic confirmation**. *AJNR Am J Neuroradiol* 1998; 19:19-27.
13. Miller LA, McLachlan RS, Bouwer MS, Hudson LP, Munoz DG. **Amygdalar sclerosis: preoperative indicators and outcome after temporal lobectomy**. *J Neurol Neurosurg Psychiatry* 1994; 57:1099-1105.
14. Hudson LP, Munoz DG, Miller L, McLachlan RS, Girvin JP, Blume WT. **Amygdaloid sclerosis in temporal lobe epilepsy**. *Ann Neurol* 1993; 33:622-631.
15. Cendes F, Andermann F, Gloor P, et al. **Relationship between atrophy of the amygdala and ictal fear in temporal lobe epilepsy**. *Brain* 1994; 117:739-746.
16. Sakamoto AC, Benbadis SR, Godoy J, et al. **Essentials for the establishment of an epilepsy surgery program (Appendice B)**. In: Luders H, Comair Y, eds. *Epilepsy Surgery*. 2nd ed. Philadelphia: Lippincott Williams & Wilkins, 2001; 979-986.
17. Cook MJ, Fish DR, Shorvon SD, Straughan K, Stevens JM. **Hippocampal volumetric and morphometric studies in frontal and temporal lobe epilepsy**. *Brain* 1992; 115:1001-1015.
18. Jackson GD, Connelly A, Duncan JS, Grunewald RA, Gadian DG. **Detection of hippocampal pathology in intractable partial epilepsy: increased sensitivity with quantitative magnetic resonance T2 relaxometry**. *Neurology* 1993; 43:1793-1799.

19. Thompson JE, Castillo M, Kwock L. **MR spectroscopy in the evaluation of epilepsy**. *Magn Reson Imaging Clin N Am* 1998; 6:21-29.
20. Jack CR, Sharbrough FW, Cascino GD, Hirschorn KA, O'Brien PC, Marsh WR. **Magnetic resonance image-based hippocampal volumetry: correlation with outcome after temporal lobectomy**. *Ann Neurol* 1992; 31:138-146.
21. Cascino GD, Trenerry MR, Sharbrough FW, So EL, Marsh WR, Strelow DC. **Depth electrode studies in temporal lobe epilepsy: relation to quantitative magnetic resonance imaging and operative outcome**. *Epilepsia* 1995; 36:230-235.
22. Kuzniecky RI, Bilir E, Gilliam F, et al. **Multimodality MRI in mesial temporal sclerosis: relative sensitivity and specificity**. *Neurology* 1997; 49:774-778.
23. Kuzniecky R, Hugg J, Hetherington H, et al. **Predictive value of ^{1}H MRSI for outcome in temporal lobectomy**. *Neurology* 1999; 53:694-698.
24. Antel SB, Li LM, Cendes F, et al. **Predicting surgical outcome in temporal lobe epilepsy patients using MRI and MRSI**. *Neurology* 2002; 58:1505-1512.
25. Wheeler-Kingshott CAM, Barker GJ, Steens SCA, van Buchem MA. **D: the Difusion of Water**. In: Tofts PS, ed. *Quantitative MRI of the brain: measuring changes caused by disease*. Chichester: John Wiley & Sons, 2003; 203-256.
26. Hugg JW, Butterworth EJ, Kuzniecky RI. **Diffusion mapping applied to mesial temporal lobe epilepsy: preliminary observations**. *Neurology* 1999; 53:173-176.
27. Wieshmann UC, Clark CA, Symms MR, Barker GJ, Birnie KD, Shorvon SD. **Water diffusion in the human hippocampus in epilepsy**. *Magn Reson Imaging* 1999; 17:29-36.
28. Kantarci K, Shin C, Britton JW, So EL, Cascino GD, Jack CR, Jr. **Comparative diagnostic utility of ^{1}H MRS and DWI in evaluation of temporal lobe epilepsy**. *Neurology* 2002; 58:1745-1753.
29. Yoo SY, Chang KH, Song IC, et al. **Apparent diffusion coefficient value of the hippocampus in patients with hippocampal sclerosis and in healthy volunteers**. *AJNR Am J Neuroradiol* 2002; 23:809-812.
30. Hufnagel A, Weber J, Marks S, et al. **Brain diffusion after single seizures**. *Epilepsia* 2003; 44:54-63.
31. Duzel E, Kaufmann J, Guderian S, et al. **Measures of hippocampal volumes, diffusion and ^{1}H MRS metabolic abnormalities in temporal lobe epilepsy provide partially complementary information**. *Eur J Neurol* 2004; 11:195-205.
32. Folstein MF, Folstein SE, McHugh PR. **"Mini-mental state". A practical method for grading the cognitive state of patients for the clinician**. *J Psychiatr Res* 1975; 12:189-198.
33. ILAE Commission on Classification and Terminology. **Proposal for revised classification of epilepsies and epileptic syndromes**. *Epilepsia* 1989; 30:389-399.
34. Gonçalves Pereira PM, Oliveira E, Forjaz Secca M. **Assessment of the preferred scout sagittal orientation for temporal lobe imaging with magnetic resonance**. *MAGMA Magnetic Resonance Materials in Physics, Biology and Medicine* 2005; 18:19-25.
35. Tamraz JC, Comair YG. **Limbic lobe and mesial temporal region**. In: Tamraz JC, Comair YG, eds. *Atlas of regional anatomy of the brain using MRI – with functional correlations*. Berlin: Springer-Verlag, 2000; 161-184.
36. Gonçalves Pereira PM, Forjaz Secca M, Ribeiro C, Evangelista P. **Diffusion-weighted imaging in chronic temporal lobe epilepsy: sensitivity analysis of the B-value and ability to detect hippocampal sclerosis**. In: *Proceedings of the 19th Annual Meeting of the European Society for Magnetic Resonance in Medicine and Biology (ESMRMB)*. Cannes, France 2002; 80.
37. Gonçalves Pereira PM, Forjaz Secca M, Oliveira E, Ribeiro C, Evangelista P. **ADC mapping of temporal lobe epilepsy at high b values: focusing on the hippocampus and**

the amygdala. *MAGMA Magnetic Resonance Materials in Physics, Biology and Medicine* 2003; 16:S 119-120.
38. Watson C, Andermann F, Gloor P, et al. **Anatomic basis of amygdaloid and hippocampal volume measurement by magnetic resonance imaging**. *Neurology* 1992; 42:1743-1750.
39. Brierley B, Shaw P, David AS. **The human amygdala: a systematic review and meta-analysis of volumetric magnetic resonance imaging**. *Brain Res Rev* 2002; 39:84-105.
40. Cendes F, Andermann F, Gloor P, et al. **MRI volumetric measurement of amygdala and hippocampus in temporal lobe epilepsy**. *Neurology* 1993; 43:719-725.
41. Humphrey T. **The development of the human hippocampal fissure**. *J Anat* 1967; 101:655-676.
42. Sasaki M, Miyuki S, Ehara S, Tamakawa Y. **Hippocampal sulcus remnant: potential cause of change in signal intensity in the hippocampus**. *Radiology* 1993; 188:743-746.
43. Soininen HS, Partanen K, Pitkänen A, et al. **Volumetric MRI analysis of the amygdala and the hippocampus in subjects with age-associated memory impairment: correlation to visual and verbal memory**. *Neurology* 1994; 44:1660-1668.
44. Gundersen HJ, Jensen EB. **The efficiency of systematic sampling in stereology and its prediction**. *J Microsc* 1987; 147:229-263.
45. Roberts N, Puddephat MJ, McNulty V. **The benefit of stereology for quantitative radiology**. *Br J Radiol* 2000; 73:679-697.
46. Kälviäinen R, Salmenperä T, Partanen K, Vainio P, Riekkinen P, Sr., Pitkänen A. **MRI volumetry and T2 relaxometry of the amygdala in newly diagnosed and chronic temporal lobe epilepsy**. *Epilepsy Res* 1997; 28:39-50.
47. Pires J, Cavaleiro Miranda P, Forjaz Secca M, Evangelista P, Jacinto A. **T2 relaxometry of the hippocampus in temporal lobe epilepsy: normal and pathological values**. In: *Proceedings of the 6th Scientific Meeting and Exhibition of the International Society of Magnetic Resonance in Medicine (ISMRM)*. Sidney, 1998; 1390.
48. Ng TC, Comair YG, Xue M, Wyllie E, Lüders HO. **Proton magnetic resonance spectroscopic imaging for the evaluation of temporal and extratemporal lobe epilepsy**. In: Lüders HO, Noachtar S, eds. *Epileptic Seizures: pathophysiology and clinical semiology*. Philadelphia: Livingstone, 2000; 796.
49. Bernasconi A, Tasch E, Cendes F, Li LM, Arnold DL. **Proton magnetic resonance spectroscopic imaging suggests progressive neuronal damage in human temporal lobe epilepsy**. In: Sutula T, Pitkänen A, eds. *Prog Brain Res*, 2002; 297-304.
50. Ende GR, Laxer KD, Knowlton RC, et al. **Temporal lobe epilepsy: bilateral hippocampal metabolite changes revealed at proton MR spectroscopic imaging**. *Radiology* 1997; 202:809-817.
51. Bernasconi N, Bernasconi A, Andermann F, Dubeau F, Feindel W, Reutens DC. **Entorhinal cortex in temporal lobe epilepsy. A quantitative MRI study**. *Neurology* 1999; 52:1870-1876.
52. Jasper H. **Report on the committee on methods of clinical electroencephalography**. *Electroencephalogr Clin Neurophysiol* 1958; 10:370-375.
53. Cendes F, Li LM, Watson C, Andermann F, Dubeau F, Arnold DL. **Is ictal recording mandatory in temporal lobe epilepsy? Not when the interictal electroencephalogram and hippocampal atrophy coincide**. *Arch Neurol* 2000; 57:497-500.
54. Helmstaedter C, Kurthen M, Linke DB, Elger CE. **Right hemisphere restitution of language and memory functions in right hemisphere language-dominant patients with left temporal lobe epilepsy**. *Brain* 1994; 117 (Pt 4):729-737.
55. Yasargil MG, Teddy PJ, Roth P. **Selective amygdalo-hippocampectomy. Operative anatomy and surgical technique**. *Adv Tech Stand Neurosurg* 1985:93-123.

56. Engel J, Jr., Van Ness PC, Rasmussen TB, Ojemann LM. **Outcome with respect to epileptic seizures**. In: Engel J, Jr., ed. *Surgical Treatment of the Epilepsies*. 2nd ed. New York: Raven Press, Ltd, 1993; 609-621.
57. Bland JM, Altman DG. **Statistical methods for assessing agreement between two methods of clinical measurement**. *Lancet* 1986; 1:307-310.
58. Kolmogorov AN. **Sulla determinazione empirica di una legge di distribuzione**. *Giorn dell' Inst Ital degli Att* 1933; 4:83-91.
59. Lilliefors HW. **On the Kolmogorov-Smirnov test for normality with mean and variance unknown**. *J Am Statistical Association* 1967; 62:399-402.
60. Hotelling H. **Relations between two sets of variates**. *Biometrika* 1936; 28:321-377.
61. Helenius J, Soinne L, Perkio J, et al. **Diffusion-weighted MR imaging in normal human brains in various age groups.** *AJNR Am J Neuroradiol* 2002; 23:194-199.
62. Branco G. **An alternative explanation of the origin of the signal in diffusion-weighted MRI**. *Neuroradiology* 2000; 42:96-98.
63. Cascino GD, Jack CR, Parisi JE, et al. **Magnetic resonance imaging-based volume studies in temporal lobe epilepsy: pathological correlations**. *Ann Neurol* 1991; 30:31-36.
64. Lencz T, McCarthy G, Bronen RA, et al. **Quantitative magnetic resonance imaging in temporal lobe epilepsy: relationship to neuropathology and neuropsychological function**. *Ann Neurol* 1992; 31:629-637.
65. Briellmann RS, Kalnins RM, Berkovic SF, Jackson GD. **Hippocampal pathology in refractory temporal lobe epilepsy: T2-weighted signal change reflects dentate gliosis**. *Neurology* 2002; 58:265-271.
66. Kuzniecky R, Palmer C, Hugg J, et al. **Magnetic resonance spectroscopic imaging in temporal lobe epilepsy: neuronal dysfunction or cell loss?** *Arch Neurol* 2001; 58:2048-2053.
67. Engel J, Jr. **Introduction to temporal lobe epilepsy**. *Epilepsy Res* 1996; 26:141-150.
68. Kälviäinen R, Salmenperä T, Partanen K, Vainio P, Riekkinen P, Pitkänen A. **Recurrent seizures may cause hippocampal damage in temporal lobe epilepsy**. *Neurology* 1998; 50:1377-1382.
69. Salmenperä T, Kälviäinen R, Partanen K, Pitkänen A. **Hippocampal and amygdaloid damage in partial epilepsy: a cross-sectional MRI study of 241 patients**. *Epilepsy Res* 2001; 46:69-82.
70. Gorter JA and Goncalves Pereira PM, van Vliet EA, Aronica E, Lopes da Silva FH, Lucassen PJ. **Neuronal cell death in a rat model for mesial temporal lobe epilepsy is induced by the initial status epilepticus and not by later repeated spontaneous seizures**. *Epilepsia* 2003; 44:647-658.
71. Li LM, Cendes F, Antel SB, et al. **Prognostic value of proton magnetic resonance spectroscopic imaging for surgical outcome in patients with intractable temporal lobe epilepsy and bilateral hippocampal atrophy**. *Ann Neurol* 2000; 47:195-200.
72. Keller SS, Denby CE, Wieshmann UC, Roberts N. **Post-surgical failure after temporal lobectomy is associated with increased medial temporal lobe damage**. In: *Proceedings of the 12nd Scientific Meeting and Exhibition of the International Society of Magnetic Resonance in Medicine (ISMRM)*. Kyoto, 2004; 1298.
73. Hakyemez B, Erdogan C, Yildiz H, Ercan I, Parlak M. **Apparent diffusion coefficient measurements in the hippocampus and amygdala of patients with temporal lobe seizures and in healthy volunteers**. *Epilepsy Behav* 2005; 6:250-256.
74. Urbach H, Siebenhaar G, Koenig R, et al. **Limbic system abnormalities associated with Ammon's horn sclerosis do not alter seizure outcome after amygdalohippocampectomy**. *Epilepsia* 2005; 46:549-555.

LEGENDS TO FIGURES

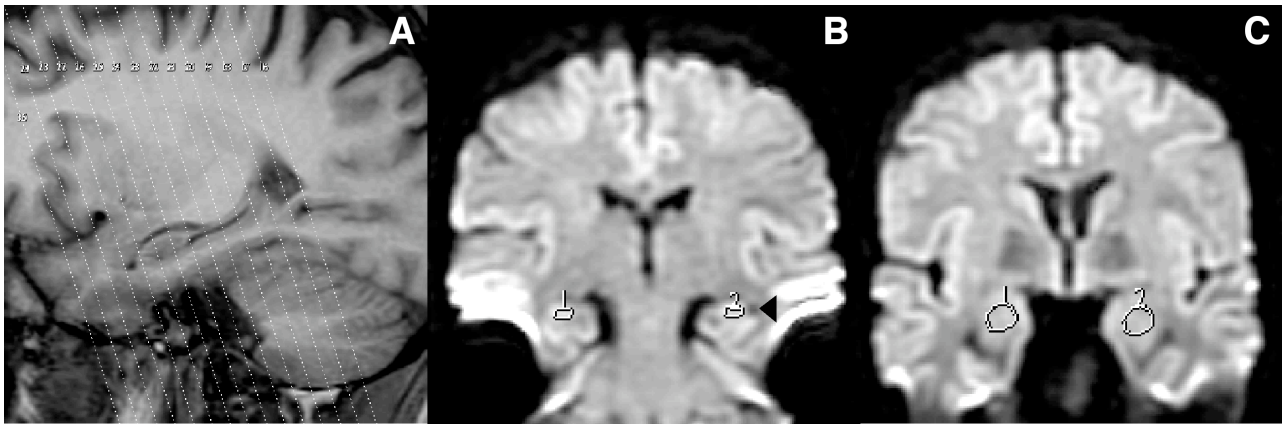


Figure 1. (*A*) Highlight of a T1-weighted sagittal scout imaging from a control subject with the tilted coronal diffusion partitions superimposed. With this protocol, at least 7 diffusion partitions can be quantified for ADC over the hippocampus (1 at the transition tail-body, 4 at the level of the body and 2 at the level of the head). For the amygdala analysis, at least 2 slices can be used. (*B* and *C*). Diffusion-maps in the coronal plane parallel to the posterior comissure-obex line from the same subject. ROIs are placed over the hippocampus (*B*) and amygdala (*C*). Note the lateral ventricle on the right side of the left hippocampus (arrowhead in *B*) and its appearance underneath both amygdalae (*C*).

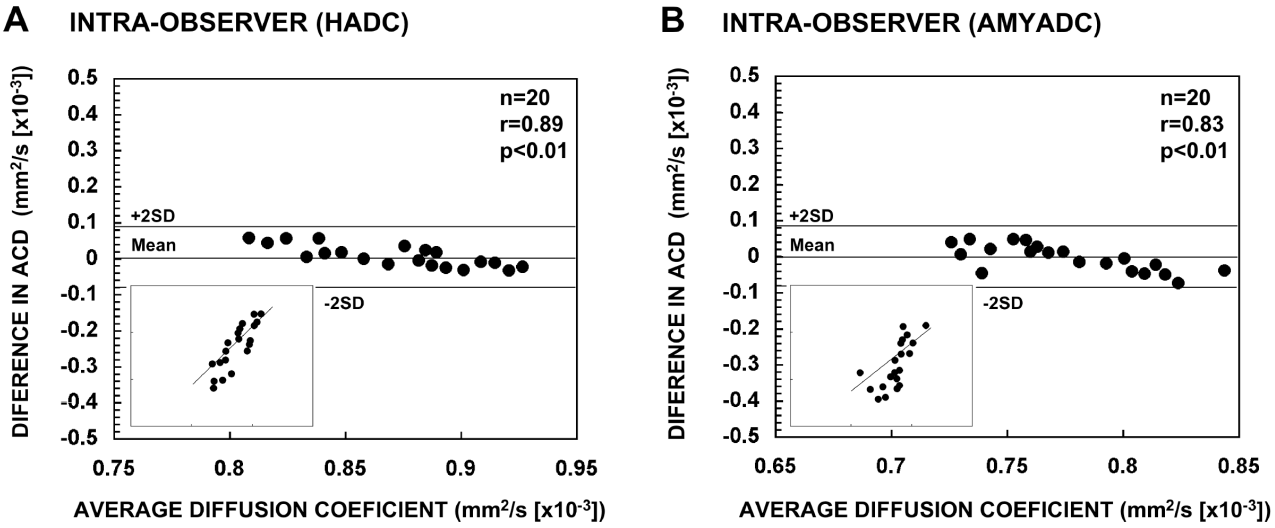


Figure 2. Scatterplots show the intra-observer variability (P.M.G.P.) of repeated measurements in the assesement of the right and left ADC values of the hippocampus (*A*), and right and left ADC values of the amygdala (*B*) in 10 control subjects. The limits of agreement between the first and second measurements are expressed as the mean difference between measurements: [first measurement minus second measurement] ± 2 SD. Inserts in the lower left corner show the association between the first (x-axis) and second (y-axis) measurements. The same test was applied to the other variables (not shown) and the results were comparable. Mean indicates mean difference; +2 SD, mean difference plus 2 SD; -2 SD, mean difference minus 2 SD.

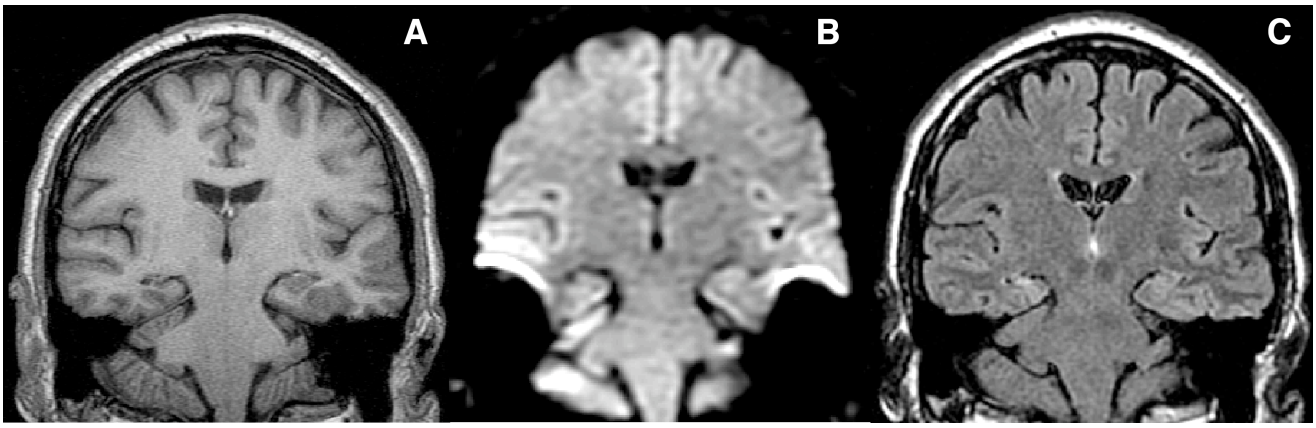


Figure 3. Tilted coronal slices from a patient with right HS illustrating the morphological (*A*), and signal (*C*) characteristics of a damaged right hippocampus (arrowhead). Compare with the diffusion-weighted image (*B*), where the right hippocampal atrophy can also be identified. (*A*) T1-weighted used for volumetry, (*B*) diffusion-weighted and (*C*) FLAIR image. The left side of the images correspond to the right side of the patient.

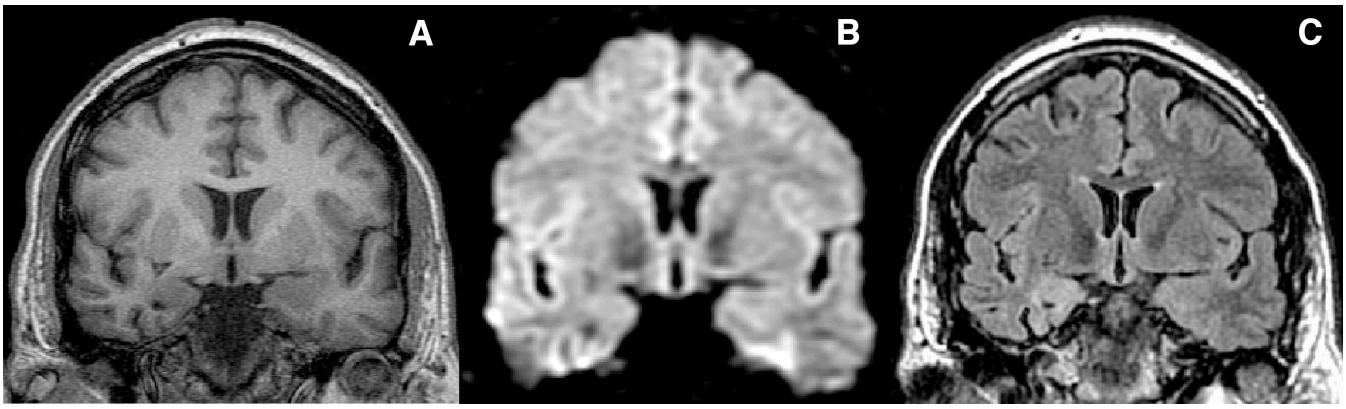


Figure 4. Tilted coronal slices from a different patient than the one presented on Figure 3 with imaging criteria for right amygdala sclerosis. Panels *A* and *C* illustrate the morphological and signal characteristics of a damaged right amygdala, respectively (arrowhead). Compare with the diffusion-weighted image (*B*), where the right amygdala atrophy can also be identified. (*A*) T1-weighted used for volumetry, (*B*) diffusion-weighted (*C*) FLAIR image. The left side of the images correspond to the right side of the patient.

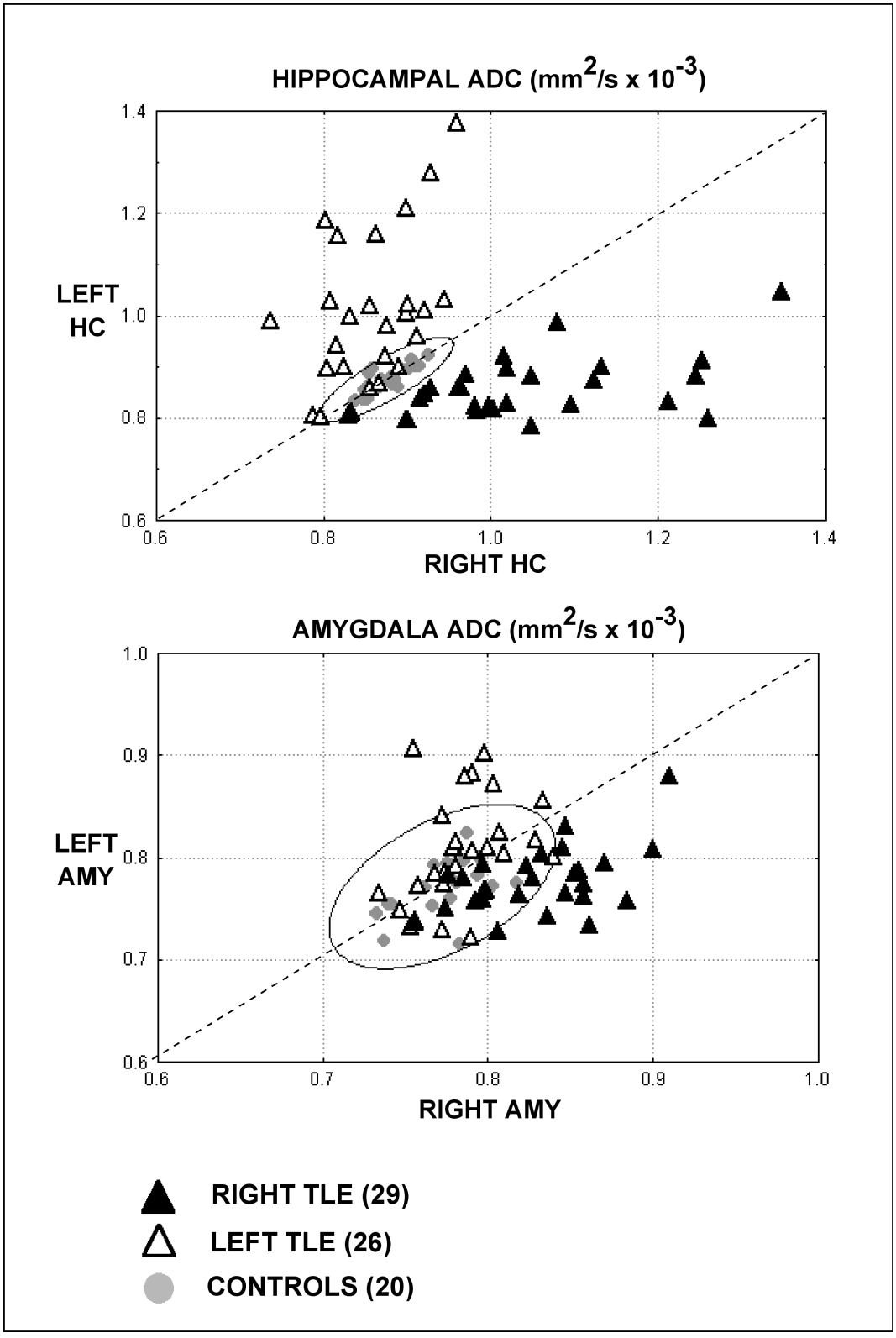


Figure 5. 99% confidence ellipses for HADC (*A*) and AMYADC (*B*).

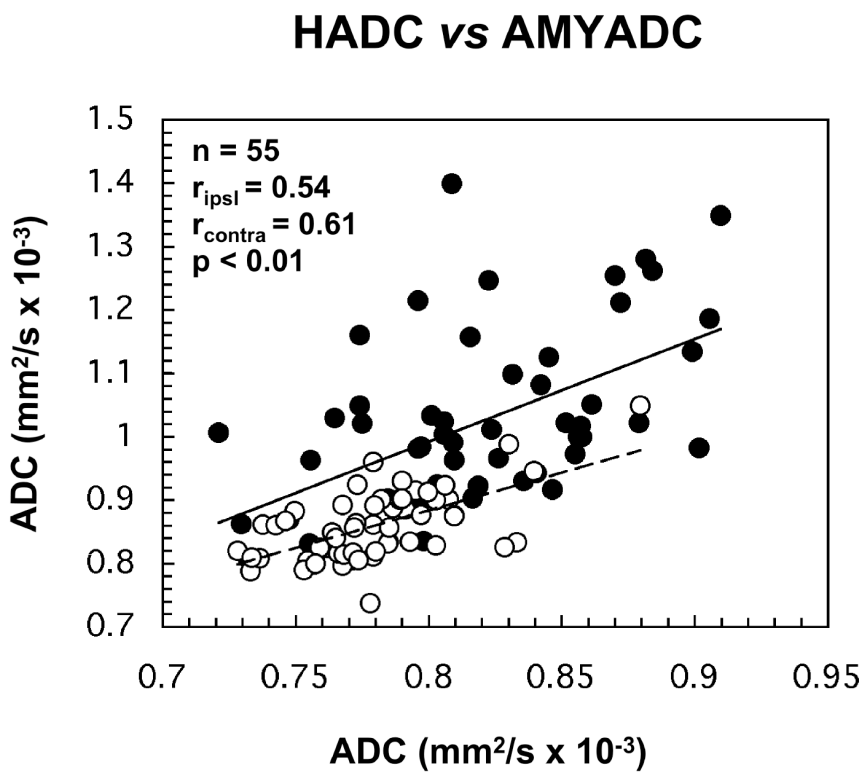


Figure 6. Scatterplots show the correlations between the ipsilateral and contralateral ADC values of the hippocampus and amygdala. *Closed circles* and solid trendline refer to the ipsilateral values; *open circles* and scattered trendline refer to the contralateral values. r_{ipsi}, Pearson's correlation coefficient for ipsilateral values; r_{contra}, Pearson's correlation coefficient for contralateral values; *n*, number of patients.

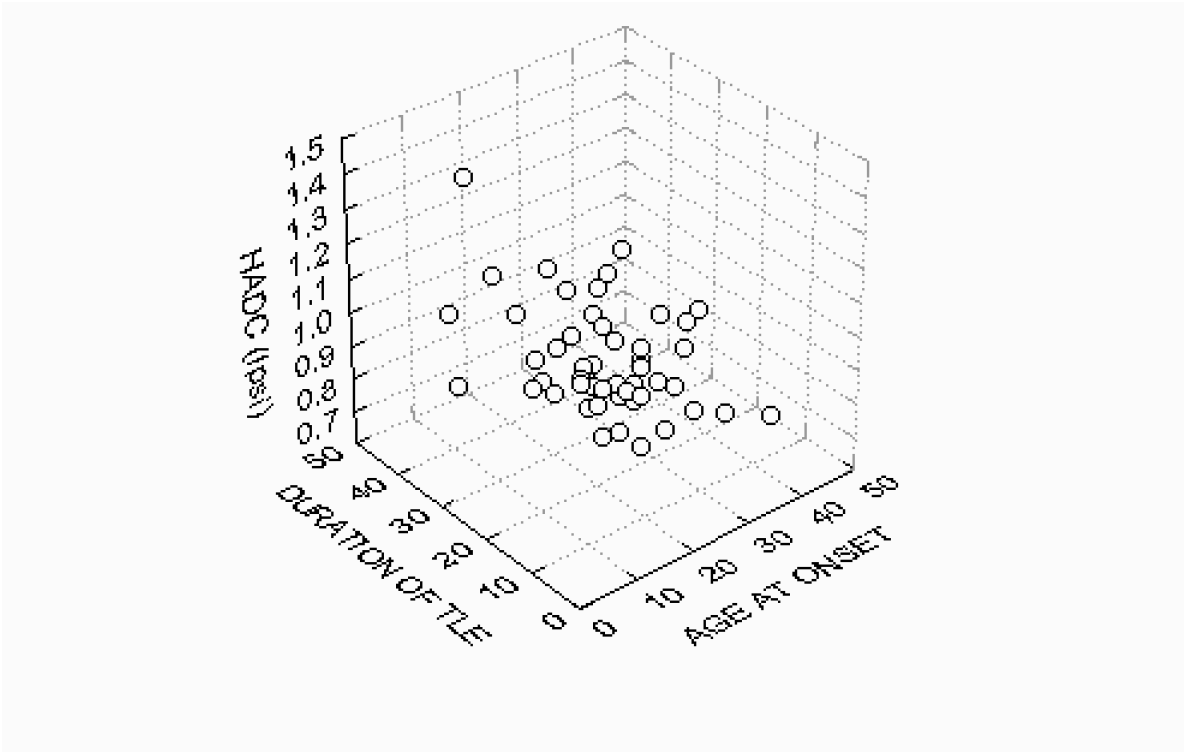


Figure 7. Scattergram displaying the association between the ipsilateral HADC (*z*-axis, mm^2/s x 10^{-3}), age at onset (*x*-axis, in years), and the duration of TLE (*y*-axis, in years).

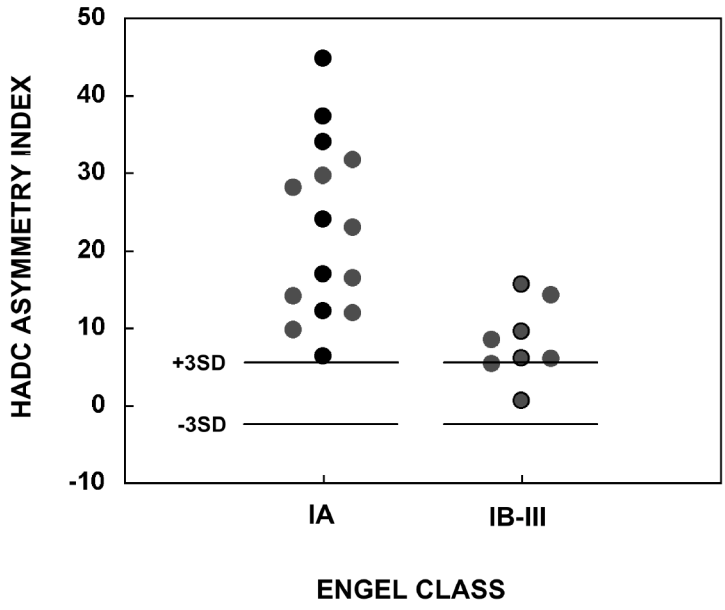


Figure 8. Hippocampal ADC asymmetry index against outcome. The A.I. is significantly greater for patients in class IA than for those in class IB-III (student *t*-test: p = 0.01; two-tailed). Horizontal bars represent ± 3 standard deviations from control mean.

Table I. Descriptive statistics for quantitative hippocampal MRI data (HADC, HCVOL, HCT2 and HCSI).

Hippocampus	**Controls (n = 20)**	**Right TLE (n = 29)**	**Left TLE (n = 26)**
ADC ($mm^2/s \times 10^5$)			
Right hippocampus	0.87 , 0.03 (0.83-0.93)	1.03 , 0.14 (0.83-1.34)#‡	0.86 , 0.05 (0.83-0.96)
Leftt hippocampus	0.88 , 0.03 (0.84-0.93)	0.85 , 0.06 (0.76-1.04)	1.01 , 0.15 (0.80-1.39)#‡
A.I.	1.3 , 1.2 (0.02-3.9)	17.6 , 10.8 (2.7-44.7)‡	15.2 , 12.5 (0.3-38.5)‡
Volume (mm^3)			
Right hippocampus	3611 , 350 (3050-4450)‡	2591 , 587 (1449-3843)#‡	3354 , 399 (2251-3947)^
Leftt hippocampus	3488 , 320 (3077-4246)	3434 , 400 (2295-4118)	2427 , 763 (1218-3660)#‡
A.I.	3.8 , 2.2 (0.8-7.5)	30.9 , 17.2 (4.1-77.8)‡	36.1 , 24.0 (0.2-78.7)‡
T2 (ms)			
Right hippocampus	83.1 , 2.3 (78.7-86.3)	92.8 , 5.7 (80.8-109)#‡	85.0 , 4.1 (72.6-92.4)
Leftt hippocampus	82.6 , 2.8 (78.1-87.0)	85.3 , 3.2 (78.9-93.2)^	93.2 , 7.3 (79.8-110.3)#‡
A.I.	1.7 , 1.0 (0.5-3.5)	9.2 , 5.0 (0.8-24.9)‡	9.6 , 7.9 (0.6-27.7)‡
NAA/(Cho+Cre) (ppm)			
Right hippocampus	0.79 , 0.05 (0.72-0.92)	0.56 , 0.12 (0.33-0.79)#‡	0.64 , 0.14 (0.46-1.03)‡
Leftt hippocampus	0.78 , 0.06 (0.66-0.87)	0.64 , 0.08 (0.42-0.81)‡	0.52 , 0.11 (0.37-0.76)#‡
A.I.	3.5 , 3.1 (0.11-11.2)	16.9 , 17.3 (1.6-62.0)‡	21.4 , 12.0 (0.9-39.3)‡

All values are expressed as mean, 1 standard deviation (range). *A.I.*, asymmetry indices.

* significantly different from the contralateral side at α level of 0.05

\# significantly different from the contralateral side at α level of 0.01

^ significantly different from the correspondent control side at α level of 0.05

‡ significantly different from the correspondent control side at α level of 0.01

Table II. Descriptive statistics for quantitative amygdala MRI data (AMYADC, AMYVOL and AMYT2).

Amygdala	Controls (n = 20)	Right TLE (n = 29)	Left TLE (n = 25)
ADC ($mm^2/s \times 10^5$)			
Right amygdala	0.77 , 0.02 (0.73-0.82)	0.82 , 0.04 (0.76-0.89)#‡	0.79 , 0.03 (0.73-0.83)
Leftt amygdala	0.77 , 0.03 (0.72-0.82)	0.77 , 0.03 (0.73-0.81)	0.81 , 0.05 (0.72-0.91)*‡
A.I.	2.5 , 1.9 (0.5-5.2)	6.3 , 4.3 (0.1-16.1)‡	4.8 , 4.5 (0.3-18.2)^
Volume (mm^3)			
Right amygdala	1870 , 112 (1667-2045)	1760 , 216 (1401-2225)#^	1847 , 158 (1640-2203)
Leftt amygdala	1877 , 095 (1673-2052)	1915 , 173 (1615-2238)	1743 , 227 (1369-2100)^
A.I.	4.1 , 2.6 (0.7-10.1)	11.1 , 8.9 (2.4-26.4)‡	12.3 , 8.8 (0.8-35.7)‡
T2 (ms)			
Right amygdala	79.9 , 2.9 (74.4-84.8)	86.3 , 4.9 (76.1-94.7)#‡	80.6 , 3.9 (73.5-87.6)
Leftt amygdala	79.8 , 2.8 (73.2-84.1)	81.4 , 4.7 (72.9-93.9)	85.0 , 5.2 (74.6-96.1)#‡
A.I.	2.3 , 1.3 (0.3-4.9)	6.7 , 3.8 (0.8-14.4)‡	6.2 , 4.8 (0.2-16.2)‡

All values are expressed as mean, 1 standard deviation (range). *A.I.*, asymmetry indices.

* significantly different from the contralateral side at α level of 0.05

\# significantly different from the contralateral side at α level of 0.01

^ significantly different from the correspondent control side at α level of 0.05

‡ significantly different from the correspondent control side at α level of 0.01

Authentication-Results: CARTMAN
from=mharder@asnr.org; domainkeys=fail (no key)
To: pmgp@fct.unl.pt, pmgp@fcsaude.ubi.pt
Subject: AJNR-04-00961.R1 ADC MAPPING OF THE HIPPOCAMPUS AND THE AMYGDALA IN PHARMACORESISTANT TEMPORAL LOBE EPILEPSY
From: grossr03@med.nyu.edu
Cc:
Date: Tue, 2 Aug 2005 10:34:36 -0400 (EDT)
X-Lookup-Warning: MAIL lookup on mharder@asnr.org does not match 206.112.78.33
X-MDRcpt-To: pmgp@fcsaude.ubi.pt
X-Rcpt-To: pmgp@fcsaude.ubi.pt
X-MDRemoteIP: 206.112.78.33
X-MDaemon-Deliver-To: pmgp@fcsaude.ubi.pt

August 2, 2005

Re: MS#04-00961.R1 ìADC Mapping of the Hippocampus and the Amygdala in Pharmacoresistant-Epilepsyî

Dear Dr. Pereira:

Thank you very much for the revisions to your manuscript entitled: ìADC Mapping of the Hippocampus and the Amygdala in Pharmacoresistant-Epilepsyî The manuscript is now accepted for publication in the American Journal of Neuroradiology.

Many thanks again for sending this interesting work to the American Journal of Neuroradiology.

Sincerely,

Robert I. Grossman, M.D.

RIG:er

Authentication-Results: CARTMAN
from=mharder@asnr.org; domainkeys=fail (no key)
To: pmgp@fct.unl.pt, pmgp@fcsaude.ubi.pt
Subject: Issue Assignment
From: jason@asnr.org
Cc:
Date: Mon, 8 Aug 2005 12:25:49 -0400 (EDT)
X-Lookup-Warning: MAIL lookup on mharder@asnr.org does not match 206.112.78.33
X-MDRcpt-To: pmgp@fcsaude.ubi.pt
X-Rcpt-To: pmgp@fcsaude.ubi.pt
X-MDRemoteIP: 206.112.78.33
X-MDaemon-Deliver-To: pmgp@fcsaude.ubi.pt

RE: AJNR-04-00961.R1 - ADC MAPPING OF THE HIPPOCAMPUS AND THE AMYGDALA IN PHARMACORESISTANT TEMPORAL LOBE EPILEPSY

Dear Dr. GonÁalves Pereira:

I am writing to inform you that the above referenced article has been accepted and is scheduled for publication in the March 2006 issue of the AJNR. As of now, we have not yet received the high-resolution .TIF image files needed for production. We must have these before the article goes to print. Please feel free to contact me with any questions regarding these materials.

Thanks very much, and congratulations on your manuscriptís acceptance.

Sincerely,

Jason Gantenberg
Editorial Assistant
American Journal of Neuroradiology
2210 Midwest Road, Suite 205
Oak Brook, IL 60523
Phone: 630.574.0220 ext. 240
FAX: 630.574.0326
Email: jason@asnr.org

STUDY V.

Relative localizing value of amygdalo-hippocampal MR biometry in temporal lobe epilepsy

Gonçalves Pereira P.M, Oliveira E, Rosado P.

Epilepsy Research (submitted).

RELATIVE LOCALIZING VALUE OF AMYGDALO-HIPPOCAMPAL MR BIOMETRY IN TEMPORAL LOBE EPILEPSY

Pedro M. Gonçalves Pereira [1,2]*; Eduardo Oliveira* [3] *; Pedro Rosado* [2,4]

[1] Department of Neuroradiology, 'Pedro Hispano' Hospital, Rua dr. Eduardo Torres, 4454-509 Matosinhos – Portugal
Phone: *-351-22-939 10 00, Fax: *-351-22-939 10 05, E-mail: pmgp@fcsaude.ubi.pt

[2] Department of Medical Science, Medical School, University of Beira Interior, Polo I, Rua Marquês d'Ávila e Bolama. 6201-001 Covilhã – Portugal

[3] Departement of Statistics, 'Egas Moniz' CRL, Health Science Institute (ISCS), Campus Universitário, Quinta da Granja, 2829-511 Monte de Caparica – Portugal

[4] Department of Neurology, Centro Hospitalar da Cova da Beira, Quinta do Alvito, 126, 6200-251 Covilhã – Portugal

Keywords: Temporal Lobe Epilepsy, Hippocampal Sclerosis, Amygdala Sclerosis, Volumetry, T2-Relaxometry, Multi-Voxel Spectroscopy, Electroencephalography, Magnetic Resonance Imaging, Epilepsy Surgery.

Support:

This study was supported by a grant from the Fundação para a Ciência e Tecnologia (BD 18498/98, awarded to P.M.G.P.) and by the Grünenthal Foundation (Portugal).

Acknowledgements:

We wish to thank neuroradiologists Constança Jordão and Pedro Evangelista for including the DWI sequence on the comprehensive magnetic resonance imaging protocol for temporal lobe epilepsy used at the "Caselas" Magnetic Resonance Centre, in Lisbon where all imaging studies were performed. Thanks also to Professor Mário Forjaz Secca and radiographer Cristina Menezes who provided us expert technical assistance. The authors further acknowledge Professor Fernando Lopes da Silva for his insightful comments on the manuscript, and the helpful criticisms of the anonymous Reviewers. All of our clinical epilepsy research occurs in collaboration with neurologists and neurosurgeons from Lisbon and Coimbra. Therefore we are very much indebted to our clinical collaborators, who include Orlando Leitão, José Pratas Vital and Luís Guerra (Hospital Egas Moniz), Alberto Leal (Hospital Júlio de Matos, referred here as A.L.), Paula Breia (Hospital Garcia de Orta), António Martins (Hospital Fernando da Fonseca), Francisco Pinto and António Gonçalves Ferreira (Hospital de Santa Maria) and Francisco Sales (Hospitais Universitários de Coimbra).

Corresponding author:
Pedro M. Gonçalves Pereira
Department of Neuroradiology
'Pedro Hispano' Hospital
Rua dr. Eduardo Torres
4454-509 Matosinhos – Portugal
Tel: *-351-22-939 10 00
Fax: *-351-22-939 10 05
E-mail: pmgp@fcsaude.ubi.pt

ABSTRACT

Objectives: The aims of the study were (i) to examine the localizing value of three MRI quantitative modalities (qMRI) currently used for the analysis of the hippocampus and amygdala in the context of pre-surgical screening and (ii) to propose a step-by-step protocol based on the sensitivity and performance of the different MR techniques. **Methods:** Ninety-two adults with chronic mesial temporal lobe epilepsy (TLE) of which 28 underwent amygdalo-hippocampal resection, and 34 age-matched controls were included in the study. High-resolution qMRI was performed at 1.5 T, including a tilted T1-weighted 3D-dataset for volumetry and four-echoes T2 relaxometry (both for hippocampus and amygdala quantifications) and multi-voxel spectroscopy [NAA/(Cho+Cre)] (exclusively in the hippocampus). Individual qMRI data were compared with electroencephalography regarding the localization of the epileptogenic area, with the neuropathological data and with postoperative outcome. MRI pathology was defined based on 99% confidence ellipses. Ten controls were used to assess the quantitative MRI intra- and inter-observer variability for all variables. **Results:** Volumetric measurements revealed unilateral damage in 77% of the patients, T2-relaxometry in 64% and spectroscopy in 53%. Additional measurements of the amygdalae (T2-relaxometry) allowed us to localize pathology that coexists with that of the hippocampus in 34%, and isolated unilateral amygdala damage in 8% of patients. Volumetry and T2-relaxometry (not spectroscopy) were associated with postoperative outcome, but accurate predictive models were computed based on hippocampal measures only. At least at one-year follow-up, volumetry predicts outcome correctly in 100% of the cases, whilst T2-relaxometry classified 96.4% (27/28) of these patients. All operated patients had hippocampal sclerosis. Concl**usions:** Hipocampal structural damage is equivocally depicted by spectroscopy. For diagnostic and pre-operative evaluation, hippocampal volumetry and T2-relaxometry provide maximal accuracy. Amygdala quantifications are irrelevant in the pre-operative evaluation but may be useful for diagnostic purposes. Of the three qMRI modalities tested, T2-relaxometry provided the best balance between diagnosis accuracy and time-efficiency to lateralize a sclerotic lesion on the majority of the patients. Cases that remain undecided after T2-relaxometry may benefit from additional measurements based on hippocampal volumetry.

INTRODUCTION

Magnetic resonance imaging (MRI) provides an objective means for studying the individual temporal lobe structures in vivo and contributes unambiguously to the identification of patients with the mesial temporal epilepsy (TLE) syndrome (ILAE, 2004) that are refractory to pharmacotherapy and have a surgical indication.

The standard surgical treatment of patients with manifest TLE is anterior temporal lobectomy, which includes the removal of the hippocampus and the amygdala (Yasargil, et al., 1985; Wiebe, et al., 2001). This effective procedure leads to improvement in up to 85% of properly selected patients. To avoid undesired effects and to optimize the results of the surgical intervention, it is necessary to identify and lateralize the seizure focus with a high degree of accuracy.

Unilateral hippocampal sclerosis (HS) is the most common pathological diagnosis in TLE, and up to 65% of cases of TLE may be attributed to lesions arising exclusively in the hippocampus (Babb, 1992; Jutila, et al., 2002). Histopathological studies have reported a concomitant pattern of tissue damage, that is, selective neuronal loss and gliosis extending to the amygdala [10-60% of the cases with a damaged hippocampus (Cavanagh and Meyer, 1956; Margerison and Corsellis, 1966; Yilmazer-Hanke, et al., 2000)] and the para-hippocampal gyrus [21-68% of the cases (Cavanagh and Meyer, 1956; Yilmazer-Hanke, et al., 2000)]. It has also been reported that isolated amygdala damage can be present in up to 10% of the patients referred for surgical treatment (Swartz, et al., 1992; Miller, et al., 1994; Lee, et al., 1998). Such widespread involvement of mesial temporal lobe structures is usually denoted by the term “mesial temporal sclerosis” (MTS).

Quantitative imaging evaluations (qMRI) are relatively unbiased when compared with qualitative observations and provide a robust means to determine the severity and extent of tissue damage in the mesial temporal lobe. Moreover, several qMRI techniques provide useful prognostic information regarding surgical outcome of those patients who are refractory to pharmacotherapy [volume: (Jack, et al., 1992; Cascino, et al., 1995; Cendes, et al., 1997); T2-relaxometry: (Kuzniecky, et al., 1997); spectroscopy: (Kuzniecky, et al., 1999; Antel, et al., 2002); diffusion (ADC-mapping): (Gonçalves Pereira, et al., 2006)].

The qMRI techniques that are mostly used in TLE include volumetry, T2-relaxometry and spectroscopy. Volumetry (Cook, et al., 1992) detects histologically proven HS in 71%-97%

of cases (Cascino, et al., 1991; Lencz, et al., 1992; Kuzniecky, et al, 1997), although volumetry may also fail to identify certain cases of HS (Jackson, et al, 1994).

The sensitivity of MRI analysis may be increased by measuring T2 relaxation times (Jackson, et al., 1993; Kuzniecky, et al., 1997; Bernasconi, et al., 2000) and hippocampal spectroscopy (Connelly, et al., 1994; Thompson, et al., 1998a; Woermann, et al., 1999; Park, et al., 2001; Capizzano, et al., 2002). In patients without any other MRI criteria of hippocampal damage, T2-relaxometry can identify HS in up to 82% of the cases (Bernasconi, et al., 2000) while spectroscopy has been reported to depict unilateral metabolic changes in 27%-71% of the subjects (Connelly, et al., 1998; Woermann, et al., 1999).

Measuring the volumes and T2-relaxometry times of the amygdalae enhances the possibilities of a correct MTS diagnosis, since there are TLE patients who can present isolated amygdala sclerosis (Swartz, et al., 1992; Miller, et al., 1994; Lee, et al., 1998).

However, current qMRI analyses have the disadvantage of being time-consuming when compared with qualitative observations. Additionally, volumetry studies depend critically on the observer's skills while T2-relaxometry and spectroscopy need dedicated software. Thus, whenever a qMRI protocol is installed for TLE pre-surgical screening a balance must be though off which considers the necessary investment in personnel training and software acquisitions.

Comparative qMRI studies have been essentially conducted in the hippocampus, namely hippocampal volumetry and spectroscopy (Cendes, et al., 1997; Kuzniecky, et al., 1998); hippocampal volumetry and T2-relaxometry (Van Paesschen, et al., 1995; von Oertzen,, et al., 2002); hippocampal volumetry, spectroscopy and diffusion-weighted imaging (Duzel, et al., 2004) and also in the amygdala [volumetry and T2-relaxometry (Kälviäinen, et al., 1997)]. Nevertheless, no study has so far investigated the relationship between hippocampal qMRI variables [volumetry (HCVOL), T2-relaxometry (HCT2) and multi-voxel spectroscopy (HCSI)] jointly with amygdala volumes (AMYVOL) and T2 maps (AMYT2).

The goal of this study was to assess the relative value of volumetry, T2 relaxometry and spectroscopy as such and in combinations, in the evaluation of the mesial temporal integrity (hippocampus and amygdala) given the context of pre-surgical screening. This is a relevant issue since no single technique may be sufficiently sensitive to detect the whole spectrum of hippocampal and amygdala pathology. An essential question is whether these techniques provide complementary or redundant information about the status of the mesio-temporal structures. This information may help us to optimize the scanning and post-processing procedure so that a multimodal MR protocol may be established with improved sensitivity in the shortest possible time.

PATIENTS AND METHODS

Control subjects

The control group included thirty-four subjects (17 women) with a mean age age [1 standard deviation (SD)] of 33.7 , 9.7 (range: 19 - 52) years. All the volunteers were interviewed to exclude those with neurologic diseases and were submitted to detailed neurological examination and a "mini-mental state" test (Folstein, et al., 1975) [obtained score and range was: 28.6 , 1.3 (26 - 30)].

Patients

Ninety-two patients (51 women) with a mean age of 32.9 , 9.8 (17 - 63) years were enrolled in the study. Classification of the patients syndromes was based on the guidelines proposed by the International League Against Epilepsy (ILAE, 1989). All had medically refractory TLE and underwent comprehensive presurgical epilepsy evaluations, which included a detailed clinical history, inter-ictal EEG, prolonged video-telemetry monitoring, MRI studies, neuropsychological assessment and intracarotid sodium amobarbital tests (in selected cases). Only patients with clinical and EEG evidence of TLE and without any neoplastic, vascular, developmental or non-hippocampal volme loss lesion demonstrated at MR imaging were included.

MR Image acquisition

All MR studies were obtained on the same 1.5T scanner [CV/i-NV/I equipped with high-capacity gradient (amplitude: 40 mT/m, slew rate: 200 (T/m)/s), General Electric Medical Systems, Milwaukee, Wisconsin, USA], over a period of approximately two years (May 2001-August 2003). Every subject underwent a single MRI session. During the scanning period (approximately 70-min.) all participants were comfortably placed and their heads were fixated within the headcoil with customized cushions. Special attention was paid to the symmetric positioning of the subjects head. Imaging processing was performed using the manufacturer's software, GE Advantage Windows 3.1 (including research modules), running on Sun workstations (SPARC 4.1, Sun Mycrosystems, Mountain View, California, USA).

Presurgical imaging consisted of standard qualitative sequences (multiplanar high-resolution T1- and T2-weighted, proton density, inversion-recovery and fluid-attenuation inversion recovery scans). For this study, patients and controls were further evaluated with a specific MR protocol in order to obtain quantitative data, part of which was described elsewhere (Gonçalves Pereira, Oliveira et al. 2006).

All sequences were obtained using a tilted orientation to the temporal lobes, orthogonal to the axis of the hippocampal body (Gonçalves Pereira, et al., 2005). Imaging for hippocampal and amygdala volumetry and relaxometry (**Figure 1**) was acquired on the coronal plane, parallel to the posterior comissure-obex line (PC-OB) (Tamraz and Comair, 2000). Two-dimensional (2D) multi-voxel hippocampal spectroscopy was acquired on the axial plane perpendicular to PC-OB (**Figure 1**). The same radiographer was used throughout.

A sagittal spin-echo T1-weighted with TR = 600 ms, TE = 15 ms, NEX = 2, FOV = 24 cm, section thicknes = 5 mm, gap = 1 mm, acquisition matrix = 512 x 192 pixels was acquired as a reference series for the following sequences (**Table 1**).

Volumetry. For volumetric studies, we used a T1 three-dimensional spoiled gradient-echo (3D SPGR) protocol with TR = 20-30 ms, TE = Min.Full, NEX = 2, FOV = 24 cm, section thickness = 1.5 mm, gap = 0 mm, acquisition matrix = 512 x 224 pixels, producing a series of 118-126 slices of the entire brain. Right and left hippocampus and amygdala volumes were measured following the general guidelines of Watson et al (1992) on images magnified four-fold, with some modifications. We relied on the multi-planar intrinsic signal of the structures of interest to adapt for the individual's anatomy. Instead of using external anatomical references, we took advantage of the gapless images with high-resolution to measure consecutively the hippocampus and amygdala areas on the coronal plane. For each subject, the posterior and anterior limits of each hippocampus were identified on the right and left para-sagittal sections, where the corresponding in-plane coronal images (with the reference image number) could be displayed. The posterior limit of the amygdala was identified using the same methodology. However, with current MRI, the anterior limit of the amygdala is difficult to identify by means of its different contrast and, thus we had to refer to external anatomical references (for a review see (Brierley, et al., 2002). We followed the borders described by Cendes et al (1993) with modifications (for the anterior limit, we choose the level where the lateral sulcus closes to form the endorhinal sulcus and, simultaneously, the optic chiasm appears continuous).

HCVOL included the volumes of the dentate gyrus, hilus, cornu ammonis, subiculum, fimbria, alveus and vertical digitations (Cook, et al., 1992). The uncus and choroids plexus were excluded (Watson, et al., 1992). Whenever present, hippocampal sulcus remmants (Humphrey, 1967) were included in the measurements and considered a normal anatomic variation (Sasaki, et al., 1993).

AMYVOL consisted of the volumes of the deep nuclei (lateral, basal, accessory basal, and paralaminar nuclei), the superficial nuclei (anterior cortical and medial nuclei, nucleus of the lateral olfactory tract, periamygdaloid cortex, posterior cortical nucleus) and the remaining

nucleus of the amygdala (anterior amygdaloid area, central nucleus, amygdalohippocampal area and intercalated nucleus) (Soininen, et al., 1994).

Volumes were calculated by measuring the hippocampal and amygdala areas within each slice using the manufacturer's interactive mouse-driven software (**Figure 1**) and multiplying it by the thickness of the section; the resulting volumes were summed to obtain a total volume [Cavalieri slices method (Gundersen and Jensen, 1987; Roberts, et al., 2000)].

Finally, to correct the absolute volumes for the individual variance in head size a ratio was used which allows obtaining 'normalized volumes'. We adopted the procedure of Cendes et al (1994), with the modifications of Kälviäinen et al (1997), accordingly to the equation:

$$Norm.Vol. = \frac{A_M}{A_I} \times Abs.Vol.$$

where *Norm.Vol.* indicates the normalized volume; A_M, the mean brain area obtained at the level of the anterior commissure (coronal plane) for the control group, A_I, the individual brain area obtained at the level of the anterior commissure (coronal plane) and *Abs.Vol*. the measured absolute volume. This procedure allows obtaining comparable volumes of the structures of interest in every subject, taking into account the differences in volume of the total brain. As subjects consecutively differ in morphometric parameters, including cranial size, overestimations of volumes (and thus misdiagnosis) will occur if two subjects with a proportionally similar hippocampal or amygdala size are compared without correction, when one of the subjects has a larger brain volume.

T2-relaxometry. The method used for T2-relaxometry was similar to that described by Jackson et al (1993), with some modifications due to time constraints (Pires, et al., 1998). We used a 4-echoes protocol (instead of 16) with TR = 3000 ms, TE = 45 – 90 – 135 – 180 ms, NEX = 2, FOV = 24 cm, section thicknes = 4 mm, gap = 1 mm, acquisition matrix = 256 x 192 pixels, producing a series of 15 oblique slices over the whole temporal lobe. To assure reproducibility, the first section was placed at the posterior end of the corpus callosum, in the mid-sagittal plane.

T2 maps were obtained by fitting, pixel by pixel, the data from successive echoes to a mono-exponential decay curve. Regions of interest (ROI) of arbitrary shape (but constant voxel number) were drawn over the hippocampi (20 mm^2) and amygdala (40 mm^2), avoiding borders where partial volume effects could alter the mean T2 value for the ROI (**Figure 1**). For each subject, the HCT2 results were obtained by averaging ROI's values from 3 central slices taken at the level of the body of the hippocampus. AMYT2 were calculated by averaging ROI's values from 2 anterior slices, which included the amygdala.

Hippocampal spectroscopy - For HCSI, a T2 fast spin-echo (TR = 4800 ms, TE = 136

ms, NEX = 2, FOV = 24 x 18 cm, section thicknes = 3 mm, gap = 1 mm, matrix = 256 x 224 pixels) localizer was acquired at an oblique transverse orientation, parallel to the long axis of the hippocampus (perpendicular to PC-OB) to reduce partial volume effects due to surrounding cerebrospinal fluid. A 2D proton magnetic resonance spectroscopy imaging sequence with point-resolved spectroscopic (PRESS) multi-volume selection (TR = 1000 ms, TE = 144 ms, NEX = 1, FOV = 24 x 24 cm, 18 x 18 encoding steps, PROBE-SI) was then acquired on the T2 image where the hippocampi were fully visible (Ng, et al., 2000; Bernasconi, et al., 2002). Shimming (GE Grad-Shim) and water suppression were performed automatically. To exclude the large lipid resonances from the extracranial fat, the length and width of the acquired volume were adjusted for each individual case, depending on head size, whereas section thickness was set to 10 mm in all cases. The volume of interest was placed behind the clivus and oriented in a similar position for all examinations to cover the entire extend of both hippocampi (**Figure 1**). Each voxel had the following nominal size: 7.5 x 7.5 x 9.9 mm^3 (volume: 557 mm^3).

The acquired chemical-shift imaging raw data were transferred to the manufacturer's workstation for Fourier transformation, curve fitting, plotting and display processing using the standard spectroscopy software (GE FuncTool). To obtain HCSI, two to tree voxels were placed along the longitudinal axis of each hippocampal structure, avoiding areas of low signal to noise ratio (**Figure 1**). In every subject, technically good-quality spectra were obtained using this standard voxel placement. Mean metabolic concentration was obtained on each hippocampus for *N*-acetyl-aspartate (NAA), Choline (Cho) and Creatine/Phosphocreatine (Cre) from signal intensities at 2.0 p.p.m. (NAA), 3.0 p.p.m. (Cre) and 3.2 p.p.m. (Cho). The NAA/(Cho + Cre) ratio was then calculated for each hippocampus, since this is a reliable measure for optimal lateralization (Ende, et al., 1997). All spectra were inspected thoroughly, and those who were artifactually broadened [i.e., with a full width at half maximum of >12 Hz (water resonance)] or if Cho and Cre peaks were not resolved, were discarded. In a small number of subjects (n=12), we had to repeat the PROBE-SI acquisition due to head motion.

For all the MRI variables, an asymmetry index (A.I.) was used to ascertain the degree of asymmetry (in percentage) between the values obtained in the right (R) and left (L) structures, according with Bernasconi et al (Bernasconi, et al., 1999) as follows:

$$A.I.(\%) = 100 \times \left| \frac{R - L}{(R + L)/2} \right|$$

EEG data

All patients were submitted to prolonged in-patient video-EEG monitoring, while anti-epileptic medication was reduced. Scalp electrodes were placed according to the International 10-20 System (Jasper, 1958) with 3 pairs of additional electrodes over the inferior temporal areas. The EEG signals were digitalized and analyzed by experts with reformatting facilities and synchronized video.

Lateralization was decided based on semiology (video) and on the electrophysiological ictal activity. In the very few patients (n=11) without seizures during video-EEG, the presence of a large majority of interictal activity localized to one hemisphere in the fronto-temporal areas was accepted as indicating lateralization (>80%, that is a ratio greater than 4:1 of interictal spikes) (Cendes, et al., 2000). Patients whose EEG didn't fit these criteria were not enrolled in the study.

Post-surgical outcome

To date, 28 patients (13 women), with a mean age of 31.8 , 9.6 (18 - 57) years underwent selective amygdalohippocampectomy accordingly to the procedure of Yasargil et al (1985) and had duration of the follow-up period longer than one year. The mean postoperative follow-up was 28 months (range: 13 - 39). In this group of patients, no reoperations were performed. Patients were assessed by epileptologists on a regular basis (months 3, 6, 12) and yearly afterwards.

The surgical outcome with respect to seizure control was assessed by means of Engel's classification (Engel, J., Jr., et al, 1993). Patients were classified as having a good outcome (Engel's class IA) or a less satisfactory outcome (classes IB to III). Such data was related to the lateralizing ability of qMRI measures, it´s degree of asymmetry and the co-occurrence of hippocampal and amygdala abnormalities. Post-surgical quality of life, memory and disability were not assessed in this study.

Pathological examination

The neuropathological data collected for this study was based on reports carried out by experienced pathologists.

The group of patients that underwent surgery (n=28) was from the "Egas Moniz" Hospital (n=23), "Santa Maria" Hospital (n=4) and "Hospitais Universitários de Coimbra" (n=3) Epilepsy Surgery Programmes.

Generally, the surgical procedure was similar across centres. Patients underwent anterior temporal lobectomy with resection of the rostral and mid hippocampus by means of microneurosurgery. The hippocampal head and anterior body were resected en bloc, and the

posterior body was then removed by subpial aspiration. This technique removes about 1.5 to 3.0 cm of the total anterior-posterior length of the hippocampus, depending on which temporal lobe is being resected (1.5 cm for the dominant temporal lobe).

Fresh surgical tissue were fixed using a formaldehyde solution (20%) and later processed into paraffin sections stained with a standard hematoxylin and eosin (H&E) technique for staining neuronal cell bodies. One centre also used the glial fibrilary acidic protein to assess reactive glia.

In all surgical cases, an estimated amount of at least > 60% of the resected hippocampus was qualitatively examined, without neuronal counting. Additional mesial temporal tissue was not consistently evaluated in all cases, although parts of the medial amygdala and portions of the subiculum and para-hippocampus were available in a group of patients.

In order to standardize the neuropathological data, our analysis concentrated on the hippocampus and on the observations of the H&E staining, according to established criteria used to diagnose HS (Lantos, et al., 2002). As a result, HS was classified into "severe", "moderate" or "end-folium" depending on the severity and extent of neuronal cell loss. "Severe HS" included major cell loss in sectors CA1, CA3 and dentate hilus, with relative sparing of CA2 and the granular cell layer. "Moderate HS" was diagnosed whenever mild neuronal loss was present in the CA3 and dentate hilus, while CA1 was severely affected. "End-folium HS" consisted of extensive dentate hilar cell loss without a similarly severe loss of dentate granule cells or hippocampal pyramidal neurons.

Statistical analysis

Group differences for age were assessed using one-way ANOVA (analysis of variance).

Statistics were performed with SPSS Statistical Software Package 11 for Macintosh OS X (SPSS, Inc., Chicago, Illinois, USA) and STATISTICA for Windows 98 (Tulsa, OK: StatSoft, Inc.).

To verify the repeatability of the imaging measurements, the same observer (P.M.G.P.) performed the quantifications twice for all the variables in 10 controls independently with a 6 week interval. To check the inter-observer variability, a second observer (A.L.) quantified also the hippocampal volumes. Intra (and inter) observer variability was tested by analysing the limits of agreement between the first and second measurements and the correlations between measurements, according to Bland and Altman (Bland and Altman, 1986), at $p < 0.05$. The intra-observer variability was expressed as the means of the coefficients of variation of each control value; it was 3.6% (HCVOL), 4.8% (AMYVOL), 3.1% (HCT2), 2.4% (AMYT2), and 0.2% (HCSI). The inter-observer variability expressed in the same way for HCVOL was 4.3%. For all

the variables, the mean difference between the two measurements was near zero and the limits of agreement were below 2 standard deviations of the mean of controls.

In order to compare the means of the variables between groups (control vs right TLE; control vs left TLE; control vs non-lateralized), we tested the equality of variances (Levene's test) and used student's t-test. Tests with respect to differences between the right and left hippocampus and amygdala values were assessed with paired t-test.

To verify the normal distribution of the values obtained by quantitative MRI, we used the Kolmogorov-Smirnov (Kolmogorov, 1933) and Lilliefors (Lilliefors, 1967) analysis. As the normal distribution was not rejected, we determined confidence ellipses for all the control values, with 99% of confidence.

Confidence ellipses describing values for both right and left hippocampus and amygdala were determined for controls applying the Hotelling's method (Hotelling, 1936), using STATISTICA software (Tulsa, OK: StatSoft, Inc.). The ellipse depends on the correlation coefficient between right and left variables and on data dispersion. The following general equation, which includes the means, the variances and the covariance of both right and left variables of controls, holds:

$$n\left[\bar{x}-\mu\right]^{T} S^{-1}\left[\bar{x}-\mu\right] \leq \frac{(n-1)p}{(n-p)} F_{p,n-p}(\alpha)$$

n - number of controls (our case: 34)

$\left[\bar{x}-\mu\right]$ - means matrix of the controls

$\left[\bar{x}-\mu\right]^{T}$ - the transpose of a means matrix

S^{-1} - inverse of the covariance matrix

p - number of variables (our case: 2, right and left)

In order to assess the level of interdependence between the MR variables, we correlated every hippocampal and amygdala independent values. We also verified whether the magnitudes of the amygdala and hippocampal damage were associated. For this analysis, we tested the level of correlation between volumes, T2 and CSI values. Pearson's coefficients (two-tailed) were used to determine the significance levels.

Fisher´s exact test was used to evaluate the probability of association between the qMRI measures, neuropathological data and surgical outcome. Whether such associations were demonstrated, the positive predictive values, odds ratios and Spearman´s correlation´s coefficient were calculated. Additionally, logistic regression models were fitted relating outcome

(dependent variable) to the side of surgery and qMRI values on the operated side. One-way analysis of variance (ANOVA) and Spearman´s correlation´s coefficients were used to verify whether there were meaningful differences in qMRI data accordingl to the pathological examination of the hippocampus.

Finally, to compare the discriminative power of the MR techniques for the detection of deviations from normality, that may indicate pathology, and to be able to propose a decision tree for the detection of imaging abnormalities, we analysed both the lateralizing ability of each modality and the corresponding acquisition and operator times.

Definition of MRI pathology

All the values that fell outside the 99% confidence ellipse for the normal values were considered pathological (**Figure 2**). This classification displays on a simple graphical representation all the deviations from normality, which includes patients that have *either* qMRI values smaller/larger than 3SD deviations from the mean of controls on right and left structures, and those patients whose qMRI values may appear within control range but show an Asymmetry Index that is larger than 3SD of the mean of controls.

Laterality was defined whenever either of the above conditions was verified and in agreement with the electroencephalographic and clinical data.

RESULTS

Patients groups

Based on neurophysiological evaluation, patients were separated in three groups according to the main seizure electrographic lateralization: right TLE (n=45), left TLE (n=39), non-lateralized TLE (n = 8). The groups did not differ statistically for demographic or illness-related variables.

The patients groups and normal controls did not differ significantly in age [ANOVA; $F(3,122) = 0.31$, $p = 0.82$] or sex distribution [χ^2; $\chi^2(1) = 2.1$, $p = 0.14$ for right TLE, χ^2; $\chi^2(1) = 0.14$, $p = 0.91$ for left TLE, and χ^2; $\chi^2(1) = 0.38$, $p = 0.54$ for bilateral TLE].

Group comparisons (Tables 2 and 3)

Comparisons were made between right and left hippocampi and amygdalae values in patients groups and controls. In patients groups, values ipsilateral and contralateral to the focus were tested and the asymmetry indices (A.I.) were compared to control values.

In the control group, the only significant asymmetry was observed regarding the hippocampal volumes (right > left; $p < 0.05$). There were no gender differences in the hippocampal or amygdala volumes, and T2 and CSI values. Also, there was no correlation between these values and age.

At a group level, these qMRI modalities presented some differences regarding the identification of amygdalo-hippocampal pathology, when compared with the control group.

In the groups with EEG focus lateralized either to the right or left TL, every qMRI analysis showed mean values that were significantly different to controls in the ipsilateral hippocampus and amygdala. HCVOL and AMYVOL didn't have any significant changes (or trend) in the contralateral mean values relative to controls. Moreover, HCVOL had the largest mean A.I. difference relative to controls (whose mean was 4.3), with values reaching a mean of 35.9.

The overall trend for HCT2, AMYT2 and HCSI showed changes in the structures that were contralateral to the focus, indicating that a certain number of patients with clear localized EEG focus and concomitant atrophy had widespread mesial abnormalities on both temporal lobes. HCT2 identified contralateral structural damage in the right TLE group, although there was a similar tendency for the left TLE group that was not significant (p=0.06 for the HCT2 mean values of the right hippocampus). There was also an additional tendency in the right TLE

group for large mean AMYT2 values in the left amygdala (p = 0.08). HCSI values from both hippocampi were significantly smaller than controls on both right and left TLE groups.

The non-lateralized patients showed significant mean bilateral differences compared with controls on every hippocampal and amygdala analysis, except for AMYT2. Furthermore, there were significant differences of the asymmetry indices of HCVOL ($p < 0.05$) suggesting that some of these patients would have pathology on a dominant side.

Since one main objective of this study was to determine the relative value of the qMRI methods to lateralize hippocampal and amygdala abnormalities, we present these data, for patients and controls, in two-dimensional plots (confidence ellipses) where the absolute values and the asymmetries can be put more clearly in evidence for the individual patients.

Confidence ellipses (Figure 3 and Table 4)

The ellipses represent the 99% confidence interval for the control group. The specificity of the three qMRI methods was 100%, since no control subject had values outside the interval defined as normal.

The present data was analysed considering, first, whether the individual values were significantly asymmetric (which may indicate lateralization of pathology) and, second, identifying the patients with asymmetry indices in the same range as controls. The latter were either indistinguishable from controls or presented bilateral abnormalities (see the summary of data on **Table 4**).

Volumetry (**Fig. 4A-B**) – There was a clear tendency for significant asymmetries (or atrophies) in agreement with the EEG data, namely for HCVOL. Considering both TLE patients groups (n = 92), HCVOL (**Fig. 4A**) detected asymmetry in 77% (71 / 92) of the patients, 6% (5 / 92) had bilateral small volumes, while the remaining (17% - 16 / 92) had normal volumes and no asymmetries. AMYVOL (**Fig. 4B**) revealed that 38% (35 / 92) of the patients had an asymmetric volume, 3% (2 / 92) had a bilateral larger AMYVOL and 59% (55 / 92) had normal volumes.

There were 39% (36 / 92) of the patients with concordant HCVOL and AMYVOL data [either pathological (n = 24) or normal (n = 12)], 43% (40 / 92) with an asymmetric HCVOL without AMYVOL changes, and 5% (4 / 92) of the patients had isolated amygdala atrophies (there were 12 cases with discordant HCVOL-AMYVOL data, that is, either asymmetries on opposite sides or bilateral HCVOL with normal or asymmetric AMYVOL).

T2-relaxometry (**Fig. 4C-D**) – These cases indicate a general trend for T2-relaxometry to be concordant with the EEG data (and with volumetry), although it detects a larger number of cases with bilateral damage. Another interesting observation was that the number of cases with pathology detected by AMYT2 nearly reaches 50% more than the ones detected by AMYVOL,

with less contralateral detections. The HCT2 showed that (**Fig. 4C**), 64% (59 / 92) of the patients had asymmetric T2 values, while 10% (9 / 92) had bilateral large T2 and the remaining 26% (24 / 92) were normal. AMYT2 data (**Fig. 4D**) showed that 45% (41 / 92) of the patients had an asymmetry index significantly larger than controls, 7% (6 / 92) had bilaterally large values and 49% (45 / 92) were normal.

There were 78% (72 / 92) patients with concomitant HCT2 and HCVOL data (either pathological or normal) and 4% (3 / 92) patients had a large T2 value and a normal hippocampal volume. In the amygdala, there were 48% (44 / 92) patients with concomitant AMYT2 and AMYVOL data (either pathological or normal) and 4% (3 / 92) patients had a large T2 value and a normal amygdala volume.

Regarding the agreement between HCT2 and AMYT2 data, 47% (43 / 92) patients had concordant values [either pathological (n = 31) or normal (n = 12)] and 8% (7 / 92) patients had isolated large T2 values in the amygdala.

Hippocampal spectroscopy (**Fig. 4E**) – HCSI showed a general trend towards low bilateral NAA/(Cho+Cre) ratios in all the TLE patients groups. In the EEG lateralized groups, nearly 50% of the patients had an A.I. in the same range as controls. Furthermore, 53% (49 / 92) of the patients had an asymmetric NAA/(Cho+Cre) ratio (ipsilateral HC > contralateral HC), 20% (18 / 92) had a bilaterally small ratio and 27% (25 / 92) were normal.

There were 53% (49 / 92) patients with concordant HCSI and HCVOL and 55% (51 / 92) patients with concomitant HCSI and HCT2 data (either pathological or normal). Other 5% (4 / 92) patients had isolated asymmetrical HCSI values.

Relations between variables

Only values from the right and left TLE patients groups (n = 84) were included in this analysis. There were significant correlations among all ipsilateral MR variables, being the strongest association between HCVOL and HCT2 (r = - 0.72, p < 0.01). The correlations between the contralateral values were non-significant, except for HCVOL vs HCT2 (r = - 0.27, p < 0.01) and HCT2 vs HCSI (r = - 0.25, p < 0.05).

The co-occurrence of amygdala and hippocampal damage was also assessed. There were significantly moderate positive correlations between hippocampal and amygdala ipsilateral volumes (r = 0.34, p < 0.01) and T2 values (r = 0.36, p < 0.01). As for the contralateral data, there was a weak positive association between the volumes (r = 0.26, p < 0.05) and a moderate correlation between the T2 values (r = 0.40, p < 0.05).

Post-surgical outcome and qMRI

During the follow-up period, 21 (75%) patients were in class IA (seizure-free), and 7 (25%) in class IB-III (3 patients in class IB, 3 in class II and 1 patient in class III). All 28 patients underwent surgery on the side of maximal EEG lateralization and had imaging features characteristic of hippocampal sclerosis on qualitative MRI. No patient was operated based on isolated amygdala sclerosis imaging.

The association between the qMRI measures and a good surgical outcome was only demonstrated with respect to the volume and T2-relaxometry independently, and either in the hippocampus and amygdala (**Table 5**). Accordingly, significant negative ρ correlations were found between the volumes, and T2-relaxometry Asymmetry Indices (HCVOL: r_s = - 0.73 ; HCT2: r_s = - 0.71, both $p < 0.0001$; AMYVOL: r_s = - 0.54 , $p < 0.01$; AMYT2: r_s = - 0.42 , $p < 0.05$), with respect to the individual Engel class. Lateralized HCSI did not associate with outcome and Spearman´s correlation was non-significant (r_s = - 0.18 , $p = 0.36$).

Although the positive predictive value was rather similar among the volumes and T2-relaxometry of the hippocampus and amygdala (**Table 5**), there were major differences in the estimated odds ratio (OR). As both HCVOL and HCT2 provided identical results regarding lateralization and outcome, the OR was the same: 120 (95% CI 2.3 – 148.4). As for AMYVOL and AMYT2, the OR was 8 and 6 times smaller than that of the hippocampus, respectively (AMYVOL: OR = 15 , 95% CI 3.2 – 33.4; AMYT2: OR = 19.2 , 95% CI 2.9 – 36.9).

Binary logistic analyses were computed for the volumes and T2-relaxometry to verify whether successful surgical outcomes could be predicted accurately by qMRI covariates and whether stepwise regression models of the hippocampus and amygdala provided complementary or redundant information regarding patient counseling.

Models that used hippocampus-only covariates obtained the maximal accuracy concerning the correct classification of these patients. For the volume all the patients (100%) were exactly grouped (Nagelkerke R^2 = 0.99; Hosmer and Lemeshow test: $p = 1$), whenever the relation between the operated side ($HCVOL_{IPSI}$; units in mm^3), the non-operated side ($HCVOL_{CONTRA}$; mm^3) and the volume asymmetry ($HCVOL_{A.I.}$) holds:

$$(0.01 \times HCVOL_{IPSI}) + (-0.08 \times HCVOL_{CONTRA}) + (-4.53 \times HCVOL_{A.I.}) + 333 < 0$$

Interestingly, all the cases with an unfavorable outcome had a side-to-side difference ($HCVOL_{CONTRA}$ minus $HCVOL_{IPSI}$) smaller than 900 mm^3, a value that matches the cut-off limit found by Jack, C.R. et al (1992) on a larger study (50 patients; difference in volume < 1000 mm^3).

As for HCT2, the model classified correctly 96.4% (27 / 28) of the patients (Nagelkerke R^2 = 0.83, Hosmer and Lemeshow test: p = 0.69) whenever the T2 asymmetry ($HCT2_{A.I.}$) assumes the following assumption:

$$(-0.91 \times HCT2_{A.I.}) + 5.10 < 0$$

For every patient that was operated with an HCT2 value in the non-operated side larger than the HCT2 in the ressected side (irrespective of the difference), the outcome was unfavourable.

Post-surgical outcome and neuropathological data

Hippocampal sclerosis, as defined, was found in all surgical specimens.

Globally, 16 (57%) hippocampi abnormalities were classified as "severe HS", 9 (32%) as "moderate HS" and 3 (11%) as end-folium sclerosis.

Of the 21 patients in class IA, 14 (66%) had a diagnosis of "severe HS", 6 (29%) had "moderate HS" and 1 (5%) patient had end-folium sclerosis. Patients whose postoperative outcome was less favourable (class IB-III, n = 7), had a neuropathological diagnosis of "severe HS" in 2 cases (29%), "moderate HS" in 3 cases (43%) and end-folium sclerosis in 2 cases (29%).

There was no significant association between the neuropathological data and surgical outcome, although a tendency could be depicted (Fisher´s exact test: p = 0.103 ; Spearman´s correlation: r_s = 0.38, p = 0,04).

Neuropathological data and hippocampal qMRI

There were significant differences in the mean values of the Asymmetry Indices of HCVOL and HCT2, accordingly to the neuropathological classification. Patients with "severe HS" had larger A.I. than "moderate HS"; similarly, the "moderate HS" class had a larger A.I. than the end-folium class ($HCVOL_{A.I.}$: p = 0.00001 ; $HCT2_{A.I.}$: p = 0.04). Furthermore, the mean value of the $HCVOL_{IPSI}$ differed significantly across pathological classes, with smaller volumes in the "severe HS" class and larger volumes in the end-folium class (p = 0.02).

Correlation analysis demonstrated a significant positive ρ between the $HCVOL_{IPSI}$ (r_s = 0.62 , p < 0.0001), with respect to the individual pathological class, and negative ρ correlations between the volumes, and T2-relaxometry Asymmetry Indices ($HCVOL_{A.I.}$: r_s = - 0.76 , p < 0.0001 ; $HCT2_{A.I.}$: r_s = - 0.48 , p < 0.01).

DISCUSSION

Accurate lesion localization is vital in order to make anatomical inferences based on clinical and neurophysiological data and to support surgical decisions. In the present study, we used a multimodal set of quantitative MRI methods to assess the occurrence and severity of hippocampal and amygdala pathology in 92 TLE patients, 30% of which underwent amygdalo-hippocampectomy, and compare the lateralizing ability of each modality. We further aimed to propose a comprehensive qMRI protocol for the pre-surgical evaluation of refractory TLE patients, based both on the ability to detect mesio-temporal damage and time efficiency.

There were four main findings in this study.

First, regarding the hippocampus, volumetry and relaxometry detected the largest number of cases with unilateral damage that agreed with the EEG, with a strong correlation between them. Accordingly, in the 4 patients (5%) with contralateral volume loss, T2-relaxometry expressed either bilateral (3 patients) or contralateral (1 patient) pathologies. Still, T2-relaxometry identified less 13 patients (14%) with unilateral damage than volumetry. In the sub-group of patients that were operated, both HCVOL and HCT2 predicted outcome with 100% and 96.4% accuracy, respectively. Both measures were also associated with the severity of hippocampal sclerosis.

Second, hippocampal spectroscopy unveiled a large number of cases with bilateral abnormalities, although the majority was asymmetric, and yielded the largest number of cases with normal symmetric values when compared with the volume and T2 analyses. Additionally, HCSI was not a predictive variable with respect to the surgical results, neither correlated with the neuropathological results. These data suggest that HCSI is less precise in the identification of tissue damage and that it detects changes, other than structural, in the normal appearing hippocampus.

Third, in the amygdala, T2-relaxometry detected nearly 50% more pathological cases than volumetry and had less contralateral detections. Moreover, there was a complete concordance between cases with isolated amygdala damage: the 4 patients with amygdala atrophy were detected by T2-relaxometry, which, additionally, detected other 3 patients with pathology. Although significantly associated with the postoperative results, none of the amygdala measures contributed decisively to the predictive models that were generated regarding outcome.

Fourth, for diagnostic purposes the co-occurrence of amygdalo-hippocampal pathology

was best assessed by the number of common cases identified by T2-relaxometry measures, which had also the highest level of correlation.

1. Lateralizing ability and technical considerations

Electroencephalography and qMRI data are independent sets of variables used to characterize different abnormalities from the area where seizures originate. Thus, concordance of the results provided by these analyses further validates the diagnostic conclusions derived from the individual studies. However, it must be realized that it is possible to encounter incongruent data between video-EEG and the newer imaging techniques and in different circumstances either one may be more indicative of the true epileptic focus.

Our first analysis revealed that the use of multiple qMRI modalities to study the hippocampus and the amygdala in patients evaluated for mesio-temporal surgeries offers advantages over individual modalities. The combined lateralizing ability of all five studies was 85% for the quantification of pathology in agreement with the EEG. However, complete concordance between all the hippocampal qMRI studies and the EEG was seen in 39% (36/92) and between both the amygdala qMRI studies and the EEG was verified in 15% (14/92). This indicates that some imaging sequences provide less than optimal sensitivity for MTS, either because they do not entirely associate with structural damage [e.g. hippocampal spectroscopy (Kuzniecky, et al. 2001)] or due to its intrinsic variation and heterogeneity of measures despite using an optimal protocol [e.g. volumetry of the amygdala (Brierley, et al., 2002)].

Our suggestion is that not all qMRI modalities are useful in the diagnosis of MTS and, thus, may increase the cost-effectiveness of the study.

Among all the qMRI modalities tested with this protocol, volume calculations using a manual segmentation method are the most time-consuming and are more prone to bias from the observer. In our hands, the total time for an amygdalo-hippocampal study with normalized volumes surpasses 1 hour (although it can be slightly shortened if the 3D set is acquired only over the temporal lobes). In this respect, multi-voxel spectroscopy studies are less demanding. Nevertheless, in our population HCSI revealed major flaws. It was the modality that detected less number of pathological cases and showed less lateralizing ability, and the single modality not associated with the surgical results. Additionally, 2D spectroscopic analyses are restricted to the hippocampus, since amygdala analyses are difficult to implement.

Our findings that a large number of cases (47%) present a symmetric NAA/(Cho+Cre) ratio are not uncommon (Connelly, et al., 1994). Thompson et al (1998b) found that only 42% of the TLE patients where effectively lateralized by the index of asymmetry of NAA/(Cho+Cre). Ende et al (1997) described a surgical series of TLE patients in which 50%, although revealed

decreased NAA and NAA/(Cho+Cre) levels in all ipsilateral temporal lobes had concomitant small metabolites values in the contralateral temporal lobe. Moreover, the patients who underwent surgery and had either a bilaterally small NAA value or normal NAA/(Cho+Cre) ratio (that is, an asymmetry index in range with control values) continued to have seizures. A similar trend has been observed by others (Duc, et al., 1998; Kantarci, et al., 2002), which emphasizes the value of MR spectroscopy in the prediction of surgical outcome. Our data indicates that spectroscopy cannot be used has a valid predictive measure for surgery success or has an adjuvant for localization. As such, further studies are needed to clarify the role of MR spectroscopy.

T2-relaxometry offers the advantage of studying both mesio-temporal structures with a single quantitative examination, which can be concluded with the present protocol in 25-30 minutes. The most relevant limitation of the T2-relaxometry analysis in our population was that it left undetected 14% of cases with an atrophic hippocampus and failed in the correct classification of one pos-surgical case. However, a detailed analysis of these cases revealed that, although pathological, the degree of atrophy was smaller (range of A.I.: 17.9 – 38.1 ; mean , 1SD = 22.6 , 9.6) when compared with the range of asymmetry for the overall patients (range up to 78.7 ; mean , 1SD = 32.1 , 19.3). Data from different laboratories (Van Paesschen, et al., 1995; Kuzniecky, et al., 1997) reported normal HCT2 maps in patients with what was considered a milder form of HS. These patients had a characteristic end-folium sclerosis, a similar trend with respect to our neuropathological data. Therefore, it is possible that HCT2 is less sensitive to milder forms of tissue damage than HCVOL. Moreover, mild forms of mesial temporal pathology may underlie surgically remediable epilepsy and not have any abnormality on MRI.

Accordingly, other studies (Woermann, et al., 1998; Bernasconi, et al., 2000) reported a higher incidence of asymmetrically bilateral HCT2, which can be due to the inclusion of hippocampal segments where T2 values can be altered by the presence of artifacts (mainly LCR), and where hippocampal borders are ill defined. Studies that included only the hippocampal body reported lower incidence of T2 bilateral abnormalities (Kuzniecky, et al., 1997). We observed these features in a sub-population (n=46) of the patients included in this study (Gonçalves Pereira, et al., 2002), where T2 values obtained at the level of the hippocampal tail and head provided more bilateral values than the ones obtained at the hippocampal body. In agreement with these results are our findings in the amygdala, where AMYT2 showed superior lateralizing ability than volumetry.

2. Relevance of amygdala studies

Intracerebral recordings from TLE patients (Kennedy and Hill, 1958; Wieser, 1991;

Maldonado, et al., 1998), usually implicate more than one mesio-temporal region on seizure onset, being the hippocampus and the amygdala commonly involved on both the onset and propagation of epileptiform activity. Amygdala sclerosis occurs mostly associated with HS, with up to 60% of the cases showing a histologically combined lesion (Cavanagh and Meyer, 1956; Bruton, 1988).

Our qMRI analysis demonstrated that T2-relaxometry performed better than volumetry in the identification of amygdala damage and showed higher level of association with the hippocampal lesion than volumetric studies. Although volumetric studies of the hippocampus bear a considerable bias among laboratories (Hasboun, et al., 1996), volume analyses of the amygdalae show highly significant variations (Brierley, et al., 2002). Moreover, amygdala sclerosis occurs in a nuclei-specific form within the complex (rather than with a layer-specific distribution within the hippocampus), being the lateral nucleus most often involved than basal or granular nuclei (Pitkänen, et al., 1998; Yilmazer-Hanke, et al., 2000). Other studies also reported increased astrocytosis in the amygdala of epileptic patients (Hudson, et al., 1993), which may underlie the polonged T2 times observed by qMRI. A detailed examination of the amygdala sub-regional pathology reported recently by Yilmazer-Hanke et al (2000) reveals that in the lateral nucleus, 45% of the specimens present severe pathology with neuronal loss and fibrillary astrogliosis (grade 4) while the remaining 55% show either moderate neuronal loss with mixed fibrillary and cellular astrogliosis (grade 3) or cellular astrogliosis without significant cell loss (grade 2). In the basal and granular nuclei, 23% showed a grade 4, 63% a grade 3-2 and 14% were normal specimens. Thus, there is a predominance of astrogliosis over neuronal cell loss, which may also explain why T2-relaxometry provides a larger detection of pathology than volumetry.

3. A comprehensive qMRI protocol for pre-surgical screening

Quantitative imaging has been recommended to be part of the whole pre-surgical evaluation of TLE patients (Sakamoto, et al., 2001). One main objective of this study was to categorize the role of three modalities of qMRI used commonly in clinical practice and define a simple step-by-step imaging protocol to be implemented on a diary routine. It must be noted that we are proposing such protocol as a complementary tool to qualitative high-resolution MRI imaging, and performed on experienced centers.

This qMRI protocol (**Figure 4**) was based on the necessity to study *both* the hippocampus and the amygdala on a time-efficient manner. As such, T2-relaxometry provided the adequate balance between scanning and processing times, on one hand, and the ability to uncover hippocampo-amygdala pathology, which agrees with the EEG and post-surgical data, on

the other. However, hippocampal volumetry must be performed on selected patients to obtain maximal predictive accuracy with respect to surgical outcome.

CONCLUSION

Previous work has indicated that approximately 20% of patients with TLE remain MRI negative after extensive qualitative imaging investigations. Such patients could benefit of additional quantitative MRI studies to study both the hippocampus and the amygadala.

For diagnostic purposes, of the three qMRI modalities tested, hippocampal T2-relaxometry provided an adequate balance between diagnosis accuracy and time-efficiency to lateralize a sclerotic lesion on the majority of the patients. Cases that are negative under this first analysis may benefit from further studies with hippocampal volumetry and amygdala T2s.

For pre-operative analysis and to maximally predict seizure freedom, hippocampal volumetry should be performed in all the patients.

Spectroscopy has limited utility to depict the structural abnormalities of the sclerotic hippocampus and in the pre-surgical evaluation of TLE patients.

REFERENCES

Antel, S. B., Li, L. M., et al., 2002. Predicting surgical outcome in temporal lobe epilepsy patients using MRI and MRSI. Neurology 58 (10), 1505-1512.

Babb, T. L., 1992. Research on the anatomy and pathology of epileptic tissue. In: Luders, H. O. (Ed) Epilepsy Surgery. Raven Press, New York, pp 719–727.

Bernasconi, A., Bernasconi, N., et al., 2000. T2 relaxometry can lateralize mesial temporal lobe epilepsy in patients with normal MRI. Neuroimage 12 (6), 739-746.

Bernasconi, A., Tasch, E., et al., 2002. Proton magnetic resonance spectroscopic imaging suggests progressive neuronal damage in human temporal lobe epilepsy. Prog Brain Res 135, 297-304.

Bernasconi, N., Bernasconi, A., et al., 1999. Entorhinal cortex in temporal lobe epilepsy. A quantitative MRI study. Neurology 52 (9), 1870-1876.

Bland, J. M. and Altman, D. G., 1986. Statistical methods for assessing agreement between two methods of clinical measurement. Lancet 1 (8476), 307-310.

Brierley, B., Shaw, P., et al., 2002. The human amygdala: a systematic review and meta-analysis of volumetric magnetic resonance imaging. Brain Res Rev 39 (1), 84-105.

Bruton, C. J., 1988. The Neuropathology of Temporal Lobe Epilepsy. Oxford University Press, Oxford, 158 p.

Capizzano, A. Vermathen, A. P., et al., 2002. Multisection Proton MR Spectroscopy for Mesial Temporal Lobe Epilepsy. AJNR Am J Neuroradiol 23 (8), 1359-1368.

Cascino, G. D., Jack, C. R., et al., 1991. Magnetic resonance imaging-based volume studies in temporal lobe epilepsy: pathological correlations. Ann Neurol 30 (1), 31-36.

Cascino, G. D., Trenerry, M. R., et al., 1995. Depth electrode studies in temporal lobe epilepsy: relation to quantitative magnetic resonance imaging and operative outcome. Epilepsia 36 (3), 230-235.

Cavanagh, J. B. and Meyer A., 1956. Aetiological aspects of Ammon's horn sclerosis associated with temporal lobe epilepsy. Br Med J 44 (5006), 1403-7.

Cendes, F., Andermann, F., et al., 1993. MRI volumetric measurement of amygdala and hippocampus in temporal lobe epilepsy. Neurology 43 (4), 719-725.

Cendes, F., Andermann, F. et al., 1994. Relationship between atrophy of the amygdala and ictal fear in temporal lobe epilepsy. Brain 117 (Pt 4), 739-746.

Cendes, F., Caramanos, Z., et al., 1997. Proton magnetic resonance spectroscopic imaging and magnetic resonance imaging volumetry in the lateralization of temporal lobe epilepsy: a series of 100 patients. Ann Neurol 42 (5), 737-746.

Cendes, F., Li, L. M., et al., 2000. Is ictal recording mandatory in temporal lobe epilepsy? Not when the interictal electroencephalogram and hippocampal atrophy coincide. Arch Neurol 57 (4), 497-500.

Connelly, A., Jackson, G. D., et al., 1994. Magnetic resonance spectroscopy in temporal lobe epilepsy. Neurology 44 (8), 1411-1417.

Connelly, A., Van Paesschen, W., et al., 1998. Proton magnetic resonance spectroscopy in MRI-negative temporal lobe epilepsy. Neurology 51 (1), 61-66.

Cook, M. J., Fish, D. R., et al., 1992. Hippocampal volumetric and morphometric studies in frontal and temporal lobe epilepsy. Brain 115 (Pt 4), 1001-1015.

Duc, C. O., Trabesinger, A. H., et al., 1998. Quantitative 1H MRS in the evaluation of mesial temporal lobe epilepsy in vivo. Magn Reson Imaging 16 (8), 969-979.

Duzel, E., Kaufmann, J., et al., 2004. Measures of hippocampal volumes, diffusion and 1H MRS metabolic abnormalities in temporal lobe epilepsy provide partially complementary information. Eur J Neurol 11 (3), 195-205.

Ende, G. R., Laxer, K. D., et al., 1997. Temporal lobe epilepsy: bilateral hippocampal metabolite changes revealed at proton MR spectroscopic imaging. Radiology 202 (3), 809-817.

Engel, J., Jr., Van Ness, P. C., et al., 1993. Outcome with respect to epileptic seizures. In: Engel, J., Jr. (Ed) Surgical Treatment of the Epilepsies. Raven Press Ltd, New York, pp. 609-621.

Folstein, M. F., Folstein, S. E., et al., 1975. Mini-mental state. A practical method for grading the cognitive state of patients for the clinician. J Psychiatr Res 12 (3), 189-198.

Gonçalves Pereira, P. M., Forjaz Secca, M., et al., 2002. Anteroposterior T2 relaxometry analysis of the hippocampus in temporal lobe epilepsy. In: Proceedings of the 10th Scientific Meeting and Exhibition of the International Society of Magnetic Resonance in Medicine (ISMRM). Honolulu, USA, p. 201.

Gonçalves Pereira, P. M., Oliveira, E., et al., 2005. Assessment of the preferred scout sagittal orientation for temporal lobe imaging with magnetic resonance. MAGMA Magnetic Resonance Materials in Physics, Biology and Medicine 18 (1), 19-25.

Gonçalves Pereira, P. M., Oliveira, E., et al., 2006. ADC mapping of the hippocampus and the amygdala in pharmacoresistant temporal lobe epilepsy. AJNR Am J Neuroradiol (*in press*).

Gundersen, H. J. and Jensen, E. B., 1987. The efficiency of systematic sampling in stereology and its prediction. J Microsc 147 (Pt 3), 229-263.

Hasboun, D., Chantome, M., et al., 1996. MR determination of hippocampal volume: comparison of three methods. AJNR Am J Neuroradiol 17 (6), 1091-1098.

Hotelling, H., 1936. Relations between two sets of variates. Biometrika 28, 321-377.

Hudson, L. P., Munoz, D. G., et al., 1993. Amygdaloid sclerosis in temporal lobe epilepsy. Ann Neurol 33 (6), 622-631.

Humphrey, T., 1967. The development of the human hippocampal fissure. J Anat 101 (4), 655-676.

ILAE Commission on Classification and Terminology, 1989. Proposal for revised classification of epilepsies and epileptic syndromes. Epilepsia 30 (4), 389-399.

ILAE Commision on Neurosurgery of Epilepsy Report (Compiled by Wieser HG), 2004. Mesial Temporal Lobe Epilepsy with Hippocampal Sclerosis. Epilepsia 45 (6), 695-714.

Jack, C. R., Sharbrough, F. W., et al. 1992. Magnetic resonance image-based hippocampal volumetry: correlation with outcome after temporal lobectomy. Ann Neurol 31 (2), 138-146.

Jackson, G. D., Connelly, A., et al. 1993. Detection of hippocampal pathology in intractable partial epilepsy: increased sensitivity with quantitative magnetic resonance T2 relaxometry. Neurology 43 (9), 1793-1799.

Jackson, G. D., Kuzniecky, R. I., et al., 1994. Hippocampal sclerosis without detectable hippocampal atrophy. Neurology 44 (1), 42-46.

Jasper, H., 1958. Report on the committee on methods of clinical electroencephalography. Electroencephalogr Clin Neurophysiol 10, 370-375.

Jutila, L., Immonen, A., et al., 2002. Long term outcome of temporal lobe epilepsy surgery: analyses of 140 consecutive patients. J Neurol Neurosurg Psychiatry 5 (73), 486-494.

Kälviäinen, R., Salmenperä, T., et al., 1997. MRI volumetry and T2 relaxometry of the amygdala in newly diagnosed and chronic temporal lobe epilepsy. Epilepsy Res 28 (1), 39-50.

Kantarci, K., Shin, C., et al., 2002. Comparative diagnostic utility of ^{1}H MRS and DWI in evaluation of temporal lobe epilepsy. Neurology 58 (12), 1745-1753.

Kennedy, W. A. and Hill, D., 1958. The surgical prognostic significance of the electroencephalographic prediction of Ammon's horn sclerosis in epileptics. J Neurochem 21 (1), 24-30.

Kolmogorov, A. N., 1933. Sulla determinazione empirica di una legge di distribuzione. Giorn dell' Inst Ital degli Att 4, 83-91.

Kuzniecky, R., Hugg, J., et al., 1999. Predictive value of ^{1}H MRSI for outcome in temporal lobectomy. Neurology 53 (4), 694-698.

Kuzniecky, R., Hugg, J. W., et al., 1998. Relative utility of ^{1}H spectroscopic imaging and hippocampal volumetry in the lateralization of mesial temporal lobe epilepsy. Neurology 51 (1), 66-71.

Kuzniecky, R., Palmer, C., et al., 2001. Magnetic resonance spectroscopic imaging in temporal lobe epilepsy: neuronal dysfunction or cell loss? Arch Neurol 58 (12), 2048-2053.

Kuzniecky, R. I., Bilir, E., et al., 1997. Multimodality MRI in mesial temporal sclerosis: relative sensitivity and specificity. Neurology 49 (3), 774-778.

Lantos, P. L., Greenfield, J. G., et al., 2002. Greenfield's Neuropathology. Arnold, London. 2 vol. (p. 1190, p. 1140).

Lee, D. H., Gao, F. Q., et al., 1998. MR in temporal lobe epilepsy: analysis with pathologic confirmation. AJNR Am J Neuroradiol 19 (1), 19-27.

Lencz, T., McCarthy, G., et al., 1992. Quantitative magnetic resonance imaging in temporal lobe epilepsy: relationship to neuropathology and neuropsychological function. Ann Neurol 31 (6), 629-637.

Lilliefors, H. W., 1967. On the Kolmogorov-Smirnov test for normality with mean and variance unknown. J Am Statistical Association 62, 399-402.

Maldonado, H. M., Delgado-Escueta, A. V., et al., 1998. Complex partial seizures of hippocampal and amygdalar origin. Epilepsia 29 (4), 420-433.

Margerison, J. H. and Corsellis, J. A. N., 1966. Epilepsy and the temporal lobes. A clinical, electroencephalographic and neuropathological study of the brain in epilepsy, with particular reference to the temporal lobes. Brain 89 (3), 499-530.

Miller, L. A., McLachlan, R. S., et al., 1994. Amygdalar sclerosis: preoperative indicators and outcome after temporal lobectomy. J Neurol Neurosurg Psychiatry 57 (9), 1099-1105.

Ng, T. C., Comair, Y. G., et al., 2000. Proton magnetic resonance spectroscopic imaging for the evaluation of temporal and extratemporal lobe epilepsy. In: Lüders, H. O. and Noachtar, S. (Eds) Epileptic Seizures: Pathophysiology and Clinical Semiology. Livingstone, Philadelphia, pp. 796.

Park, S. W., Chang, K. H., et al., 2001. Lateralizing ability of single-voxel proton MR spectroscopy in hippocampal sclerosis: comparison with MR imaging and positron emission tomography. AJNR Am J Neuroradiol 22 (4), 625-631.

Pires, J., Cavaleiro Miranda, P., et al., 1998. T2 relaxometry of the hippocampus in temporal lobe epilepsy: normal and pathological values. In: Proceedings of the 6th Scientific Meeting and Exhibition of the International Society of Magnetic Resonance in Medicine (ISMRM). Sidney, Australia, p. 1390.

Pitkänen, A., Tuunanen, J., et al., 1998. Amygdala damage in experimental and human temporal lobe epilepsy. Epilepsy Res 32 (1-2), 233-253.

Roberts, N., Puddephat, M. J., et al., 2000. The benefit of stereology for quantitative radiology. Br J Radiol 73 (871), 679-97.

Sakamoto, A. C., Benbadis, S. R., et al., 2001. Essentials for the establishment of an epilepsy surgery program (Appendice B). In: Lüders, H. O. and Comair, Y. Epilepsy Surgery. Lippincott Williams & Wilkins, Philadelphia, pp. 979-986.

Sasaki, M., Miyuki, S., et al., 1993. Hippocampal sulcus remnant: potential cause of change in signal intensity in the hippocampus. Radiology 188 (3), 743-6.

Soininen, H. S., Partanen, K., et al., 1994. Volumetric MRI analysis of the amygdala and the hippocampus in subjects with age-associated memory impairment: correlation to visual and verbal memory. Neurology 44 (9), 1660-1668.

Swartz, B. E., Tomiyasu, U., et al., 1992. Neuroimaging in temporal lobe epilepsy: test sensitivity and relationships to pathology and postoperative outcome. Epilepsia 33 (4), 624-634.

Tamraz, J. C. and Comair Y. G., 2000. Limbic lobe and mesial temporal region. In: Tamraz, J. C. and Comair Y. G. (Eds) Atlas of Regional Anatomy of the Brain using MRI – with Functional Correlations. Springer-Verlag, Berlin, pp. 161-184.

Thompson, J. E., Castillo, M., et al., 1998a. MR spectroscopy in the evaluation of epilepsy. Magn Reson Imaging Clin N Am 6 (1), 21-29.

Thompson, J. E., Castillo, M., et al. 1998b. Usefulness of proton MR spectroscopy in the evaluation of temporal lobe epilepsy. AJR Am J Roentgenol 170 (3), 771-776.

Van Paesschen, W., Sisodiya, S., et al., 1995. Quantitative hippocampal MRI and intractable temporal lobe epilepsy. Neurology 45 (12), 2233-2240.

von Oertzen, J., Urbach, H., et al., 2002. Time-efficient T2 relaxometry of the entire hippocampus is feasible in temporal lobe epilepsy. Neurology 58 (2), 257-264.

Watson, C., Andermann, F., et al., 1992. Anatomic basis of amygdaloid and hippocampal volume measurement by magnetic resonance imaging. Neurology 42 (9), 1743-1750.

Wiebe, S., Blume, W. T., et al., 2001. A randomized, controlled trial of surgery for temporal-lobe epilepsy. N Engl J Med 345 (5), 311-318.

Wieser, H. G., 1991. "Selective amygdalohippocampectomy: indications and follow-up." Can J Neurol Sci 18 (4 Suppl), 617-627.

Woermann, F. G., Barker, G. J., et al., 1998. Regional changes in hippocampal T2 relaxation and volume: a quantitative magnetic resonance imaging study of hippocampal sclerosis. J Neurol Neurosurg Psychiatry 65 (5), 656-664.

Woermann, F. G., McLean, M. A., et al., 1999. Short echo time single-voxel ^{1}H magnetic resonance spectroscopy in magnetic resonance imaging-negative temporal lobe epilepsy: different biochemical profile compared with hippocampal sclerosis. Ann Neurol 45 (3): 369-76.

Yasargil, M. G., Teddy, P. J., et al., 1985. Selective amygdalo-hippocampectomy. Operative anatomy and surgical technique. Adv Tech Stand Neurosurg 12, 93-123.

Yilmazer-Hanke, D. M., Wolf, H. K., et al., 2000. Subregional pathology of the amygdala complex and entorhinal region in surgical specimens from patients with pharmacoresistant temporal lobe epilepsy. J Neuropathol Exp Neurol 59 (10), 907-920.

LEGENDS TO FIGURES

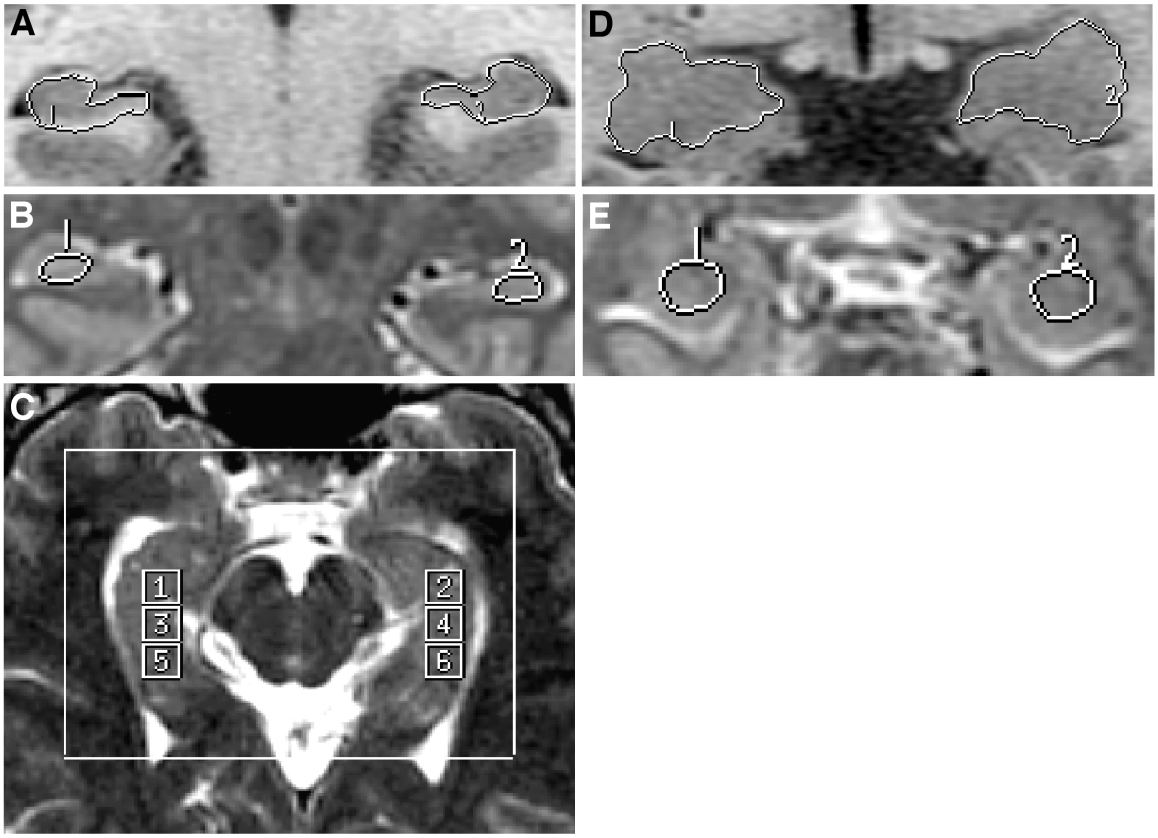


Figure 1. Multimodal quantitative MRI as performed in a control subject. *A*, *B* and *C* – Hippocampus. *D* and *E* – Amygdala. Coronal T1-weighted MR images demonstrate the outlining of the cross-sectional areas of the hippocampus (*A*) and amygdala (*D)* as performed on the workstation (*1* marks the first ROI to be drawn, in the structure of the right side). Highlights of coronal T2-weighted relaxometry images, demonstrate the positioning of the ROIs over the hippocampal body (*B*) and amygdala (*E*), for direct calculation of the relaxometry values. Axial T2-weighted localizer image for multi-voxel spectroscopy (*C*), demonstrate the positioning of the volumes of interest over the hippocampus. Individual NAA, Cho and Cre values are obtained for each voxel (see text for other details).

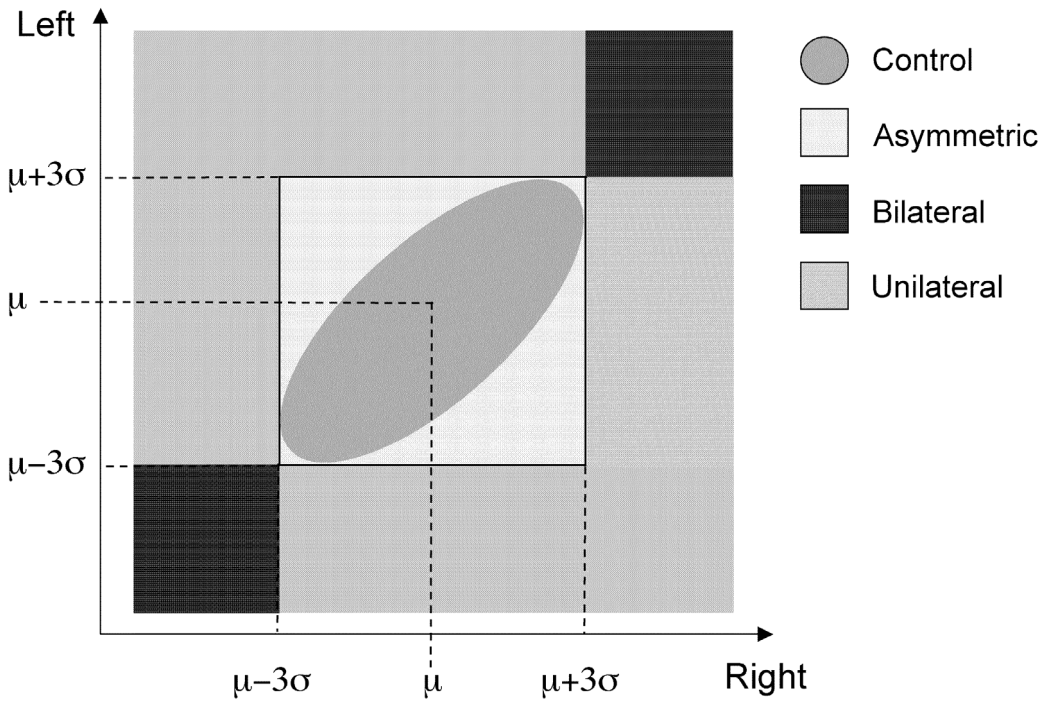


Figure 2. A representation of the general confidence ellipse for quantitative MRI calculated with 99% confidence over normal control values. With a simple graphic illustration, every case localized outside the ellipse is immediately categorized as "Asymmetrical", "Unilateral" or "Bilateral". Such method can be used to plot every data obtained from paired structures with a normal distribution within the brain. Abbreviations: μ – mean value, σ – standard deviation, $\mu \pm 3\sigma$ – mean ± 3 standard deviations.

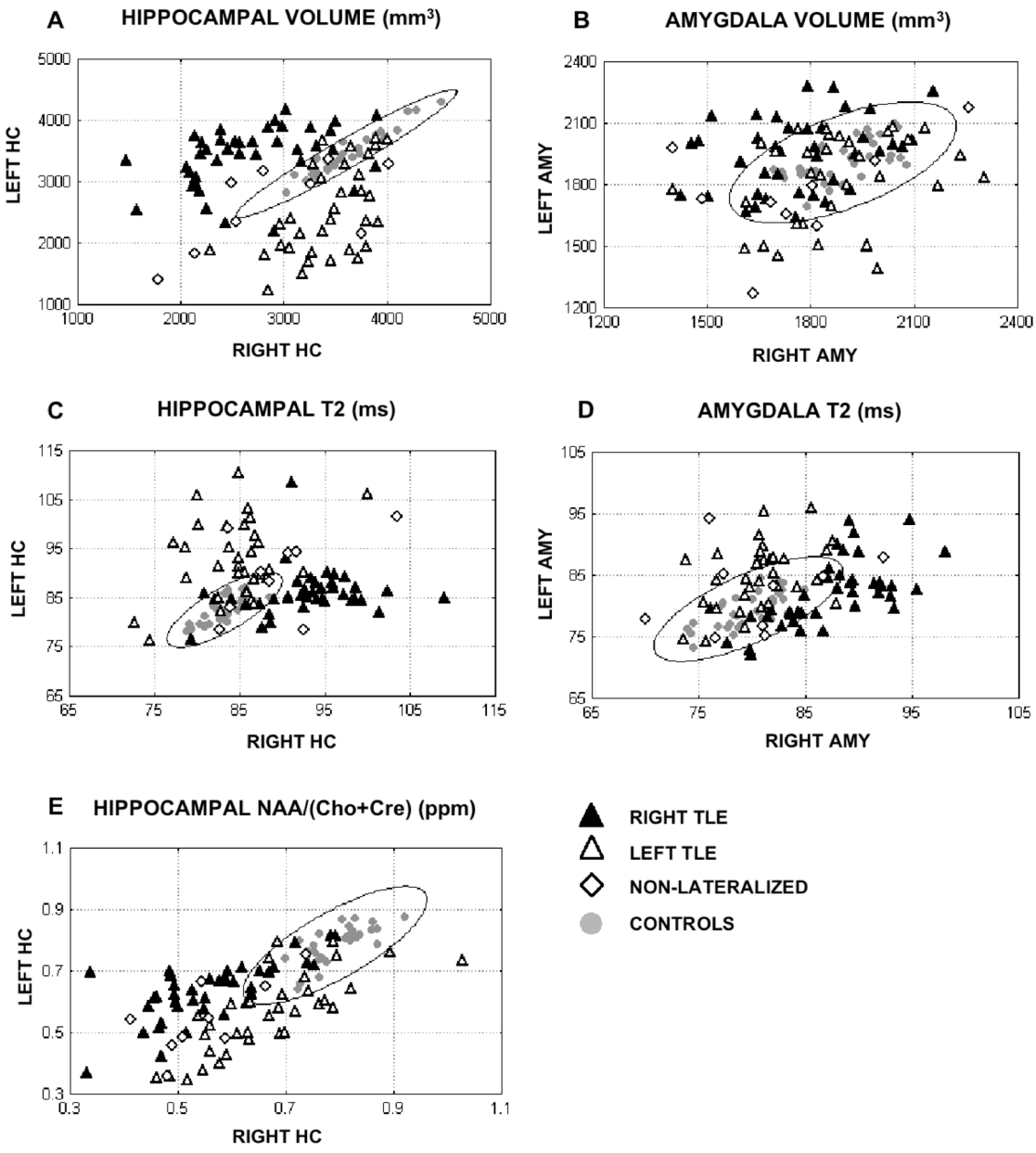


Figure 3. 99% confidence elipses for HCVOL (*A*), AMYVOL (*B*), HCT2 (*C*), AMYT2 (*D*) and HCSI (*E*).

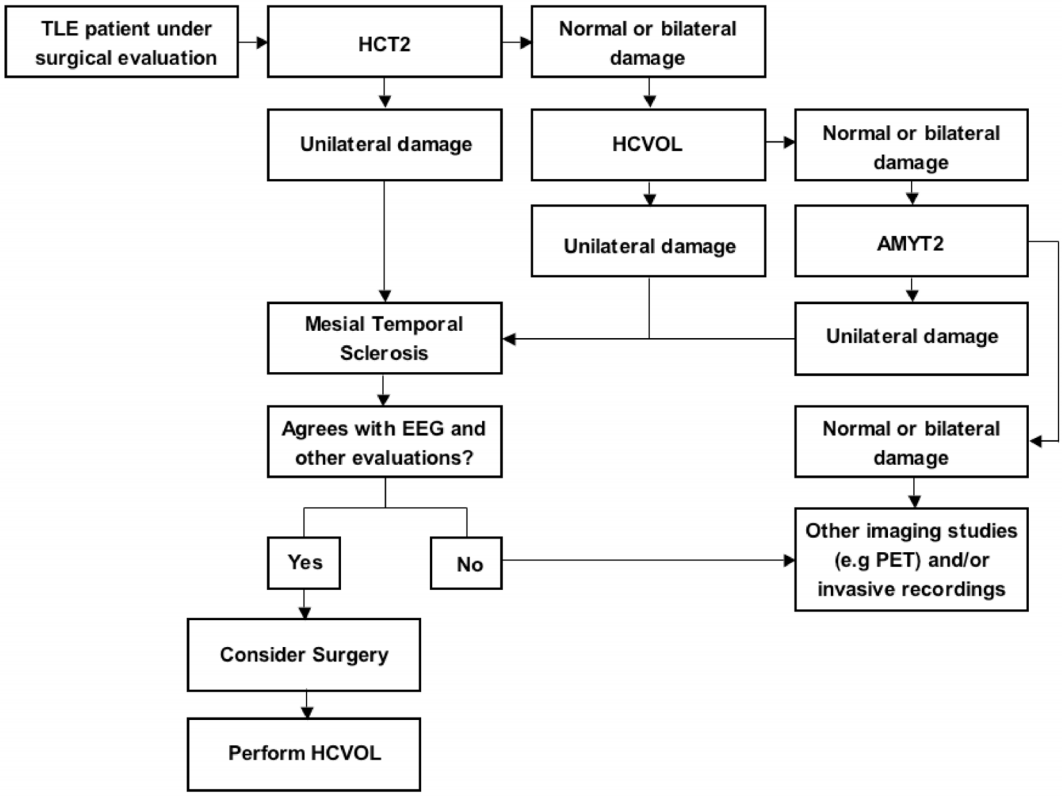


Figure 4. Proposed qMRI protocol for pre-surgical evaluation privileges T2-relaxometry as the single diagnostic method to study hippocampo-amygdala pathology, reserving hippocampal volumetry for a secondary analysis due to the excessive processing time. Whenever a surgical decision is reached, hippocampal volumetry can be performed since it guarantees a higher predictive value than T2-relaxometry. Hippocampal multi-voxel spectroscopy and amygdala volumetry are exluded. *HCT2*, hippocampal T2-relaxometry; *HCVOL*, hippocampal volumetry; AMYT2, amygdala T2-relaxometry; *PET*, positron emission tomograpphy.

Table 1. Brief description of the quantitative MRI protocol performed on a 1.5T. scanner, with scanning and processing times.

qMRI method	Summary of technical description	Scanning time	Processing time
Volumetry	T1 3D SPGR with continuous 1.5mm slices (coronal)	12 min. #	50-55 min.
T2-relaxometry	Four-echoes with interleaved 4mm slices (coronal)	15 min.	10-12 min.
Multi-voxel spectroscopy	2D chemical-shift with PRESS and TE=144ms (axial)	10 min.	5-8 min.

See text for details. Processing time includes the quantification of hippocampal and amygdala volumes and T2-relaxometry. Multi-voxel spectroscopy was performed only in the hippocampus. PRESS - point-resolved spectroscopy. Time in minutes.

Acquisition time for SPGR can be shortened to 6 min. if the 3D set is restricted to the temporal lobes.

Table 2. Descriptive statistics for quantitative hippocampal MRI data (HCVOL, HCT2 and HCSI).

Hippocampus	Controls (n = 34)	Right TLE (n = 45)	Left TLE (n = 39)	Non-Lateralized (n = 8)
Volume				
Right hippocampus	3604±353 (3023-4516)*	2640±586 (1471-3901)**‡	3404±391 (2285-4007)	2926±803 (1778-4010)^
Leftt hippocampus	3463±344 (2824-4310)	3387±456 (2192-4180)	2445±699 (1235-3716)**‡	2544±715 (1411-3290)‡
A.I.	4.3±2.1 (0.8-7.5)	29.3±16.3 (1.4-77.8)‡	35.9±21.8 (0.2-78.7)‡	18.7±15.8 (2.2-53.9)^
T2				
Right hippocampus	83.2±2.2 (79.0-88.4)	92.8±5.6 (79.4-109)**‡	84.8±4.7 (72.6-100)	88.9±6.7 (82.6-103.4)^
Leftt hippocampus	82.6±2.5 (78.1-87.0)	85.6±4.7 (76.4-108.6)‡	93±7.4 (76.3-110.3)**‡	91.2±7.8 (78.5-101.5)^
A.I.	1.8±1.1 (0.2-3.3)	9.4±5.1 (0.9-24.9)‡	9.5±7.4 (0.3-27.7)‡	4.3±5.4 (0.2-17.1)
NAA/(Cho+Cre)				
Right hippocampus	0.79±0.06 (0.66-0.92)	0.56±0.11 (0.33-0.79)**‡	0.65±0.13 (0.46-1.03)‡	0.57±0.09 (0.48-0.73)‡
Leftt hippocampus	0.78±0.06 (0.64-0.88)	0.64±0.09 (0.37-0.82)‡	0.54±0.13 (0.34-0.80)**‡	0.55±0.13 (0.36-0.75)‡
A.I.	4.1±3.5 (0.1-11.9)	16.2±14.6 (1.5-69.4)‡	19.8±11.5 (0.9-40.3)‡	10.9±10.6 (2.1-29.3)

All values are expressed as mean ± 1 standard deviation (range). *A.I.*, asymmetry indexes. Volume in mm^3; T2 in ms; NAA/(Cho+Cre) in ppm.

* significantly different from the contralateral side at α level of 0.05

** significantly different from the contralateral side at α level of 0.01

^ significantly different from the correspondent control side at α level of 0.05

‡ significantly different from the correspondent control side at α level of 0.01

Table 3. Descriptive statistics for quantitative amygdala MRI data (AMYVOL and AMYT2).

Amygdala	Controls (n = 34)	Right TLE (n = 45)	Left TLE (n = 39)	Non-Lateralized (n = 8)
Volume				
Right amygdala	1893±108 (1692-2076)	1779±207 (1422-2266)**‡	1872±182 (1400-2236)	1694±189 (1400-1989)^
Leftt amygdala	1909±097 (1698-2099)	1948±178 (1639-2277)	1805±225 (1389-2083)^	1708±217 (1271-1976)^
A.I.	4.2±2.6 (0.2-10.1)	11.4±8.9 (0.5-34.1)‡	11.9±8.4 (0.3-35.7)‡	12.2±12.1 (0.4-34.1)
T2				
Right amygdala	79.6±2.9 (73.8-84.9)	86.8±5.2 (76.1-98.1)**‡	80.5±3.5 (73.5-87.8)	80.3±6.9 (70.1-92.3)
Leftt amygdala	79.5±2.8 (73.2-84.5)	82.1±5.1 (72.1-93.9)	84.9±4.9 (74.2-96.1)**‡	83.1±6.4 (76.7-94.3)
A.I.	2.3±1.5 (0.6-5.5)	6.7±3.9 (0.5-15.8)‡	6.1±4.5 (0.2-17.1)‡	7.3±6.6 (1.5-21.4)

All values are expressed as mean ± 1 standard deviation (range). *A.I.*, asymmetry indexes. Volume in mm^3; T2 in ms.

* significantly different from the contralateral side at α level of 0.05

** significantly different from the contralateral side at α level of 0.01

^ significantly different from the correspondent control side at α level of 0.05

‡ significantly different from the correspondent control side at α level of 0.01

Table 4. Summary of data for quantitative hippocampal and amygdala MRI analysis.

Study	Group	Pathological A.I. (Ipsilateral – Contralateral cases)	Normal A.I. (Normal – Bilateral cases)
HCVOL	*Lateralized (n=84)*	82% (77%-5%)	18% (15%-3%)
	Non-lateralized (n=8)	38% #	62% (24%-38%)
HCT2	*Lateralized (n=84)*	69% (68%-1%)	31% (24%-7%)
	Non-lateralized (n=8)	12%	88% (50%-38%)
HCSI	*Lateralized (n=84)*	55% (53%-2%)	45% (27%-18%)
	Non-lateralized (n=8)	38%	62% (24% -38%)
AMYVOL	*Lateralized (n=84)*	37% (27%-10%)	63% (60%-3%*)
	Non-lateralized (n=8)	50%	50% (50%-0%)
AMYT2	*Lateralized (n=84)*	44% (43%-1%)	56% (49%-7%)
	Non-lateralized (n=8)	50%	50% (50%-0%)

All values are expressed in percentage for the respective group. *A.I.*, asymmetry indices.

the ipsilateral-contralateral distinction does not apply to the non-lateralized patients

* 2 patients with a bilateral large AMYVOL

Table 5. Post-surgical outcome and relation with quantitative hippocampal and amygdala MRI analysis for the 28 patients operated.

Study	Lateralization	Favourable Outcome (Engel I)	Unfavourable Outcome (Engel IB – III)	Positive Predictive Value
HCVOL ***	*Concordant*	20	1	0.95
	Discordant/Non-lateralized	1	6	
HCT2 ***	*Concordant*	20	1	0.95
	Discordant/Non-lateralized	1	6	
HCSI #	*Concordant*	14	2	0.88
	Discordant/Non-lateralized	7	5	
AMYVOL *	*Concordant*	15	1	0.93
	Discordant/Non-lateralized	6	6	
AMYT2 **	*Concordant*	16	1	0.94
	Discordant/Non-lateralized	5	6	

Fisher exact test regarding a concordant lateralization to the side of major qMRI and EEG abnormalities and surgery:

#	non-significant
*	$p < 0.05$
**	$p < 0.01$
***	$p < 0.0001$

EPILEPSY RESEARCH

An International Multidisciplinary Journal devoted to Experimental and Clinical Research in Epilepsy

Managing Editors

Prof. I.E. Leppik
Epilepsy Clinical Research Program
University of Minnesota
5775 Wayzata Blvd, Suite 255
Minneapolis, MN 55416 - 1227
USA
Fax: +1-952-525-1560
E-mail: kraus012@tc.umn.edu

Prof. W. Löscher
Dept. of Pharmacology,
Toxicology and Pharmacy,
School of Veterinary Medicine
Bünteweg 17
D-30559 Hannover
Germany
Fax: +49-511-953-8581
E-mail: Wolfgang.Loescher@tiho-hannover.de

Prof. R.L. Macdonald
Dept. of Neurology
Vanderbilt University
2100 Pierce Ave., 320 MCS
Nashville, TN 37212
USA
Fax: +1-615-936-0223
E-mail: Robert.Macdonald@mcmail.vanderbilt.edu

Prof. D. Schmidt
Epilepsy Research Group
Goethestrasse 5
D-14163 Berlin
Germany
Fax: +49-30-8017679
E-mail: dbschmidt@t-online.de

Pedro M. Goncales Pereira
Rua Gregorio Lopes 1524 - 3 Esq.
1400 Lisboa
Portugal

Berlin, October 17,2004

Dear Dr. Pereira,

thank you for sending your manuscript "Relative localizing value of amygdalo-hippocampal MR biometry in temporal lobe epilepsy" to Epilepsy Research. It has been reviewed by two experts, enclosed are their comments. Please revise your manuscript accordingly and send it back as soon as possible,. It will be reviewed again before final decision can be made. Thank you.

Sincerely yours

Prof.Dr.Dieter Schmidt

PUBLISHER: ELSEVIER SCIENCE B.V.
www.elsevier.com/locate/epilepsyres

VI – CONCLUSIONS

1.

Recurrent seizures are not the main determinant cause of cell loss in the hippocampus, para-hippocampus and in the piriform cortex in experimental Temporal Lobe Epilepsy. Tissue damage in these regions, mainly consisting of neuronal cell loss and glial overexpression, develops immediately after the initial insult (*status epilepticus*) during the latent period and it is already present when the first spontaneous seizures arise. No meaningful cell loss occurs afterwards.

2.

The spatio-temporal progression of cell death across the limbic temporal lobe has regional variations. Although it occurs in the hippocampus, para-hippocampal gyrus and piriform cortex during the latent period, its magnitude varies within this time frame. In the hilus of the hippocampus, neuronal loss is apparent early in the latent period (24 hours after *status epilepticus*) and remains without further evolution throughout the late phases of the latent period and in the chronic phase. In the para-hippocampus, cell loss progresses during the latent period and reaches a maximum in the late phase (that is 7-10 days after *status epilepticus*). Moreover, it affects specifically cell layers III (and II) of the entorhinal cortex. Similarly in the piriform cortex, cell loss is maximal at 7-10 days after *status epilepticus*, and implicates specifically layer II and the deep nuclei (endopiriform nuclei and claustrum).

3.

The extent of neuronal cell death observed in the chronic phase is not related to the frequency of spontaneous short-duration seizures. Rather, it is associated with the duration of the initial insult; a significant negative correlation was seen between the number of surviving neurons and the duration of *status epilepticus*. A shorter duration of *status epilepticus* is also associated with the later development of a nonprogressive form of epilepsy.

4.

In human patients with chronic TLE, the piriform-cortical amygdala ribbon is an area extensively damaged, showing a mean of 20% atrophy in nearly 50% of the patients (up to 30% in cases with hippocampal sclerosis) on the side of the EEG focus as compared to reference values.

5.

Detection of tissue atrophy in the piriform cortex is feasible in human subjects, non-invasively, by means of quantitative MRI and using current 1.5 T machines. Moreover it is reproducible, given that an adequate volumetric protocol based on anatomical landmarks is followed. Qualitative inspection of the piriform cortex morphometry in images with optimal resolution is ineffective in the detection of tissue damage.

6.

The piriform cortex damage is generally associated with the damage quantified in the hippocampus, amygdala, and entorhinal cortex, following a pattern observed experimentally. However, there is a specific association with hippocampal atrophy.

7.

In chronic TLE, there is no association between the piriform cortex damage and the duration of seizure frequency.

8.

The concept of mesial temporal sclerosis, originally formulated to include the human hippocampus, amygdala and entorhinal cortex should now be extended to include the piriform cortex.

9.

In order to obtain a gain in reproducibility, orthogonal MRI sequences of the temporal lobe (not only for quantitative studies) can be programmed according to the mid-sagittal posterior commissure-obex line.

10.

Diffusion-weighed imaging with ADC-mapping has a sensitivity of at least 82% and 35% in the detection of hippocampal and amygdala abnormalities, respectively, in accordance with the electroencephalographic and clinical manifestations. These figures are within the range of detection of other structural MRI modalities, to which it correlates, except for hippocampal spectroscopy.

11.

Interictal pre-surgical ADC-mapping predicts the surgical outcome of patients who undergo selective amygdalo-hippocampectomy for the relief of recurrent seizures that are pharmacoresistant. Major determinants of a successful outcome are the concordant lateralization of the hippocampal ADC increase ipsilateral to the side of major electroencephalographic abnormalities and a larger side-to-side difference in hippocampal ADCs.

12.

Amygdalo-hippocampal ADCs are insensitive to the subject's age and gender, at least up to the 5th decade. Hippocampal ADCs on the side of the seizure focus (along with hippocampal volumes and T2-relaxometry) associate moderately with the duration of epilepsy. The coexistent increase in ADC/T2 plus atrophy in the ipsilateral hippocampus correlates selectively with the time elapsed after the onset of seizures. Age of onset correlates only with the ipsilateral hippocampal ADCs.

13.

Amygdalo-hippocampal volumetry and T2-relaxometry, plus hippocampal spectroscopy provide redundant information about mesial temporal integrity. Although these techniques are distinct, their ability to detect amygdalo-hippocampal damage mostly overlaps.

14.

In the context of pre-surgical screening, the predictive values of hippocampal volumetry and of T2-relaxometry are similar. Both analyses are useful as diagnostic and prognostic tools. Hippocampal spectroscopy and amygdala studies are less precise in the prediction of post-operative outcome.

15.

Considering the time it takes to reach a diagnosis with these tools, we propose an optimized algorithm to be used in the pre-surgical evaluation of TLE patients where hippocampal T2-relaxometry is the reference modality.

VII – DISCUSSION

Symptomatic seizure disorders such as temporal lobe epilepsy are among the most prevalent and least medically responsive forms of epilepsy. With this Thesis we sought to determine the progression, severity and extent of mesial temporal sclerosis, and to refine the diagnostic and prognostic capabilities of state-of-the-art magnetic resonance imaging by selecting appropriate quantitative methods.

One of the conclusions of the experimental part of this Thesis is that neuronal loss does not depend primarily on the chronic occurrence of seizures, at least in the experimental model used by us, namely the *post-status epilepticus* temporal lobe epileptic rat model. This concept argues against the hypothesis that mesial temporal sclerosis is a progressive disorder that depends on the occurrence of seizures for its development. The latter theory is mostly based on human studies in which the morphological pattern of hippocampal sclerosis is analyzed when the disease is already fully developed, thus not allowing the assessment of how TLE develops at the early stages of the pathological process.

Nevertheless, we found in our chronic patients a moderate correlation between the years of symptomatic epilepsy and the coexistent increase of ADC/T2 values plus atrophy in the hippocampus ipsilateral to the seizure focus.

In addition several case-reports and longitudinal MRI studies [212, 228, 414, 415] indicate a progressive decrease of the hippocampal volume that might depend on the cumulative effect of brief recurrent seizures. This has been shown both in humans and in experimental models (pilocarpine) [175, 416].

However, although hippocampal volumes and T2 relaxation values correlate with the amount of neuronal cells and astrocytosis [17, 328] it must be realized that neither a reduction in volume reflects solely cell loss, nor an increased T2 value corresponds simply to gliosis. As we were able to demonstrate with ADC-mapping, micro-structural changes (such as shrinkage of neurons and surrounding cells) occur extensively in hippocampal sclerosis, modifying tissue architectonics and the balance between intra and extra-cellular water content. As MRI is sensitive to the protonic content of tissues, these changes are also reflected in the T1 signal morpho-intensity and in the T2 values.

Taking all these different observations, experimental, neuroradiological and clinical into account we may suggest that mesial temporal sclerosis may be induced by a previous brain insult (such as an episode of *status epilepticus*), or by some kind of (genetical and structural)

predisposition, although the imaging appearance might undergo progressive changes in the course of the evolution of the pathological process.

Another essential assumption of our work was to inquire whether the concept of mesial temporal sclerosis should be broaden to include the piriform cortex as one of the limbic cortices showing volume loss in human patients. In recent years there has been a growing body of experimental evidence implicating the piriform cortex in the generation and propagation of seizures. However, there were no means to demonstrate its involvement in human TLE due to the lack of clear anatomical determinants in order to identify its location in MR images. Moreover, its appearance on visual inspection may be equivocal. Based on an accurate anatomical protocol it was possible to detect atrophy in the human piriform cortex, the magnitude of which was associated with that of the hippocampus. These results support the unifying theory of an epileptogenic circuit distributed throughout the limbic system with the possibility to initiate seizures at any point within the network [116] whose core would be located in the mesial temporal lobe [19, 417].

One novel result of this study was to identify piriform-cortical amygdala atrophy in drug-refractory TLE patients. More interestingly, though, we were able to find a subset of patients without hippocampal sclerosis but marked piriform-cortical amygdala atrophy/asymmetry. These data suggest that a reduced volume, or an abnormal asymmetry index, can be a useful addition to the tools currently used to determine the side of the seizure focus, particularly if the hippocampus is identified as apparently normal. In addition we were unable to confirm our data histologically and to establish a clear-cut regional boundary for the region displaying loss of volume. Indeed, to date there exists no gold standard combining MR imaging and histologic analysis of the same TLE cases. Future post-surgical or autopsy-based studies[3] are needed to substantiate our data and to definitively establish the role that the human piriform cortex and cortical amygdala have as critical areas in epileptogenesis.

The third relevant contribution of this study was to demonstrate the clinical utility of diffusion-weighted imaging, both as diagnostic and prognostic tool, in the characterization of amygdalo-hippocampal abnormalities. Previous investigations suggested that ADC-mapping reveals the impairment of water difusibility associated to mesial temporal sclerosis. However, there has been no attempt to establish its prognostic utility in the context of pre-surgical screening. This study is

[3] By the time this Thesis was being completed, we received the information of ongoing studies at the Montreal Neurological Institute and Hospital (Department of Cognitive Neurosciences), using our imaging protocol to assess the behavioural performance of TLE patients on odor tasks previous and in the aftermath of selective amygdalo-hippocampectomy (Joelle Crane and Brenda Milner´s personal communication).

important because (1) it is possible to extract rigorous information from ADC-mapping in a relatively short time (faster than any other qualitative or quantitative MR sequence available), (2) current MRI, despite its ability to produce images of high quality, is unable to document the full spectrum of structural changes associated with epilepsy, and (3) MRI lesions have an unpredictable spatial relationship to seizures, as seizures may originate within, adjacent to or remote from such lesions.

Diffusion-weighted imaging also stands in a class apart from the remaining quantitative imaging techniques. ADC maps are easily generated from routine fast diffusion-weighted imaging by use of software available on most MR systems. Therefore, diffusion values can be obtained without a great deal of effort. Most importantly, ADC may be a more direct indicator of changes in the brain than are other physical parameters, because in the majority of cases, these parameters evaluate submicroscopic, molecular-level phenomena. T1 and T2 reflect changes in the interactions between water protons, macromolecules and their hydration shells. The degree of diffusion is strongly affected by microscopic biological structures such as the number, type, and spatial arrangement of cells. These structures create barriers to the free diffusion of water. Therefore, changes in diffusion may more directly reflect changes occurring at the cellular level.

The original contribution of this study was to show the capability of hippocampal ADC to predict the postoperative results regarding seizure control. Accordingly, there were similar results with respect to the lateralizing ability of hippocampal ADC in agreement with the electroencephalographic data, volumetric data and T2 values. We further extended those observations to the amygdala, where 35% of the patients had ADC abnormalities compatible with tissue damage, the detection of which may be likely missed on current MRI studies. As such, we propose that diffusion-weighted imaging holds great promisse in the context of epilepsy surgery given its ability to identify the site and nature of a causative lesion on a time-efficient manner. Subsequent clinical studies are needed to validate these hypotheses and extend the ADC analysis to the remaining limbic regions.

Finally, we were able to demonstrate the usefulness of *multimodal quantitative imaging* in the pre-surgical screening of TLE patients by proposing an algorithm tailored to disclose both diagnostic and prognostic data. Given that MR sequences are programmed with a reproducible anatomical orientation, MR volumes and T2 relaxation measurements yield unbiased, objective information regarding the co-localization of amygdalo-hippocampal damage, while hippocampal multi-voxel spectroscopy is less precise. Moreover, we developed logistic regression models, which allow predicting outcome with 100% (volume) and 96.4% (T2-relaxometry) accuracy. Ultimately, this statistical modelling might be applied to study other patients analysed accordingly.

Due to some limitations of the study, we were unable to fully compare ADC-mapping with the remaining quantitative MR measures. Further work is required in order to test this algorithm and re-arrange it, in order to better define the promising role of ADC-mapping in a general context.

One major interest in pre-surgical evaluation is to provide sound insights into the outcome of surgery. Quantitative MR imaging is specially tailored to provide such insight, given its excellent objectivity and reproducibility.

VIII – FUTURE STUDIES

Taking into consideration the results presented in this Thesis we propose for future research the following:

1. To correlate histological and MR studies in animal models of temporal lobe epilepsy and to perform longitudinal studies in order to better understand the evolution of the human condition pointing to a progressive, seizure-dependent nature of mesial temporal sclerosis.

2. To validate the observations of the human piriform cortex by analysing histological post-surgical or autopsy-derived specimens in relation with MRI data. Further, to

3. To extend the quantitative MRI analyses (diffusion-weighted imaging in particular) to the para-hippocampus and remaining limbic cortices, while evaluating also the status of limbic interconnectivity by means of MR tractography with diffusion tensor imaging (DTI). DTI is a development of DWI, which allows better delineation of the magnitude of diffusion as well as identifying the principal direction of diffusion in any voxel.

4. To test the pre-surgical evaluation algorithm in additional and larger TLE populations in order to better validate its predictive modeling.

5. To improve the ability of multimodal quantitative imaging to provide predictive data of surgical outcome by using polynomial quadratic statistical models in order to overcome the limitations of linear regressional analysis.

6. To evaluate newly developed software (e.g. statistical parametric mapping) and additional imaging techniques (e.g. magnetization transfer and arterial spin labelling perfusion) for diagnostic and prognostic purposes. Continuous arterial spin labelling perfusion MRI is a non-invasive tool for investigation of cerebral blood flow and is a potentially useful tool for investigation of both interictal and ictal states.

IX – REFERENCES

1. Hauser, W.A., *Incidence and prevalence*, in *Epilepsy: A Comprehensive Textbook*, J. Engel and T.A. Pedley, Editors. 1997, Lippincott-Raven: Philadelphia. p. 47-57.
2. Hauser, W.A., *The natural history of temporal lobe epilepsy*, in *Epilepsy surgery*, L.H. A., Editor. 1992, Raven Press: New York. p. 133-141.
3. Sander, J.W., *The epidemiology of epilepsy revisited.* **Curr Opin Neurol**, 2003. 16 (2): p. 165-70.
4. Hauser, W.A. and D.C. Hesdorffer, *Epidemiology of intractable epilepsy*, in *Epilepsy Surgery*, H.O. Luders and Y.G. Comair, Editors. 2001, Lippincott Williams and Wilkins: Philadelphia. p. 55-61.
5. Wieser, H.G., et al., *Surgically remediable temporal lobe syndromes*, in *Surgical Treatment of the Epilepsies*, J. Engel, Editor. 1993, Raven Press: New York. p. 49-63.
6. Bruton, C.J., *The neuropathology of temporal lobe epilepsy*. Maudsley monographs, ed. 1988, Oxford: Oxford University Press. 158 p.
7. Margerison, J.H. and Corsellis, J.A.N., *Epilepsy and the temporal lobes. A clinical, electroencephalographic and neuropathological study of the brain in epilepsy, with particular reference to the temporal lobes.* **Brain**, 1966. 89 (3): p. 499-530.
8. Du, F., et al., *Preferential neuronal loss in layer III of the entorhinal cortex in patients with temporal lobe epilepsy.* **Epilepsy Res**, 1993. 16 (3): p. 223-233.
9. Yilmazer-Hanke, D.M., et al., *Subregional pathology of the amygdala complex and entorhinal region in surgical specimens from patients with pharmacoresistant temporal lobe epilepsy.* **J Neuropathol Exp Neurol**, 2000. 59 (10): p. 907-20.
10. Cavanagh, J.B. and Meyer, A., *Aetiological aspects of Ammon's horn sclerosis associated with temporal lobe epilepsy.* **Br Med J**, 1956. 44 (5006): p. 1403-7.
11. Falconer, M.A., Serafetinides, E.A. and Corsellis, J.A.N. *Etiology and pathogenesis of temporal lobe epilepsy.* **Arch Neurol**, 1964. 10: p. 233-248.
12. Mathern, G.W., et al., *Hippocampal neuron damage in human epilepsy: Meyer's hypothesis revisited.* **Prog Brain Res**, 2002. 135: p. 237-51.
13. Sloviter, R.S., *"Epileptic" brain damage in rats induced by sustained electrical stimulation of the perforant path. I. Acute electrophysiological and light microscopic studies.* **Brain Res Bull**, 1983. 10 (5): p. 675-97.
14. Cavazos, J.E., Das, I. and Sutula, T.P., *Neuronal loss induced in limbic pathways by kindling: evidence for induction of hippocampal sclerosis by repeated brief seizures.* **J Neurosci**, 1994. 14 (5 Pt 2): p. 3106-21.
15. Mathern, G.W., et al., *The clinical-pathogenic mechanisms of hippocampal neuron loss and surgical outcomes in temporal lobe epilepsy.* **Brain**, 1995. 118 (Pt 1): p. 105-18.
16. Sloviter, R.S., *On the relationship between neuropathology and pathophysiology in the epileptic hippocampus of humans and experimental animals.* **Hippocampus**, 1994. 4 (3): p. 250-3.
17. Cascino, G.D., et al., *Magnetic resonance imaging-based volume studies in temporal lobe epilepsy: pathological correlations.* **Ann Neurol**, 1991. 30 (1): p. 31-36.
18. Cascino, G.D., et al., *MRI in the presurgical evaluation of patients with frontal lobe epilepsy and children with temporal lobe epilepsy: pathologic correlation and prognostic importance.* **Epilepsy Res**, 1992. 11 (1): p. 51-9.
19. Lopes da Silva, F.H. and Wadman, W.J. *Pathophysiology of epilepsy*, in *Handbook of Clinican Neurology: The Epilepsies, Part I*, H. Meinardi, Editor. 1999, Elsevier Science B.V.: Amsterdam; New York. p. 39-81.
20. ILAE Commission on Epidemiology and Prognosis Report, *Guidelines for epidemiologic studies on epilepsy.* **Epilepsia**, 1993. 34 (4): p. 592-6.
21. Shorvon, S.D., *The epidemiology and treatment of chronic and refractory epilepsy.* **Epilepsia**, 1996. 37 **(**Suppl 2): p. S1-S3.
22. McNamara, J.O., *Emerging insights into the genesis of epilepsy.* **Nature**, 1999. 399 (Suppl): p. A15-22.
23. Lopes da Silva, F.H., et al., *Dynamical diseases of brain systems: different routes to epileptic seizures.* **IEEE Trans Biomed Eng**, 2003. 50 (5): p. 540-8.

24. Suffczynski, P., Kalitzin, S. and Lopes da Silva, F.H. *Dynamics of non-convulsive epileptic phenomena modeled by a bistable neuronal network.* **Neuroscience**, 2004. 126 (2): p. 467-84.
25. Hauser, W.A. and Kurland, L.T. *The epidemiology of epilepsy in Rochester, Minnesota, 1935 through 1967.* **Epilepsia**, 1975. 16 (1): p. 1-66.
26. Goodridge, D.M. and Shorvon, S.D. *Epileptic seizures in a population of 6000. I: Demography, diagnosis and classification, and role of the hospital services.* **Br Med J** (Clin Res Ed), 1983. 287 (6393): p. 641-4.
27. Hauser, W.A., Annegers, J.F. and Kurland, L.T. *Incidence of epilepsy and unprovoked seizures in Rochester, Minnesota: 1935-1984.* **Epilepsia**, 1993. 34 (3): p. 453-68.
28. Lopes Lima, J.M.L., *Levantamento epidemiológico das epilepsias e dos síndromos epilépticos no Norte de Portugal*, in *Serviço de Neurologia, Hospital Geral de Santo António*. PhD Thesis 1998, Universidade do Porto, Portugal. 114 p.
29. Keränen, T., *Epilepsy in adults. An epidemiological study in Eastern Finland*, in *Department of Neurology, Kuopio University Hospital.* PhD Thesis 1988, University of Kuopio, Finland. 130 p.
30. Auslandsstatistische Daten, *Statistisches Bundesamt Deutchland.* Wiesbaden, Germany, 1999.
31. Goodridge, D.M. and Shorvon, S.D., *Epileptic seizures in a population of 6000. II: Treatment and prognosis.* **Br Med J** (Clin Res Ed), 1983. 287 (6393): p. 645-7.
32. Hauser, W.A., Annegers, J.F. and Kurland, L.T., *Prevalence of epilepsy in Rochester, Minnesota: 1940-1980.* **Epilepsia**, 1991. 32 (4): p. 429-445.
33. ILAE Commission on Classification and Terminology Report, *Proposal for revised clinical and electroencephalographic classification of epileptic seizures.* **Epilepsia**, 1981. 22 (4): p. 489-501.
34. Annegers, J.F., *The epidemiology of epilepsy*, in *The Treatment of Epilepsy: Principles and Practice*, E. Willie, Editor. 1996, Williams & Wilkins: Baltimore. p. 165-172.
35. Li, L.M., et al., *High resolution magnetic resonance imaging in adults with partial or secondary generalized epilepsy attending a tertiary referral unit.* **J Neurol Neurosurg Psychiatry**, 1995. 59 (4): p. 384-87.
36. Guerrini, R., et al., *Cortical dysplasias, genetics, and epileptogenesis.* **Adv Neurol**, 1999. 79: p. 95-121.
37. Leal, A.J., et al., *Different electroclinical manifestations of the epilepsy associated with hamartomas connecting to the middle or posterior hypothalamus.* **Epilepsia**, 2003. 44 (9): p. 1191-5.
38. Picard, F., et al., *Dominant partial epilepsies. A clinical, electrophysiological and genetic study of 19 European families.* **Brain**, 2000. 123 (Pt 6): p. 1247-62.
39. Cavalheiro, A.E., et al., *Long-term effects of pilocarpine in rats: structural damage of the brain triggers kindling and spontaneous recurrent seizures.* **Epilepsia**, 1991. 32 (6): p. 778-82.
40. Gorter, J.A., et al., *Progression of spontaneous seizures after status epilepticus is associated with mossy fibre sprouting and extensive bilateral loss of hilar parvalbumin and somatostatin-immunoreactive neurons.* **Eur J Neurosci**, 2001. 13 (4): p. 657-69.
41. Annegers, J.F., et al., *Seizures after head trauma: a population study.* **Neurology**, 1980. 30 (7 Pt 1): p. 683-89.
42. Sutula, T., et al., *Mossy fiber synaptic reorganization in the epileptic human temporal lobe.* **Ann Neurol**, 1989. 26 (3): p. 321-30.
43. Houser, C.R., *Neuronal loss and synaptic reorganization in temporal lobe epilepsy.* **Adv Neurol**, 1999. 79: p. 743-61.
44. Gorter, J.A. and Lopes da Silva, F.H. *Abnormal plastic changes in a rat model for mesial temporal lobe epilepsy: a short review.* **Prog Brain Res**, 2002 (138): p. 61-72.
45. Shorvon, S.D. and Reynolds, E.H. *The nature of epilepsy: evidence from studies of epidemiology, temporal pattern of seizures, prognosis and treatment*, in *What is Epilepsy?*, Trimble M.R. and Reynolds, E.H. Editors. 1986, Churchill Livingstone: Edinburgh. p. 36-45.
46. Engel, J., Jr., et al., *Neurobiological evidence for epilepsy-induced interictal disturbances*, in *Advances in Neurology*, Smith, D., Treiman, D., and Trimble, M.R. Editors. 1991, Raven Press: New York. p. 97-111.
47. French, J.A., et al., *Characteristics of medial temporal lobe epilepsy: I. Results of history and physical examination.* **Ann Neurol**, 1993. 34 (6): p. 774-80.

48. Williamson, P.D., et al., *Characteristics of medial temporal lobe epilepsy: II. Interictal and ictal scalp electroencephalography, neuropsychological testing, neuroimaging, surgical results and pathology.* **Ann Neurol**, 1993. 34 (6): p. 781-7.
49. Jokeit, H. and Ebner, A. *Long term effects of refractory temporal lobe epilepsy on cognitive abilities: a cross sectional study.* **J Neurol Neurosurg Psychiatry**, 1999. 67 (1): p. 44-50.
50. Pitkänen, A., et al., *Seizure-induced damage to the medial temporal lobe in temporal lobe epilepsy.*, in *Epilepsy and Mental Retardation*, M. Sillanpää, et al., Editors. 1999, Wrightson Biomedical Publishing LTD. p. 147-63.
51. Annegers, J.F., Hauser, W.A. and Elveback, L.R. *Remission of seizures and relapse in patients with epilepsy.* **Epilepsia**, 1979. 20 (6): p. 729-37.
52. Brodie, M.J. and Dichter, M.A. *Antiepileptic drugs.* **N Engl J Med**, 1996. 334 (3): p. 168-175.
53. Sillanpää, M., *Children with epilepsy as adults: outcome after 30 years of follow-up.* **Acta Paediatr Scand**, 1990. 79 (suppl 368): p. 1-78.
54. MacDonald, B.K., et al., *Factors predicting prognosis of epilepsy after presentation with seizures.* **Ann Neurol**, 2000. 48 (6): p. 833-41.
55. Collaborative Group for the Study of Epilepsy, *Prognosis of epilepsy in newly referred patients: a multicenter prospective study of the effects of monotherapy on the long-term course of epilepsy.* **Epilepsia**, 1992. 33 (1): p. 45-51.
56. Bill, P.A., et al., *A double-blind controlled clinical trial of oxcarbazepine versus phenytoin in adults with previously untreated epilepsy.* **Epilepsy Res**, 1997. 27 (3): p. 195-204.
57. Marson, A.G. and Chadwick, D.W. *New drug treatments for epilepsy.* **J Neurol Neurosurg Psychiatry**, 2001. 70 (2): p. 143-7.
58. Cascino, G.D., *Intractable partial epilepsy: evaluation and treatment.* **Mayo Clin Proc**, 1990. 65 (12): p. 1578-86.
59. Sander, J.W. and Sillanpää, M., *Natural History and Prognosis*, in *Epilepsy. The Comprehensive CD-ROM*, J.J. Engel and T.A. Pedley, Editors. 1999, Lippincott Williams and Wilkins: Baltimore.
60. Benbadis, S.R., Tatum, W.O. and Vale, F.L. *When drugs don't work: an algorithmic approach to medically intractable epilepsy.* **Neurology**, 2000. 55 (12): p. 1780-4.
61. Lüders, H., *Epilepsy Surgery*. 1992, New York: Raven Press. xxvi, 854 p.
62. Jutila, L., et al., *Long term outcome of temporal lobe epilepsy surgery: analyses of 140 consecutive patients.* **J Neurol Neurosurg Psychiatry**, 2002. 5 (73): p. 486-94.
63. Berg, A.T., et al., *Early development of intractable epilepsy in children: a prospective study.* **Neurology**, 2001. 56 (11): p. 1445-52.
64. Shorvon, S.D., *Epidemiology, classification, natural history, and genetics of epilepsy.* **Lancet**, 1990. 336 (8707): p. 93-6.
65. Sillanpää, M., *Long-term outcome of epilepsy.* **Epileptic Disord**, 2000. 2 (2): p. 79-88.
66. Annegers, J.F., *Mortality*, in *Epilepsy. The Comprehensive CD-ROM*, J.J. Engel and T.A. Pedley, Editors. 1999: Baltimore.
67. Walczak, T.S., et al., *Incidence and risk factors in sudden unexpected death in epilepsy: a prospective cohort study.* **Neurology**, 2001. 27 (56): p. 519-25.
68. Gastaut, H., *Clinical and electroencephalographical classification of epileptic seizures.* **Epilepsia**, 1970. 11 (1): p. 102-103.
69. Lowenstein, D.H. and Alldredge, B.K., *Status Epilepticus.* **N Engl J Med**, 1998. 338 (14): p. 970-6.
70. Mathern, G.W., Pretorius, J.K. and Babb, T.L., *Influence of the type of initial precipitating injury and at what age it occurs on course and outcome in patients with temporal lobe seizures.* **J Neurosurg**, 1995. 82 (2): p. 220-7.
71. Mayer, S.A., et al., *Refractory status epilepticus: frequency, risk factors, and impact on outcome.* **Arch Neurol**, 2002. 59 (2): p. 205-10.
72. Leppik, I.E., *Status epilepticus: the next decade.* **Neurology**, 1990. 40 (5 Suppl. 2): p. 4-9.
73. DeLorenzo, R.J., et al., *A prospective, population-based epidemiologic study of status epilepticus in Richmond, Virginia.* **Neurology**, 1996. 46 (4): p. 1029-35.
74. Lothman, E.W., *The biochemical basis and pathophysiology of status epilepticus.* **Neurology**, 1990. 40 (5 Suppl. 2): p. 13-23.

75. Wasterlain, C.G., et al., *Chronic epilepsy with damage restricted to the hippocampus: possible mechanisms.* **Epilepsy Res**, 1996. 26 (1): p. 255-65.
76. Nohria, V., et al., *Magnetic resonance imaging evidence of hippocampal sclerosis in progression: a case report.* **Epilepsia**, 1994. 35 (6): p. 1332-6.
77. Wieshmann, U.C., et al., *Development of hippocampal atrophy: a serial magnetic resonance imaging study in a patient who developed epilepsy after generalized status epilepticus.* **Epilepsia**, 1997. 38 (11): p. 1238-41.
78. Meierkord, H., et al., *Structural consequences of status epilepticus demonstrated with serial magnetic resonance imaging.* **Acta Neurol Scand**, 1997. 96 (3): p. 127-32.
79. Wieshmann, U.C., Symms, M.R. and Shorvon, S.D., *Diffusion changes in status epilepticus.* **Lancet**, 1997. 350 (9076): p. 493-4.
80. Krumholz, A., et al., *Complex partial status epilepticus accompanied by serious morbidity and mortality.* **Neurology**, 1995. 45 (8): p. 1499-504.
81. Lothman, E.W., et al., *Self-sustained limbic status epilepticus induced by "continuous" hippocampal stimulation: electrographic and behavioral characteristics.* **Epilepsy Res**, 1989. 3 (2): p. 107-19.
82. Broca, P., *Anatomie Comparée des Circonvolutions Cérébrales. Le Grand Lobe Limbique et la Scisure Limbique dans la série des Mammifères.* **Rev. Anthropol**. Paris, 1878. 2: p. 285-498.
83. Lopes da Silva, F.H., et al., *Anatomic organization and physiology of the limbic cortex.* **Physiol Rev**, 1990. 70 (2): p. 453-511.
84. Papez, J., *A proposed mechanism of emotion.* **Arch Neurol Psychiatry**, 1937. 38: p. 725-743.
85. MacLean, P.D., *Some psychiatric implications of physiological studies on frontotemporal portion of limbic system (visceral brain).* **Electrencephalogr Clin Neurophysiol Suppl**, 1952. 4 (4): p. 407-18.
86. Phan, K.L., et al., *Functional neuroanatomy of emotion: a meta-analysis of emotion activation studies in PET and fMRI.* **Neuroimage**, 2002. 16 (2): p. 331-48.
87. Swanson, L.W., *The hippocampus and the concept of the limbic system*, in *Neurobiology of the Hippocampus*, W. Seifert, Editor. 1983, Academic: London. p. 3-20.
88. Amaral, D.G. and Insausti, R. *Hippocampal formation*, in *The Human Nervous System*, G. Paxinos, Editor. 1990, Academic Press, Inc.: San Diego. p. 711-755.
89. Witter, M.P., et al., *Functional organization of the extrinsic and intrinsic circuitry of the parahippocampal region.* **Prog Neurobiol**, 1989. 33 (3): p. 161-253.
90. Amaral, D.G. and Witter, M.P. *The three-dimensional organization of the hippocampal formation: a review of anatomical data.* **Neuroscience**, 1989. 31 (3): p. 571-91.
91. Brodmann, K., *Verleichende Lokalisationslehre der Grosshirnrinde in ihren Prinzipien dargestellet auf Grund des Zellenbaues*. 1909, Leipzig: Barth.
92. Insausti, R., et al., *The human entorhinal cortex: a cytoarchitectonic analysis.* **J Comp Neurol**, 1995. 355 (2): p. 171-98.
93. Witter, M.P., *Organization of the entorhinal-hippocampal system: a review of current anatomical data.* **Hippocampus**, 1993. 3 (special number): p. 33-44.
94. Insausti, R., Amaral, D.G. and Cowan, W.M., *The entorhinal cortex of the monkey: II. Cortical afferents.* **J Comp Neurol**, 1987. 264 (3): p. 356-95.
95. Insausti, R., Herrero, M.T. and Witter, M.P. *Entorhinal cortex of the rat: cytoarchitectonic subdivisions and the origin and distribution of cortical efferents.* **Hippocampus**, 1997. 7 (2): p. 146-83.
96. Insausti, R., et al., *MR volumetric analysis of the human entorhinal, perirhinal, and temporopolar cortices.* **AJNR Am J Neuroradiol**, 1998. 19 (4): p. 659-71.
97. Price, J.L., *Olfactory System*, in *The Human Nervous System*, G. Paxinos, Editor. 1990, Academic Press, Inc.: San Diego. p. 979-998.
98. Zatorre, R.J., et al., *Functional localization and lateralization of human olfactory cortex.* **Nature**, 1992. 360 (6402): p. 339-40.
99. Fujikawa, D.G., et al., *Status epilepticus-induced neuronal loss in humans without systemic complications or epilepsy.* **Epilepsia**, 2000. 41 (8): p. 981-91.
100. Bertram, E.H., *Functional anatomy of spontaneous seizures in a rat model of limbic epilepsy.* **Epilepsia**, 1997. 38 (1): p. 95-105.

101.Löscher, W. and Ebert, U., *The role of the piriform cortex in kindling.* **Prog Neurobiol**, 1996. 50 (5-6): p. 427-81.
102.Haberly, L.B. and Presto, S., *Ultraestrutural analysis of synaptic relationships of intracellularly stained pyramidal cell axons in piriform cortex.* **J Comp Neurol**, 1986. 4 (248): p. 464-474.
103.Price, J.L., *An autoradiographic study of complementary laminar patterns of termination of afferent fibers to the olfactory cortex.* **J Comp Neurol**, 1973. 1 (150): p. 87-108.
104.Haberly, L.B. and Feig, S.L., *Structure of the piriform cortex of the opossum. II. Fine structure of cell bodies and neuropil.* **J Comp Neurol**, 1983. 1 (216): p. 69-88.
105.Carmichael, S.T., Clugnet, M.C. and Price, J.L. *Central olfactory connections in the macaque monkey.* **J Comp Neurol**, 1994. 346 (3): p. 403-34.
106.Amaral, D.G., *Memory: anatomical organization of candidate brain regions*, in *Higher Functions of the Brain, Handbook of Physiology, Part I.*, Plum, F. and Mountcastle, V. Editors. 1987, Am Physiol Soc: Washington, DC. p. 211-294.
107.Price, J.L., Russchen, F.T. and Amaral, D.G., *The Limbic Region. II. The amygdaloid complex*, in *Handbook of Chemical Neuroanatomy*, Björklund, A., Hokfelt, T., and Swanson, L.W. Editors. 1987, Elsevier: Amsterdam. p. 279-388.
108.Pitkänen, A., Savander, V. and LeDoux, J.E. *Organization of intra-amygdaloid circuitries in the rat: an emerging framework for understanding functions of the amygdala.* **Trends Neurosci**, 1997. 20 (11): p. 517-23.
109.Pitkänen, A., et al., *Reciprocal connections between the amygdala and the hippocampal formation, perirhinal cortex, and postrhinal cortex in rat. A review.* **Ann N Y Acad Sci**, 2000. 911: p. 369-91.
110.Jolkkonen, E., R. Miettinen, and A. Pitkänen, *Projections from the amygdalo-piriform transition area to the amygdaloid complex: a PHA-l study in rat.* **J Comp Neurol**, 2001. 432 (4): p. 440-65.
111.Motokizawa, F., et al., *The principal pathway from the piriform cortex to the deep amygdaloid nuclei in the cat.* **Neurosci Res**, 1985. 3 (2): p. 167-70.
112.Witter, M.P., et al., *Reciprocal connections of the insular and piriform claustrum with limbic cortex: an anatomical study in the cat.* **Neuroscience**, 1988. 24 (2): p. 519-39.
113.Insausti, R., et al., *Plasticity in the entorhinal-hippocampal system.* **Hippocampus**, 1993. 3 (special number): p. 289-92.
114.Lothman, E.W., Bertram, E.H., and Stringer, J.L., *Functional anatomy of hippocampal seizures.* **Prog Neurobiol**, 1991. 37 (1): p. 1-82.
115.Pare, D., deCurtis, M. and Llinas, R. *Role of the hippocampal-entorhinal loop in temporal lobe epilepsy: extra- and intracellular study in the isolated guinea pig brain in vitro.* **J Neurosci**, 1992. 12 (5): p. 1867-81.
116.Bertram, E.H., et al., *Functional anatomy of limbic epilepsy: a proposal for central synchronization of a diffusely hyperexcitable network.* **Epilepsy Res**, 1998. 32 (1-2): p. 194-205.
117.ILAE Commission on Classification and Terminology Report, *Proposal for revised classification of epilepsies and epileptic syndromes* **Epilepsia**, 1989. 30 (4): p. 389-99.
118.ILAE Commission on Neurosurgery of Epilepsy Report, *Mesial Temporal Lobe Epilepsy with Hippocampal Sclerosis.* **Epilepsia**, 2004. 45 (6): p. 695-714.
119.Engel, J., Jr., *Diagnostic evaluation*, in *Seizures and epilepsy*, J. Engel, Jr., Editor. 1989, F. A. Davis Company: Philadelphia. p. 303-309.
120.Cahan, L.D., et al., *Review of the 20-year UCLA experience with surgery for epilepsy.* **Cleve Clin Q**, 1984. 51 (2): p. 313-8.
121.Tureczek, I.E., Fandino-Franky, J. and Wieser, H.G. *Comparison of the epilepsy surgery programs in Cartagena, Colombia, and Zurich, Switzerland.* **Epilepsia**, 2000. 41 (Suppl 4): p. 35-40.
122.Williamson, P.D., *Complex Partial Status Epilepticus*, in *Epilepsy: A Comprehensive Textbook*, Engel, J. and Pedley, T.A. Editors. 1997, Lippincott-Raven: Philadelphia.
123.Williamson, P.D., Wieser, H.G. and Delgado-Escueta, A.V. *Clinical characteristics of partial seizures*, in *Surgical Treatment of the Epilepsies*, J.J. Engel, Editor. 1987, Raven Press: New York. p. 101-20.
124.Williamson, P.D. and Jobst, B.C. *Frontal lobe epilepsy.* **Adv Neurol**, 2000. 84: p. 215-42.

125.Wiebe, S., *Epidemiology of temporal lobe epilepsy.* **Can J Neurol Sci**, 2000. 27 (Suppl 1): p. S6-10; discussion S20-1.
126.Engel, J., Jr. and Shewmon, D.A. *Overview: who should be considered a surgical candidate?*, in *Surgical Treatment of the Epilepsies*, Engel, J. Jr. Editor. 1996, Lippincott-Raven: Philadelphia.
127.Gloor, P., et al., *The role of the limbic system in experiential phenomena of temporal lobe epilepsy.* **Ann Neurol**, 1982. 12 (2): p. 129-44.
128.Henkel, A., et al., *The localizing value of the abdominal aura and its evolution: A study in focal epilepsies.* **Neurology**, 2002. 58 (2): p. 271-6.
129.Engel, J., Jr., *Introduction to temporal lobe epilepsy.* **Epilepsy Res**, 1996. 26 (1): p. 141-50.
130.Niedermeyer, E., *Epileptic seizure disorders*, in *Electroencephalography: basic principles, clinical applications and related fields*, Niedermeyer, E. and Lopes da Silva, F.H. Editors. 1999, Williams & Wilkins: Baltimore. p. 476-585.
131.Gibbs, E.L., Fuster, B. and Gibbs, F.A., *Peculiar low temporal localization of sleep-induced seizure discharges of psychomotor epilepsy.* **Arch Neurol Psychiatry** (Chicago), 1948. 60: p. 95-97.
132.Jasper, H.H., Pertuiset, B. and Flanigin, H.F. *EEG and cortical electrograms in patients with temporal lobe seizures.* **Arch Neurol Psychiatry** (Chicago), 1951. 65: p. 272-290.
133.Spencer, S.S., et al., *Combined depth and subdural electrode investigation in uncontrolled epilepsy.* **Neurology**, 1990. 40 (1): p. 74-9.
134.Schiller, Y., Cascino, G.D. and Sharbrough, F.W., *Chronic intracranial EEG monitoring for localizing the epileptogenic zone: an electroclinical correlation.* **Epilepsia**, 1998. 39 (12): p. 1302-8.
135.Hamati-Haddad, A. and Abou-Khalil, B., *Epilepsy diagnosis and localization in patients with antecedent childhood febrile convulsions.* **Neurology**, 1998. 50 (4): p. 917-22.
136.Verity, C.M., Ross, E.M. and Golding, J., *Outcome of childhood status epilepticus and lengthy febrile convulsions: findings of national cohort study.* **BMJ**, 1993. 307 (6898): p. 225-8.
137.Hudson, L.P., et al., *Amygdaloid sclerosis in temporal lobe epilepsy.* **Ann Neurol**, 1993. 33 (6): p. 622-31.
138.Zentner, J., et al., *Clinical relevance of amygdala sclerosis in temporal lobe epilepsy.* **J Neurosurg**, 1999. 91 (1): p. 59-67.
139.Racine, R.J., Moscher, M. and Kairiss, E.W. *The role of the pyriform cortex in the generation of interictal spikes in the kindled preparation.* **Brain Res**, 1988. 454 (1-2): p. 251-63.
140.Löscher, W., et al., *Susceptibility of different cell layers of the anterior and posterior part of the piriform cortex to electrical stimulation and kindling: comparison with the basolateral amygdala and "area tempestas".* **Neuroscience**, 1995. 66 (2): p. 265-76.
141.Kelly, M.E., Staines, W.A. and McIntyre, D.C., *Secondary generalization of hippocampal kindled seizures in rats: examining the role of the piriform cortex.* **Brain Res**, 2002. 957 (1): p. 152-61.
142.Piredda, S. and Gale, K., *A crucial epileptogenic site in the deep prepiriform cortex.* **Nature**, 1985. 317 (6038): p. 623-625.
143.Piredda, S., Pavlick, M. and Gale, K., *Anticonvulsant effects of GABA elevation in the deep prepiriform cortex.* **Epilepsy Res**, 1987. 1 (2): p. 102-6.
144.Halonen, T., et al., *Posterior piriform and perirhinal cortex relay seizures evoked from the area tempestas: role of excitatory and inhibitory amino acid receptors.* **Brain Res**, 1994. 652 (1): p. 145-8.
145.Gale, K., et al., *Amino acid neurotransmitter interactions in 'area tempestas': an epileptogenic trigger zone in the deep prepiriform cortex.* **Epilepsy Res Suppl**, 1992. 8: p. 229-34.
146.Gale, K. and Dubach, M., *Localization of area tempestas in piriform cortex of the monkey.* **Soc Neurosci Abstr**, 1993. 19: p. 21.
147.Wilson, C.L., et al., *Functional connections in the human temporal lobe. I. Analysis of limbic system pathways using neuronal responses evoked by electrical stimulation.* **Exp Brain Res**, 1990. 82 (2): p. 279-92.
148.Spencer, S.S. and Spencer, D.D. *Entorhinal-hippocampal interactions in medial temporal lobe epilepsy.* **Epilepsia**, 1994. 35 (4): p. 721-7.
149.Velasco, A.L., et al., *Functional and anatomic correlates of two frequently observed temporal lobe seizure-onset patterns.* **Neural Plast**, 2000. 7 (1-2): p. 49-63.

150.Gonçalves Pereira, P.M., et al., *Spatio-temporal evolution of cell death in the hippocampus and entorhinal cortex in the post-status epilepticus model.* **European Journal of Neuroscience**, 2000. 12 (Suppl 11): p. 210.
151.Gorter, J.A. and Gonçalves Pereira, P.M., et al., *Neuronal cell death in a rat model for mesial temporal lobe epilepsy is induced by the initial status epilepticus and not by later repeated spontaneous seizures.* **Epilepsia**, 2003. 44 (5): p. 647-58.
152.Wieser, H.G., et al., *Long-term seizure outcomes following amygdalohippocampectomy.* **J Neurosurg**, 2003. 98 (4): p. 751-63.
153.Yasargil, M.G., Teddy, P.J. and Roth, P. *Selective amygdalo-hippocampectomy. Operative anatomy and surgical technique.* **Adv Tech Stand Neurosurg**, 1985. 12: p. 93-123.
154.Wiebe, S., et al., *A randomized, controlled trial of surgery for temporal-lobe epilepsy.* **N Engl J Med**, 2001. 345 (5): p. 311-8.
155.McIntyre, D.C. and Kelly, M.E. *Pyriform cortex involvement in limbic kindling.* **Soc Neurosci Abstr**, 1990. 166: p. 1107.
156.Babb, T.L. and W.J. Brown, *Pathological findings in epilepsy*, in *Surgical Treatment of the Epilepsies*, Engel, J. J. Editor. 1987, Raven Press: New York. p. 511-540.
157.Meyer, A., Falconer, M.A. and Beck, E. *Pathological findings in temporal lobe epilepsy.* **J Neurochem**, 1954. 17 (4): p. 276-85.
158.Mathern, G.W., Babb, T.L. and Armstrong, D.L. *Hippocampal sclerosis*, in *Epilepsy: a comprehensive textbook*, J. Engel and T.A. Pedley, Editors. 1997, Lippincott-Raven: Philadelphia. p. 133-155.
159.Babb, T.L., et al., *Temporal lobe volumetric cell densities in temporal lobe epilepsy.* **Epilepsia**, 1984. 25 (6): p. 729-40.
160.Houser, C.R., *Morphological changes in the dentate gyrus in human temporal lobe epilepsy.* **Epilepsy Res Suppl**, 1992. **7**: p. 223-34.
161.Houser, C.R., *Granule cell dispersion in the dentate gyrus of humans with temporal lobe epilepsy.* **Brain Res**, 1990. 535 (2): p. 195-204.
162.Babb, T.L., *Bilateral pathological damage in temporal lobe epilepsy.* **Can J Neurol Sci**, 1991. 18 (4 Suppl): p. 645-8.
163.Levesque, M.F., et al., *Surgical treatment of limbic epilepsy associated with extrahippocampal lesions: the problem of dual pathology.* **J Neurosurg**, 1991. 75 (3): p. 364-70.
164.Pitkänen, A., et al., *Amygdala damage in experimental and human temporal lobe epilepsy.* **Epilepsy Res**, 1998. 32 (1-2): p. 233-53.
165.Lee, D.H., et al., *MR in temporal lobe epilepsy: analysis with pathologic confirmation.* **AJNR Am J Neuroradiol**, 1998. 19 (1): p. 19-27.
166.Swartz, B.E., et al., *Neuroimaging in temporal lobe epilepsy: test sensitivity and relationships to pathology and postoperative outcome.* **Epilepsia**, 1992. 33 (4): p. 624-34.
167.Miller, L.A., et al., *Amygdalar sclerosis: preoperative indicators and outcome after temporal lobectomy.* **J Neurol Neurosurg Psychiatry**, 1994. 57 (9): p. 1099-105.
168.Mikkonen, M., et al., *Remodeling of neuronal circuitries in human temporal lobe epilepsy: increased expression of highly polysialylated neural cell adhesion molecule in the hippocampus and the entorhinal cortex.* **Ann Neurol**, 1998. 44 (6): p. 923-34.
169.Honack, D., Wahnschaffe, U. and Löscher, W., *Kindling from stimulation of a highly sensitive locus in the posterior part of the piriform cortex. Comparison with amygdala kindling and effects of antiepileptic drugs.* **Brain Res**, 1991. 538 (2): p. 196-202.
170.Clark, M., et al., *Regional expression of c-fos mRNA in rat brain during the evolution of amygdala kindled seizures.* **Mol Brain Res**, 1991. 11 (1): p. 55-64.
171.Maggio, R., et al., *Expression of c-fos mRNA following seizures evoked from an epileptogenic site in the deep prepiriform cortex: regional distribution in brain as shown by in situ hybridization.* **Exp Neurol**, 1993. 1 (119): p. 11-9.
172.Ebert, U. and Löscher, W. *Strong induction of c-fos in the piriform cortex during focal seizures evoked from different limbic brain sites.* **Brain Res**, 1995. 671 (2): p. 338-44.
173.McIntyre, D.C. and M.E. Kelly, *The parahippocampal cortices and kindling.* **Ann N Y Acad Sci**, 2000. 911: p. 343-54.

174.Pirttila, T.R., et al., *Ex vivo MR microimaging of neuronal damage after kainate-induced status epilepticus in rat: correlation with quantitative histology.* **Magn Reson Med**, 2001. 46 (5): p. 946-54.
175.Roch, C., et al., *Magnetic resonance imaging in the study of the lithium-pilocarpine model of temporal lobe epilepsy in adult rats.* **Epilepsia**, 2002. 43 (4): p. 325-35.
176.Sperling, M.R., *Neuroimaging in epilepsy: contribution of MRI, PET and SPECT.* **Semin Neurol**, 1990. 10 (4): p. 349-56.
177.Lamusuo, S., et al., *[18F]FDG-PET reveals temporal hypometabolism in patients with temporal lobe epilepsy even when quantitative MRI and histopathological analysis show only mild hippocampal damage.* **Arch Neurol**, 2001. 58 (6): p. 933-9.
178.Toczek, M.T., et al., *PET imaging of 5-HT1A receptor binding in patients with temporal lobe epilepsy.* **Neurology**, 2003. 5 (60): p. 749-56.
179.Moran, N.F., et al., *Extrahippocampal temporal lobe atrophy in temporal lobe epilepsy and mesial temporal sclerosis.* **Brain**, 2001. 124 (Pt 1): 167-75.
180.Mamourian, A.C. and Brown, D.B. *Asymmetric mamillary bodies: MR identification.* **AJNR Am J Neuroradiol**, 1993. 14 (6): p. 1332-5; discussion 1336-42.
181.Baldwin, G.N., et al., *The fornix in patients with seizures caused by unilateral hippocampal sclerosis: detection of unilateral volume loss on MR images.* **AJR Am J Roentgenol**, 1994. 162 (5): p. 1185-9.
182.DeCarli, C., et al., *Extratemporal atrophy in patients with complex partial seizures of left temporal origin.* **Ann Neurol**, 1998. 43 (1): p. 41-5.
183.Natsume, J., et al., *MRI volumetry of the thalamus in temporal, extratemporal, and idiopathic generalized epilepsy.* **Neurology**, 2003. 60 (8): p. 1296-300.
184.Chan, S., Erickson, J.K. and Yoon, S.S., *Limbic system abnormalities associated with mesial temporal sclerosis: a model of chronic cerebral changes due to seizures.* **Radiographics**, 1997. 17 (5): p. 1095-110.
185.Nelson, K.B. and Ellenberg, J.H., *Predictors of epilepsy in children who have experienced febrile seizures.* **N Engl J Med**, 1976. 295 (19): p. 1029-33.
186.Mathern, G.W., et al., *The pathogenic and progressive features of chronic human hippocampal epilepsy.* **Epilepsy Res**, 1996. 26 (1): p. 151-61.
187.Dam, A.M., *Epilepsy and neuron loss in the hippocampus.* **Epilepsia**, 1980. 21 (6): p. 617-29.
188.Beach, T.G., et al., *Reactive microglia in hippocampal sclerosis associated with human temporal lobe epilepsy.* **Neurosci Lett**, 1995. 191 (1-2): p. 27-30.
189.Cendes, F., et al., *Early childhood prolonged febrile convulsions, atrophy and sclerosis of mesial structures, and temporal lobe epilepsy: an MRI volumetric study.* **Neurology**, 1993. 43 (6): p. 1083-7.
190.Kuks, J.B., et al., *Hippocampal sclerosis in epilepsy and childhood febrile seizures.* **Lancet**, 1993. 342 (8884): p. 1391-4.
191.Trenerry, M.R., et al., *Quantitative MRI hippocampal volumes: association with onset and duration of epilepsy, and febrile convulsions in temporal lobectomy patients.* **Epilepsy Res**, 1993. 15 (3): p. 247-52.
192.Harvey, A.S., et al., *Febrile seizures and hippocampal sclerosis: frequent and related findings in intractable temporal lobe epilepsy of childhood.* **Pediatr Neurol**, 1995. 12 (3): p. 201-6.
193.Van Paesschen, W., et al., *The spectrum of hippocampal sclerosis: a quantitative magnetic resonance imaging study.* **Ann Neurol**, 1997. 41 (1): p. 41-51.
194.Theodore, W.H., et al., *Hippocampal atrophy, epilepsy duration, and febrile seizures in patients with partial seizures.* **Neurology**, 1999. 52 (1): p. 132-6.
195.Fernandez, G., et al., *Hippocampal malformation as a cause of familial febrile convulsions and subsequent hippocampal sclerosis.* **Neurology**, 1998. 50 (4): p. 909-17.
196.VanLandingham, K.E., et al., *Magnetic resonance imaging evidence of hippocampal injury after prolonged focal febrile convulsions.* **Ann Neurol**, 1998. 43 (4): p. 413-26.
197.Bigler, E.D., et al., *Hippocampal volume in normal aging and traumatic brain injury.* **AJNR Am J Neuroradiol**, 1997. 18 (1): p. 11-23.
198.Free, S.L., et al., *Bilateral hippocampal volume loss in patients with a history of encephalitis or meningitis.* **Epilepsia**, 1996. 37 (4): p. 400-5.

199.Tien, R.D. and G.J. Felsberg, *The hippocampus in status epilepticus: demonstration of signal intensity and morphologic changes with sequential fast spin-echo MR imaging.* **Radiology**, 1995. 194 (1): p. 249-56.
200.Grunewald, R.A., et al., *MR detection of hippocampal disease in epilepsy: factors influencing T2 relaxation time.* **AJNR Am J Neuroradiol**, 1994. 15 (6): p. 1149-56.
201.Kuzniecky, R.I., et al., *Qualitative MRI segmentation in mesial temporal sclerosis: clinical correlations.* **Epilepsia**, 1996. 37 (5): p. 433-9.
202.Barr, W.B., Ashtari, M. and Schaul, N. *Bilateral reductions in hippocampal volume in adults with epilepsy and a history of febrile seizures.* **J Neurol Neurosurg Psychiatry**, 1997. 63 (4): p. 461-7.
203.Spencer, S.S., McCarthy, G. and Spencer, D.D. *Diagnosis of medial temporal lobe seizure onset: relative specificity and sensitivity of quantitative MRI.* **Neurology**, 1993. 43 (10): p. 2117-24.
204.Tasch, E., et al., *Neuroimaging evidence of progressive neuronal loss and dysfunction in temporal lobe epilepsy.* **Ann Neurol**, 1999. 45 (5): p. 568-76.
205.Marsh, L., et al., *Cortical and hippocampal volume deficits in temporal lobe epilepsy.* **Epilepsia**, 1997. 38 (5): p. 576-87.
206.Van Paesschen, W., *Quantitative MRI of mesial temporal structures in temporal lobe epilepsy.* **Epilepsia**, 1997. 38 (Suppl. 10): p. 3-12.
207.Van Paesschen, W., et al., *Quantitative neuropathology and quantitative magnetic resonance imaging of the hippocampus in temporal lobe epilepsy.* **Ann Neurol**, 1997. 42 (5): p. 756-66.
208.Van Paesschen, W., et al., *Etiology and early prognosis of newly diagnosed partial seizures in adults: a quantitative hippocampal MRI study.* **Neurology**, 1997. 49 (3): p. 753-7.
209.Kälviäinen, R., et al., *Recurrent seizures may cause hippocampal damage in temporal lobe epilepsy.* **Neurology**, 1998. 50 (5): p. 1377-82.
210.Salmenperä, T., et al., *Hippocampal damage caused by seizures in temporal lobe epilepsy.* **Lancet**, 1998. 351 (9095): p. 35.
211.Pitkänen, A., et al., *Severity of hippocampal atrophy correlates with the prolongation of MRI T2 relaxation time in temporal lobe epilepsy but not in Alzheimer's disease.* **Neurology**, 1996. 46 (6): p. 1724-30.
212.O'Brien, T.J., et al., *Progressive hippocampal atrophy in chronic intractable temporal lobe epilepsy.* **Ann Neurol**, 1999. 45 (4): p. 526-9.
213.Garcia, P.A., Laxer, K.D. and Ng, T. *Application of spectroscopic imaging in epilepsy.* **Magn Reson Imaging**, 1995. 13 (8): p. 1181-5.
214.Ebisu, T., et al., *MR spectroscopic imaging and diffusion-weighted MRI for early detection of kainate-induced status epilepticus in the rat.* **Magn Reson Med**, 1996. 36 (6): p. 821-8.
215.Cendes, F., et al., *Proton magnetic resonance spectroscopic imaging and magnetic resonance imaging volumetry in the lateralization of temporal lobe epilepsy: a series of 100 patients.* **Ann Neurol**, 1997. 42 (5): p. 737-46.
216.Cendes, F., et al., *Proton magnetic resonance spectroscopic imaging for discrimination of absence and complex partial seizures.* **Ann Neurol**, 1997. 41 (1): p. 74-81.
217.Garcia, P.A., et al., *Correlation of seizure frequency with N-acetyl-aspartate levels determined by 1H magnetic resonance spectroscopic imaging.* **Magn Reson Imaging**, 1997. 15 (4): p. 475-8.
218.Bernasconi, A., et al., *Proton magnetic resonance spectroscopic imaging suggests progressive neuronal damage in human temporal lobe epilepsy*, in *Prog Brain Res*, Sutula, T. and Pitkänen, A. Editors. 2002. p. 297-304.
219.Ende, G.R., et al., *Temporal lobe epilepsy: bilateral hippocampal metabolite changes revealed at proton MR spectroscopic imaging.* **Radiology**, 1997. 202 (3): p. 809-17.
220.Knowlton, R.C., et al., *Presurgical multimodality neuroimaging in electroencephalographic lateralized temporal lobe epilepsy.* **Ann Neurol**, 1997. 42 (6): p. 829-37.
221.Vermathen, P., et al., *Hippocampal N-acetylaspartate in neocortical epilepsy and mesial temporal lobe epilepsy.* **Ann Neurol**, 1997. 42 (2): p. 194-9.
222.Vermathen, P., et al., *Temporal lobectomy for epilepsy: Recovery of the contralateral hippocampus measured by (1)H MRS.* **Neurology**, 2002. 59 (4): p. 633-636.
223.Kuzniecky, R., et al., *Magnetic resonance spectroscopic imaging in temporal lobe epilepsy: neuronal dysfunction or cell loss?* **Arch Neurol**, 2001. 58 (12): p. 2048-53.

224.Salmenperä, T., et al., *Hippocampal and amygdaloid damage in partial epilepsy: a cross-sectional MRI study of 241 patients.* **Epilepsy Res**, 2001. 46 (1): p. 69-82.
225.Kälviäinen, R., et al., *MRI volumetry and T2 relaxometry of the amygdala in newly diagnosed and chronic temporal lobe epilepsy.* **Epilepsy Res**, 1997. 28 (1): p. 39-50.
226.Van Paesschen, W., et al., *The amygdala and temporal lobe simple partial seizures: a prospective and quantitative MRI study.* **Epilepsia**, 2001. 42 (7): p. 857-62.
227.Liu, R.S., et al., *A longitudinal quantitative MRI study of community-based patients with chronic epilepsy and newly diagnosed seizures: methodology and preliminary findings.* **Neuroimage**, 2001. 14 (1, Pt 1): p. 231-43.
228.Fuerst, D., et al., *Hippocampal sclerosis is a progressive disorder: a longitudinal volumetric MRI study.* **Ann Neurol**, 2003. 53 (3): p. 413-6.
229.Williamson, A., Spencer, D.D. and Shepherd, G.M. *Comparison between the membrane and synaptic properties of human and rodent dentate granule cells.* **Brain Res**, 1993. 622 (1-2): p. 194-202.
230.Cummins, T.R., Xia, Y. and Haddad, G.G. *Functional properties of rat and human neocortical voltage-sensitive sodium currents.* **J Neurophysiol**, 1994. 71 (3): p. 1052-64.
231.Schwob, J.E., et al., *Widespread patterns of neuronal damage following systemic or intracerebral injections of kainic acid: a histological study.* **Neuroscience**, 1980. 6 (5): p. 991-1014.
232.Tuunanen, J., Halonen, T. and Pitkänen, A. *Status epilepticus causes selective regional damage and loss of GABAergic neurons in the rat amygdaloid complex.* **Eur J Neurosci**, 1996. 8 (12): p. 2711-25.
233.Mathern, G.W., *Hippocampal Pathophysiology in Experimental Models.*, in *The Epilepsies. Etiologies and Prevention.*, Kotagal, P. and Lüders, H.O. Editors. 1999, Academic Press. p. 149-166.
234.Covolan, L., et al., *Cell damage and neurogenesis in the dentate granule cell layer of adult rats after pilocarpine- or kainate-induced status epilepticus.* **Hippocampus**, 2000. 10 (2): p. 169-80.
235.Koh, S., et al., *Early-life seizures in rats increase susceptibility to seizure-induced brain injury in adulthood.* **Neurology**, 1999. 53 (5): p. 915-21.
236.Goddard, G.V., McIntyre, D.C. and Leech, C.K. *A permanent change in brain function resulting from daily electrical stimulation.* **Exp Neurol**, 1969. 25 (3): p. 295-330.
237.Lopes da Silva, F.H., et al., *An experimental model of progressive epilepsy: the development of kindling of the hippocampus of the rat.* **Ital J Neurol Sci**, 1995. 16 (1-2): p. 45-57.
238.Bengzon, J., et al., *Apoptosis and proliferation of dentate gyrus neurons after single and intermittent limbic seizures.* **Proc Natl Acad Sci USA**, 1997. 94 (19): p. 10432-7.
239.Bertram, E.H. and Lothman, E.W. *Morphometric effects of intermittent kindled seizures and limbic status epilepticus in the dentate gyrus of the rat.* **Brain Res**, 1993. 603 (1): p. 25-31.
240.Adams, B., et al., *Nerve growth factor accelerates seizure development, enhances mossy fiber sprouting, and attenuates seizure-induced decreases in neuronal density in the kindling model of epilepsy.* **J Neurosci**, 1997. 17 (14): p. 5288-96.
241.Tuunanen, J., Halonen, T. and Pitkänen, A., *Decrease in somatostatin-immunoreactive neurons in the rat amygdaloid complex in a kindling model of temporal lobe epilepsy.* **Epilepsy Res**, 1997. 26 (2): p. 315-27.
242.Nissinen, J., et al., *A new model of chronic temporal lobe epilepsy induced by electrical stimulation of the amygdala in rat.* **Epilepsy Res**, 2000. 38 (2-3): p. 177-205.
243.Mathern, G.W., Pretorius, J.K. and Babb, T.L. *Quantified patterns of mossy fiber sprouting and neuron densities in hippocampal and lesional seizures.* **J Neurosurg**, 1995. 82 (2): p. 211-9.
244.Milgram, N.W., et al., *Establishment of status epilepticus by limbic system stimulation in previously unstimulated rats.* **Exp Neurol**, 1985. 2 (88): p. 253-64.
245.Vicedomini, J.P. and Nadler, J.V. *A model of status epilepticus based on electrical stimulation of hippocampal afferent pathways.* **Exp Neurol**, 1987. 96 (3): p. 681-91.
246.Bertram, E.H. and Cornett, J.F. *The evolution of a rat model of chronic spontaneous limbic seizures.* **Brain Res**, 1994. 661 (1-2): p. 157-62.
247.Racine, R.J., *Modification of seizure activity by electrical stimulation. II. Motor seizure.* **Electroencephalogr Clin Neurophysiol**, 1972. 32 (3): p. 281-94.

248.Scoville, W.B. and Milner, B., *Loss of recent memory after bilateral hippocampal lesions.* **J Neurol Neurosurg Psychiatry**, 1957. 20 (1): p. 11-21.
249.Kroll, N.E., et al., *Retrieval of old memories: the temporofrontal hypothesis.* **Brain**, 1997. 120 (Pt 8): p. 1377-99.
250.Stone, V.E., et al., *Selective impairment of reasoning about social exchange in a patient with bilateral limbic system damage.* **Proc Natl Acad Sci USA**, 2002. 99 (17): p. 11531-6.
251.Squire, L.R. and S. Zola-Morgan, *The medial temporal lobe memory system.* **Science**, 1991. 253 (5026): p. 1380-6.
252.McGaugh, J.L., *Memory consolidation and the amygdala: a systems perspective.* **Trends Neurosci**, 2002. 25 (9): p. 456.
253.Zola-Morgan, S., et al., *Independence of memory functions and emotional behavior: separate contributions of the hippocampal formation and the amygdala.* **Hippocampus**, 1991. 1 (2): p. 207-20.
254.Wilson, D.A. and Stevenson, R.J., *The fundamental role of memory in olfactory perception.* **Trends Neurosci**, 2003. 26 (5): p. 243-7.
255.Zola-Morgan, S., Squire, L.R. and Amaral, D.G. *Human amnesia and the medial temporal lobe region: enduring memory impairment following a bilateral lesion limited to field CA1 of the hippocampus.* **J Neurosci**, 1986. 6 (10): p. 2950-67.
256.Habib, M. and A. Sirigu, *Pure topographical disorientation: a definition and anatomical basis.* **Cortex**, 1987. 23 (1): p. 73-85.
257.Meunier, M., et al., *Effects of aspiration versus neurotoxic lesions of the amygdala on emotional responses in monkeys.* **Eur J Neurosci**, 1999. 11 (12): p. 4403-18.
258.de Gennes, P.G., *Organization of a primitive memory: Olfaction.* **Proc Natl Acad Sci USA**, 2004. 101 (44): p. 15778-81.
259.Eichenbaum, H., et al., *Selective olfactory deficits in case H.M.* **Brain**, 1983. 106 (Pt 2): p. 459-72.
260.Schab, F.R. and Crowder, R.G., *Memory for odors*. 1995, Mahwah, N.J.: L. Erlbaum Associates. viii, 187 p.
261.Rausch, R. and Babb, T.L. *Hippocampal neuron loss and memory scores before and after temporal lobe surgery for epilepsy.* **Arch Neurol**, 1993. 50 (8): p. 812-7.
262.Aikia, M., et al., *Predictors of seizure outcome in newly diagnosed partial epilepsy: memory performance as a prognostic factor.* **Epilepsy Res**, 1999. 37 (2): p. 159-67.
263.Rausch, R., Serafetinides, E.A. and Crandall, P.H. *Olfactory memory in patients with anterior temporal lobectomy.* **Cortex**, 1977. 4 (13): p. 445-52.
264.Mungas, D., et al., *Verbal learning differences in epileptic patients with left and right temporal lobe foci.* **Epilepsia**, 1985. 26 (4): p. 340-5.
265.Hermann, B.P., et al., *Neuropsychological characteristics of the syndrome of mesial temporal lobe epilepsy.* **Arch Neurol**, 1997. 54 (4): p. 369-76.
266.Leonard, G., *Temporal lobe surgery for epilepsy: neuropsychological variables related to surgical outcome.* **Can J Neurol Sci**, 1991. 18 (4 Suppl): p. 593-7.
267.Alpherts, W.C., et al., *Long-term effects of temporal lobectomy on intelligence.* **Neurology**, 2004. 62 (4): p. 607-11.
268.Weissbecker, K.A., et al., *Genetic epidemiology and the search for epilepsy genes.* **Adv Neurol**, 1999. 79: p. 323-40.
269.Lindsay, J., Ounsted, C. and Richards, P. *Long-term outcome in children with temporal lobe seizures. III: Psychiatric aspects in childhood and adult life.* **Dev Med Child Neurol**, 1979. 21 (5): p. 630-6.
270.Bazil, C.W. and Pedley, T.A., *Advances in the medical treatment of epilepsy.* **Annu Rev Med**, 1998. **49**: p. 135-62.
271.Feely, M., *Fortnightly review: drug treatment of epilepsy.* **BMJ**, 1999. 318 (7176): p. 106-9.
272.Engel, J., Jr., *Surgery for seizures.* **N Engl J Med**, 1996. 334 (10): p. 647-52.
273.Duncan, J.S. and Sagar, H.J. *Seizure characteristics, pathology, and outcome after temporal lobectomy.* **Neurology**, 1987. 37 (3): p. 405-9.
274.Salanova, V., Markand, O. and Worth, R. *Temporal lobe epilepsy surgery: outcome, complications, and late mortality rate in 215 patients.* **Epilepsia**, 2002. 43 (2): p. 170-4.

275.Kuzniecky, R., et al., *Magnetic resonance imaging in temporal lobe epilepsy: pathological correlations.* **Ann Neurol**, 1987. 22 (3): p. 341-7.
276.Lehericy, S., et al., *Temporal lobe epilepsy with varying severity: MRI study of 222 patients.* **Neuroradiology**, 1997. 39 (11): p. 788-96.
277.Kramer, D.M., *Basic principles of magnetic resonance imaging.* **Radiol Clin North Am**, 1984. 22 (4): p. 765-78.
278.Jackson, G.D., et al., *Hippocampal sclerosis can be reliably detected by magnetic resonance imaging.* **Neurology**, 1990. 40 (12): p. 1869-75.
279.Berkovic, S.F., et al., *Hippocampal sclerosis in temporal lobe epilepsy demonstrated by magnetic resonance imaging.* **Ann Neurol**, 1991. 29 (2): p. 175-82.
280.Jackson, G.D., et al., *Optimizing the diagnosis of hippocampal sclerosis using magnetic resonance imaging.* **AJNR Am J Neuroradiology**, 1993. 14 (3): p. 753-62.
281.Kim, J.H., et al., *Fast spin-echo MR in hippocampal sclerosis: correlation with pathology and surgery.* **AJNR Am J Neuroradiol**, 1995. 16 (4): p. 627-36.
282.Bronen, R.A., et al., *Qualitative MR imaging of refractory temporal lobe epilepsy requiring surgery: correlation with pathology and seizure outcome after surgery.* **AJR Am J Roentgenol**, 1997. 169 (3): p. 875-82.
283.Bronen, R.A., et al., *Regional distribution of MR findings in hippocampal sclerosis.* **AJNR Am J Neuroradiol**, 1995. 16 (6): p. 1193-200.
284.Kuzniecky, R.I., et al., *Multimodality MRI in mesial temporal sclerosis: relative sensitivity and specificity.* **Neurology**, 1997. 49 (3): p. 774-8.
285.McBride, M.C., et al., *Failure of standard magnetic resonance imaging in patients with refractory temporal lobe epilepsy.* **Arch Neurol**, 1998. 55 (3): p. 346-8.
286.Von Oertzen, J., et al., *Standard magnetic resonance imaging is inadequate for patients with refractory focal epilepsy.* **J Neurol Neurosurg Psychiatry**, 2002. 73 (6): p. 643-7.
287.Meiners, L.C., et al., *Fast fluid-attenuated inversion recovery (FLAIR) compared with T2-weighted spin-echo in the magnetic resonance diagnosis of mesial temporal sclerosis.* **Invest Radiol**, 1999. 34 (2): p. 134-42.
288.Jack, C.R., et al., *Temporal lobe volume measurement from MR images: accuracy and left- right asymmetry in normal persons.* **J Comput Assist Tomogr**, 1988. 12 (1): p. 21-9.
289.Watson, C., et al., *Anatomic basis of amygdaloid and hippocampal volume measurement by magnetic resonance imaging.* **Neurology**, 1992. 42 (9): p. 1743-50.
290.Cook, M.J., et al., *Hippocampal volumetric and morphometric studies in frontal and temporal lobe epilepsy.* **Brain**, 1992. 115 (Pt 4): p. 1001-15.
291.Lencz, T., et al., *Quantitative magnetic resonance imaging in temporal lobe epilepsy: relationship to neuropathology and neuropsychological function.* **Ann Neurol**, 1992. 31 (6): p. 629-37.
292.Cheon, J.E., et al., *MR of hippocampal sclerosis: comparison of qualitative and quantitative assessments.* **AJNR Am J Neuroradiol**, 1998. 19 (3): p. 465-8.
293.Jack, C.R., et al., *MR imaging-based volume measurements of the hippocampal formation and anterior temporal lobe: validation studies.* **Radiology**, 1990. 176 (1): p. 205-9.
294.Jack, C.R., *Hippocampal Volumetry in Mesial Temporal Sclerosis*, in *The Epilepsies, Etiologies and Prevention*. Kotagal, P. and Lüders, H.O. Editors. 1999, Academic Press. p. 235-40.
295.Sakamoto, A.C., et al., *Essentials for the establishment of an epilepsy surgery program (Appendice B)*, in *Epilepsy Surgery*, Luders, H. and Comair, Y. Editors. 2001, Lippincott Williams & Wilkins: Philadelphia. p. 979-86.
296.Antel, S.B., et al., *Predicting surgical outcome in temporal lobe epilepsy patients using MRI and MRSI.* **Neurology**, 2002. 58 (10): p. 1505-12.
297.Kral, T., et al., *Preoperative evaluation for epilepsy surgery (Bonn Algorithm).* **Zentralbl Neurochir**, 2002. 63 (3): p. 106-10.
298.Gundersen, H.J. and Jensen, E.B. *The efficiency of systematic sampling in stereology and its prediction.* **J Microsc**, 1987. 147 (Pt 3): p. 229-63.
299.Mayhew, T.M. and Olsen, D.R. *Magnetic resonance imaging (MRI) and model-free estimates of brain volume determined using the Cavalieri principle.* **J Anat**, 1991. 178: p. 133-44.
300.Hasboun, D., et al., *MR determination of hippocampal volume: comparison of three methods.* **AJNR Am J Neuroradiol**, 1996. 17 (6): p. 1091-8.

301.Gonçalves Pereira, P.M., Oliveira, E. and Insausti, R. *Quantitative volumetric analysis of the Hippocampus, Amygdala and Entorhinal Cortex: normative database for the adult portuguese population.* **Rev Neurol** (submited), 2005.
302.Blatter, D.D., et al., *Quantitative volumetric analysis of brain MR: normative database spanning 5 decades of life.* **AJNR Am J Neuroradiol**, 1995. 16 (2): p. 241-51.
303.Brierley, B., Shaw, P. and David, A.S. *The human amygdala: a systematic review and meta-analysis of volumetric magnetic resonance imaging.* **Brain Res Rev**, 2002. 39 (1): p. 84-105.
304.Gonçalves Pereira, P.M., et al., *Magnetic resonance volumetric analysis of the piriform cortex and cortical amygdala in drug-refractory temporal lobe epilepsy.* **AJNR Am J Neuroradiol**, 2005. 26 (2): p. 319-332.
305.Free, S.L., et al., *Methods for normalization of hippocampal volumes measured with MR.* **AJNR Am J Neuroradiol**, 1995. 16 (4): p. 637-43.
306.Hotelling, H., *Relations between two sets of variates.* **Biometrika**, 1936. 28: p. 321-377.
307.Cascino, G.D., et al., *Identification of the epileptic focus: magnetic resonance imaging.* **Epilepsy Res Suppl**, 1992. 5: p. 95-100.
308.Cendes, F., et al., *MRI volumetric measurement of amygdala and hippocampus in temporal lobe epilepsy.* **Neurology**, 1993. 43 (4): p. 719-25.
309.Jack, C.R., et al., *Magnetic resonance image-based hippocampal volumetry: correlation with outcome after temporal lobectomy.* **Ann Neurol**, 1992. 31 (2): p. 138-46.
310.Kuzniecky, R., et al., *Predictive value of magnetic resonance imaging in temporal lobe epilepsy surgery.* **Arch Neurol**, 1993. 50 (1): p. 65-9.
311.Arruda, F., et al., *Mesial atrophy and outcome after amygdalohippocampectomy or temporal lobe removal.* **Ann Neurol**, 1996. 40 (3): p. 446-50.
312.Engel, J., Jr., et al., *Outcome with respect to epileptic seizures*, in *Surgical Treatment of the Epilepsies*, Engel, J. Jr. Editor. 1993, Raven Press, Ltd: New York. p. 609-21.
313.Trenerry, M.R., et al., *MRI hippocampal volumes and memory function before and after temporal lobectomy.* **Neurology**, 1993. 43 (9): p. 1800-5.
314.Trenerry, M.R., M. Westerveld, and K.J. Meador, *MRI hippocampal volume and neuropsychology in epilepsy surgery.* **Magn Reson Imaging**, 1995. 13 (8): p. 1125-32.
315.Jack, C.R., et al., *Bilaterally symmetric hippocampi and surgical outcome.* **Neurology**, 1995. 45 (7): p. 1353-8.
316.Boulby, P.A. and F.J. Rugg-Gunn, *T2: the tranverse relaxation time*, in *Quantitative MRI of the brain: measuring changes caused by disease.* Tofts, P. Editor. 2003, John Wiley & Sons: Chichester. p. 143-201.
317.Brooks, B.S., et al., *MR imaging in patients with intractable complex partial epileptic seizures.* **AJNR Am J Neuroradiol**, 1990. 11 (1): p. 93-9.
318.Bronen, R.A., et al., *Imaging findings in hippocampal sclerosis: correlation with pathology.* **AJNR Am J Neuroradiol**, 1991. 12 (5): p. 933-40.
319.Dowd, C.F., et al., *Magnetic resonance imaging of intractable complex partial seizures: pathological and electroencephalographic correlation.* **Epilepsia**, 1991. 32 (4): p. 454-9.
320.Jackson, G.D., et al., *Detection of hippocampal pathology in intractable partial epilepsy: increased sensitivity with quantitative magnetic resonance T2 relaxometry.* **Neurology**, 1993. 43 (9): p. 1793-9.
321.Namer, I.J., et al., *Contribution of T2 Relaxation Time Mapping in the Evaluation of Cryptogenic Temporal Lobe Epilepsy.* **Neuroimage**, 1998. 7 (4): p. 304-13.
322.Duncan, J.S., Bartlett, P. and Barker, G.J., *Technique for measuring hippocampal T2 relaxation time.* **AJNR Am J Neuroradiol**, 1996. 17 (10): p. 1805-10.
323.Duncan, J.S., Bartlett, P. and Barker, G.J., *Measurement of hippocampal T2 in epilepsy.* **AJNR Am J Neuroradiol**, 1997. 18 (9): p. 1791-2.
324.Bernasconi, A., et al., *T2 relaxometry can lateralize mesial temporal lobe epilepsy in patients with normal MRI.* **Neuroimage**, 2000. 12 (6): p. 739-46.
325.Von Oertzen, J., et al., *Time-efficient T2 relaxometry of the entire hippocampus is feasible in temporal lobe epilepsy.* **Neurology**, 2002. 58 (2): p. 257-64.
326.Okujava, M., et al., *Measurement of temporal lobe T2 relaxation times using a routine diagnostic MR imaging protocol in epilepsy.* **Epilepsy Res**, 2002. 48 (1-2): p. 131-42.

327.Van Paesschen, W., et al., *Quantitative hippocampal MRI and intractable temporal lobe epilepsy.* **Neurology**, 1995. 45 (12): p. 2233-40.
328.Briellmann, R.S., et al., *Hippocampal pathology in refractory temporal lobe epilepsy: T2-weighted signal change reflects dentate gliosis.* **Neurology**, 2002. 58 (2): p. 265-71.
329.Jackson, G.D., Kuzniecky, R.I. and Cascino, G.D., *Hippocampal sclerosis without detectable hippocampal atrophy.* **Neurology**, 1994. 44 (1): p. 42-6.
330.Incisa della Rocchetta, A., et al., *Verbal memory impairment after right temporal lobe surgery: role of contralateral damage as revealed by 1H magnetic resonance spectroscopy and T2 relaxometry.* **Neurology**, 1995. 45 (4): p. 797-802.
331.Kälviäinen, R., et al., *MRI-based hippocampal volumetry and T2 relaxometry: correlation to verbal memory performance in newly diagnosed epilepsy patients with left-sided temporal lobe focus.* **Neurology**, 1997. 48 (1): p. 286-7.
332.Wood, A.G., et al., *Components of verbal learning and hippocampal damage assessed by T2 relaxometry.* **J Int Neuropsychol Soc**, 2000. 6 (5): p. 529-38.
333.Woermann, F.G., et al., *Regional changes in hippocampal T2 relaxation and volume: a quantitative magnetic resonance imaging study of hippocampal sclerosis.* **J Neurol Neurosurg Psychiatry**, 1998. 65 (5): p. 656-64.
334.Sasaki, M., et al., *Hippocampal sulcus remnant: potential cause of change in signal intensity in the hippocampus.* **Radiology**, 1993. 188 (3): p. 743-6.
335.Woermann, F.G., et al., *A fast FLAIR dual-echo technique for hippocampal T2 relaxometry: First experiences in patients with temporal lobe epilepsy.* **J Magn Reson Imaging**, 2001. 13 (4): p. 547-52.
336.Hugg, J.W., et al., *Neuron loss localizes human temporal lobe epilepsy by in vivo proton magnetic resonance spectroscopic imaging.* **Ann Neurol**, 1993. 34 (6): p. 788-94.
337.Hugg, J.W., et al., *Normalization of contralateral metabolic function following temporal lobectomy demonstrated by ^{1}H magnetic resonance spectroscopic imaging.* **Ann Neurol**, 1996. 40 (2): p. 236-9.
338.Cendes, F., et al., *Normalization of neuronal metabolic dysfunction after surgery for temporal lobe epilepsy. Evidence from proton MR spectroscopic imaging.* **Neurology**, 1997. 49 (6): p. 1525-33.
339.Moffett, J.R., et al., *Immunohistochemical localization of N-acetylaspartate in rat brain.* **Neuroreport**, 1991. 2 (3): p. 131-4.
340.Simmons, M.L., Frondoza, C.G. and Coyle, J.T. *Immunocytochemical localization of N-acetyl-aspartate with monoclonal antibodies.* **Neuroscience**, 1991. 45 (1): p. 37-45.
341.Urenjak, J., et al., *Proton nuclear magnetic resonance spectroscopy unambiguously identifies different neural cell types.* **J Neurosci**, 1993. 13 (3): p. 981-9.
342.Bjartmar, C., et al., *N-acetylaspartate is an axon-specific marker of mature white matter in vivo: a biochemical and immunohistochemical study on the rat optic nerve.* **Ann Neurol**, 2002. 51 (1): p. 51-8.
343.Kuzniecky, R., et al., *Relative utility of ^{1}H spectroscopic imaging and hippocampal volumetry in the lateralization of mesial temporal lobe epilepsy.* **Neurology**, 1998. 51 (1): p. 66-71.
344.Nakano, M., et al., *Measurement of regional N-acetylaspartate after transient global ischemia in gerbils with and without ischemic tolerance: an index of neuronal survival.* **Ann Neurol**, 1998. 44 (3): p. 334-40.
345.Frahm, J., et al., *Localized high-resolution proton NMR spectroscopy using stimulated echoes: initial applications to human brain in vivo.* **Magn Reson Med**, 1989. 9 (1): p. 79-93.
346.Mader, I., et al., *Proton chemical shift imaging, metabolic maps, and single voxel spectroscopy of glial brain tumors.* **MAGMA**, 1996. 4 (2): p. 139-50.
347.Maton, B., et al., *Reproducibility of proton magnetic resonance spectroscopy imaging measurements of normal human hippocampus at 1.5 T: clinical implications.* **J Neuroimaging**, 2001. 11 (2): p. 194-201.
348.Hsu, Y.Y., et al., *Proton MR spectroscopy in patients with complex partial seizures: single-voxel spectroscopy versus chemical-shift imaging.* **AJNR Am J Neuroradiol**, 1999. 20 (4): p. 643-51.
349.Gadian, D.G., et al., *^{1}H magnetic resonance spectroscopy in the investigation of intractable epilepsy.* **Acta Neurol Scand Suppl**, 1994. 152: p. 116-21.

350.Connelly, A., et al., *Magnetic resonance spectroscopy in temporal lobe epilepsy.* **Neurology**, 1994. 44 (8): p. 1411-7.
351.Achten, E., et al., *Value of single-voxel proton MR spectroscopy in temporal lobe epilepsy.* **AJNR Am J Neuroradiol**, 1997. 18 (6): p. 1131-9.
352.Cendes, F., et al., *Lateralization of temporal lobe epilepsy based on regional metabolic abnormalities in proton magnetic resonance spectroscopic images.* **Ann Neurol**, 1994. 35 (2): p. 211-6.
353.Burneo, J.G., et al., *Chronic temporal lobe epilepsy: spatial extent and degree of metabolic dysfunction studied with magnetic resonance spectroscopy (MRS).* **Epilepsy Res**, 2004. 62 (2-3): p. 119-24.
354.Stejskal, E. and Tanner, J. *Spin diffusion measurements: spin-echos in the presence of a time dependent field gradient.* **J Chem Phys**, 1965. 42: p. 288-292.
355.Wheeler-Kingshott, C.A.M., et al., *D: the Difusion of Water*, in *Quantitative MRI of the brain: measuring changes caused by disease.* Tofts, P.S. Editor. 2003, John Wiley & Sons: Chichester. p. 203-256.
356.Hugg, J.W., Butterworth, E.J. and Kuzniecky, R.I. *Diffusion mapping applied to mesial temporal lobe epilepsy: preliminary observations.* **Neurology**, 1999. 53 (1): p. 173-6.
357.Wieshmann, U.C., et al., *Water diffusion in the human hippocampus in epilepsy.* **Magn Reson Imaging**, 1999. 17 (1): p. 29-36.
358.Kantarci, K., et al., *Comparative diagnostic utility of ^{1}H MRS and DWI in evaluation of temporal lobe epilepsy.* **Neurology**, 2002. 58 (12): p. 1745-53.
359.Yoo, S.Y., et al., *Apparent diffusion coefficient value of the hippocampus in patients with hippocampal sclerosis and in healthy volunteers.* **AJNR Am J Neuroradiol**, 2002. 23 (5): p. 809-12.
360.Hufnagel, A., et al., *Brain diffusion after single seizures.* **Epilepsia**, 2003. 44 (1): p. 54-63.
361.Duzel, E., et al., *Measures of hippocampal volumes, diffusion and ^{1}H MRS metabolic abnormalities in temporal lobe epilepsy provide partially complementary information.* **Eur J Neurol**, 2004. 11 (3): p. 195-205.
362.Londono, A., et al., *Apparent diffusion coefficient measurements in the hippocampi in patients with temporal lobe seizures.* **AJNR Am J Neuroradiol**, 2003. 24 (8): p. 1582-6.
363.Quigg, M., et al., *Volumetric magnetic resonance imaging evidence of bilateral hippocampal atrophy in mesial temporal lobe epilepsy.* **Epilepsia**, 1997. 38 (5): p. 588-94.
364.Blum, D.E., et al., *Bilateral temporal hypometabolism in epilepsy.* **Epilepsia**, 1998. 39 (6): p. 651-9.
365.Martin, R.C., et al., *Bilateral hippocampal atrophy: Consequences to verbal memory following temporal lobectomy.* **Neurology**, 2001. 57 (4): p. 597-604.
366.King, D., et al., *Bilateral hippocampal atrophy in medial temporal lobe epilepsy.* **Epilepsia**, 1995. ***36*** (9): p. 905-10.
367.Fish, D.R. and Spencer, S.S. *Clinical correlations: MRI and EEG.* **Magn Reson Imaging**, 1995. 13 (8): p. 1113-7.
368.Watson, C., et al., *Specificity of volumetric magnetic resonance imaging in detecting hippocampal sclerosis.* **Arch Neurol**, 1997. 54 (1): p. 67-73.
369.Cascino, G.D., et al., *Operative strategy in patients with MRI-identified dual pathology and temporal lobe epilepsy.* **Epilepsy Res**, 1993. 14 (2): p. 175-82.
370.Adam, C., et al., *Value of magnetic resonance imaging-based measurements of hippocampal formations in patients with partial epilepsy.* **Arch Neurol**, 1994. 51 (2): p. 130-8.
371.Cendes, F., et al., *Frequency and characteristics of dual pathology in patients with lesional epilepsy.* **Neurology**, 1995. 45 (11): p. 2058-64.
372.Li, L.M., et al., *Surgical outcome in patients with epilepsy and dual pathology.* **Brain**, 1999. 122 (Pt 5): p. 799-805.
373.Eriksson, S.H., et al., *Parenchymal lesions in pharmacoresistant temporal lobe epilepsy: dual and multiple pathology.* **Acta Neurol Scand**, 2005. 112 (3): p. 151-6.
374.Van Paesschen, W., et al., *The amygdala and intractable temporal lobe epilepsy: a quantitative magnetic resonance imaging study.* **Neurology**, 1996. 47 (4): p. 1021-31.

375.Salmenperä, T., et al., *MRI volumetry of the hippocampus, amygdala, entorhinal cortex, and perirhinal cortex after status epilepticus.* **Epilepsy Res**, 2000. 40 (2-3): p. 155-70.
376.Bartlett, P.A., Richardson, M.P. and Duncan, J.S. *Measurement of amygdala T2 relaxation time in temporal lobe epilepsy.* **J Neurol Neurosurg Psychiatry**, 2002. 73 (6): p. 753-5.
377.Bernasconi, N., et al., *Mesial temporal damage in temporal lobe epilepsy: a volumetric MRI study of the hippocampus, amygdala and parahippocampal region.* **Brain**, 2003. 126 (Pt 2): p. 462-9.
378.Convit, A., et al., *MRI volume of the amygdala: a reliable method allowing separation from the hippocampal formation.* **Psychiatry Res**, 1999. 90 (2): p. 113-23.
379.Cendes, F. and et al, *MRI volumetric measurements of amygdaloid body and hippocampal formation: inter and intra ratter differences.* **Can J Neuro Sci**, 1992. 19: p. 285.
380.Achten, E., et al., *Intra- and interobserver variability of MRI-based volume measurements of the hippocampus and amygdala using the manual ray-tracing method.* **Neuroradiology**, 1998. 40 (9): p. 558-66.
381.Salmenperä, T., *Damage in the hippocampus, amygdala, entorhinal and perirhinal cortex of adults with partial epilepsy*, in *Departement of Neurology, Kuopio University Hospital*. PhD Thesis 2001, University of Kuopio, Finland. 125 p.
382.Cendes, F., et al., *MRI of amygdala and hippocampus in temporal lobe epilepsy.* **J Comput Assist Tomogr**, 1993. 17 (2): p. 206-10.
383.Cendes, F., et al., *Relationship between atrophy of the amygdala and ictal fear in temporal lobe epilepsy.* **Brain**, 1994. 117 (Pt 4): p. 739-46.
384.Bernasconi, N., et al., *Entorhinal cortex in temporal lobe epilepsy. A quantitative MRI study.* **Neurology**, 1999. 52 (9): p. 1870-1876.
385.Salmenperä, T., et al., *Quantitative MRI volumetry of the entorhinal cortex in temporal lobe epilepsy.* **Seizure**, 2000. 9 (3): p. 208-15.
386.Saukkonen, A., et al., *Do seizures cause neuronal damage? A MRI study in newly diagnosed and chronic epilepsy.* **Neuroreport**, 1994. 6 (1): p. 219-23.
387.Bernasconi, N., et al., *Entorhinal cortex atrophy in epilepsy patients exhibiting normal hippocampal volumes.* **Neurology**, 2001. 56 (10): p. 1335-9.
388.Jutila, L., et al., *MR Volumetry of the Entorhinal, Perirhinal, and Temporopolar Cortices in Drug-Refractory Temporal Lobe Epilepsy.* **AJNR Am J Neuroradiol**, 2001. 22 (8): p. 1490-1501.
389.Bernasconi, N., et al., *Entorhinal cortex MRI assessment in temporal, extratemporal, and idiopathic generalized epilepsy.* **Epilepsia**, 2003. 44 (8): p. 1070-4.
390.Briellmann, R.S., et al., *Hemicranial volume deficits in patients with temporal lobe epilepsy with and without hippocampal sclerosis.* **Epilepsia**, 1998. 39 (11): p. 1174-81.
391.Lee, J.W., et al., *Morphometry in temporal lobe epilepsy.* **Magn Reson Imaging**, 1995. 13 (8): p. 1073-80.
392.Kim, J.H., et al., *Clinical significance of asymmetry of the fornix and mamillary body on MR in hippocampal sclerosis.* **AJNR Am J Neuroradiol**, 1995. 16 (3): p. 509-15.
393.Ng, S.E., et al., *MRI of the fornix and mamillary body in temporal lobe epilepsy.* **Neuroradiology**, 1997. 39 (8): p. 551-5.
394.Woermann, F.G., et al., *Voxel-by-voxel comparison of automatically segmented cerebral gray matter - A rater-independent comparison of structural MRI in patients with epilepsy.* **Neuroimage**, 1999. 10 (4): p. 373-84.
395.Keller, S.S., et al., *Voxel based morphometry of grey matter abnormalities in patients with medically intractable temporal lobe epilepsy: effects of side of seizure onset and epilepsy duration.* **J Neurol Neurosurg Psychiatry**, 2002. 73 (6): p. 648-655.
396.Keller, S.S., et al., *Voxel-based morphometric comparison of hippocampal and extrahippocampal abnormalities in patients with left and right hippocampal atrophy.* **Neuroimage**, 2002. 16 (1): p. 23-31.
397.McMillan, A.B., et al. *Voxel-based morphometry of gray and white matter in lateralized temporal lobe epilepsy*. in *ISMRM 2004, 12 Intl. Soc. Mag. Reson. Med.* 2004.
398.Pell, G.S., et al. *Combined Voxel-based analysis of volume and T2-relaxometry in temporal lobe epilepsy*. in *ISMRM 2004, 12 Intl. Soc. Mag. Reson. Med.* 2004.
399.Bonilha, L., et al., *Voxel-based morphometry reveals gray matter network atrophy in refractory medial temporal lobe epilepsy.* **Arch Neurol**, 2004. 61 (9): p. 1379-84.

400.Bonilha, L., et al., *Voxel-based morphometry of the thalamus in patients with refractory medial temporal lobe epilepsy.* **Neuroimage**, 2005. 25 (3): p. 1016-21.
401.Achten, E., et al., *An MR protocol for presurgical evaluation of patients with complex partial seizures of temporal lobe origin.* **AJNR Am J Neuroradiol**, 1995. 16 (6): p. 1201-13.
402.Meiners, L.C., et al., *Assessment of the preferred plane and sequence in the depiction of mesial temporal sclerosis using magnetic resonance imaging.* **Invest Radiol**, 1997. 32 (5): p. 268-76.
403.Ng, T.C., et al., *Temporal lobe epilepsy: presurgical localization with proton chemical shift imaging.* **Radiology**, 1994. 193 (2): p. 465-72.
404.Jack, C.R., et al., *MR-based hippocampal volumetry in the diagnosis of Alzheimer's disease.* **Neurology**, 1992. 42 (1): p. 183-8.
405.Du, A.T., et al., *Magnetic resonance imaging of the entorhinal cortex and hippocampus in mild cognitive impairment and Alzheimer's disease.* **J Neurol Neurosurg Psychiatry**, 2001. 71 (4): p. 441-7.
406.Capizzano, A.A., et al., *Temporal lobe epilepsy: qualitative reading of ^{1}H MR spectroscopic images for presurgical evaluation.* **Radiology**, 2001. 218 (1): p. 144-51.
407.Tamraz, J.C. and Comair, Y.G. *Cephalic reference lines suitable for neuroimaging*, in *Atlas of regional anatomy of the brain using MRI – with functional correlations.* Tamraz, J.C. and Comair, Y.G. Editors. 2000, Springer-Verlag: Berlin. p. 11-50.
408.Jack, C.R., *Medial temporal lobe volumetrics in traumatic brain injury.* **AJNR Am J Neuroradiol**, 1997. 18 (1): p. 25-8.
409.Bigler, E.D., Andersob, C.V. and Blatter, D.D. *Temporal lobe morphology in normal aging and traumatic brain injury.* **AJNR Am J Neuroradiol**, 2002. 23 (2): p. 255-66.
410.Strassburger, T.L., et al., *Interactive effects of age and hypertension on volumes of brain structures.* **Stroke**, 1997. 28 (7): p. 1410-7.
411.Folstein, M.F., Folstein, S.E. and McHugh, P.R., *"Mini-mental state". A practical method for grading the cognitive state of patients for the clinician.* **J Psychiatr Res**, 1975. 12 (3): p. 189-98.
412.Bland, J.M. and Altman, D.G. *Statistical methods for assessing agreement between two methods of clinical measurement.* **Lancet**, 1986. 1 (8476): p. 307-10.
413.Tofts, P.S., *QA: quality assurance, accuracy, precision and phantoms*, in *Quantitative MRI of the brain: measuring changes caused by disease.* Tofts, P. Editor. 2003, John Wiley & Sons: Chichester. p. 55-81.
414.Jackson, G.D., Chambers, B.R. and Berkovic, S.F., *Hippocampal sclerosis: development in adult life.* **Dev Neurosci**, 1999. 21 (3-5): p. 207-14.
415.Worrell, G.A., et al., *Rapidly progressive hippocampal atrophy: evidence for a seizure-induced mechanism.* **Neurology**, 2002. 58 (10): p. 1553-6.
416.Bouilleret, V., et al., *Mapping of the progressive metabolic changes occurring during the development of hippocampal sclerosis in a model of mesial temporal lobe epilepsy.* **Brain Res**, 2000. 852 (2): p. 255-62.
417.Gale, K., *Subcortical structures and pathways involved in convulsive seizure generation.* **J Clin Neurophysiol**, 1992. 9 (2): p. 264-77.
418. ILAE Commission on Classification Report, *Proposal for a new classification of outcome with respect to epileptic seizures following epilepsy surgery.* **Epilepsia**, 2001. 42 (2): p. 282-6.